A Microalgae-Based Platform for the Beneficial Re-use of Carbon Dioxide Emissions from Power Plants

Final Technical Report

Principal Author
Mark Crocker
University of Kentucky, Lexington KY

Contributing Co-authors
Jack Groppo, Stephanie Kesner, Daniel Mohler, Robby Pace, Eduardo Santillan-Jimenez and Michael Wilson, *University of Kentucky, Lexington, KY*
Jenna Schambach and Jennifer Stewart, *University of Delaware, Lewes, DE*
Ashton Zeller, *Algix, Meridian, MS*

Reporting Period
October 1, 2015 – September 30, 2017

Submission Date
December 2017

Work Performed Under Award Number
DE-FE0026396

Submitted By
University of Kentucky Research Foundation
109 Kinkead Hall
Lexington, KY 40506-0057

Principal Investigator
Mark Crocker
859-257-0295
mark.crocker@uky.edu

DOE Program Manager
Isaac ‘Andy’ Aurelio
304-285-0244
Isaac.Aurelio@NETL.DOE.GOV

Submitted To
U.S. Department of Energy, National Energy Technology Laboratory

Disclaimer

Acknowledgement

This material is based upon work supported by the Department of Energy under Award Number DE-FE0026396.

Table of Contents

List of Tables

List of Figures

1. Executive Summary

This project sought to address the technical and economic barriers to carbon dioxide (CO_2) capture and utilization using microalgae. Key findings are as follows:

- Culturing experiments confirmed the suitability of urea as a nitrogen source for *Scenedesmus acutus* (versus the more expensive alternative, $NaNO_3$). Both N sources gave similar growth rates, while protein content in the algae was higher for cultures grown using urea. Growth rates for cultures grown using 9%CO_2/N_2 and simulated flue gas (9%CO_2/N_2 with 25 ppm SO_2 and 55 ppm NO added) were equivalent — independent of the N-source — indicating that SO_2 and NO do not affect *Scenedesmus* growth at these concentrations.
- $NaHCO_3$ supplementation and sparging with air were examined as methods of providing C to algae cultures in the event of a power plant outage. The addition of solid bicarbonate stimulated the greatest biomass productivity among the treatments examined, followed by addition of an aqueous $NaHCO_3$ solution, whereas the biomass density of the cultures bubbled with air declined. Under all treatments biomass productivity was still less than that of cultures maintained on flue gas. However, the cells treated with $NaHCO_3$ remained healthy and maintained a high protein content.
- A full prototype of an integrated dewatering process was built, tested, and operated. Using the lamellar clarifier, solids recovery efficiency of >95% could be obtained for *Scenedesmus acutus* algae that had first been flocked using a polymeric cationic flocculant (5-7 ppm). In separate experiments, it was shown that the combined use of cationic (5 ppm) and anionic (2 ppm) polymeric flocculants affords even better results.
- The potential of leveraging low grade waste heat to elevate the temperatures of algae cultures in winter was evaluated. A scenario was studied in which algae cultures are heated by pumping culture medium through shell-tube heat exchangers, using circulating water that flows between the power plant boiler and the cooling towers as a heat source. Calculations showed that even when the ambient temperature was 0 °C, this approach would enable the temperature in the PBR to be maintained at ≥12 °C while maintaining net CO_2 capture. However, dramatic increases in CAPEX result from the purchase of the required heat integration equipment, which includes feed tanks, additional pumps and shell tube heat exchangers. Consequently, the increase in CAPEX associated with the purchase of heat integration equipment incurs an increase in the biomass production cost that is untenable
- Operating data were collected during algae cultivation in a 1200 L cyclic flow PBR at Duke Energy's East Bend Station in 2016 and 2017 for inclusion in techno-economic and lifecycle analyses. Analysis of the data revealed that the growth of *Scenedesmus acutus* shows a greater degree of temperature than previously realized, peak O_2 production (a proxy for growth) occurring in the range 35-38.5 °C. Carbon mass balance calculations in which CO_2 uptake was compared with the mass of biomass produced gave generally good agreement, indicating that the cyclic flow PBR at East Bend was free of major gas leaks.
- Harvested algae grown using flue gas as the CO_2 source were analyzed for heavy metals (As, Hg, Se). Very low heavy metal concentrations were detected, consistent with heavy metals incorporation from the supplied nutrients. All dry algae samples fell within acceptable levels for plastics used for food packaging that has an unregulated industry standard level of 60

mg/kg as outlined by the World Health Organization. All samples had As, Cd, Hg and Se concentrations below the MCLs for biosolids and fertilizer MCLs, although Cd levels in dry algae were too high for use in raw materials for dietary supplements and animal feed. Finding a phosphate source that has a lower Cd content should mitigate Cd levels within the final products.

- Techno-economic analysis and lifecycle assessment were performed to quantify the economics and the magnitude of GHG emission reductions that can be achieved using algae-based CO_2 capture in the UK cyclic flow PBR. LCA showed that the cyclic flow PBR qualifies as a net CO_2 capture technology; over a 30-year period, net CO_2 capture equated to 43% of the targeted amount. TEA indicates a best case scenario production cost of $875/ton for *Scenedesmus acutus* biomass in the USA, excluding the cost of capital.
- A procedure was developed for lipid extraction from wet *Scenedesmus* biomass (10-20 wt% solids) based on chemical lysing of the algae cells using HCl/MeOH followed by the addition of hexane. The yield of extracted esterifiable lipids was found to be comparable to that obtained from dry biomass. Extracted lipids were upgraded to diesel-range hydrocarbons in high yield using a supported Ni catalyst, while the defatted solid (5 kg) was provided to Algix for bioplastic compounding studies. Subsequently, a second batch of biomass (2.2 kg) was prepared for Algix that was subjected to lipid extraction and an additional washing step to remove free sugars.
- Molded bioplastic test specimens were prepared and evaluated for mechanical performance and material characterization. It was found that while some properties of the newly formed bioplastic products improved upon the neat material properties, other properties lessened. Overall, the potential for the UK CAER supplied algae to become a viable and processable bioplastic with adequate mechanical properties was clearly shown. The best candidate for further review was the lipid and sugar extracted material, which showed the highest extension values with comparable load values to other UK-derived samples. Moreover, it demonstrated extension benefits against the Algix Bloom product (currently offered commercially), even though it had quite a few agglomerates which generally exert a negative effect on mechanical properties. This suggests that with the enhanced milling that exists on the commercial scale, the sugar and fat extracted product may be even more competitive.

2. Project Objectives

2.1. Goals

Specific goals of this project were as follows:

(i) Optimize UK's current technology with respect to cost and performance, particularly with regard to harvesting and dewatering operations;

(ii) Develop strategies to monitor and maintain algae culture health, based on a sound understanding of algal biology;

(iii) Develop a biomass utilization strategy which simultaneously produces lipid feedstock for the direct upgrading to fuels and a proteinaceous feedstock for the production of algal-based bioplastics, thereby maximizing the value of the algal biomass;

(iv) Perform techno-economic analyses to calculate the cost of CO_2 capture and recycle using this approach, and lifecycle analyses to evaluate the greenhouse gas emission reduction potential.

2.2. Milestones

The outcome of the various milestones associated with important activities in the project is summarized below (see Table 1).

Table 1. Outcome of Project Milestones

Budget Period	Task Number	Milestone Title/ Description	Planned Completion Date	Actual Completion Date	Verification Method	Outcome
1	1.0	Updated Project Management Plan	11/30/2015	10/27/2015	PMP File	Completed
1	1.1	Kickoff Meeting	12/15/2015	10/20/2015	Presentation file	Completed
1	1.1	Material & Energy Balances	12/15/2015	12/16/2015	Data file	Completed
1	1.1	Presentation at NETL	12/15/2015	12/16/2015	Presentation file	Completed
2	1.1	Final Presentation at NETL	9/15/2017	10/13/2017	Presentation file	Completed
2	1.2	Final Report to NETL	9/30/2017	Dec. 2017	Final Report	Completed
1	1.2	Presentation at ABO	10/15/2016	10/25/2016	Presentation File	Completed
1	1.3	Year 1 Go/No-Go	11/15/2016	8/5/2016	Presentation File	Completed
1	2.4	Demonstration of Continuous Dewatering	9/15/2016	9/30/2016	Report w/ data	Completed
1	3.2	Flue Gas Biomass Effect Study Complete	9/15/2016	6/30/2017	Report w/ data	Completed
1	4.3	Scaled Up Lipid Extraction	9/15/2016	5/31/2016	Sample + report file	Completed
2	5.6	Life Cycle Assessment	9/15/2017	9/30/2017	Report File	Completed
2	5.6	Techno-economic Analysis	9/15/2017	9/30/2017	Report w/data	Completed
2	6.1	Demonstration of Alternative Carbon Delivery System	9/15/2017	6/30/2017	Report w/data	Completed
2	7.2	Product Delivery of Whole and Defatted Algae to Algix	7/15/2017	8/31/2017	Report	Completed
2	7.3	Comparative Analysis of Bioplastics From Whole and Defatted Algae	9/15/2017	9/30/2017	Samples + report w/data	Completed

2.3. Success Criteria

The outcomes for the project's various success criteria are summarized in Table 2.

Table 2. Outcome of Success Criteria

Decision Point	Target Date	Success Criteria	Outcome
Lipid extraction	9/30/16	>50 wt% total lipid recovery demonstrated for wet extraction	>80 wt% total lipid recovery; >95 wt% esterifiable lipid recovery (see section 3.3.1)
Demonstration of continuous dewatering	9/30/16	Solids recovery of >95% demonstrated	>95% solids recovery achieved in lamellar clarifier (see section 3.2.3)_
Verification of methodology for culture maintenance	9/30/17	Maintenance of culture viability for 2 weeks without flue gas	Culture supplementation with $NaHCO_3$ shown to be effective for culture maintenance (see section 3.1.2)
Validation of bioplastic properties	9/30/17	Mechanical properties of bioplastics derived from defatted algae better or equal to bioplastics based on whole cell algae	Compared to raw UK CAER algal biomass, plastic samples prepared from defatted & sugar extracted biomass were equivalent/slightly better (see section 3.3.2)
Lifecycle analysis	9/30/17	Lifecycle analysis shows net positive greenhouse gas emission reduction	~43% net CO_2 equivalent emission reduction calculated (see section 3.2.6)

3. Technical Results

3.1. System Biology

3.1.1. Influence of Flue Gas on the Growth and Composition of *Scenedesmus acutus*

As expected, the productivity of *S. acutus* was very low when grown with bubbled air only (0.018 ± 0.006 g L^{-1} d^{-1}). Biomass productivity was significantly (15x) higher than air ($p<0.05$) for the CO_2 (0.267 ± 0.016 g L^{-1} d^{-1}) and flue gas (0.269 ± 0.039 g L^{-1} d^{-1}) treatments, with no significant difference between the two ($p>0.05$, Figure 1). Specific growth rates, however, were significantly different between all treatments ($p<0.05$), with the greatest specific growth rate for the CO_2 treatment (0.389 ± 0.021 d^{-1}), followed by the flue gas treatment (0.307 ± 0.020 d^{-1}), and finally the air control (0.217 ± 0.087 d^{-1}).

The initial pH for the urea media was between 6.5 and 7.0. The pH for the air-bubbled cultures increased to 9.7 ± 0.01 by day 6, whereas pH decreased to 4.2 ± 0.14 and 3.5 ± 0.19 in the CO_2 and flue gas treatments, respectively (Figure 2). Despite a much lower pH in this experiment as compared to the outdoor PBR (pH 6-7; Wilson et al, 2016), the productivity of *S. acutus* was greater in this experiment. The maximum quantum yield of PSII (Fv/Fm), a proxy for cell health, was comparable for all treatments, which further indicated that the high CO_2 concentrations and low pH in these treatments were not inhibitory (Figure 3).

These results are in agreement with previous studies that noted increased biomass productivity of other economically important chlorophytes, such as *Chlorella* sp., *Chlamydomonas* sp., and other *Scenedesmus* sp., when grown in high CO_2 concentrations (Mudimu et al., 2015, Papazi et al., 2008, Yang and Gao 2003, Hanagata et al., 1992). They are also consistent with studies that evaluated the use of microalgae to biologically capture CO_2 from industrial flue gas sources (Mortensen and Gislerod 2016, Jiang et al., 2013, Huang et al., 2016). For example, Hanagata et al. (1992) showed that *Scenedesmus* sp. successfully grows in up to 80% CO_2; Jiang et al. (2013) reported that *Scenedesmus* sp. grew well at NO concentrations of 150-500 ppm and SO_2 concentrations below 100 ppm, which are much higher than in the simulated flue gas used in this experiment. Here, NO and SO_2 in flue gas were not inhibitory, but the similar results observed for growth on flue gas and 9% CO_2 suggests that the high CO_2 concentration in the flue gas is driving the enhanced growth.

In this experiment, pH was unregulated and the continuous introduction of excess CO_2 caused the pH to decline considerably in the CO_2 and flue gas treatments. Additionally, the final pH in the flue gas treatment (3.5) was almost one pH unit below that of the final pH in the CO_2 treatment. This was likely due to the accumulation of acidic species of NO and SO_2 in the media (Yen et al., 2015, Jiang et al. 2013, Lee et al., 2002, Maeda et al., 1995). It was surprising that we observed such enhanced growth under these acidic conditions, considering the optimum pH for most microalgae is near neutral (Juneja et al., 2013). Many algal species, however, have adapted to the fluctuations in pH often seen in freshwater environments by regulating their internal pH (Juneja et al., 2013, Gehl and Colman 1984, Goldman et al., 1982). Some freshwater green algae, including *Scenedesmus,* can maintain a near neutral internal pH even under low external pH conditions (Gehl and Colman 1984, Lane and Burris 1981). This would allow for normal cell functions to proceed, although it would be necessary for cells to allocate a significant amount of energy to proton pumping via P-type H^+ ATPases found on the plasma membrane (Juneja et al., 2013, Taylor et al., 2012). While there was an increase in *S. acutus* biomass

productivity in 9% CO_2 and flue gas, maximum productivity might not have been reached in these treatments if the cells diverted energy from CO_2 fixation and growth to such proton pumping (Gerloff-Elias et al., 2005). Thus, optimal culture pH for maximal growth at scale should be determined for this species. A pH-stat strategy is employed in the pilot PBR at the East Bend Station to stabilize culture pH in the range of 6-7, where gas is sparged for 20 seconds and then turned off for 40 seconds (Wilson, personal communication). Results from these experiments, however, suggest that the optimal pH may be lower than 6.

As expected, macronutrients were more quickly consumed in the CO_2 and flue gas treatments compared to air, where the culture media for these treatments became N-depleted between days 3 and 6 (Table 3). Urea declined by 67% in the air-bubbled cultures and by 95% in the CO_2 and flue gas treatments by day 3, and were below the limit of detection in the CO_2 and flue gas treatments on day 6. The decline in phosphate concentrations followed the same trend as urea, but phosphate was not entirely depleted in any treatment on day 6 (Table 4).

Sub-inhibitory levels of NO are known to promote microalgal growth, since the NO can be used as an additional nitrogen source (Yen et al. 2015, Matsumoto et al., 1997, Nagase et al., 1997). As NO is dissolved into the media, it is oxidized to form nitrite (NO_2^-) via inlet gas or photosynthetically derived oxygen (Nagase et al., 1997), and the NO_2^- may then be taken up and assimilated by the algae (Nagase et al., 1997). Dissolution and removal of NO by the algae was not directly measured in this experiment, but a small amount of bioavailable nitrogen as nitrite was detected (approximately 15 μmol L^{-1} NO_2^-) in flue gas cultures. The presence of this additional N source, however, did not result in increased productivity when compared to cultures grown on CO_2 alone, suggesting that this algal strain is not utilizing NO-derived nitrogen in the presence of urea. Although the culture media was depleted of urea by day 6 in both CO_2-supplemented treatments, cultures had not yet reached stationary phase, suggesting that internal nitrogen pools were sufficient for growth at this time point. In general, algae prefer to utilize reduced nitrogen sources such as urea and ammonium, even in the presence of nitrate/nitrite, so it is possible that NO-derived nitrogen could contribute to sustained growth as these internal N pools are further depleted, over longer timelines than were measured here. Even so, this phenomenon would not contribute to an operational advantage at scale, as biomass would be harvested long before severe urea depletion would occur.

Influence of Flue Gas on Biochemical Composition

Biomass samples were taken on days 0, 3, and 6 to determine protein content, total lipid content, FAME profile, and carbohydrate content for each treatment. Protein content was similar across treatments, peaking on day 3 (Figure 4). Total protein was higher in both CO_2-supplemented cultures compared to air, despite the fact that air-bubbled cultures exhibited significantly >2x more chlorophyll a content ($p<0.05$; Figure 5). Protein content (% of total biomass) was of particular importance in this study, since *S. acutus* biomass is being explored for the production of biodegradable plastic from the defatted fraction. When exposed to CO_2 and flue gas, protein content was enhanced by 25% during log phase growth (day 3, Figure 4). Sarat et al. (2016) also found that protein content in *S. obtusus* increased by 15% when grown under 10% CO_2. In the current study, total protein content was about 30% on day 3, which is comparable to that reported for *S. acutus* grown using flue gas in an outdoor pilot-PBR (Santillan-Jimenez et al., 2016), as well as that for *S. obtusus* in Sarat et al. (2016).

From lipid and carbohydrate measurements, it is apparent that under CO_2-limited conditions carbon is shunted to the production of lipids, whereas carbohydrate synthesis is the main depot for carbon when cultures are supplemented with 9% CO_2 (Figure 6 and Figure 7). Other studies have noted increased lipids with increased CO_2 concentration in *Scenesdesmus* and *Chlorella* sp., as lipid biosynthesis is a sink for excess products of carbon fixation, and it is thought that channeling these products to energy rich compounds may be an adaptation to high CO_2 tolerance (Sarat et al., 2016, Xia et al., 2013, Solovchenko and Goldberg 2013). This was not the case in this experiment, where the cells in the flue gas and CO_2 treatments stored their fixed carbon as carbohydrates. At nearly 50% of the total biomass, the carbohydrate content in *S. acutus* could be extracted and utilized as a feedstock for fermentation into bio-ethanol, which would increase the purity of the protein fraction bio-plastic production (Laurens et al., 2015). Since the storage of large amounts of carbohydrates, at the expense of lipids, occurs when cultures are exposed to flue gas, an extraction and processing strategy specific for carbohydrates may add to the economic value of this system at scale.

In terms of the overall FAME composition of the lipid fraction, saturated and monounsaturated fatty acid content was similar between the CO_2 and flue gas treatments and significantly greater than the control on all days ($p<0.05$, Figure 8). Notably, polyunsaturated fatty acids represented >20% of FAMEs in air-grown cultures, but were largely absent in the CO_2 and flue gas treatments. However, *S. acutus* grown in the field and other species of *Scenedesmus* were reported to have as much as 50% of the total fatty acids as polyunsaturated fatty acids (Ji et al., 2017). This difference in fatty acid composition could be due to the low pH in this experiment versus the near neutral pH seen in the field and in these other experiments (Ji et al., 2017). Increased saturated fatty acid content in microalgae is another response to increased external acidity, since saturation of membrane fatty acids reduces its fluidity and inhibits proton infiltration (Juneja et al., 2013). This difference highlights the idea that fatty acid content and composition in microalgae is largely species-specific and can significantly change under different environmental conditions (Ji et al., 2017, Juneja et al., 2013).

There were a few prominent fatty acids found among all treatments on all sampling days, including C16:0, C18:1n9c, and C18:1n9t (Figure 9). Additionally, C18:2n6 was the only polyunsaturated fatty acid that made up at least 2% of the total composition, and it was only found in the control. The air-bubbled cultures also contained several other fatty acids that were not seen at all in the other treatments throughout the experiment, including multiple short chain fatty acids, C8:0, C10:0, C11:0, and C16:1. These profile differences resulted in the CO_2 and flue gas treatments having greater calculated cetane numbers compared to air cultures (Table 5), although cetane numbers exceeded US premium diesel standards (55) for all cases.

Table 3. Concentrations of urea (μmol/L) in *S. acutus* cultures when grown under air (0.04% CO_2), 9%CO_2, and simulated flue gas (9% CO_2, 50 ppm NO, 25 ppm SO_2). Values are means ± SD.

	Day		
	0	3	6
Air	1950.0 ± 35.3	660.5 ± 8.1	508.8 ± 61.9
9% CO_2	1963.2 ± 88.9	122.2 ± 30.4	0
Flue Gas	1961.5 ± 20.8	133.3 ± 49.9	0

Table 4. Concentrations of phosphate (μmol/L) in *S. acutus* cultures grown under air (0.04% CO_2), 9%CO_2, and simulated flue gas (9% CO_2, 50 ppm NO, 25 ppm SO_2). Values are means ± SD.

	Day		
	0	3	6
Air	736.7 ± 49.0	650.1 ± 42.4	326.0 ± 42.7
9% CO_2	731.9 ± 99.0	462.2 ± 28.2	73.1 ± 27.2
Flue Gas	715.1 ± 87.1	487.4 ± 42.1	119.7 ± 41.8

Table 5. Average cetane number for *S. acutus* FAME content grown under air, 9% CO_2, and simulated flue gas (9% CO_2, 55 ppm NO, 25 ppm SO_2).

	0	3	6	Overall
Air	58	59	59	58
9% CO_2	65	68	65	66
Flue Gas	65	68	66	66

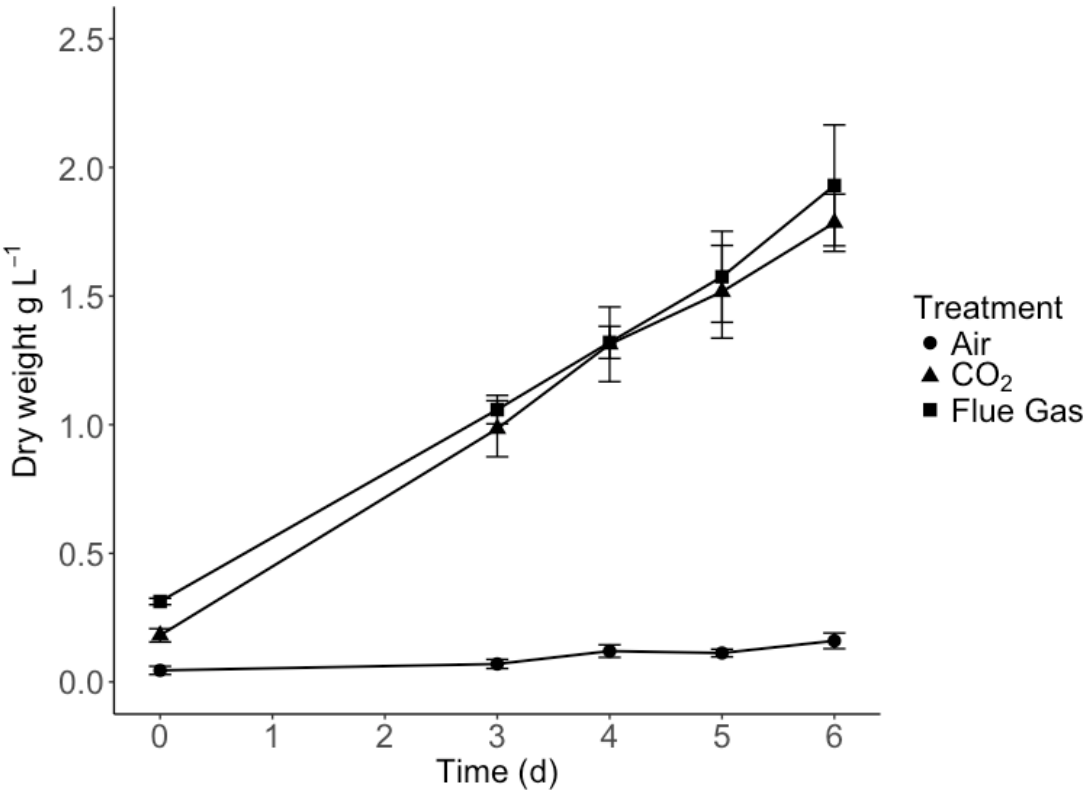

Figure 1. Growth of *S. acutus* cultures when grown under air (0.04% CO_2), 9%CO_2, and simulated flue gas (9% CO_2, 55 ppm NO, 25 ppm SO_2). Values are means ± SD.

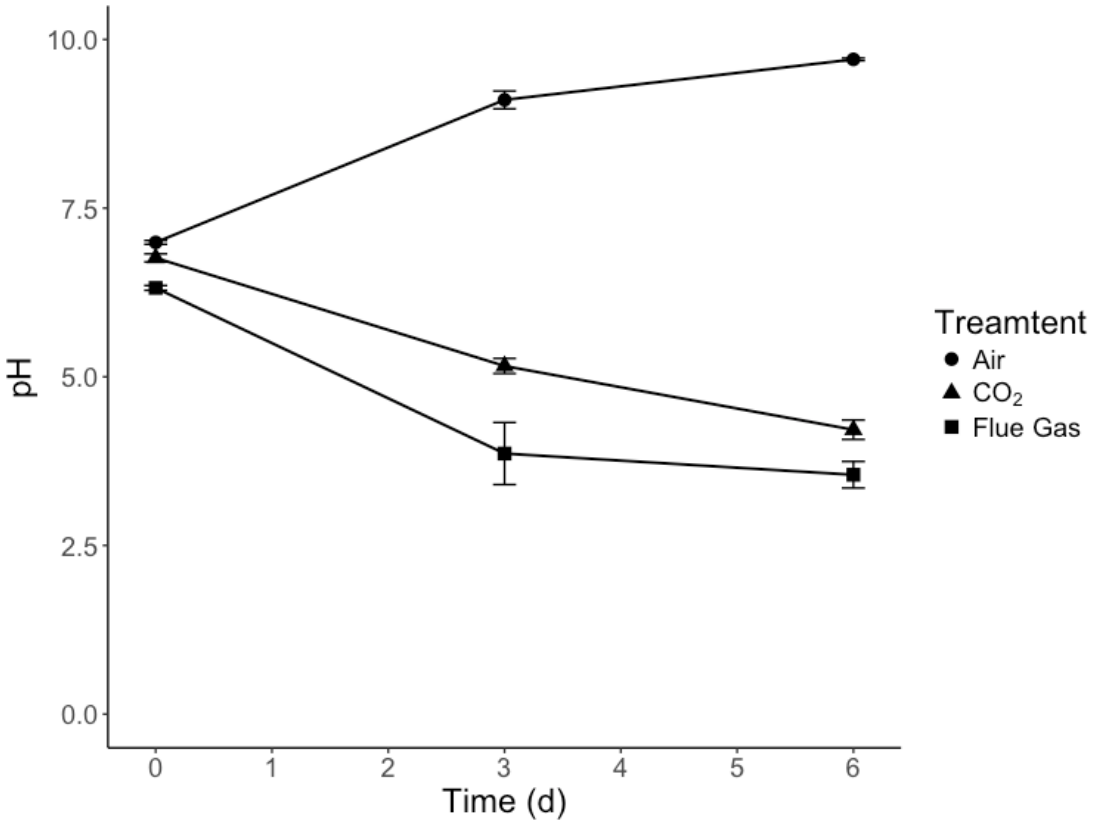

Figure 2. pH of *S. acutus* cultures when grown under air (0.04% CO_2), 9%CO_2, and simulated flue gas (9% CO_2, 50 ppm NO, 25 ppm SO_2). Values are means ± SD.

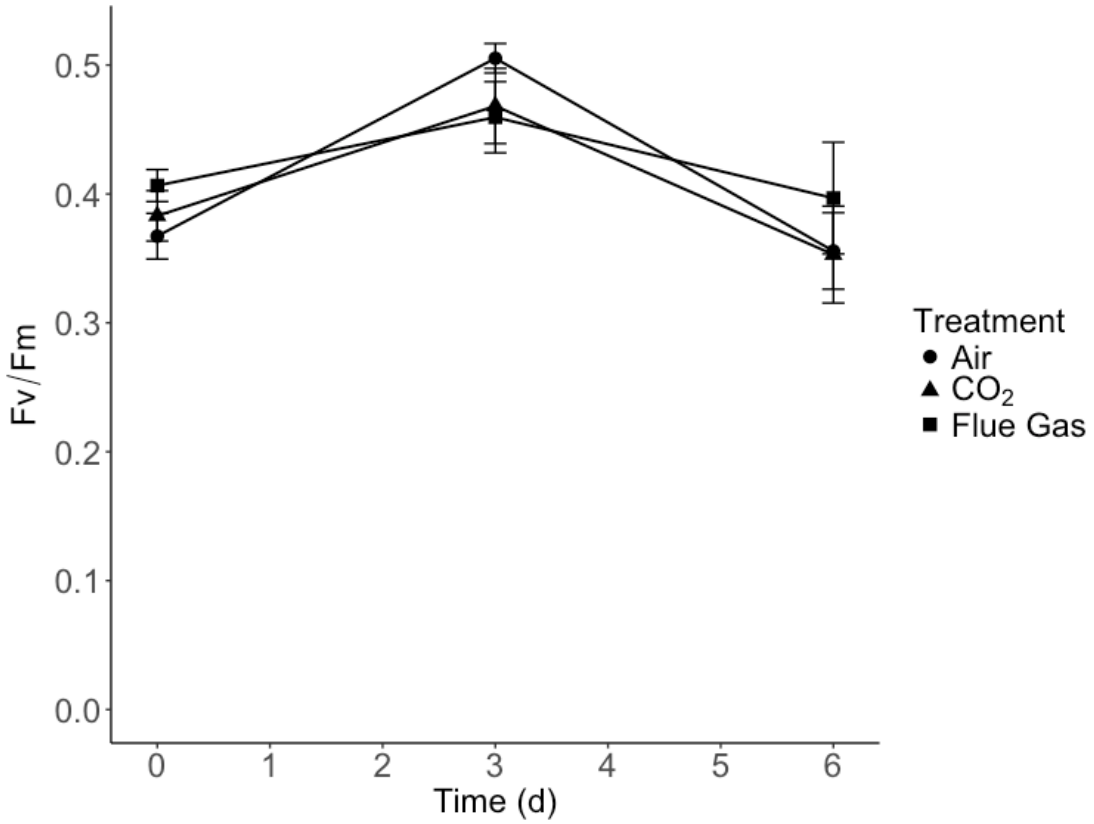

Figure 3. Maximum quantum yield of PSII (single turnover) of *S. acutus* when grown under air (0.04% CO_2), 9% CO_2, and simulated flue gas (9% CO_2, 55 ppm NO, 25 ppm SO_2). Values are means ± SD.

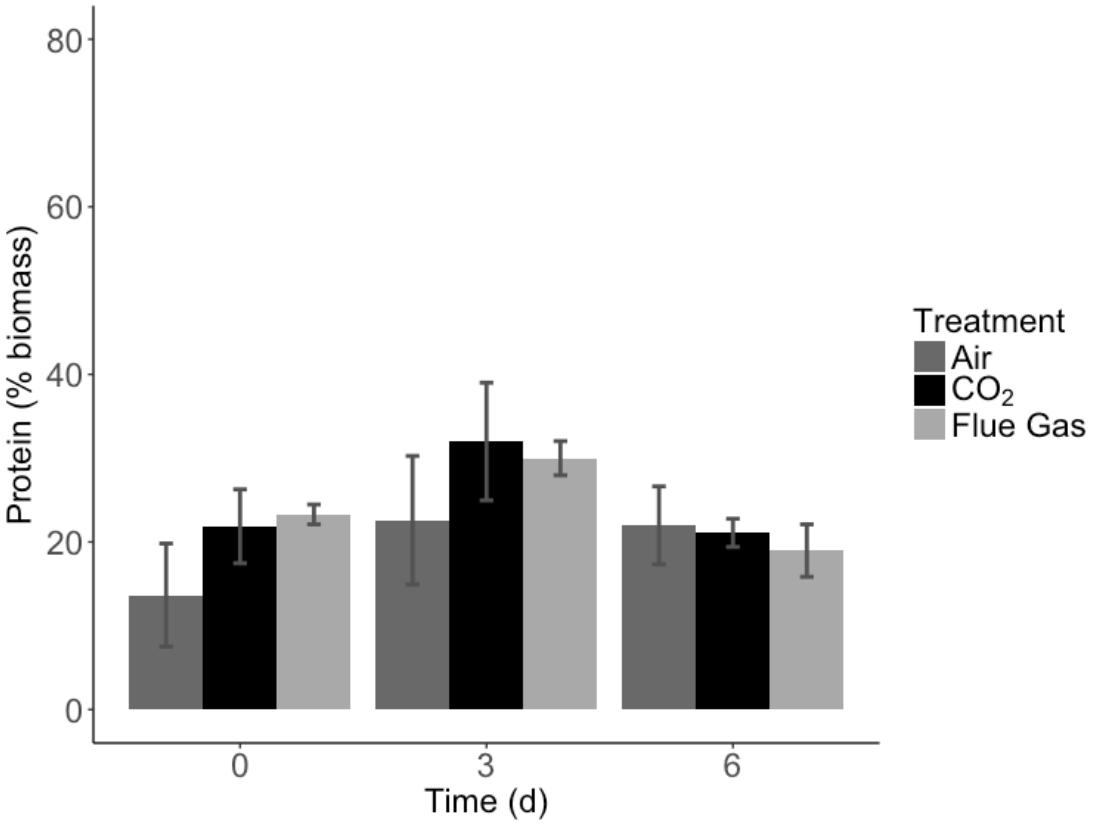

Figure 4. Protein content as a percentage of the total biomass in *S. acutus* grown under air (0.04% CO_2), 9% CO_2, and simulated flue gas (9% CO_2, 55 ppm NO, 25 ppm SO_2). Values are means ± SD.

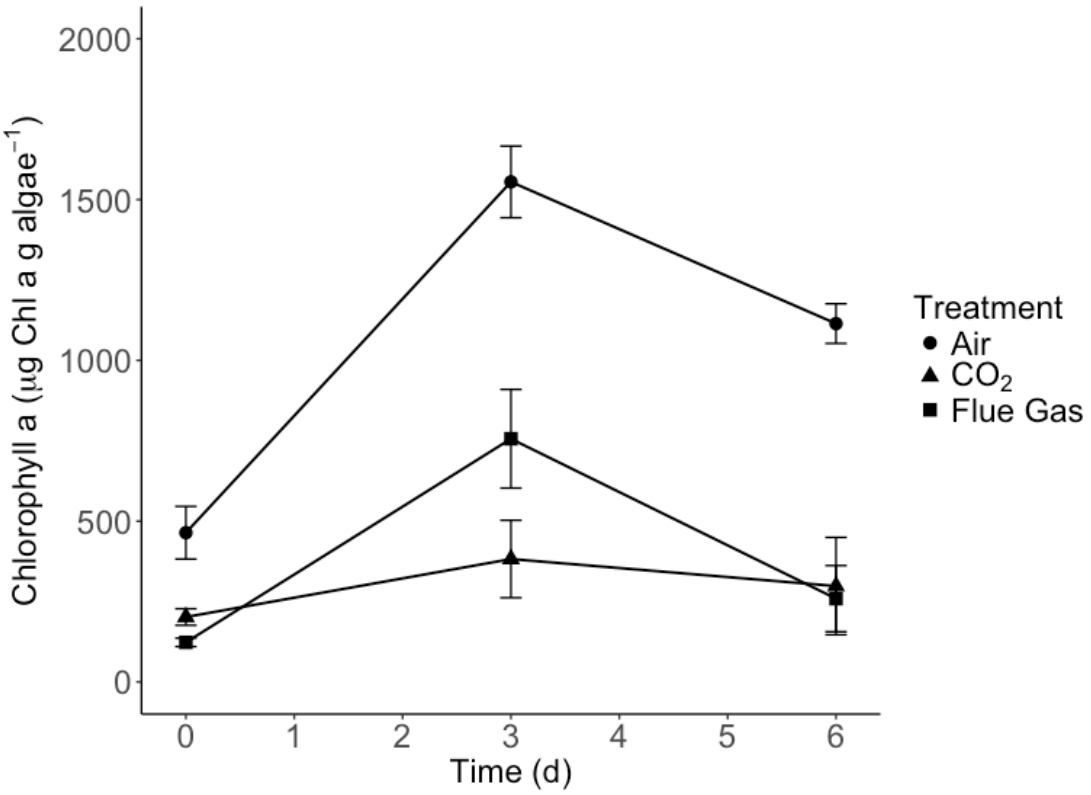

Figure 5. Chlorophyll a content per gram of algal biomass of *S. acutus* when grown under air (0.04% CO_2), 9% CO_2, and simulated flue gas (9% CO_2, 55 ppm NO, 25 ppm SO_2). Values are means ± SD.

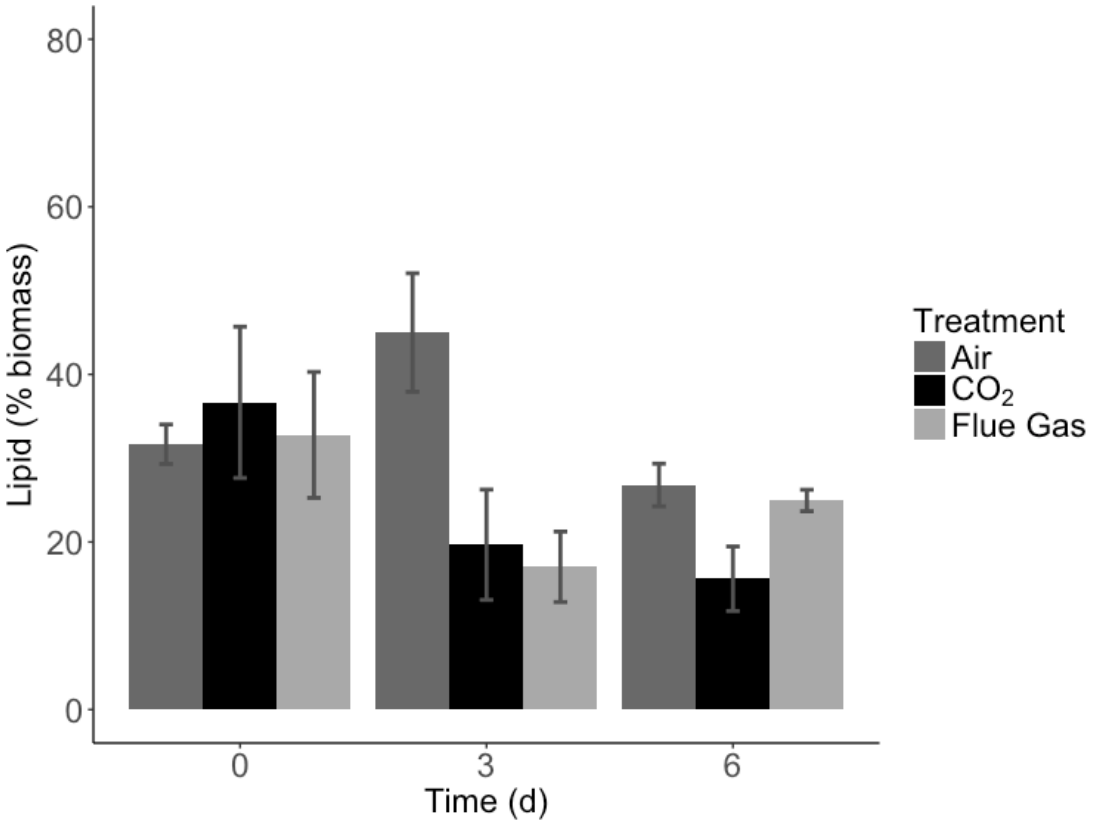

Figure 6. Total lipid content as a percentage of the total biomass in *S. acutus* grown under air (0.04% CO_2), 9% CO_2, and simulated flue gas (9% CO_2, 55 ppm NO, 25 ppm SO_2). Values are means ± SD.

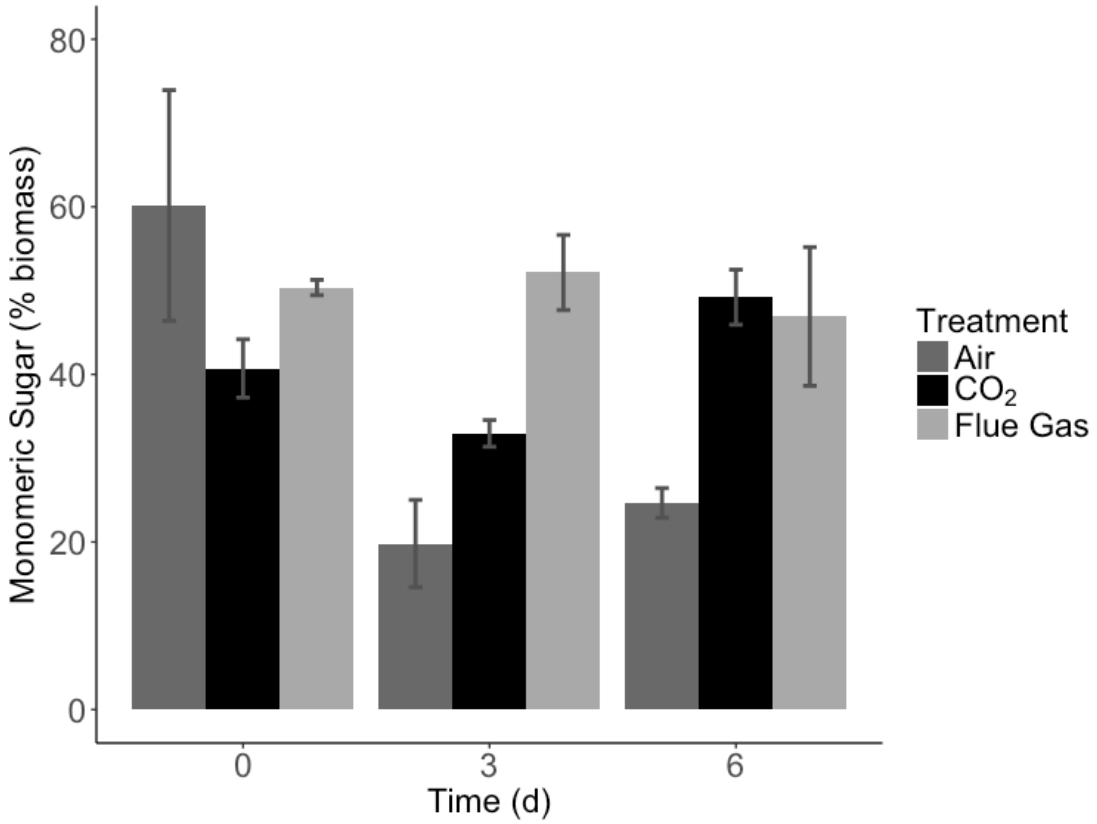

Figure 7. Total carbohydrate content as a percentage of the total biomass in *S. acutus* grown under air (0.04% CO_2), 9% CO_2, and simulated flue gas (9% CO_2, 55 ppm NO, 25 ppm SO_2). Values are means ± SD.

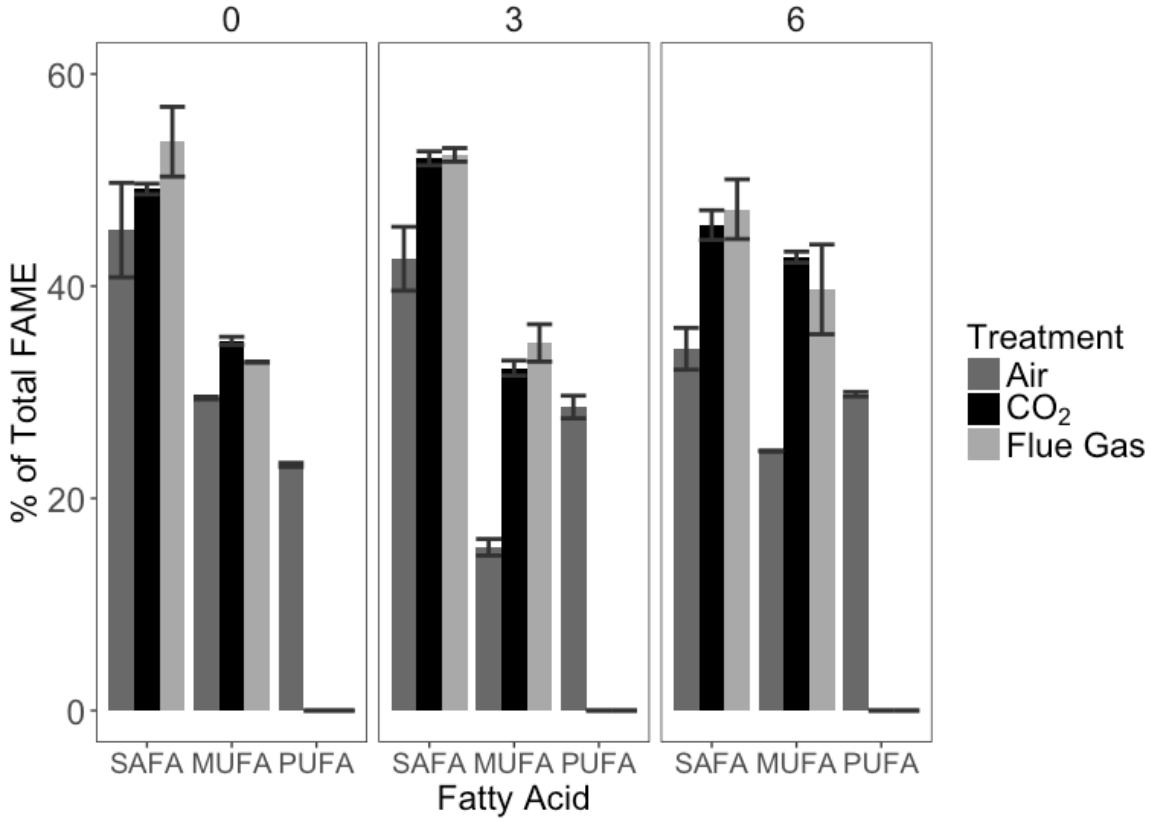

Figure 8. Saturated (SAFA), monounsaturated (MUFA), and polyunsaturated (PUFA) fatty acid content for *S. acutus* grown under air (0.04% CO_2), 9% CO_2, and simulated flue gas (9% CO_2, 55 ppm NO, 25 ppm SO_2). Values are percent means ± SD of the total fatty acid methyl ester (FAME) content. Only fatty acids that contributed to 2% or more of the total FAME composition were included in the calculation of each fatty acid.

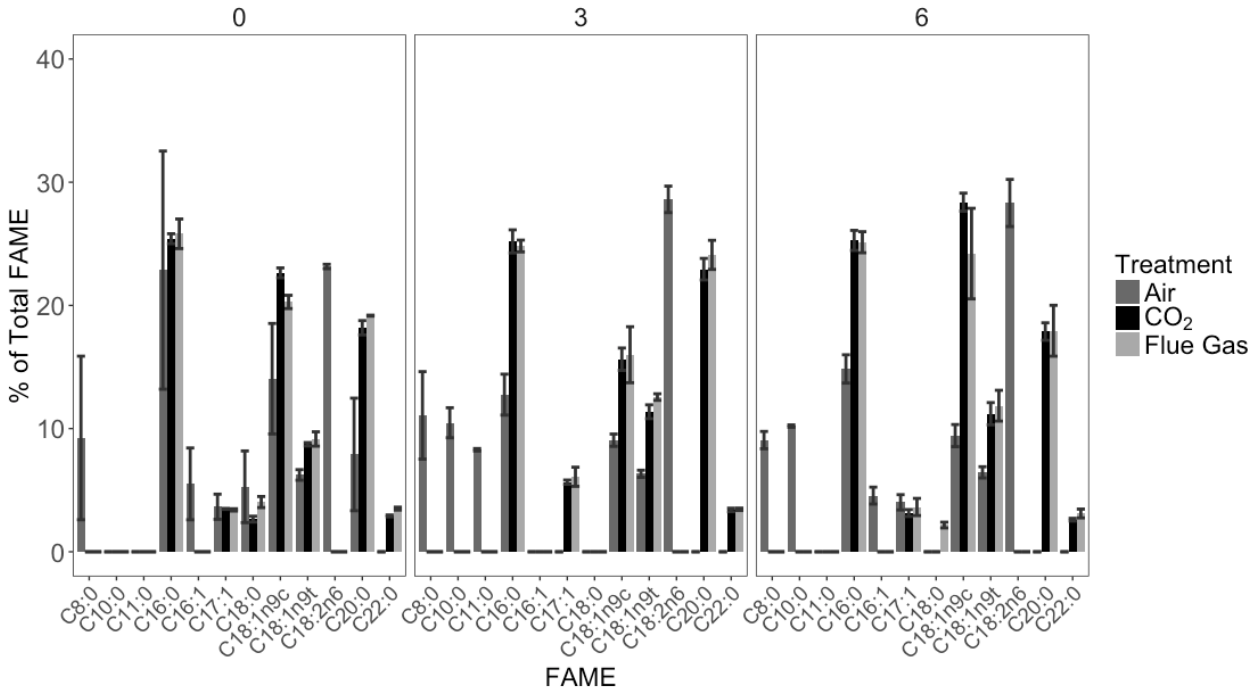

Figure 9. Fatty acid methyl ester (FAME) profiles of *S. acutus* when grown under air (0.04% CO_2), 9% CO_2, and simulated flue gas (9% CO_2, 55 ppm NO, 25 ppm SO_2). Values are means ± SD.

3.1.2. Mitigation of Power Plant Outages

The biomass productivity of cultures exposed to flue gas (0.23 g L^{-1} day^{-1}) for the first four days was not significantly different from that seen in the previous experiment ($p<0.05$). After the flue gas was shut off, cultures supplemented with bicarbonate continued to grow, although at a significantly reduced rate compared to those maintained on uninterrupted flue gas ($p<0.05$; Table 6, Figure 10). Conversely, the biomass of those maintained on air declined (Figure 10), indicating that maintaining cultures on air alone is not feasible. The pH increased in all treatments after the flue gas was shut off, and, as expected, it was highest in the two $NaHCO_3$ treatments at the end of the experiment (Figure 11).

Despite significant differences in growth, the biomass composition remained similar for air-grown cultures compared to those receiving bicarbonate supplementation. However, significant differences were observed in biomass composition for all treatments compared to those maintained on flue gas without interruption. On day 7, all treatments contained ~25% of total biomass as protein, which was significantly greater than that in cultures maintained on flue gas without interruption (Figure 12, $p<0.01$). In contrast, total lipids were ~5% less ($p<0.05$) and carbohydrate content was ~50% less ($p<0.05$) in all treatments compared to cultures when flue gas supply was not interrupted (Figure 13 and Figure 14). Furthermore, there was a significant increase in respiration rate (normalized to total carbon content), as reflected in the significant decline in P:R for all treatments after the flue gas was shut off ($p <0.05$, Figure 15). The lowest P:R ratio was observed for the two $NaHCO_3$ treatments.

This overall loss in carbon, decreased P:R, and decreased productivity suggests that cells become C-limited as soon as the flue gas supply is interrupted, and that a significant loss in biomass and shift in biochemical characteristics should be expected even if bicarbonate is supplied as an alternative C-source. Optimizing the concentration of supplemented bicarbonate at scale may narrow the productivity gap, however, it is unlikely that a bicarbonate supplementation regimen could achieve the levels observed for cultures grown on uninterrupted flue gas, as increasing bicarbonate concentrations are known to be inhibitory to cell growth and can result in stress-induced TAG accumulation (Gardner, Cooksey et al. 2012, Gardner, Lohman et al. 2013, Lohman, Gardner et al. 2015).

Saturated fatty acid content in all treatments was significantly greater than uninterrupted flue gas cultures on day 7 ($p<0.05$, Figure 16). Conversely, monounsaturated fatty acid content in all treatments was significantly less than in flue gas maintained cultures on day 7 ($p<0.05$). A few fatty acids were common across all samples before and after the flue gas disruption, including C16:0, C18:0, C18:1n9c/t, and C20:0 (Figure 17). C22:6n3 was the only polyunsaturated fatty acid that contributed to 2% or more of the total FAME content and it was only seen on day 4 prior to flue gas disruption. Average calculated cetane numbers for air, flue gas, solid $NaHCO_3$, and $NaHCO_3$ solution on day 7 were 67, 65, 66, and 65, respectively.

Table 6. Productivity and specific growth rates of *S. acutus* cultures maintained on flue gas compared to those amended with bicarbonate or air from days 4 to 7. Letters denote significant differences between treatments ($p<0.05$).

	Flue Gas	Air	Solid $NaHCO_3$	$NaHCO_3$ Solution
Productivity (g L^{-1} day^{-1})	0.260 ± 0.084^{A}	-0.028 ± 0.012^{B}	0.079 ± 0.02^{C}	0.048 ± 0.016^{D}
Specific growth rate (μ)	0.270 ± 0.027^{A}	-0.033 ± 0.042^{B}	0.061 ± 0.017^{C}	0.039 ± 0.013^{D}

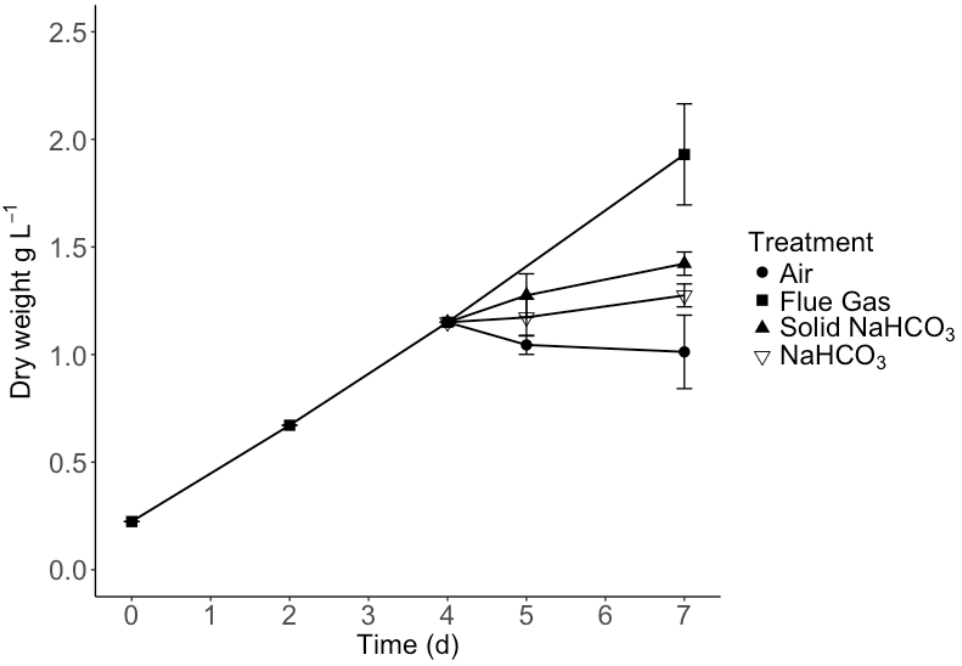

Figure 10. Growth of *S. acutus* cultures before and after flue gas was shut off and cultures were supplemented with bicarbonate or air. Values are means ± SD. Arrow indicates when flue gas was shut off.

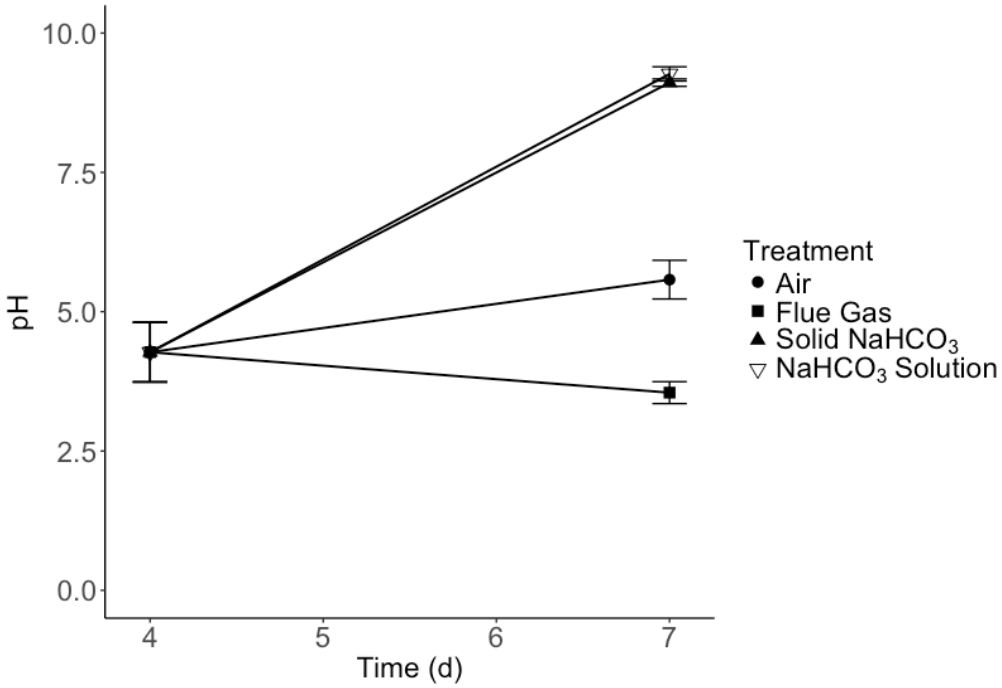

Figure 11. pH in *S. acutus* cultures before and after flue gas was shut off and cultures were supplemented with bicarbonate or air. Values are means ± SD.

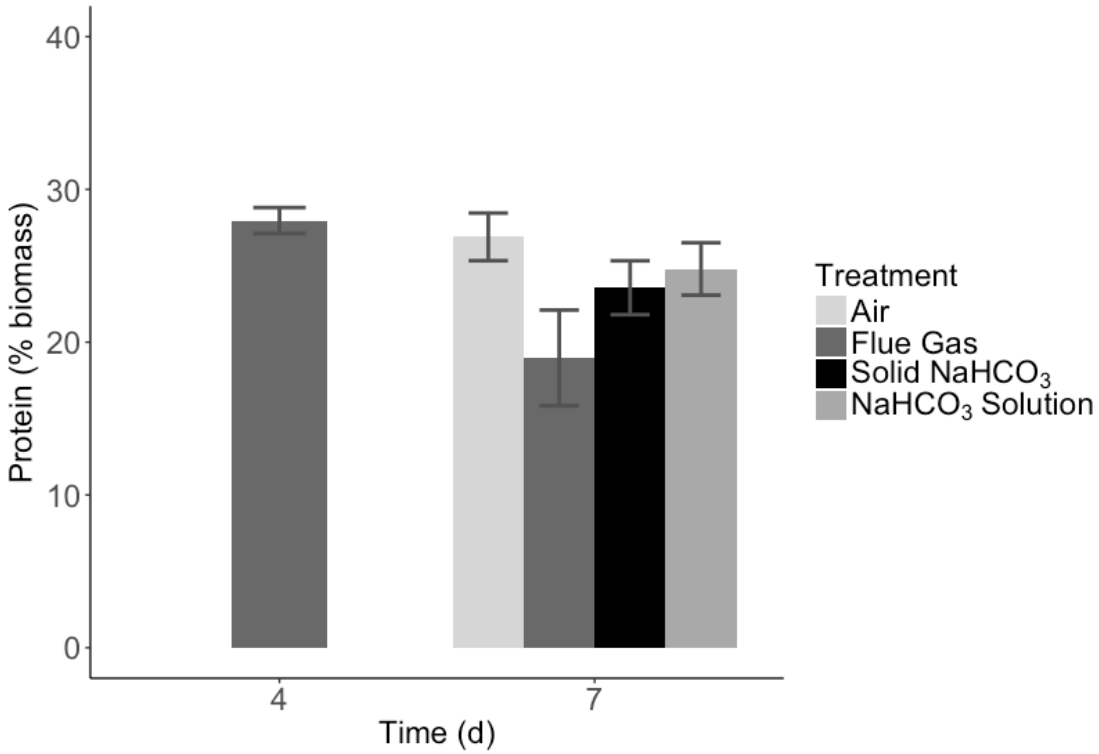

Figure 12. Protein content (% of biomass) in *S. acutus* before (day 4) and after (day 7) flue gas was shut off and cultures were supplemented with bicarbonate or air. Values are means ± SD.

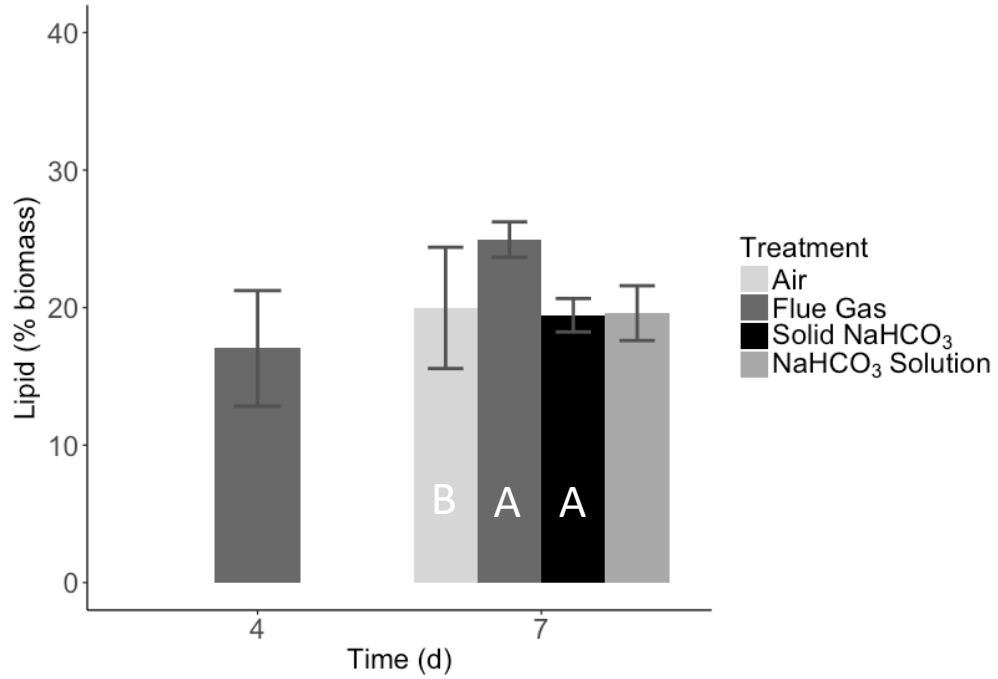

Figure 13. Lipid content (% of biomass) in *S. acutus* before and after flue gas was shut off and cultures were supplemented with bicarbonate or air. Values are means ± SD.

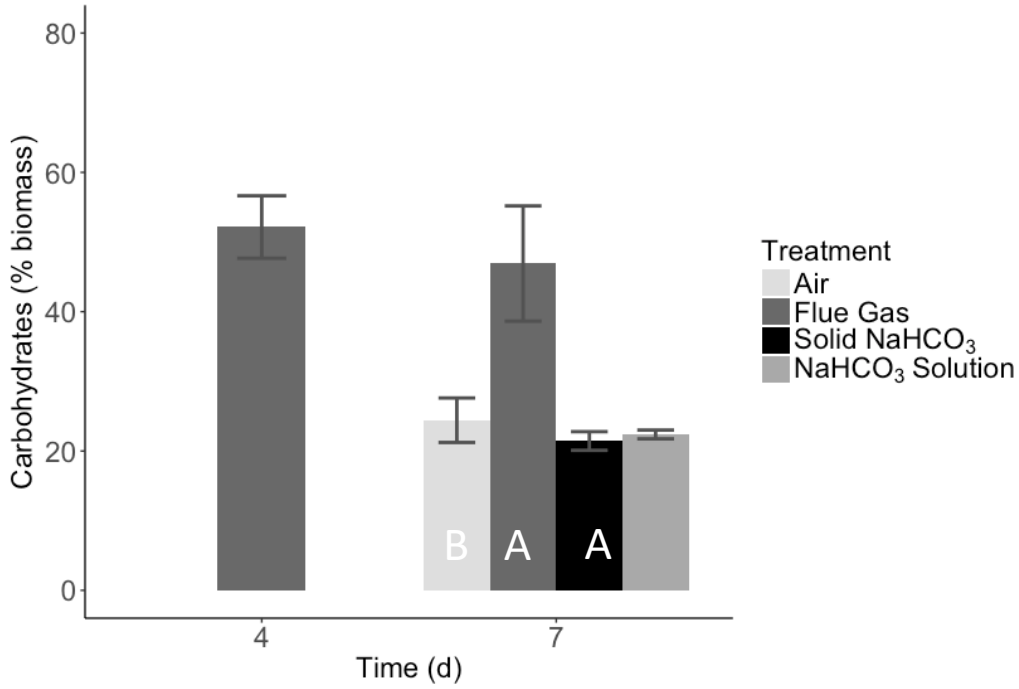

Figure 14. Carbohydrate content (% of biomass) in *S. acutus* before and after flue gas was shut off and cultures were supplemented with bicarbonate or air. Values are mean ± SD.

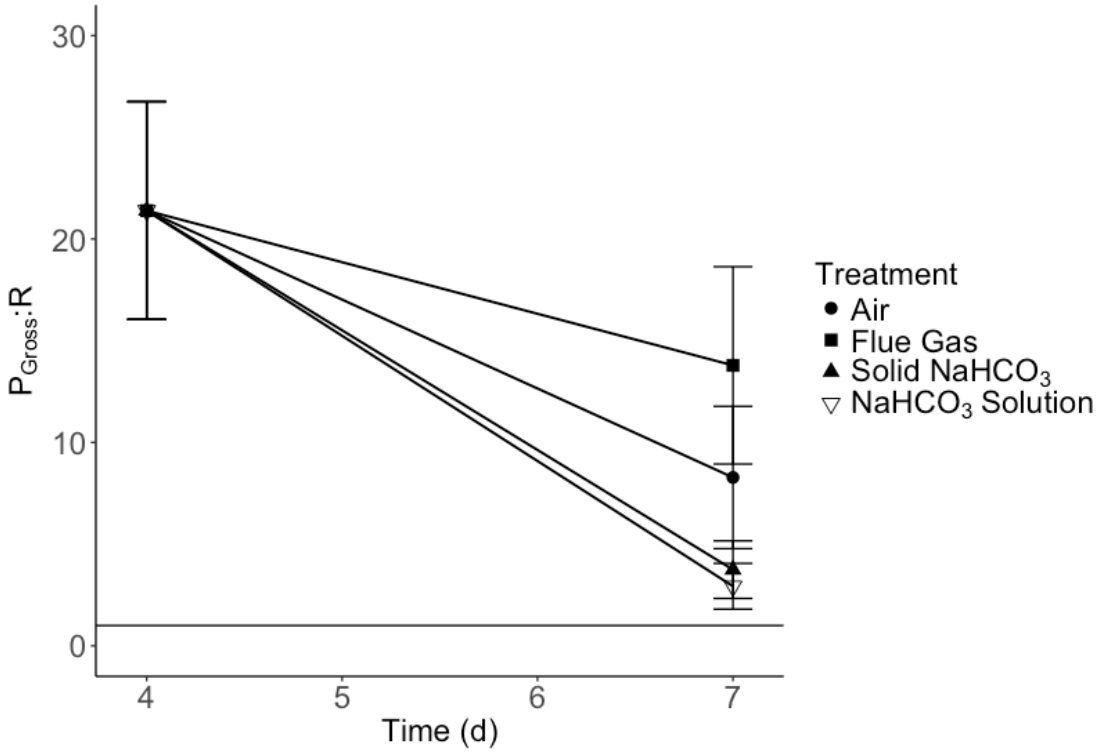

Figure 15. Gross photosynthesis to respiration ratios (P:R) for *S. acutus* before and after flue gas was shut off and cultures were supplemented with bicarbonate or air. Black solid line represents the 1:1 line. Values are means ± SD.

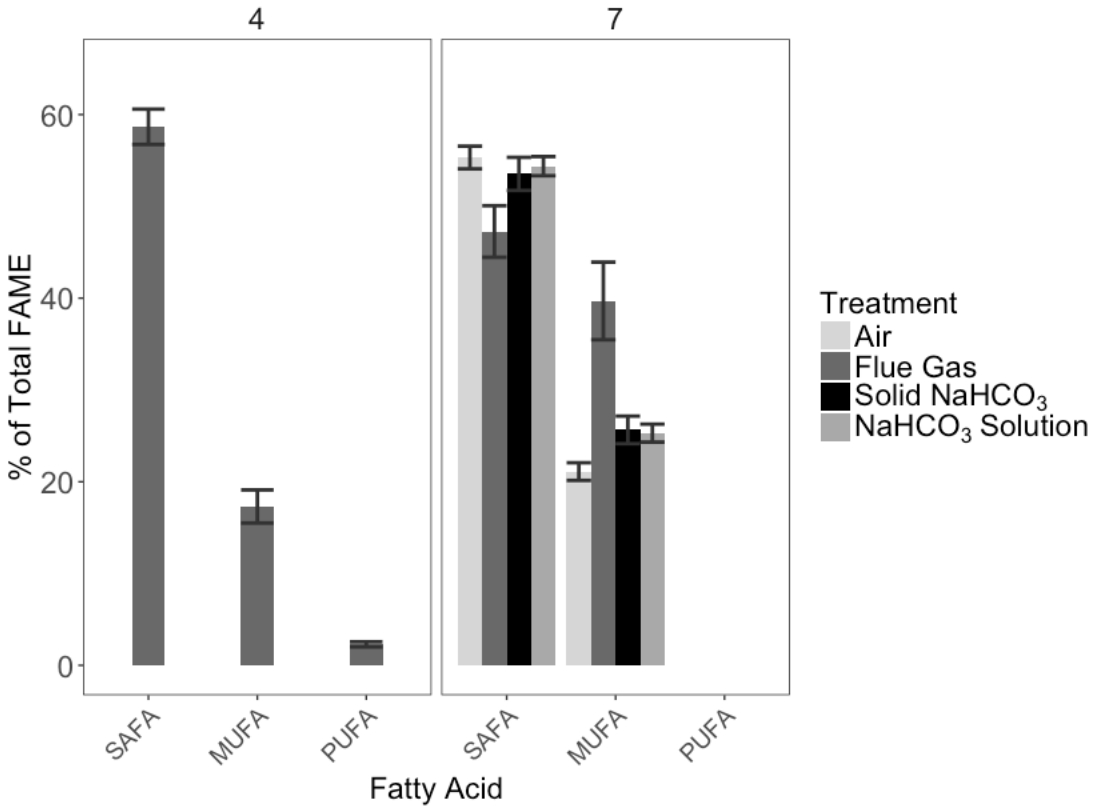

Figure 16. Saturated (SAFA), monounsaturated (MUFA), and polyunsaturated (PUFA) fatty acid content for *S. acutus* before and after flue gas was shut off and cultures were supplemented with bicarbonate or air. Values are percent means ± SD of the total fatty acid methyl ester (FAME) content. Only fatty acids that contributed to 2% or more of the total FAME composition were included in the calculation of each fatty acid

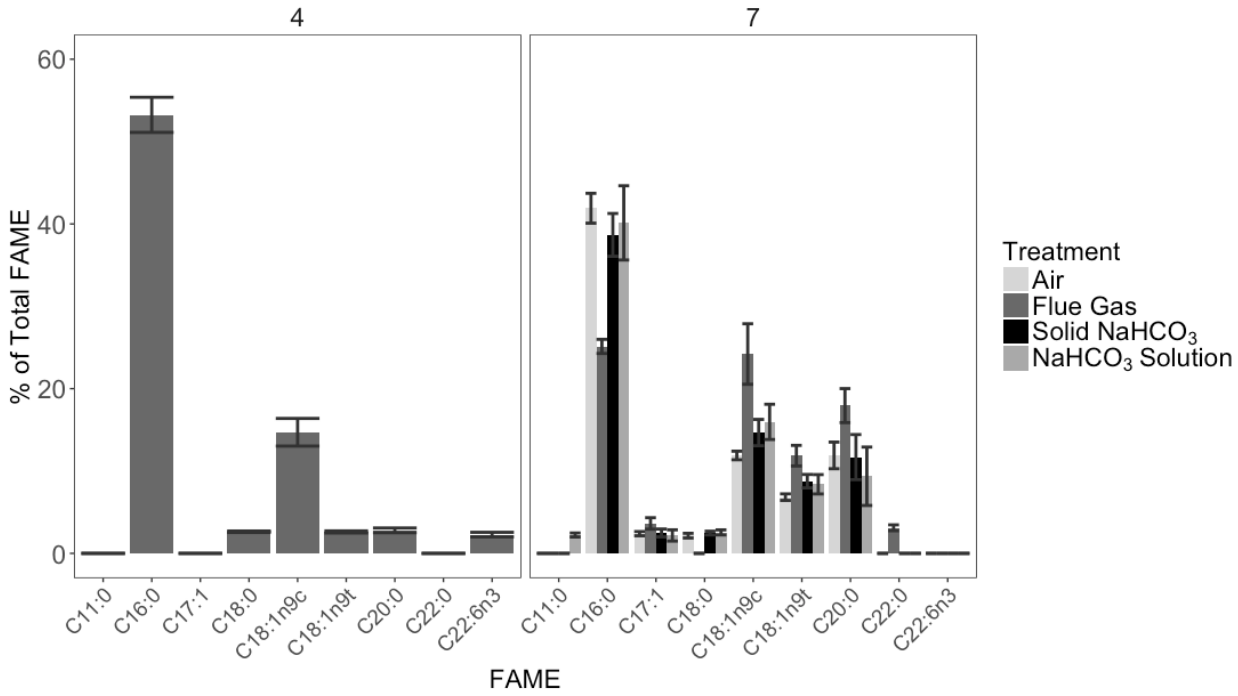

Figure 17. Fatty acid methyl ester (FAME) profiles of *S. acutus* before and after flue gas was shut off and cultures were supplemented with bicarbonate or air. Values are mean ± SD.

3.1.3. Analysis of PBR Algae Culture Grown at East Bend Station (Summer 2016)

Samples were taken for DNA sequencing of *S. acutus* cultures grown on flue gas in an outdoor PBR from June to October 2016. Adequate biomass densities of 0.80-1.0 g L^{-1} were reached throughout the season (Figure 18). However, it is evident from the composition of eukaryotes that the culture was not predominantly *Scenedesmus* for a good portion of the season (Figure 19). It is apparent that there were also shifts in the bacterial and fungal communities over time (Figure 20 and 21, respectively).

There were four instances where the PBR had to be re-inoculated with new seed cultures of *S. acutus*: July 6, July 18, August 17, and September 15. The first instance was due to a power outage at the plant, during which time the culture was switched to bottled CO_2 until harvest on June 27. Upon harvest, the composition of eukaryote community was still about 80% *Scenedesmus* (Figure 19). However, there was low gas flow in the PBR and the culture began to turn yellow, indicating that it was dying. The system was subsequently drained and re-inoculated with culture at a biomass density of 0.10 g L^{-1} on July 6. The first harvest of viable biomass took place on July 11, with a biomass density of 1.15 g L^{-1} and about 80% of the composition was identified as *Scenedesmus*, although three days later it was clear that the culture had died (Figure 19). No samples were taken at this time to know if the eukaryotic community had changed significantly at the time of the culture crash, but some of the equipment was destroyed, possibly due to a weather event, which could have also caused the culture to die.

The PBR was bleached and rinsed prior to re-inoculating on July 18. However, it was reported that there was residual biofilm on the inside of the tubes. The eukaryotic community remained

greater than 95% *Scenedesmus* for one week after inoculation, but the pre-harvest sample taken on July 25 indicated that the culture had been compromised by a *Chlorococcum* species, another green chlorophyte (Figure 19). The culture did appear to be dying at this time, so fresh culture from the greenhouse was added to the reactor post-harvest in hopes that it would recover. From visual inspection on July 27, the culture seemed to recover as it had maintained its signature green color it is evident that *Chlorococcum* sp. actually made up a majority of the composition (Figure 19). From July 29 until the culture death on August 11, *Scenedesmus* only made up 10-35% of the eukaryotic composition, with the exception of the post-harvest sample on August 4, where it made up 60%. Notable contaminating eukaryotes that were identified during this time were organisms of the Ichthyophonida family, and *Pseudorhizidium* sp. The presence of contaminating organisms was not evident from visual inspection, but signs of declining culture health were reported on August 9, two days prior to the culture death. After the PBR was bleached, residual biofilm still appeared to be growing in it and 85% of the eukaryotic composition of this biofilm was made up of *Pseudorhizidium* sp., the bacteria were largely from the Alpha- and Betaproteobacteria classes, and 86% of the fungi composition was of the Agaricomycetes class (Figures 20-21).

The third re-inoculation of the PBR took place on August 17. The initial culture density was about 0.2 g L^{-1}. *Scenedesmus* made up the majority of the composition for a week following inoculation, but it was reported that the culture turned a yellow-green color on harvest days August 25 and August 29. At this time, the population of *Scenedesmus* declined to about 40% of the composition. By September 2, the green color returned, although large flocs of cells were observed in the culture which was a visual indication that there was contamination and the results from sequencing agreed. Thus, the PBR was drained, rinsed, and bleached.

Scenedesmus also made up the majority of the composition for a week after the last inoculation of the season on September 15. The pre-harvest sample on September 23 indicated that about half of the eukaryotic community was *Scenedesmus*, but upon harvest the *Scenedesmus* population rebounded and made up 80% of the composition. However, a severe decline followed shortly thereafter and lasted until the final harvest on October 18. During that time, *Scenedesmus* only made up 10% or less of the eukaryotic community, and this was not recognized by visual observations.

The bacterial populations largely varied over time and between seed cultures. Alpha-, Beta- and Gammaproteobacteria made up a vast majority of the composition throughout the entire season, but no obvious trends in populations were detected (Figure 20). The fungi composition was largely dominated by the Agaricomycetes class, especially from mid-July to mid-September (Figure 21). While ITS primers are often utilized to distinguish between fungal species, other protozoa and metazoans were identified by this method, including Cryptomycotes and Enopleans.

Lastly, DNA was extracted from a stock culture of *S. acutus* to use as a representative sample to compare against the compositions of the 5 seed cultures (Figures 22-24). While over 95% of the composition of the stock and most seed cultures was *Scenedesmus*, it is apparent that they were not axenic. Furthermore, the compositions of bacteria and fungi varied between these cultures.

One of the primary advantages of using a closed PBR system for large scale cultivation of microalgae is that it prevents the large contamination events that are often seen in open pond systems (Hannon et al., 2011). However, this survey not only provides evidence that these large

events occur in closed PBRs, but also that they can go unnoticed for a considerable amount of time and ultimately cause culture death. Over the 2016 season, the target alga, *Scenedesmus acutus*, would remain the dominant organism for about a week after inoculation, then the culture either died soon after or it was compromised by other organisms. Among these invading organisms were other species of green algae that were most likely directly competing with *S. acutus* for light and nutrients. *Chlorococcum* sp. and *Choricystis* sp. are notable organisms that invaded at the end of July and end of September, respectively.

Invasion by other microalgae could be detrimental to the health of the target alga, but if the overall carbon capture efficiency does not significantly decline, and the biochemical composition are not markedly different, the harvested biomass may still be viable for downstream processing. *Chlorococcum* sp. has been described as a high CO_2 tolerant alga, that can grow in a pH range of 6.5-9 (Ota et al., 2009, Harwati et al. 2012). The total fatty acid content for *Chlorococcum* grown under 6% CO_2 reached about 15% of the total biomass composition, which is comparable to that reported for *S. acutus* under 9% CO_2 (Ota et al., 2009, see section 3.3.2). Furthermore, Chen et al. (2017) found that *Choricystis* sp., isolated from wastewater, grew well in an outdoor PBR and had a total lipid content of 25-30% of the total biomass. The biodiesel properties calculated for this alga also met the standard requirements of the US and Europe (Chen et al., 2017). While the lipid content of these organisms could make it a good feedstock for biodiesel, more tests would be necessary to determine how their presence influences the overall biochemical composition of the biomass. The presence of these two organisms in this system indicates that they are robust to the flue gas and the fluctuations in other environmental parameters, which could make them ideal candidates for polyculture studies.

Other notable eukaryotes included organisms of the Ichthyophonida family that were present at the end of July and in October, as well as *Pseudorhizidium* species that proliferated after the Ichthyophonida in August. Ichthyophonida is a group of protozoa, some of which are known fish parasites, and others are saprotrophic microbes (Mendoza et al., 2002). *Pseudorhizidium* sp. are chytrid fungi, which are a group known to parasitize microalgae in freshwater environments (Carney and Lane, 2014). Chytrid fungi have caused production losses of microalgae in commercial settings, including loss of *Scenedesmus* in open pond systems (Ilkov 1975). Other fungi, in particular those of the classes agaricomycetes and cryptomycota, were also identified by sequencing the ITS region of the rRNA operon. Of the cryptomycota, aphelids were a prominent taxon and are known to be intracellular parasites of microalgae (Karpov et al., 2013). A species of aphelid was identified in commercial ponds growing *Scenedesmus dimorphus* (Letcher et al., 2013). Many fungi and fungi-like organisms are known to produce spores that may be able to withstand sterilization of the PBR using bleach, allowing them to infect subsequent cultures (Carney and Lane 2014). The biofilm sample taken from the inside of the PBR after it was bleached corroborates this idea. Of the organisms identified by sequencing of the 18S rRNA gene in this sample, 85% was identified as a *Pseudorhizidium* species, and 86% of the organisms identified by ITS sequencing were agaricomycetes. Quantitative PCR would be necessary to determine how these organisms contribute to the overall composition of this sample, but it is clear that fungi are dominant in the residual biofilm.

Alpha-, Beta-, and Bammaproteobacteria, as well as Flavobacteria, made up a large portion of the bacterial composition in the stock and seed cultures that were all healthy upon inoculating the PBR. Although, the large variability seen in the bacterial composition, and the broad level of identification make it difficult to hypothesize how these bacteria influence the growth of *S.*

acutus. It is known that certain bacteria can promote microalgal growth by releasing vitamins or growth factors (Schwenk et al., 2014). Gonzalez and Bashan (2000) saw a significant increase in growth of the commercially important chlorophyte, *Chlorella vulgaris*, when grown with the bacterium *Azospirillum brasilense*, possibly from the production of phytohormones like indole-3-acetic acid by the bacterium. Schwenk et al. (2014) found several strains of bacteria in laboratory cultures of *Scenedesmus obliquus* from the *Rhodobacteraceae* and *Rhizobiaceae* families (both Alphaproteobacteria). These bacteria had coexisted with the algae for several years of culturing in an artificial medium, indicating that there could be a symbiosis between the algae and bacteria (Schwenk et al., 2014). Algae-bacteria interactions are complex, can be species-specific, and have yet to be widely investigated, especially in commercial settings (Schwenk et al., 2014). Future studies should focus on identifying these bacteria at the genus or species level, and if they are cultivable, growth experiments should be performed to see how they influence the overall growth of *S. acutus*.

Lastly, there can be numerous sources of contamination with any outdoor large-scale algae cultivation (Wang et al., 2008). Exposure of the culture to air for any amount of time poses the risk of introducing a contaminating organism. This study provided some insight on two potential sources of contamination in this system. It was apparent that many of the invading organisms seen throughout the season were actually identified in the seed cultures. Although these organisms were only present in small numbers, the variability in the outdoor environment could have been detrimental to the health of *S. acutus*, thereby allowing a contaminant to take over, or provided favorable conditions that directly allowed a contaminant to proliferate. Another source of contamination was the residual biofilm on the tubes of the PBR due to ineffective sterilization after draining the system.

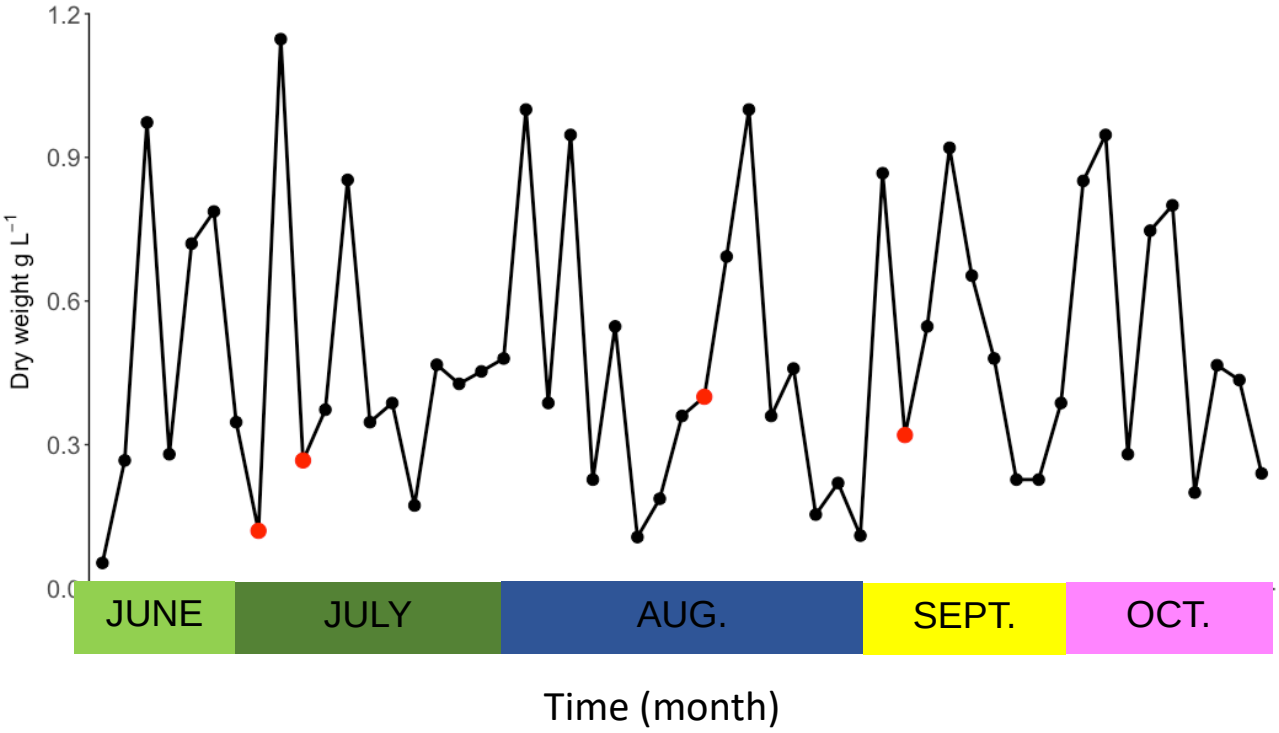

Figure 18. Dry weights for *S. acutus* grown on flue gas emissions in a 1200 L outdoor PBR from June to October 2016. Seed cultures are represented by the red points.

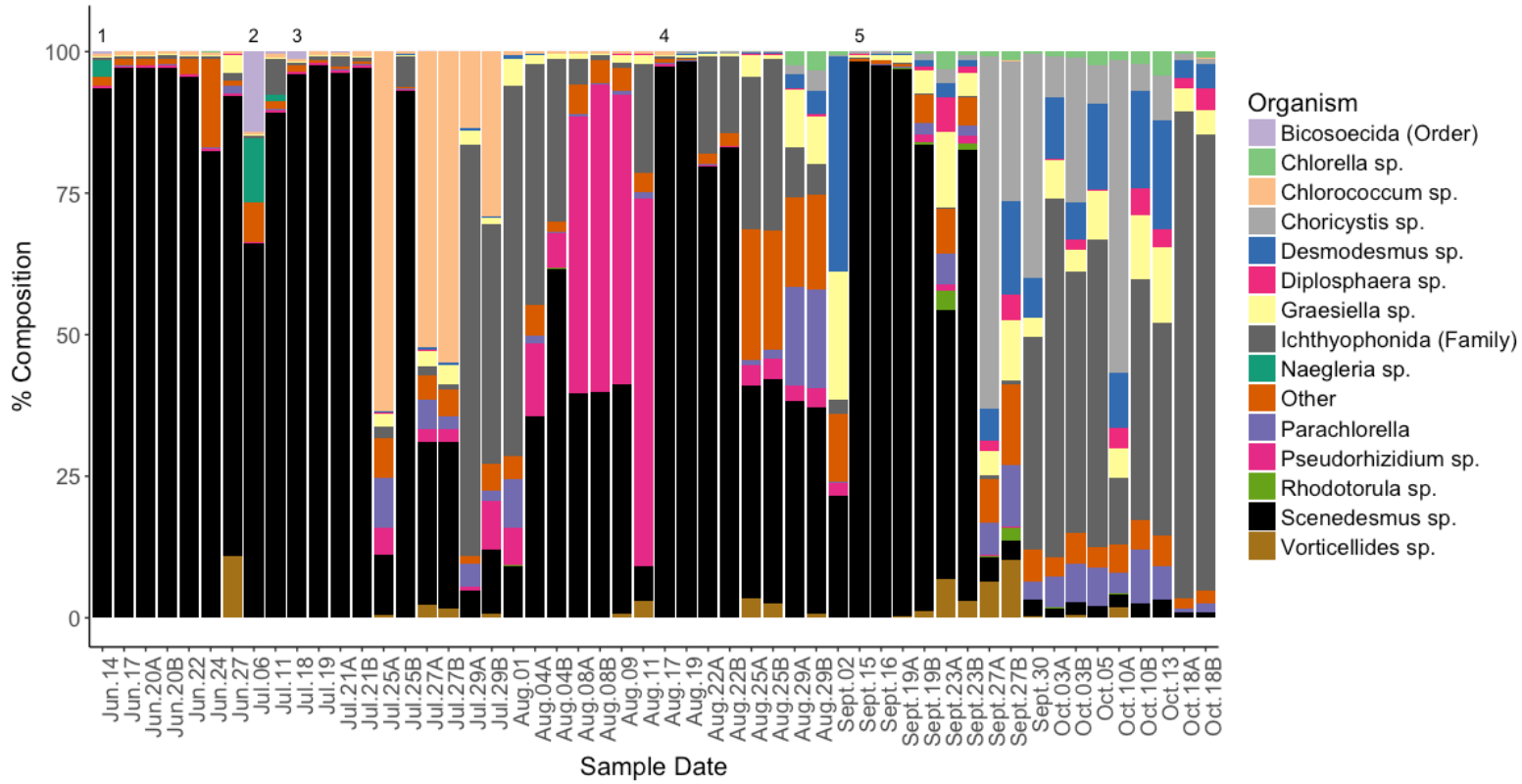

Figure 19. Composition of eukaryotic organisms in the outdoor PBR from June to October 2016, identified by sequencing the 18S rRNA gene.

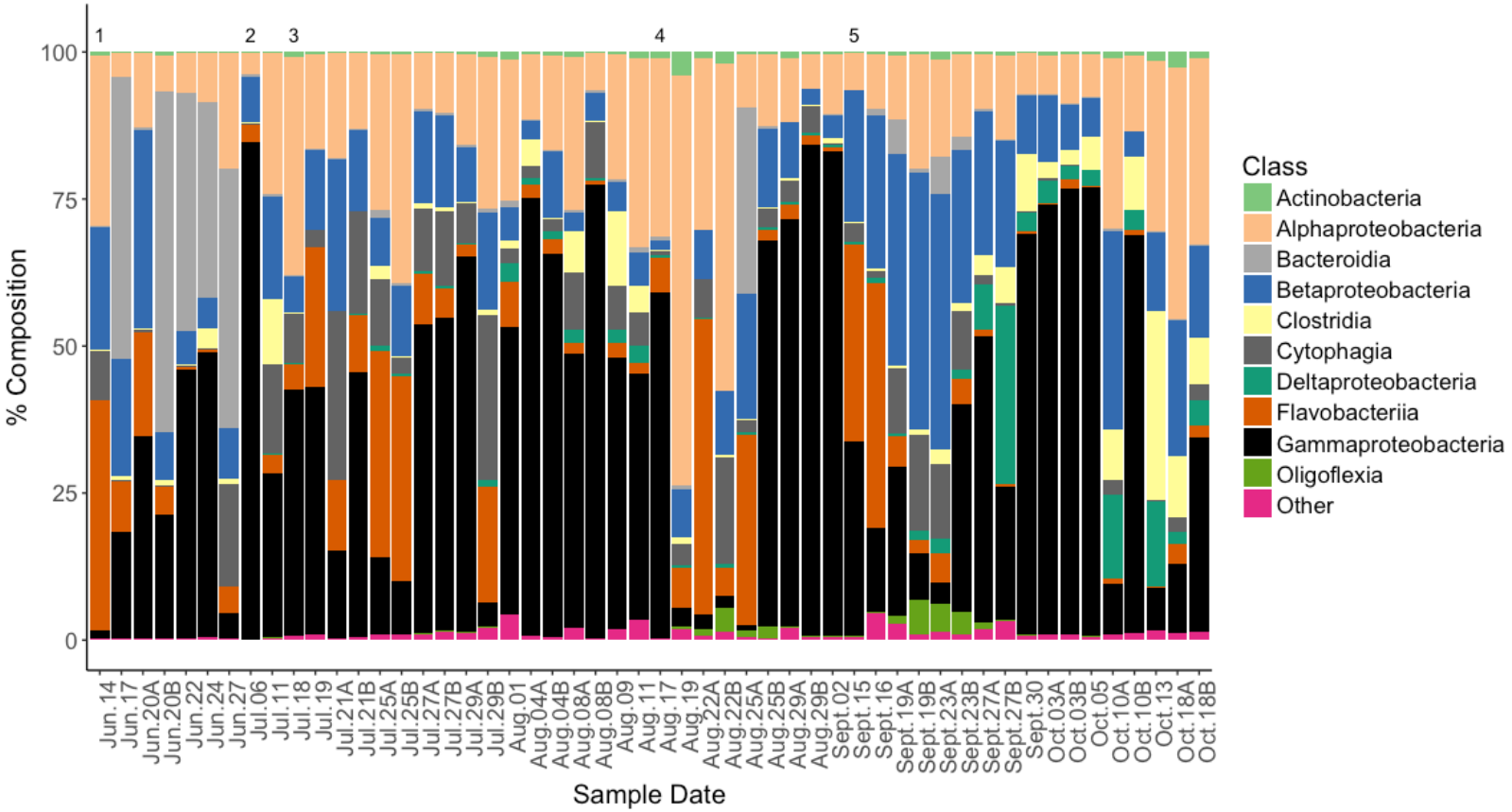

Figure 20. Composition of bacteria in the outdoor PBR from June to October 2016, identified by sequencing the 16S rRNA gene.

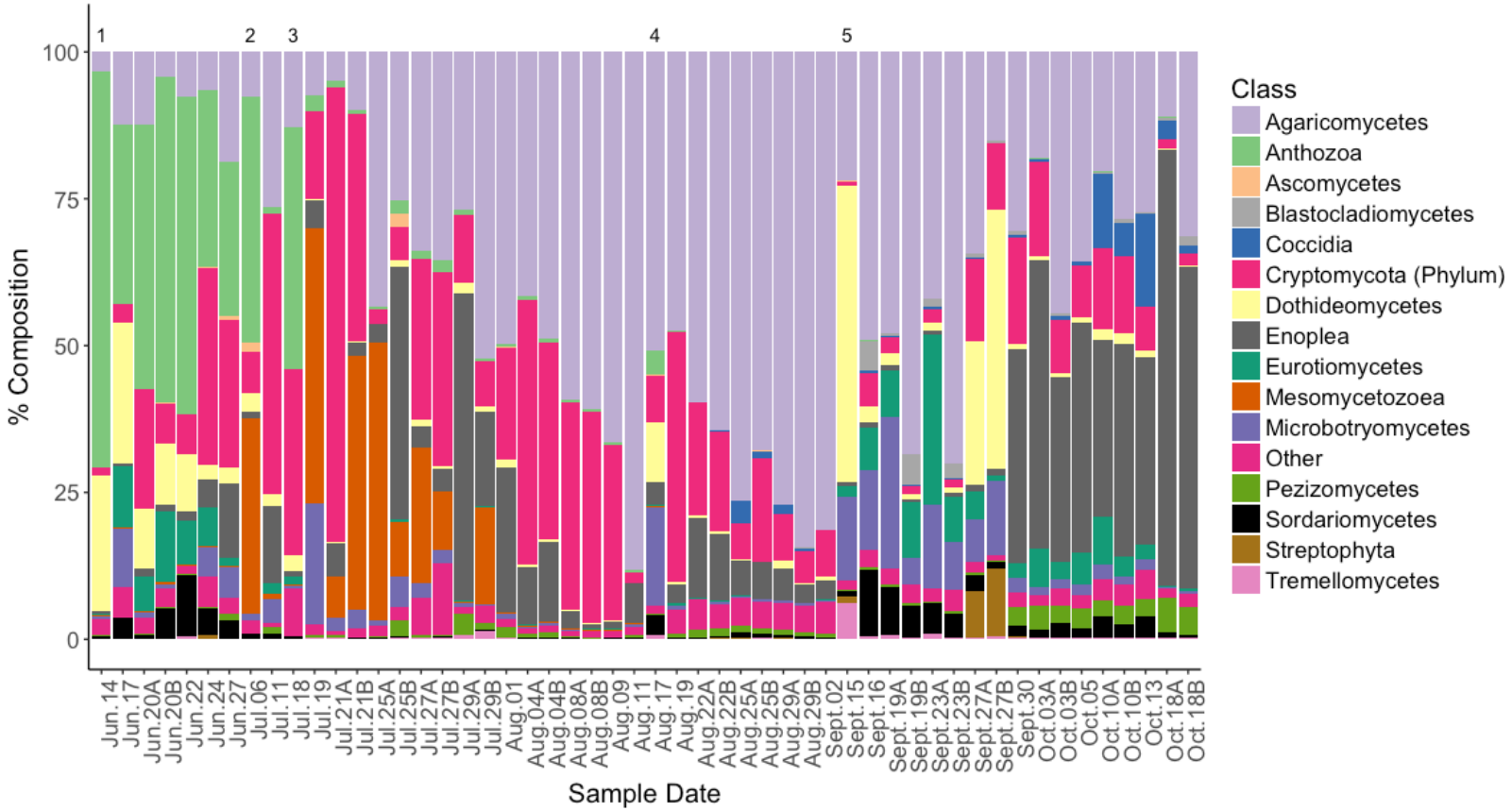

Figure 21. Composition of fungi in the outdoor PBR from June to October 2016, identified by sequencing the ITS region in the rRNA opero

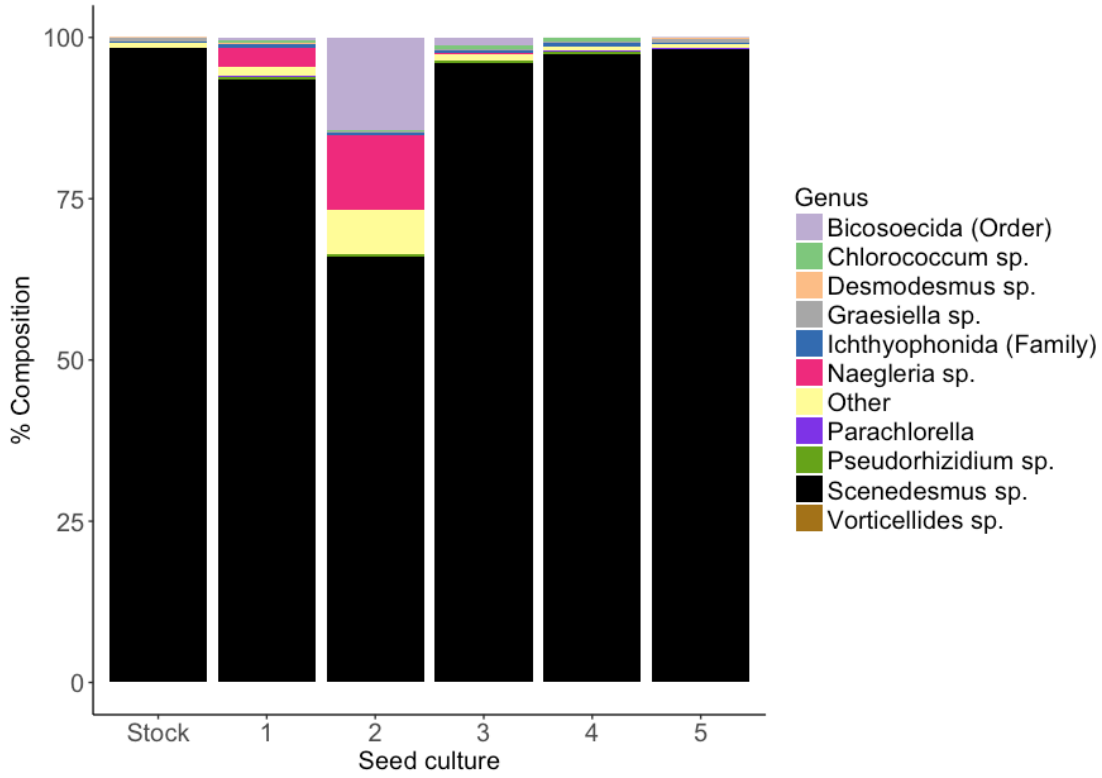

Figure 22. Composition of eukaryotes in a stock culture of *S. acutus* compared to the five seed cultures used to inoculate the PBR

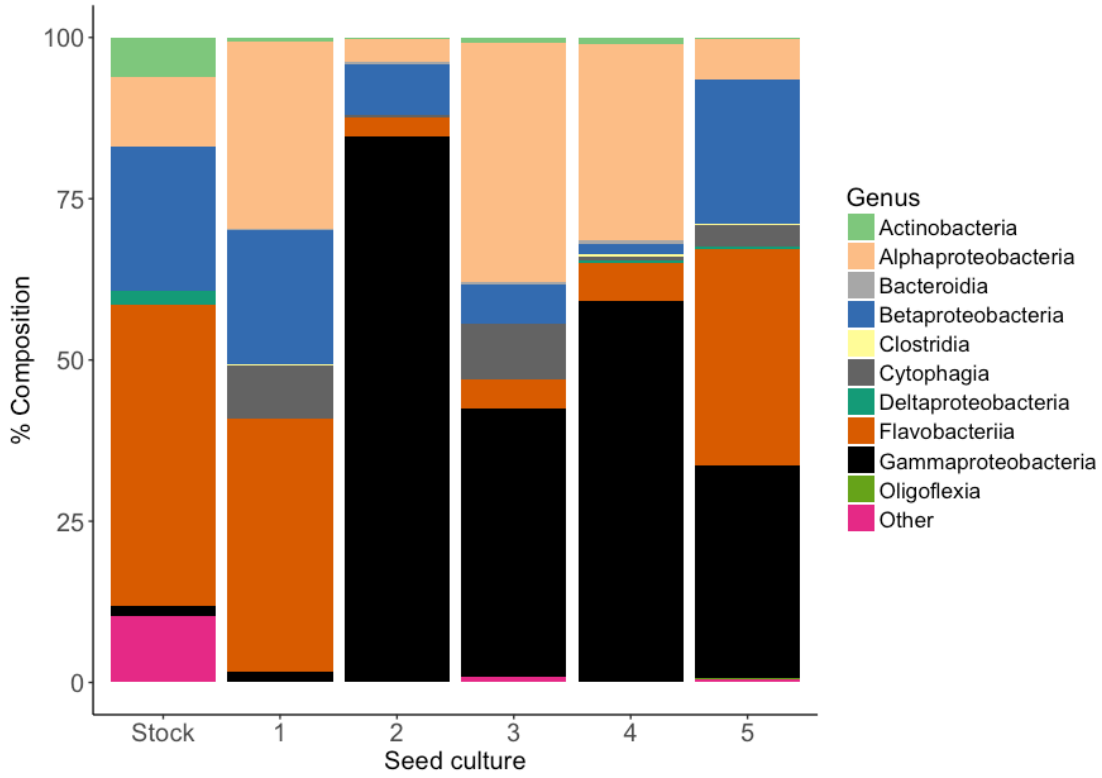

Figure 23. Composition of bacteria in a stock culture of *S. acutus* compared to the five seed cultures used to inoculate the PBR.

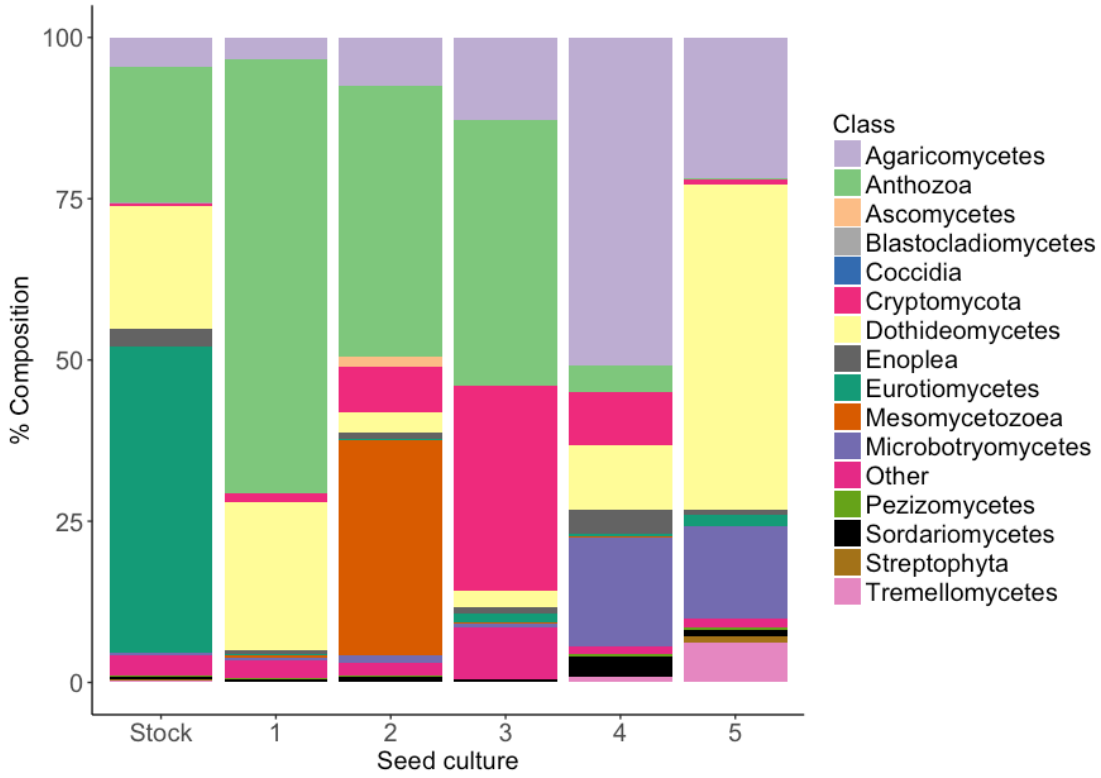

Figure 24. Composition of fungi in a stock culture of *S. acutus* compared to the five seed cultures used to inoculate the PBR.

3.2. Engineering Analysis and Testing

3.2.1. Field Testing at East Bend Station

Efforts were made in April and May 2016 to improve the design of the cyclic flow PBR to be deployed at Duke Energy's East Bend Station for field testing and production of algae biomass. These activities consisted of:

- Testing of various materials for flue gas injection to the system, including different types of tubing as well as microporous PVC pipe, with the goal of obtaining a more even distribution of flue gas throughout the PBR.
- Improvement of the control and data acquisition system to enhance operational stability and flexibility, while incorporating additional analytical inputs.
- Design, procurement, and installation of an enhanced flue gas injection system to maintain constant delivery pressure, measure the flow rate of the injected gas, as well as provide continuous temperature and pressure readings.

The improved East Bend Station photobioreactor was inoculated on June 14, 2016 at a biomass density of 0.06 g/l from seed cultures maintained in the CAER greenhouse. The reactor moved quickly through its 'grow out' phase, overcoming an initial lag period to achieve a culture density >1.0 g/l (see Figures 25 and 26). A regular harvesting schedule was established to maintain and quantify the reactor performance, as well as obtain biomass for characterization and valorization studies.

Figure 25. Cyclic flow reactor at initial culture density of 0.06 g/l

Figure 26. Cyclic flow reactor ready to be harvested (1.1 g/l culture density)

The updated control and data acquisition system was deployed once the reactor was inoculated. Figures summarizing the process data from June 6-11, 2016 are shown below, including temperature (ambient, reactor, and flue gas), dissolved oxygen, photosynthetically active radiation (PAR), pH, and the composition of the gas exhaust from the system (Figures 27-29).

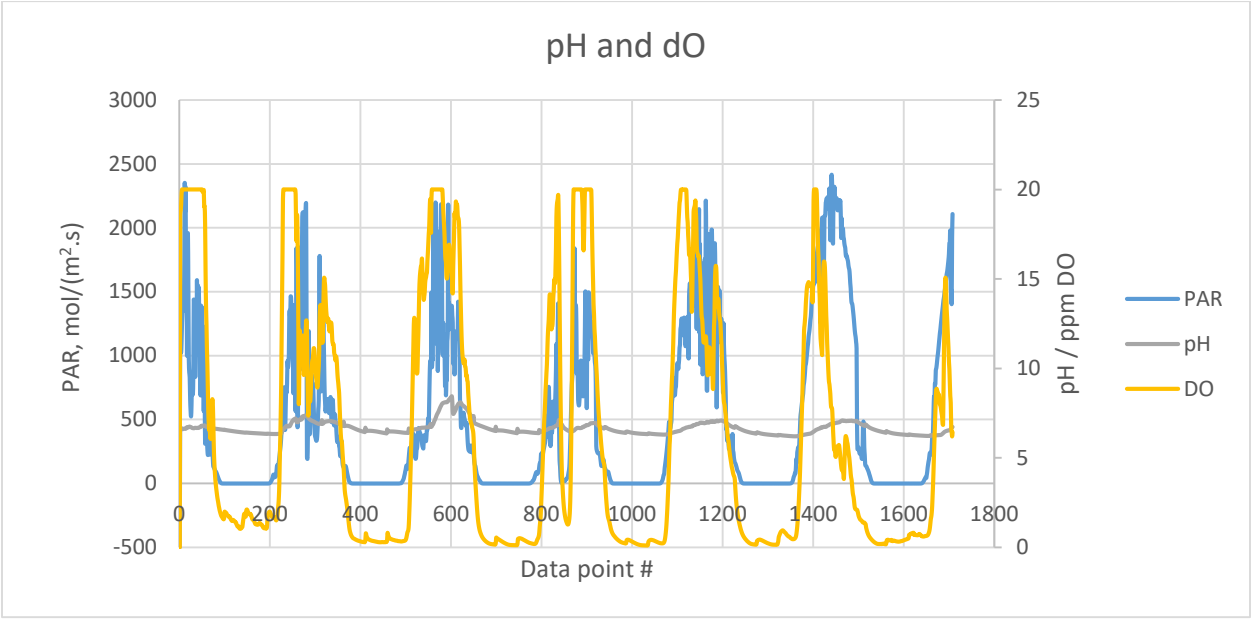

Figure 27. Process pH and dissolved oxygen (DO) versus PAR showing photosynthetic activity in response to available sunlight

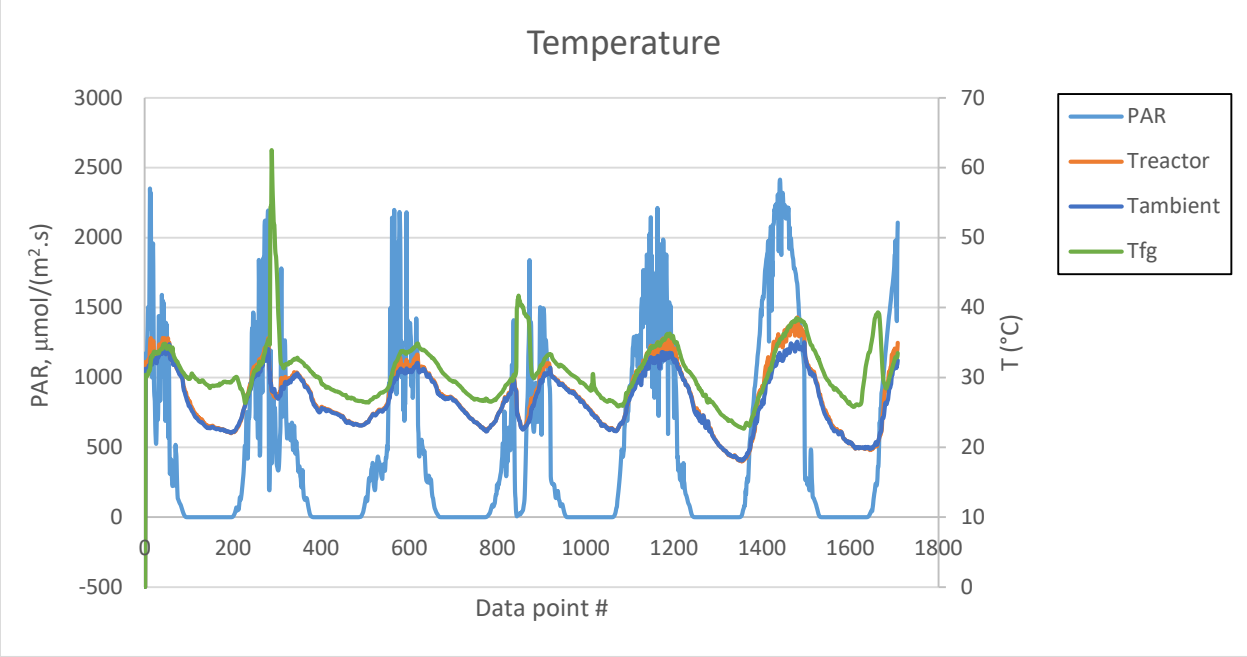

Figure 28. Ambient, photobioreactor and inlet flue gas temperatures versus PAR

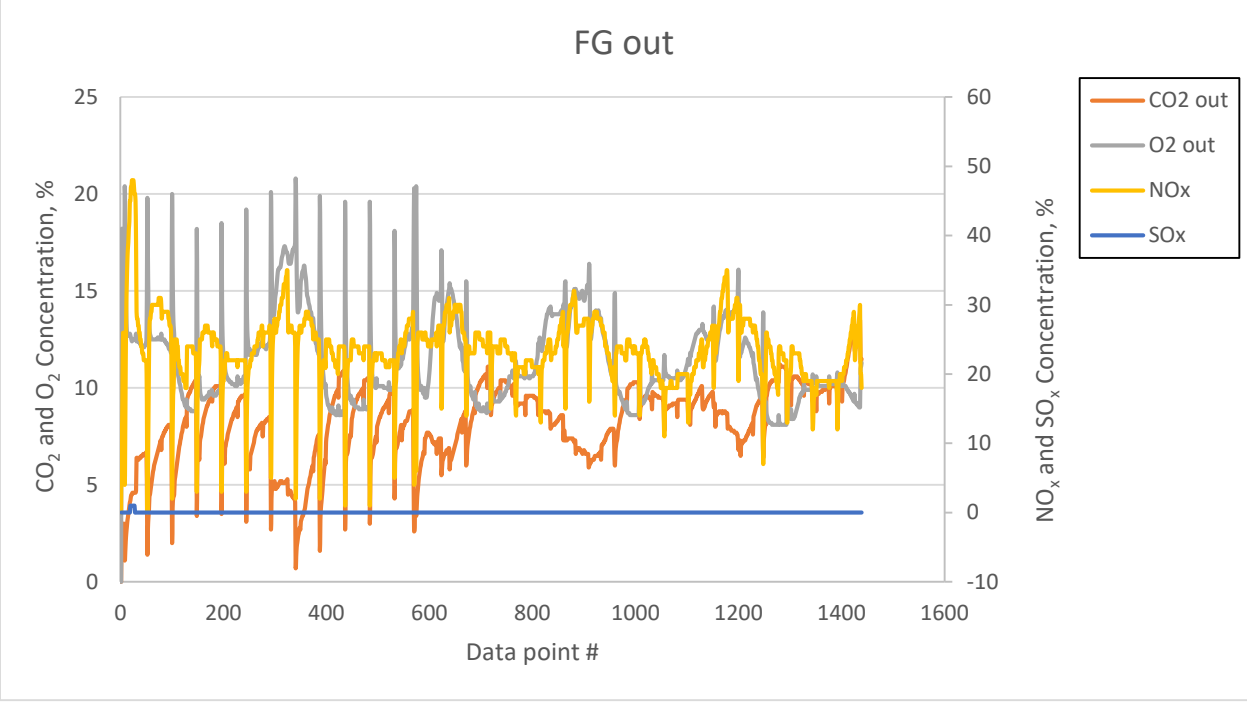

Figure 29. PBR exhaust gas composition showing oxygen production (co-product of photosynthesis) paired with CO_2 reduction and almost complete removal of SOx. Note: NOx and SOx concentrations correspond to ppm values shown on the right hand y axis.

Operations at East Bend Station continued throughout July-Sep 2016 although a number of obstacles were encountered. In mid-July, the East Bend PBR suffered a lightning strike which destroyed a significant amount of sensors and automation instrumentation. This was followed by a plant shut down, during which the culture was maintained on bottled CO_2 and air. Two culture crashes, one in mid-August and the other in mid-September, subsequently occurred, most likely due to high temperatures within the reactor.

Temperature plays a critical role in algae cell growth, reproduction and metabolism. Each species has a range of temperatures it can tolerate; the tolerance range observed for this particular culture of S*cenedesmus acutus* is approximately 12°C-38°C. Green algae are, by their nature, adaptable and at times can be pushed beyond the limits of unfavorable conditions by a cellular response mechanism through the synthesis of heat shock proteins (HSP). This specific class of stress-induced proteins improve cellular thermotolerance through altered gene expression. Unfortunately, even HSP have their limits. If an unfavorable environmental parameter occurs more quickly than the culture can adapt, the stress proteins can misform, expressing further misformed proteins thus leading to a culture whose characteristic morphology is no longer metabolically viable.

Figure 30 shows the CO_2 concentration in the PBR's inlet and outlet gas streams, PAR and reactor temperature for late July 2016. Missing PAR data in Figure 30 are the result of a previous lightning strike that destroyed the sensor. Significant carbon capture upwards of 40% can be seen from July 18-22, 2016, with less significant night losses. The culture was observed to be dying on July 23, exhibiting a brown color and foul odor. The cause of death was likely exposure to high temperatures for a prolonged period as can be seen in temperature data from a few days prior. A large seed culture was added to the reactor without using normal rinse and sterilization procedures. This was done in hopes that the culture would "bounce back." As carbon capture data for July 25 shows, it did recover, proving that adding fresh culture to a culture on the verge of crashing can, in effect, save it. This is verified by Figure 31, oxygen production providing a measure of culture health and activity.

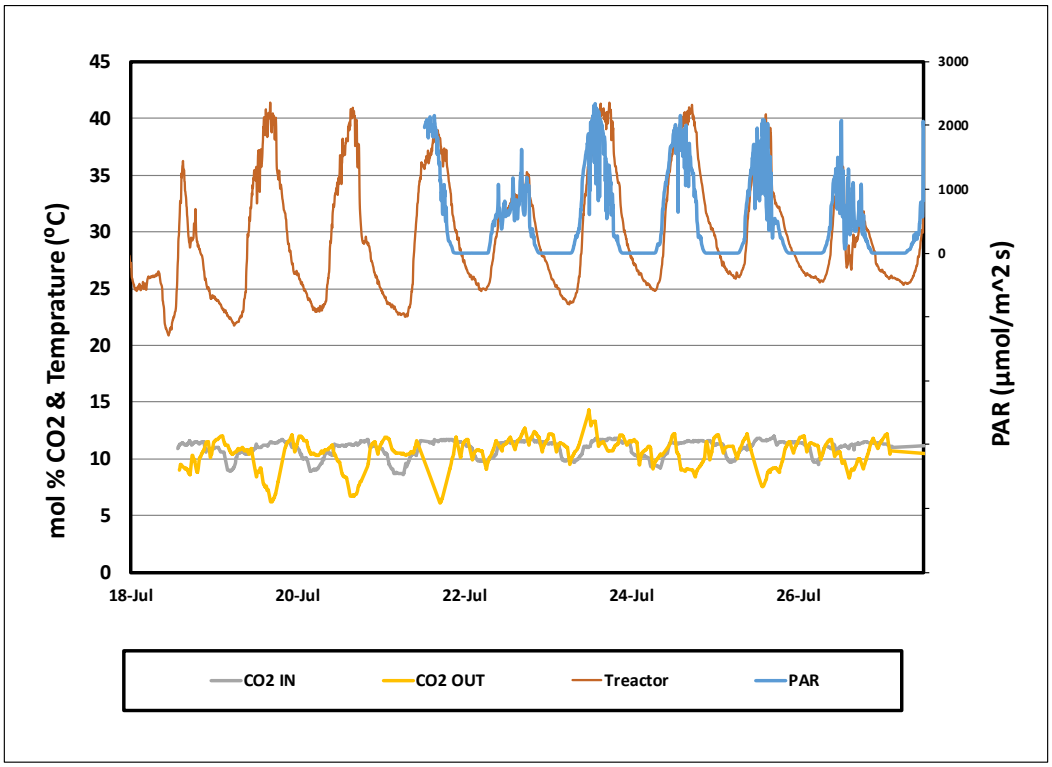

Figure 30. Inlet and outlet CO_2 (mol%), PAR and process temperature for late July 2016.

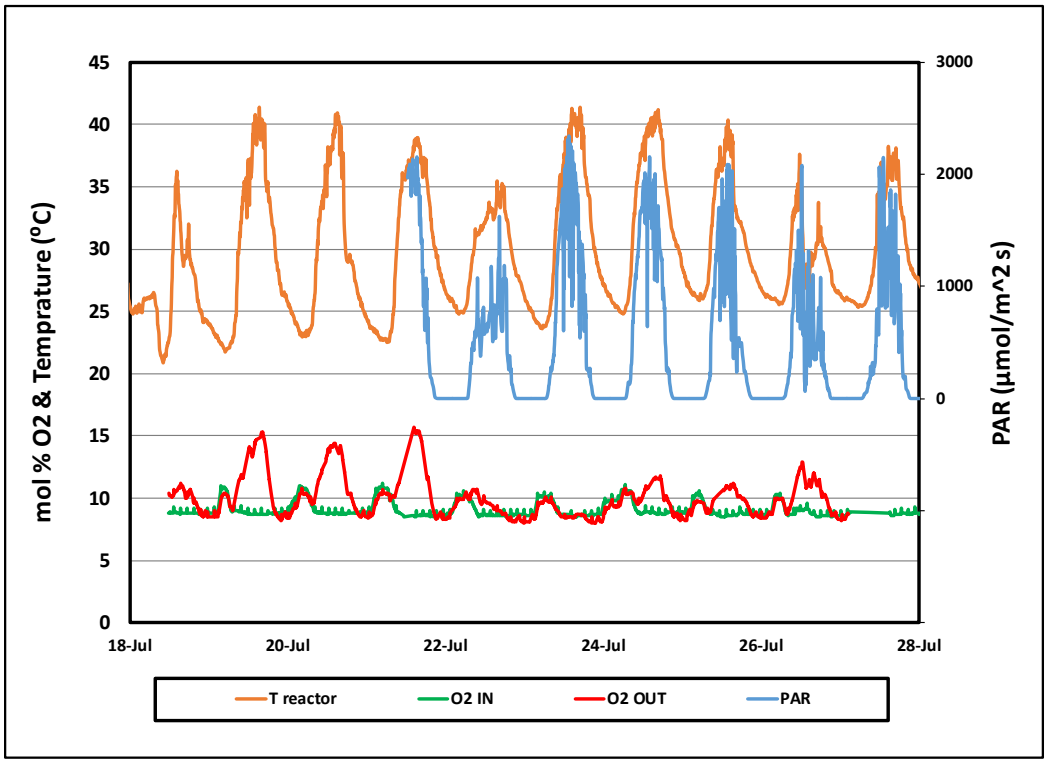

Figure 31. Inlet and outlet O_2 concentration, PAR and process temperature for late July 2016.

Two similar situations played out in August and September 2016. However, in both these instances, the culture could not be saved, requiring rinse, sterilization and re-seeding procedures to be performed. The culture crash that occurred in August cannot be definitively attributed to higher temperatures, although high temperatures did follow the culture crash, ensuring that it could not recover. Decreased photosynthetic activity was verified by decreased oxygen production, as exemplified by the data in Figure 32. The cause of the crash was likely a takeover by invasive species, as microscopy shows in Figure 33. This culture crash resulted in a complete rinse, disinfection and re-seeding procedure beginning September 2. Seed culture limitations did not allow for re-seeding of the reactor until September 16.

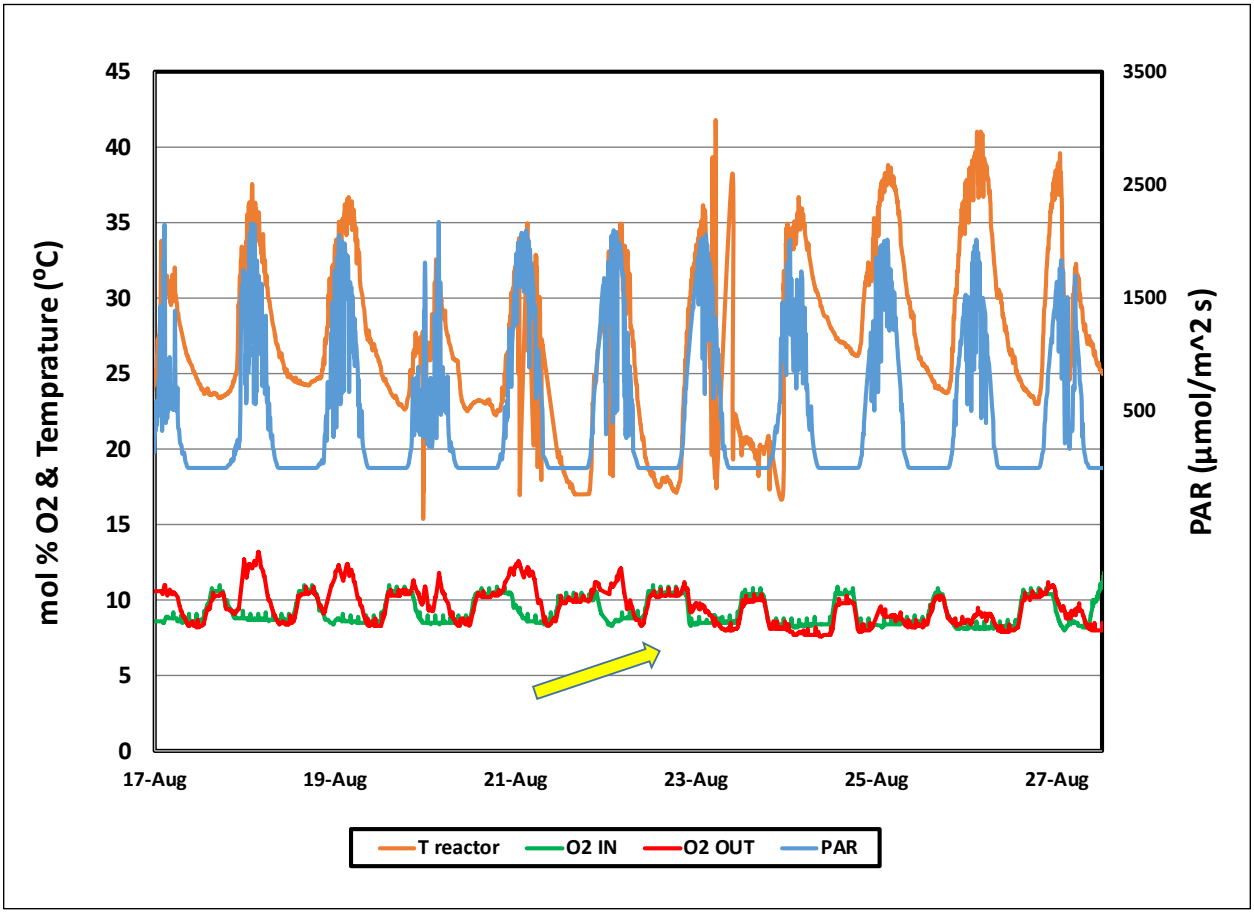

Figure 32. Inlet and outlet O_2 concentration, PAR and process temperature for late August 2016. The arrow indicates the onset of decreased oxygen production.

CO_2 capture efficiencies for September 2016 were not as high as those in July, but still significant. Figure 34 shows CO_2 capture of roughly 20-30%, with more significant night losses, presumably due to respiration of the algae. High temperatures on September 20 are likely the cause of the culture crash that occurred thereafter.

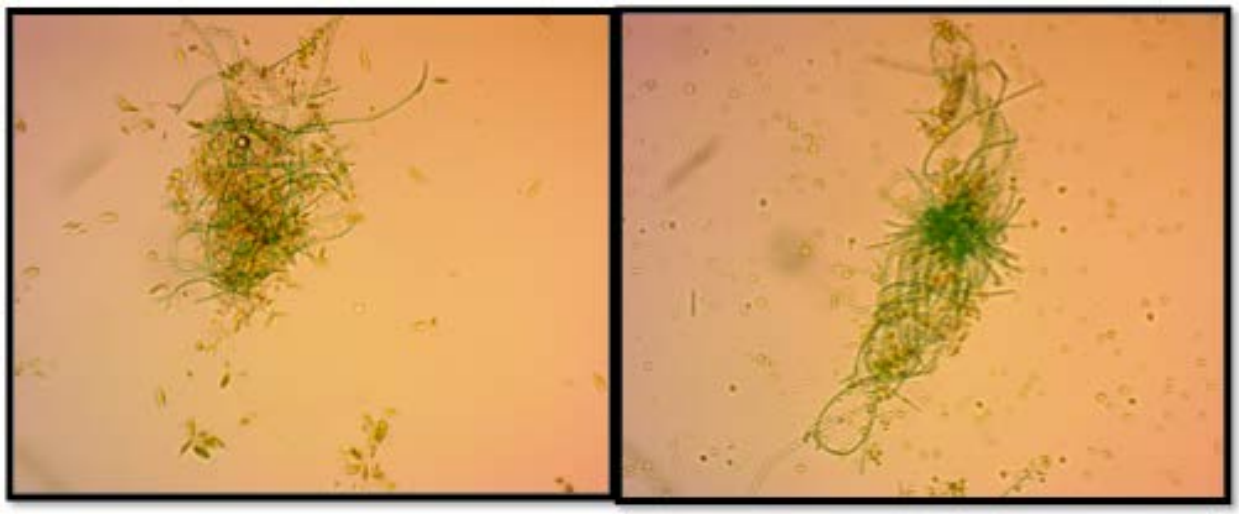

Figure 33. Microscopy images of East Bend algae culture from August 23 (left) and August 25 (right). Left photo shows the presence of invasive cyanobacteria in the presence of a decreased *Scenedesmus acutus* culture. Right photo shows cyanobacteria and other invasive green algae with little to no *Scenedesmus acutus* present.

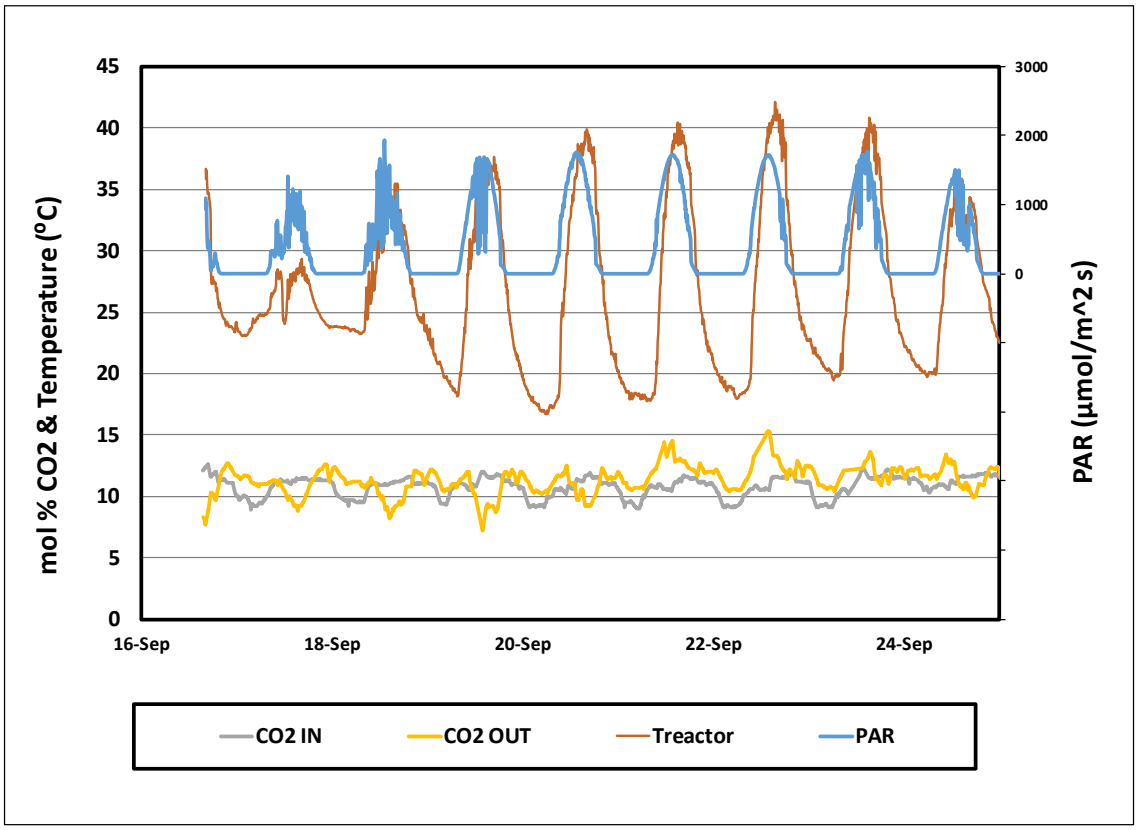

Figure 34. Inlet and outlet CO_2 (mol%), PAR and process temperature from September 2016.

The growth campaign at East Bend Station was suspended in mid-October 2016 due to a combination of worker availability, scheduled travel, and inclement weather. Subsequently, a detailed analysis of the data collected at East Bend Station during 2016 was conducted. More specifically, the dependence of O_2 production, indicative of photosynthesis and algae culture growth, on factors such as CO_2 consumption, PAR (photosynthetically active radiation) and process temperature was examined.

Figure 35 shows the relationship between CO_2 consumed and O_2 generated, the data corresponding to measurements made during the period July 18-28, 2016. CO_2 consumption and O_2 production are based on measurements of mole % composition of inlet and outlet gas, volumetric flow rate and pressure, which were collected by a MRU VarioPlus Industrial SDIR gas analyzer, an American Meter Co. DTM 200A flow meter and a Noshok high accuracy pressure gauge, respectively. Gas measurements were logged by the MRU analyzer. It is important to note that gas measurement units denote Δn over periods of five minutes.

PAR and process temperature were measured using an Apogee SQ-215 quantum sensor and a J thermocouple, respectively, and data were logged as part of the PBR's control system which uses National Instruments (NI) Labview software deployed to a NI cRIO CPU. Data points are averages taken over a five minute period.

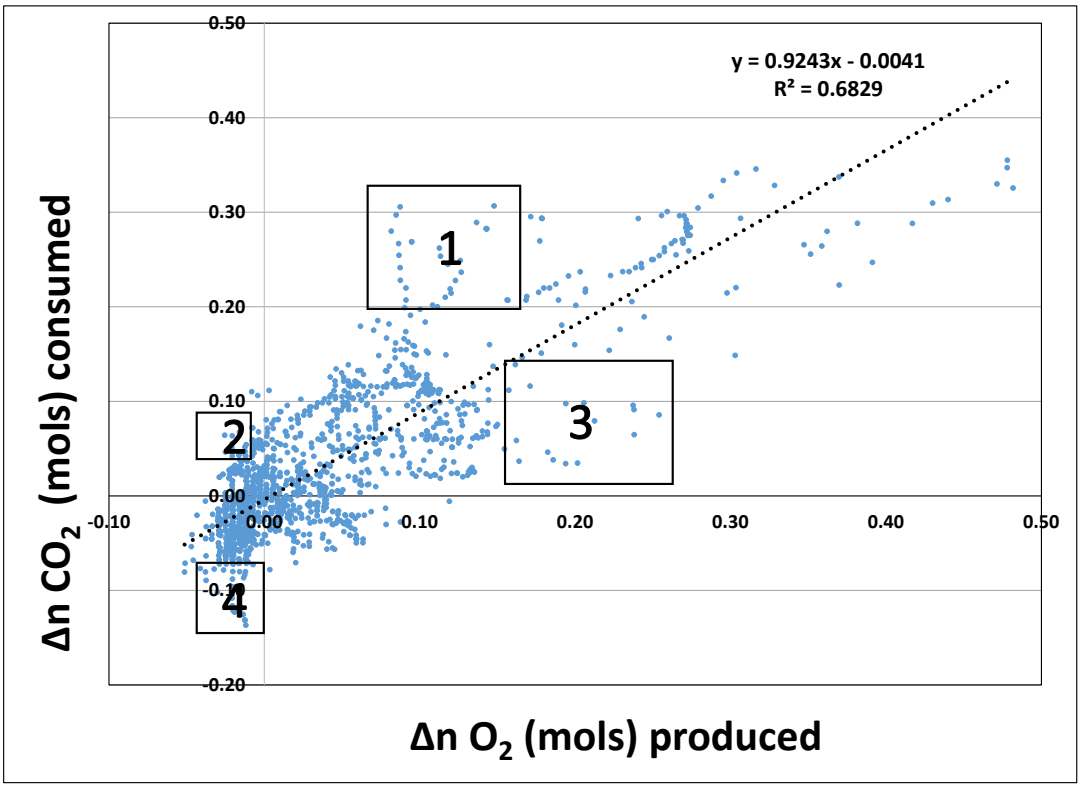

Figure 35. CO_2 consumed vs. O_2 produced (5 s data). The graph indicates a linear correlation between CO_2 consumed and O_2 produced with a slope of 0.92 and intercept of 0.0041. Boxes and numbers denote groups of outliers of interest. Data include all data points taken, including night data. All data are calculations made from averages taken over a five minute period.

The slope of linear regression for Figure 35 represents a ratio of 0.92 moles of CO_2 consumed per moles of O_2 produced (R_{CO_2}/R_{O_2}). The inverse of this ratio is 1.08 R_{O_2}/R_{CO_2} and is within the range of 0.8 to 1.2 R_{O_2}/R_{CO_2} which has been previously reported in the literature (Sobczuk *et al*., 2000). According to the generalized equation for photosynthesis, one mole of O_2 should be produced for every mole of CO_2 consumed:

$$CO_2 + H_2O \rightarrow (CH_2O)_n + O_2$$

However, given that this assumes the production of carbohydrate only, and given that algae actually consist of (mainly) carbohydrate, protein and lipids, some deviation from this stoichiometry is to be expected. Indeed, values commonly reported in the literature range between *ca.* 1.04 and 1.1.

Outliers lying within the bounds of the boxes in Figure 35 were investigated based on the time of occurrence and coinciding data from the East Bend log book (which logs seed/harvest times, visual observations, etc.). The outliers in box 3, representing low CO_2 consumption and high O_2 production, were found to have taken place directly after re-seeding, i.e., the high O_2 production numbers are an artifact of air which is pulled into the system during re-seeding and then expelled by flue gas. The outliers in box 1, representing high CO_2 consumption and low O_2 production, were found to have taken place around two hours after re-seeding, the high CO_2 consumption numbers being indicative of CO_2 dissolution in the make-up water that had been added to the system. The outliers in box 2, representing low CO_2 consumption with negative O_2 production, were found to have taken place at the end of daylight periods which, when coupled with PAR data, are indicative of a transition between photosynthesis and respiration by the algae. The outliers in box 4, representing negative CO_2 consumption and negative O_2 production, were found to have taken place at a time when the culture was observed to be dying, suggesting that organic degradation was taking place. Additional culture and nutrients were added and the culture recovered.

The analysis also indicated that some O_2 production numbers were artificially high due to air being pulled into the system during cycling. This was indicated by O_2 production spikes (not shown) that coincided with the cycling schedule of four hours. In order to gain a more meaningful understanding of O_2 production during daylight hours, in subsequent analyses these data points were removed (around 20 minutes of data occurring every four hours) along with data taken up to four hours after PBR re-seeding, as well as data collected during the night hours.

Figure 36 shows the relationship between O_2 production and PAR. The trend line evinces a rise and subsequent fall in O_2 production as PAR increases, with peak production occurring around 1500 µmol/(m^2s). A sharp drop off in O_2 production can be seen at PAR levels of near 2200 µmol/(m^2s), suggesting that high levels of PAR result in photo-inhibition. This phenomenon has been reported in the literature for algae grown in photobioreactors under strong sunlight (Rebolloso Fuentes *et al*., 1999).

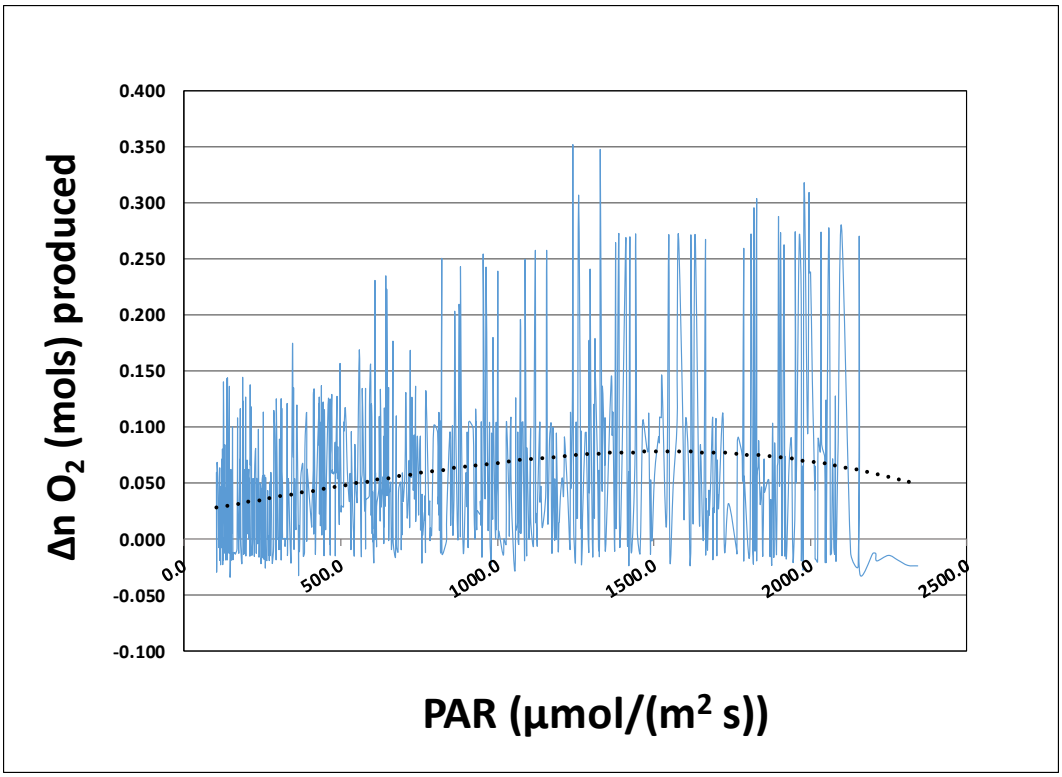

Figure 36. O_2 production vs. photosynthetically active radiation (PAR) (5 s data). Data corresponding to system cycling, re-seeding and night time operation have been removed. The trend line is a polynomial fit used for illustration.

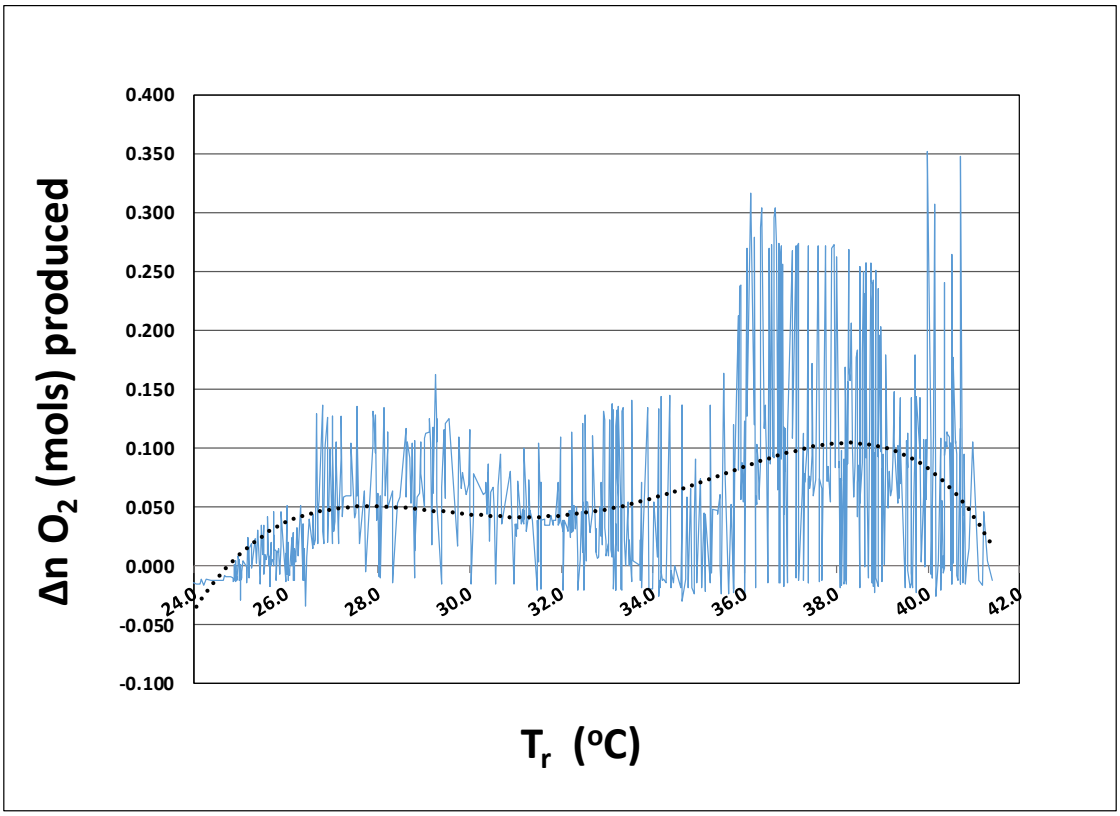

Figure 37. O_2 production vs. process temperature (5 s data). Data corresponding to system cycling, re-seeding and night time operation have been removed. The trend line is a polynomial fit used for illustration.

Figure 37 shows the relationship between O_2 production and temperature. The trend line indicates that peak O_2 production occurs in a temperature range of 36 to 38.5 ºC. A sharp drop can be seen around 40 ºC. Indeed, during the 2016 growth campaign at East Bend Station, several instances of culture death were attributed to sustained process temperatures at or above 40 ºC.

Figure 38 shows 3D plots which combine the data from Figures 36 and 37. The 3D plots show a clear ridgeline for peak O_2 production, corresponding to a temperature range of 36-38.5 ºC. A similar observation can be made when examining Figure 37. However, the 3D plot shows that peak O_2 production is much more dependent on temperature than PAR. The ridge line of peak O_2 production extends over a PAR range of 600-2000 µmol/(m^2 s), a range that encompasses 66% of the total range of given data and hence a majority of the data points. Conversely, the ridge line of peak O_2 production extends over a narrow process temperature range of 36-38.5 ºC. Based on these data, O_2 production is far more temperature dependent than previously thought.

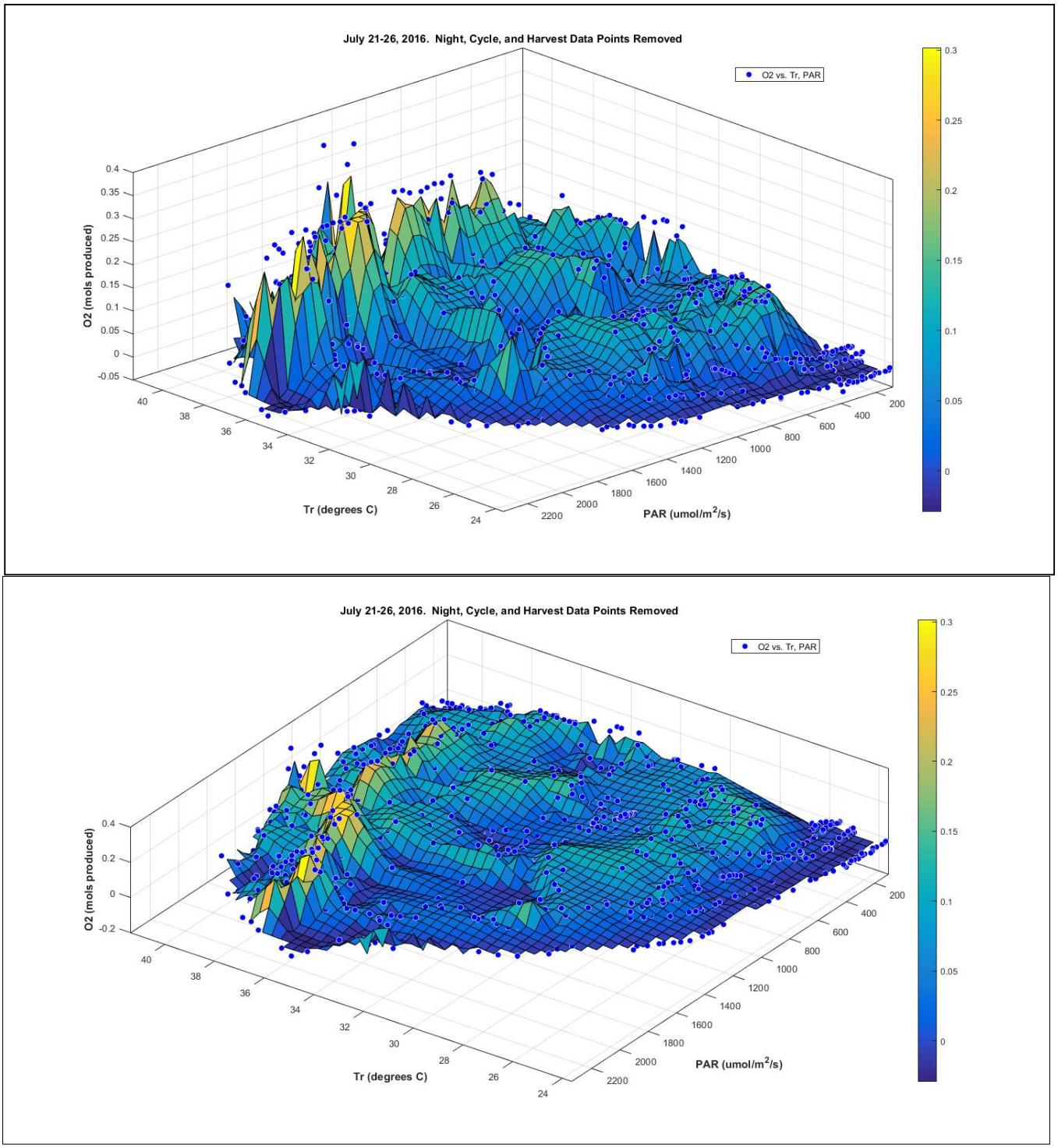

Figure 38. O_2 production vs. process temperature and PAR (5 s data). 3D plots are of identical data shown at different rotations. Data corresponding to system cycling, re-seeding and night time operation have been removed. The legend refers to O_2 production numbers on the Z axis: darker blues and lighter yellows indicating lower and higher O_2 production, respectively.

Inherent in the O_2 production data are O_2 "spikes" as can be seen in the red line in Figure 39. These spikes in O_2 production are a consequence of the cyclic flow PBR design. As the tube banks drain, gas from the feed tank displaces the volume within the tube banks. However, during this procedure, air is pulled into the system through filtered outlets installed on the feed tank. The normal operating O_2 composition of the outlet gas stream from the tube banks is around 4-8%. Consequently, when air containing 20.8% O_2 enters the system, there is a temporary increase in the measured O_2 concentration.

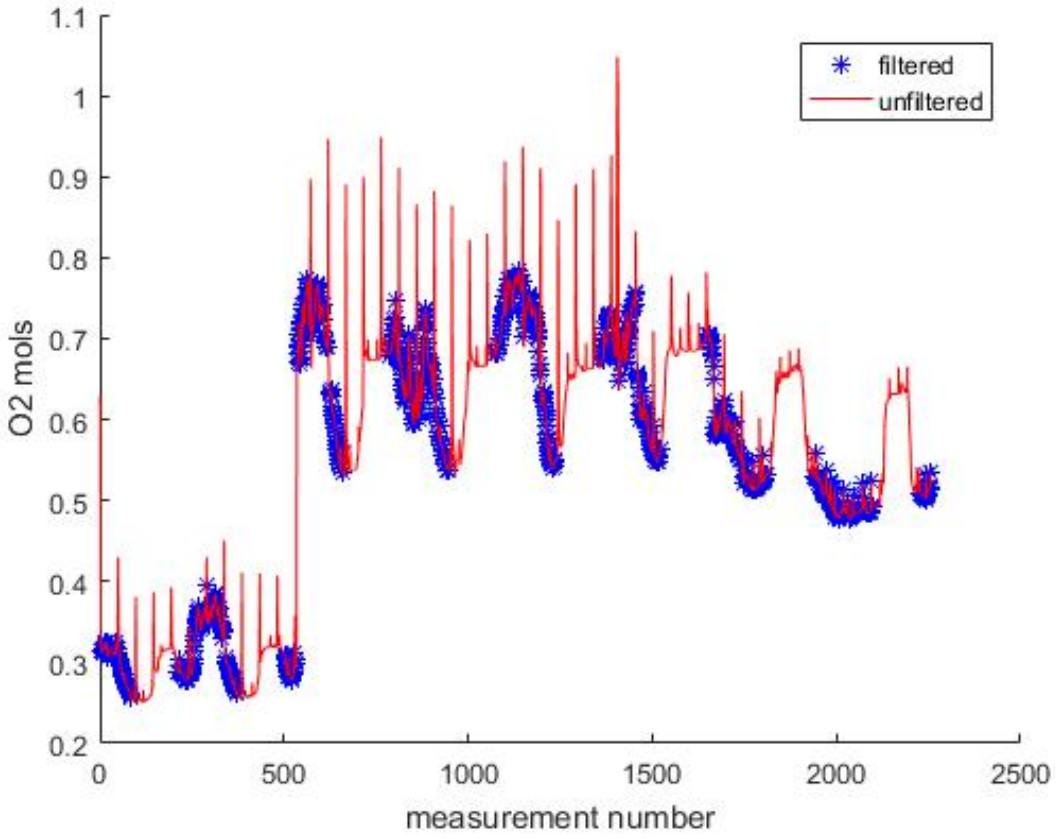

Figure 39. O_2 production data: unfiltered data in red and filtered data in blue. The filter removes night data as well as data associated with the intake of air during PBR cycling.

These "spikes" follow the exact cycling schedule of the PBR, their removal from the data being essential to characterize true system performance. Manual removal of these "spikes" is plausible for small amounts of data, but cumbersome and, in some instances, impossible for larger data sets. For this reason, a data filter was created using Matlab to remove the "spikes" and allow for analysis of data sets regardless of size. The filter uses if/else time series regression techniques, examining data points before and after the point in question. If the difference in data points is too large, that data point is removed. The blue points in Figure 39 also represent the removal of nighttime data. The filter was applied to all data points where a PAR level lower than 50 µmol m^{-2} s^{-1} was recorded.

Using the filtered data, contour plots were created in Minitab to verify optimal ranges for O_2 production (photosynthetic activity). Figure 40 verifies optimal ranges of system performance as hypothesized from data presented in the last quarterly report. As CO_2 consumption increases, so does O_2 production, the optimal ranges of pH, PAR and reactor temperature being 7-7.5, 1200-2200 µmol $m^{-2}s^{-1}$, and 36-38ºC, respectively.

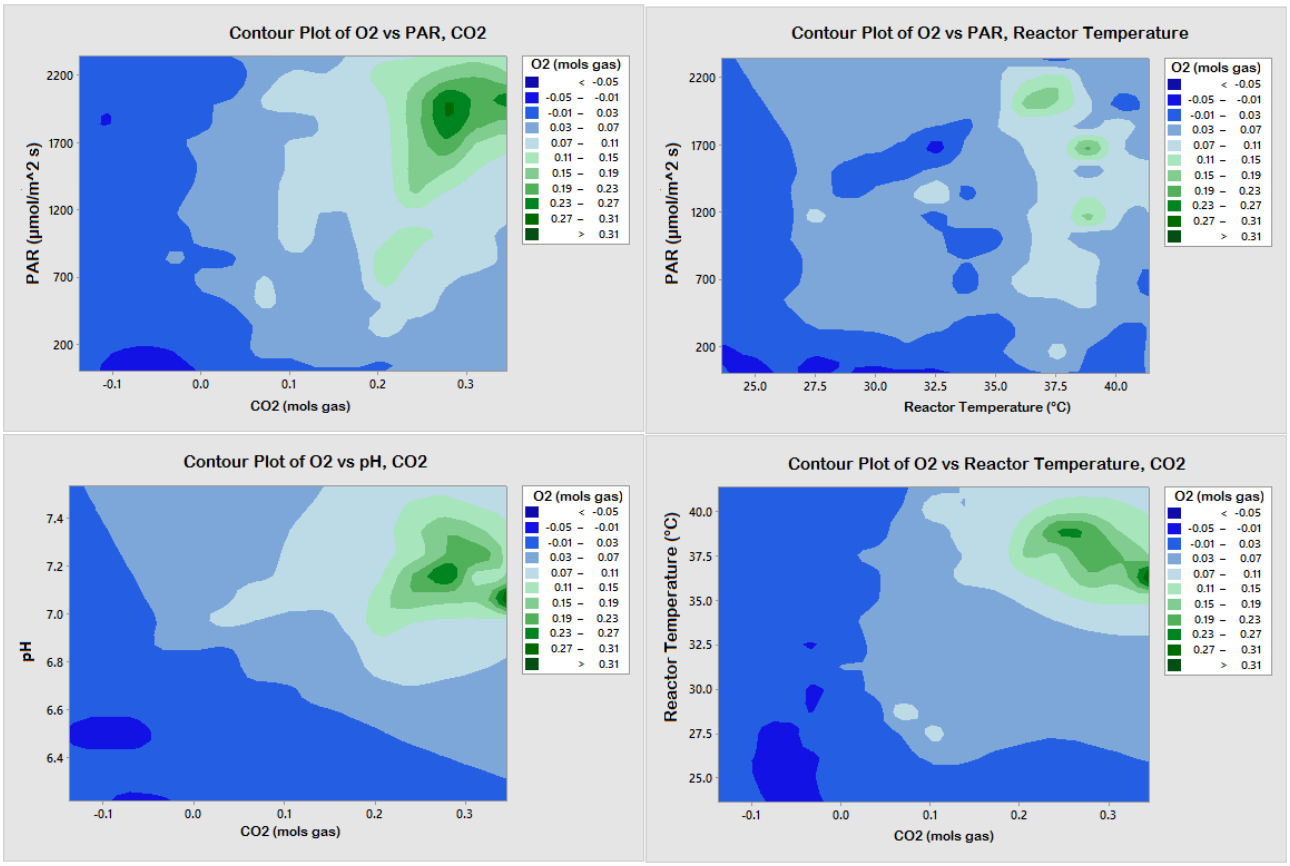

Figure 40. O_2 production as a function of two parameters (corresponding to 5 days of the 2016 East Bend data). The units of CO_2 and O_2 are mols of gas consumed and produced, respectively, over a five minute period and are correlated with pH, PAR and reactor temperature.

Activities in 2017 focused on the production of algae biomass for lipid extraction experiments. Biomass was being produced at the UK CAER in the 1200 L cyclic flow PBR (Figure 41).

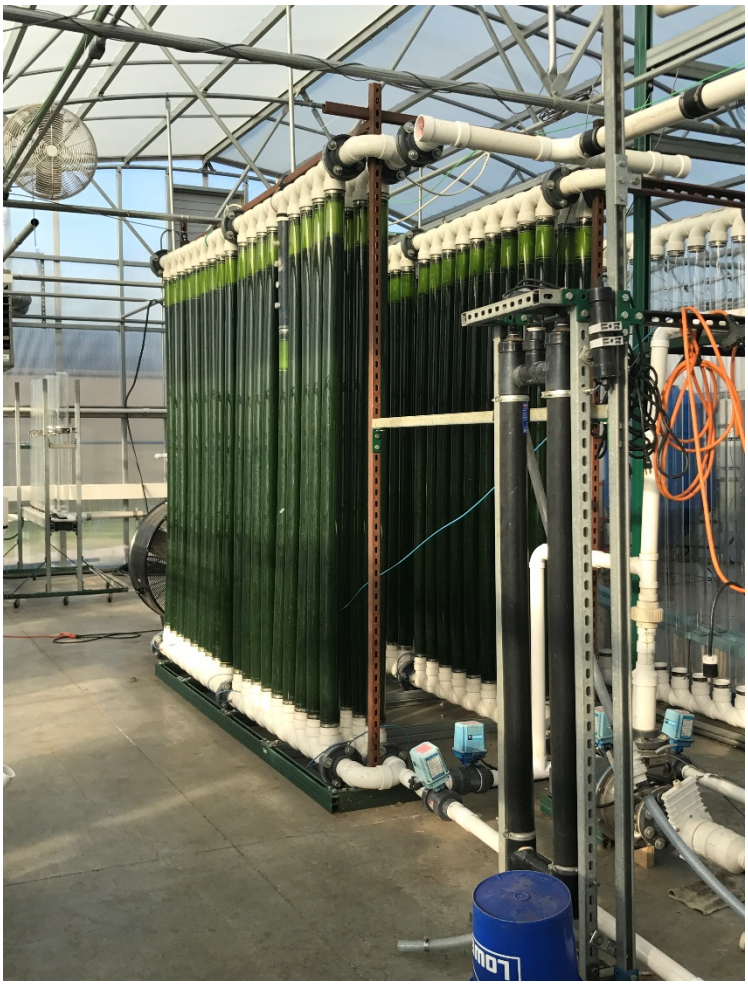

Figure 41. Cyclic flow photobioreactor in the greenhouse at UK CAER.

The PBR was seeded on April 6th, 2017 and was operated continuously using simulated flue gas to produce biomass for utilization studies. Strong growth was observed and important culturing parameters (PAR, T, pH, dissolved O_2) were monitored. Daily culture density (dry mass) measurements also afforded the opportunity to examine the relationship between dry mass and culture absorbance in the UV-vis region. As shown in Figure 42, a reasonably linear relationship was obtained. Consequently, UV-vis spectrophotometry was used as an acceptable alternative to dry mass measurements in instances when the latter are deemed to be too time consuming.

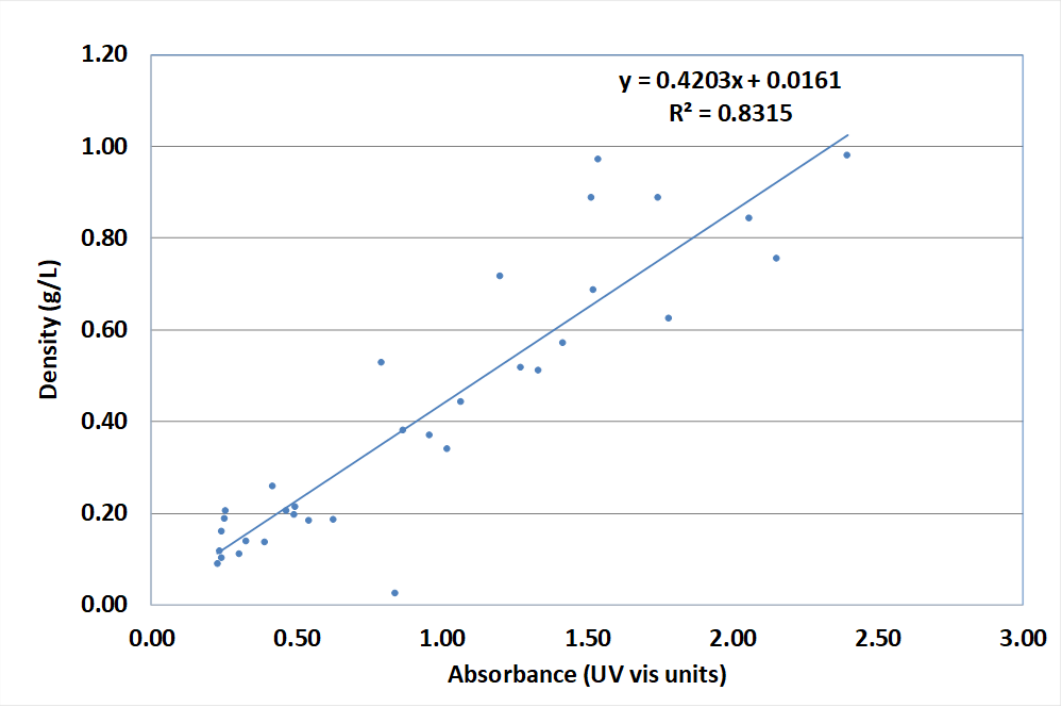

Figure 42. Linear regression of culture density (g/L) vs UV-vis absorbance units. Data represents samples taken from the cyclic flow PBR at the UK CAER greenhouse from April-June 2017.

Figure 43 summarizes select data from the PBR that confirms previous findings drawn from the 2016 East Bend data: optimal O_2 production follows an ideal temperature range of 35-38 ºC. The lower range of PAR numbers are indicative of measurements taken inside the greenhouse. On average the PAR levels in the greenhouse are some 800-1000 µmol $m^{-2}s^{-1}$ lower than those outside. It is important to note that O_2 numbers in this graph are measured as dissolved oxygen levels and not the number of mols of O_2 produced.

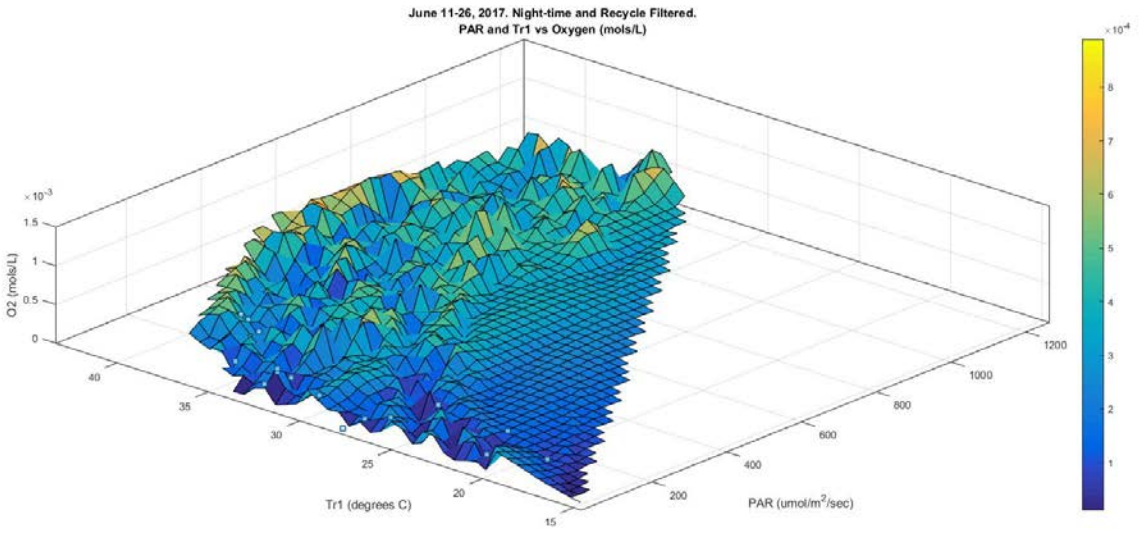

Figure 43. Process data from cyclic flow reactor in UK CAER greenhouse from June 11-26, 2017. Night data and O_2 "spikes" (due to liquid cycling) have been removed.

Carbon Mass Balance

Carbon mass balance calculations were performed on a comprehensive and qualifiable data set obtained from the East Bend Station PBR. The data for these calculations were taken from a ten-day period in late July 2016 and were selected on the basis of several factors, including the presence of a monoculture, proper equipment function and good weather.

Traditionally, dry mass (g/L) measurements are obtained on the algae culture by filtering a sample of the culture through a 0.5 µm filter. The filter, having been weighed before filtration, is dried in an oven at 100 ^{o}C. The filter is then weighed again after all remaining water has evaporated. The difference in initial and final filter weight is the measured dry mass.

Other means of measuring algal carbon capture were needed to validate these filtered dry mass numbers and, in the process, close the mass balance on the system. Consequently, a method for calculating algal carbon capture was developed, based on gas measurements, urea consumption measurements and Henry's Law (eqn. 1). The term "target carbon dry mass" implies that, theoretically, this calculated value should equal the filtered dry mass value.

$$m_{C\,target} = m_{C\,gas} + m_{C_{urea\,consumption}} - m_{C_{soln}} \qquad (1)$$

During the 2016 growing season, samples were taken during seeding, pre-harvest and post-harvest of the PBR. Samples were also taken on days when trips were made to East Bend station for maintenance or repair. Culture growth and growth rates were measured by the difference in

filtered dry mass measurements. Carbon capture for the PBR as a whole can be calculated by multiplying the difference in algae dry mass concentrations by the volume of the reactor and the mass fraction of carbon within the algae (determined by elemental analysis):

$$m_{C_{dry\ mass}} = (\rho_{t_2} - \rho_{t_1}) V_R w_c \quad (2)$$

The inlet gas stream volumetric flow rate, pressure and mole % CO_2 and O_2 were measured using an Elster American Meter Co. DTM-200A flowmeter, a Noshok high accuracy pressure gauge and an MRU Instruments Vario Plus Industrial gas analyzer, respectively. Mole % CO_2 and O_2 were measured in the outlet gas stream using a duplicate MRU Instruments Vario Plus Industrial gas analyzer. The gas analyzers also measured temperature. Data were taken continuously every five minutes for those time periods during the summer growing season. The length of this period varied based on extenuating factors such as culture health, plant shutdowns, etc., but typically lasted 2-5 days.

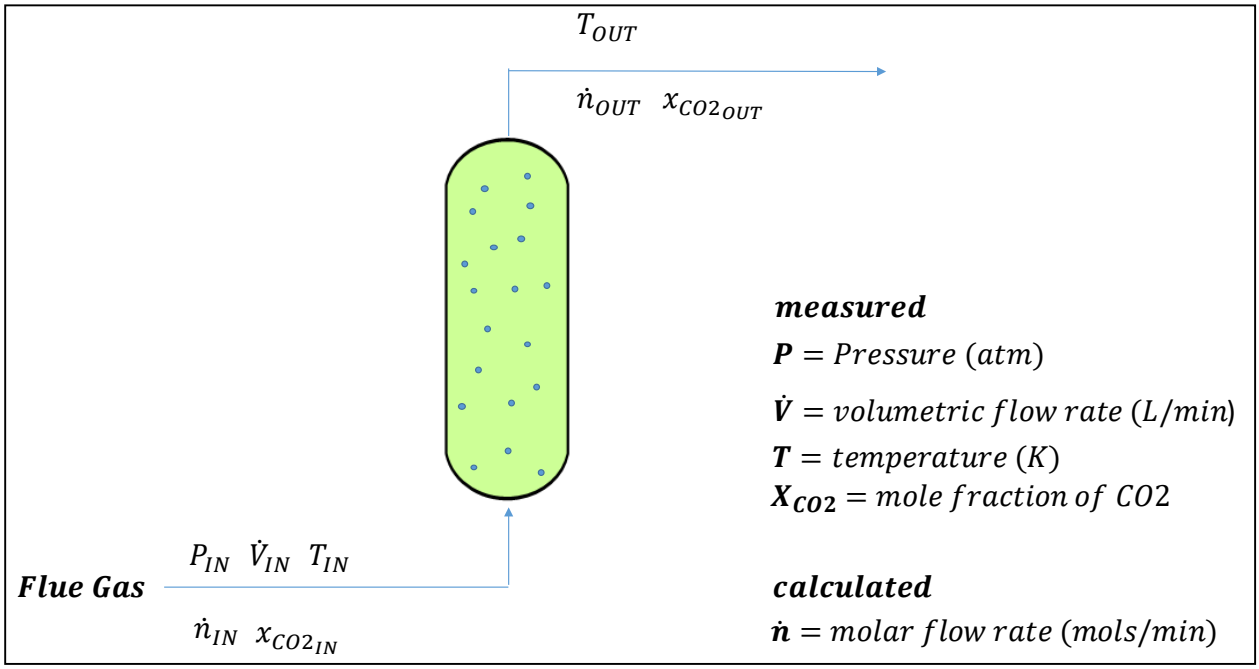

Figure 44. Flow diagram for carbon mass balance based on gas measurements.

Molar flow rates were calculated using the ideal gas law (eqn. 3). An ideal equation of state was appropriate for these calculations based on the pressure and temperature ranges of gas flowing

into and out of the PBR (Figure 44). Compressibility factors for air range from 0.9992 to 1.0000 at temperatures of 250-300 K at pressures of 1-2 bar (D.W. Green and R.H. Perry, Perry's Chemical Engineers' Handbook, 1984). The inlet gas stream flowed at a pressure of *ca*. 1.8 bar. Flue gas closely resembles air in its molecular composition, containing around 70% N_2 and 10% O_2. Thus, it stands to reason that compressibility factors for flue gas are similar to those of air at identical temperatures and pressures. For air, the compressibility factors are so close to 1 that they did not need to be included in calculations.

$$\dot{n}_i = \frac{P_i \dot{V}}{R T_{AVG_i}} \tag{3}$$

Data points were taken from an average over a five minute period. Molar flow rates of CO_2 were calculated and multiplied by the time period to acquire the moles of CO_2 accumulated (eqn. 4).

$$n_{CO2_{accum}} = \left(\dot{n}_{IN}\, x_{CO2_{IN_{AVG}}} - \dot{n}_{OUT}\, x_{CO2_{OUT_{AVG}}}\right) \Delta t \tag{4}$$

The mass of accumulated carbon was calculated using mole ratios and the molecular weight of carbon (eqn. 5).

$$m_C = n_{CO_2} \left(\frac{1 mol\ C}{1 mol\ CO_2}\right) MW_C \tag{5}$$

The mass amounts of carbon for each five minute period were summed over the of growth periods from the time of seeding to the time of harvest. (eqn. 6).

$$\boldsymbol{m_{C_{gas}}} = \sum_{\boldsymbol{i=Day\ 1}}^{\boldsymbol{Day\ n}} \boldsymbol{m_{C_{accum_i}}} = \boldsymbol{m_{C_{accum_{Day\ 1}}}} + \boldsymbol{m_{C_{accum_{Day\ 2}}}} + \cdots + \boldsymbol{m_{C_{accum_{Day\ n}}}} \tag{6}$$

Urea was measured by a method developed at the UK CAER that used ion chromatography. After filtration, samples were partitioned into hydrolyzed and non-hydrolyzed aliquots. Urease was used to hydrolyze all urea into NH_4^+ and CO_2 in the hydrolyzed aliquots. A mass balance of NH_4^+ ions in hydrolyzed and non-hydrolyzed samples allowed for quantifiable detection of urea.

Urea consumption was calculated by comparing the difference in urea concentration at the times of seeding and harvest (eqn. 7).

$$\boldsymbol{m_{C_{urea\ consumed}}} = [Urea]_{t_{seed}} - [Urea]_{t_{harvest}} \quad (7)$$

Carbon addition associated with the addition of nutrients other than urea was not considered. Elemental analysis of dry nutrients at UK CAER confirms that the mass amount of carbon in all non-urea nutrients is so low that its contribution can be considered negligible.

During the growth period in question, top-up water was added to the reactor after each harvest. Using Henry's law, the concentration of CO_2 required to saturate the top-up water was estimated (eqns. 8 and 9). An average of the molar composition of the outlet gas was used in estimating an average partial pressure of CO_2 in the system (eqn. 8) and well as the mass of carbon in solution.

$$[CO_2(aq)] = \frac{P_{CO2}}{K_{H_{CO_2}}} \quad (8)$$

$$m_{c_{soln}} = [CO_2(aq)] V_{newwater} MW_C \quad (9)$$

Finally, the target dry mass of carbon was calculated according to eqn. 1, i.e., by summing the mass of carbon accumulated according to the gas analyzers and the carbon consumed by the algae as urea, and subtracting the carbon absorbed into solution upon addition of the top-up water.

Figure 45 shows a comparison of the target dry mass and measured dry mass for three sequential harvest periods. For the growth periods of 7/18-7/21 and 7-25-7/27, errors associated with each growth period were not statistically significant. However, for the growth period spanning 7/21-7/25, there was a statistically significant discrepancy. During this period, biofilm formation was visually observed and noted in the East Bend activity log. Upon arrival at East Bend station on 7/25, the culture did not look healthy. Accumulation of biofilm within the reactor could explain the larger target dry mass number, since carbon captured as biofilm within the reactor would not be sampled during harvesting or culture sampling.

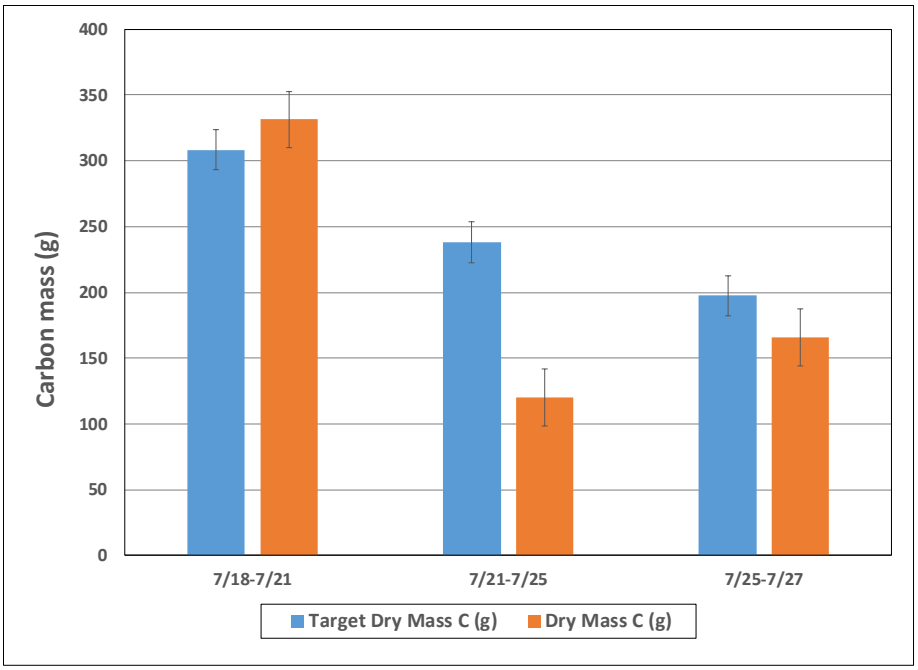

Figure 45. Mass of carbon accumulation in algae as calculated by target dry mass calculations and dry mass measurements. Error bars for target dry mass (blue) represent the error associated with the CO_2 gas analyzer. Error bars for the measured dry mass (orange) represent the standard deviations of triplicate measurements.

The discrepancy for the growth period of 7/21-7/27 served as an impetus for further investigation. The question of night losses often comes into play when considering carbon capture efficiencies. Comparing day gains to night losses (associated with respiration) not only helps to clarify the overall carbon capture efficiencies of a system, but may also indicate the health of an algae culture.

Figure 46 shows carbon uptake during daylight hours and carbon losses during night hours. Clearly, when culture health is strong, the day gains far eclipse the night losses. For the dates of 7/22 and 7/23, however, no net carbon was gained during daylight hours. A variety of factors could influence this outcome. The culture harvested on 7/21 was diluted to a dry mass concentration of 0.17 g/L. The rule of thumb for *Scenedesmus* cultivation dictates that the culture concentration should ideally not fall below 0.2 g/L. If a culture is stressed, it could extend the lag phase of culture growth. This low culture density combined with low PAR (photosynthetically active radiation) levels on 7/23 and high temperatures (around 40 $^{\circ}$C in the PBR) on 7/24 could explain the lack of CO_2 uptake for those days.

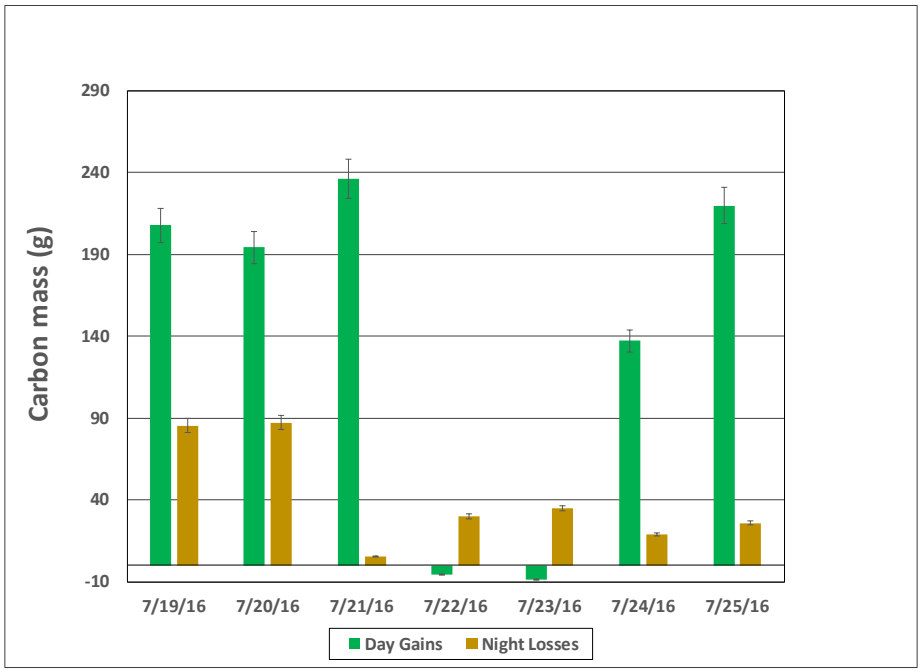

Figure 46. Comparison of carbon gains (day) and losses (night) for the East Bend PBR. Error bars represent the error associated with the gas analyzers. It is important to note that although night losses are represented as positive values in the graph, they represent a net expulsion of carbon from the PBR and their values should be considered as "negative gains."

Indeed, culture growth for the 5-day period of 7/21-7/25, 2016 was lower than the neighboring growth periods. An unhealthy *Scenedesmus* culture most likely served as an opportunity for the establishment of invasive species and/or biofilm formation on 7/23 and 7/24.

In September, 2017, the opportunity was taken to perform mass balance calculations on a data set obtained during biomass production taking place in the UK CAER greenhouse PBR. The data for these calculations were taken from a 3-day period in late September 2017 and as before were selected on the basis of factors which included the presence of a monoculture, proper equipment function and good weather.

The inlet gas stream volumetric flow rate, pressure and mole % CO_2 and O_2 were measured using an Omega PMR-011030 rotameter, a Noshok high accuracy pressure gauge and an MRU Instruments Vario Plus Industrial gas analyzer, respectively. Mole % CO_2 and O_2 were measured in the outlet gas stream using a duplicate MRU Instruments Vario Plus Industrial gas analyzer. The gas analyzers also measured temperature.

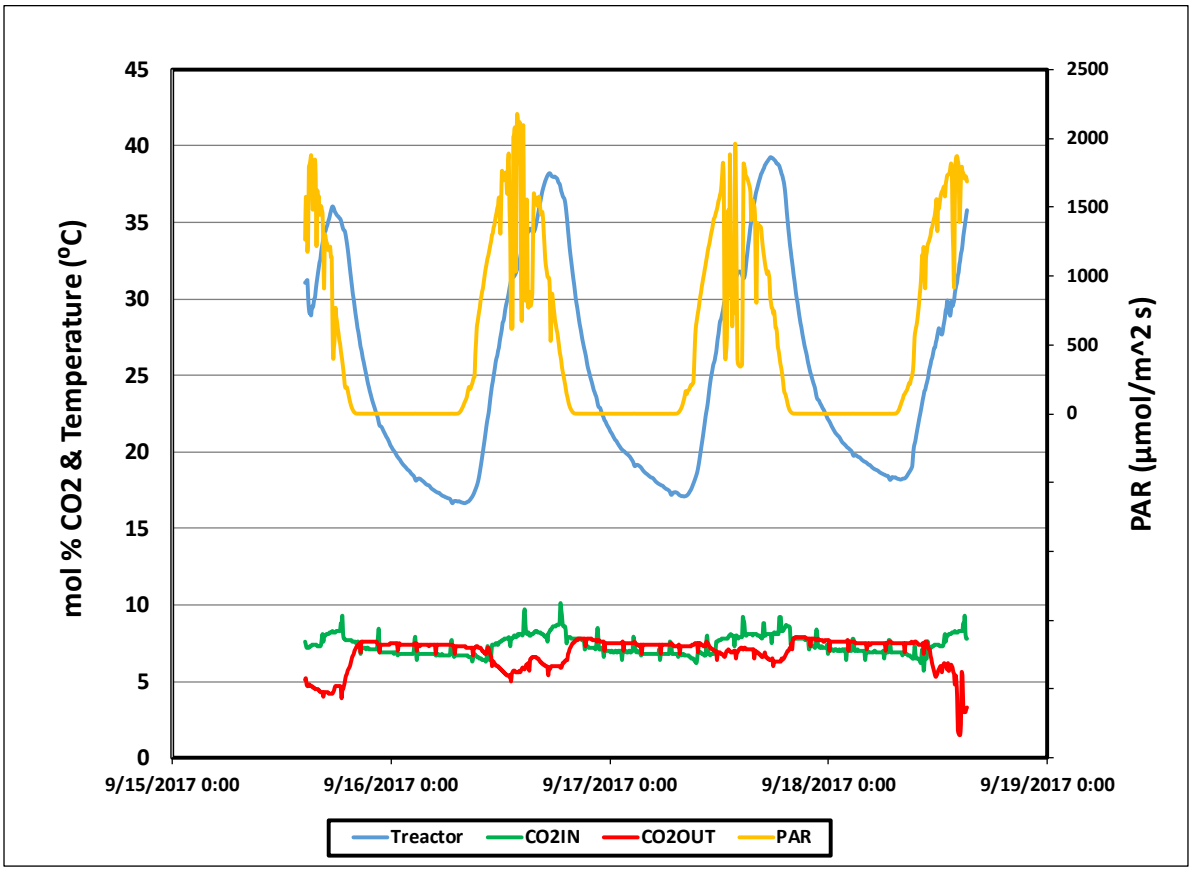

Figure 47. Mole % CO_2, reactor temperature and PAR (photosynthetically active radiation) vs. date/time. Data were obtained from an outdoor cyclic flow PBR operating at the UK CAER campus from 9/15/17 to 9/18/17. The figure collects process data used in mass balance calculations.

Process data depicted in Figure 47 show a direct correlation between PAR and reactor temperature. Also shown is an expected increase in CO_2 capture associated with increasing PAR due to photosynthesis. Both inlet and outlet CO_2 gas data show "spikes" in the composition of the analyzed gas. This phenomenon is graphically similar to spikes in O_2 production seen in previous data analyses. However, previously presented spikes in O_2 production data were relics of the PBR's recycle function as air is pulled in during liquid recycling. The spikes in CO_2 concentration also correlate to the recycle function, but were caused by gas line pressure equilibration during periods when sparging of gas into the PBR had ceased.

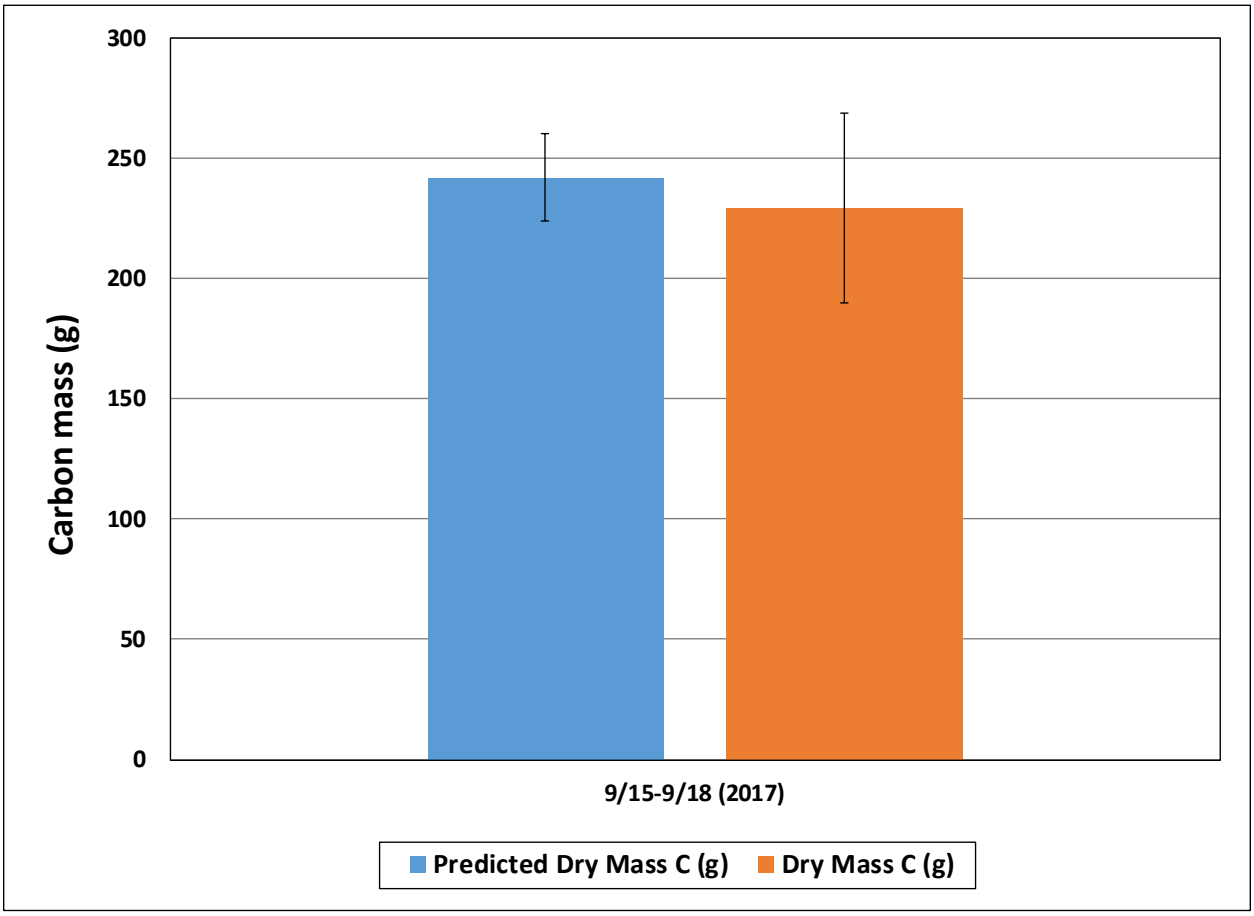

Figure 48. Mass of carbon accumulated in cyclic flow PBR as calculated from gas analyses ("predicted dry mass") and determined from algae dry mass measurements ("dry mass"). Error bars for predicted dry mass (blue) represent the error associated with the CO_2 gas analyzer. Error bars for the measured dry mass (orange) represent the standard deviations of triplicate measurements.

Figure 48 shows a comparison of the predicted dry mass and measured dry mass for the growth period of 9/15-9/18. Note that the predicted dry mass number in Figure 48 assumes that all of the urea in solution was consumed by the algae. The normal concentration of urea in the culture medium is 130 mg/L, which corresponds to a carbon consumption amount of 32.7 g carbon for one culture/harvest cycle in the cyclic flow PBR. As shown in Figure 48, carbon capture values based on the dry mass measurements and the gaseous CO_2 measurements show excellent agreement. This confirms that the cyclic flow PBR was free from significant gas leaks.

3.2.2. Heavy Metals Analysis

Quantitative analysis for the presence of As, Cd, Hg and Se in algae samples grown in the UK CAER cyclic flow photobioreactor at East Bend Station began in late 2015 and analyses

continued into 2017. Also analyzed were the dry industrial agricultural fertilizers that make up the nutrient media recipe used in the PBR. All of these analyses were done on an ICP-MS mass spectrometer according to EPA Method 6020A (SW-846) (U.S.C.o.F., 2010a) in a NELAC certified laboratory (National Environmental Laboratory Accreditation Program).

It is the conclusion of this study that the metals present in algae in various stages of cultivation and processing are derived from the industrial fertilizers used as nutrients. The results were also compared with standardized and/or regulated maximum contaminant levels (MCLs) for the presence of metals in various possible by-products of algae production. Details are presented below.

Each dry nutrient used in the culture medium was analyzed for heavy metals as shown in Figure 49. Higher concentrations of cadmium were found in triple super phosphate than were found in any other ingredient, around 43 mg/kg (ppm). The weighted dry nutrient numbers represent metals in the combined dry nutrients on a mass basis that reflect the proportionality of the target nutrient concentrations (Table 7).

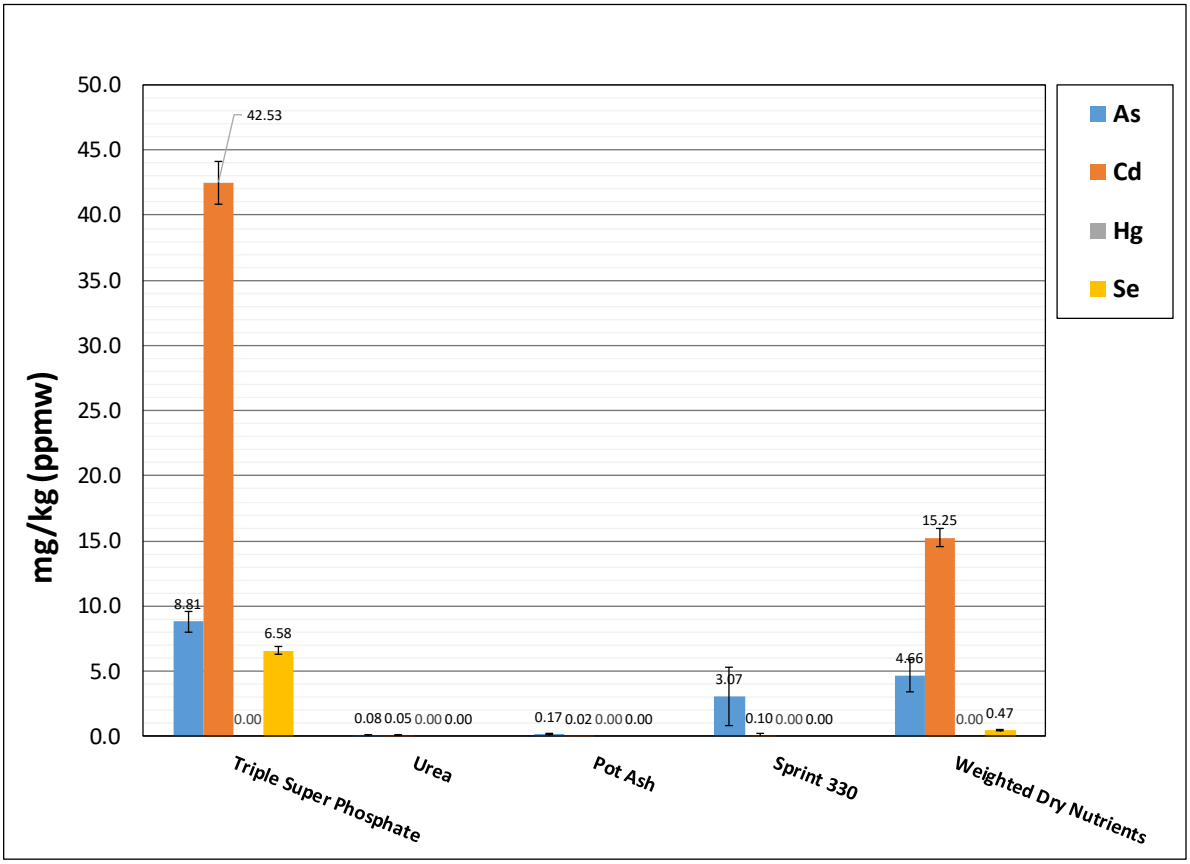

Figure 49. Analysis of triple super phosphate, urea, pot ash and Sprint 330 nutrients for As, Cd, Hg and Se. Weighted Dry Nutrients numbers represent the weighted sum of all metals present in dry nutrients. Numbers are weighted to reflect the nutrient recipe as it is added to the photobioreactor. Error bars represent standard deviations (n=3).

Table 7. Target nutrient concentrations in culture medium.

TSP	140	mg/L
Urea	130	mg/L
Pot Ash	68	mg/L
Sprint 330	26	mg/L

Figure 50 represents the concentration of As, Cd, Hg and Se measured in liquid samples taken from the East Bend PBR on three separate occasions in 2016. The metal concentrations are very close in range to the theoretical (calculated) values based on the corresponding concentrations in the supplied nutrients (Table 8). The results are also rather consistent throughout two months of sampling.

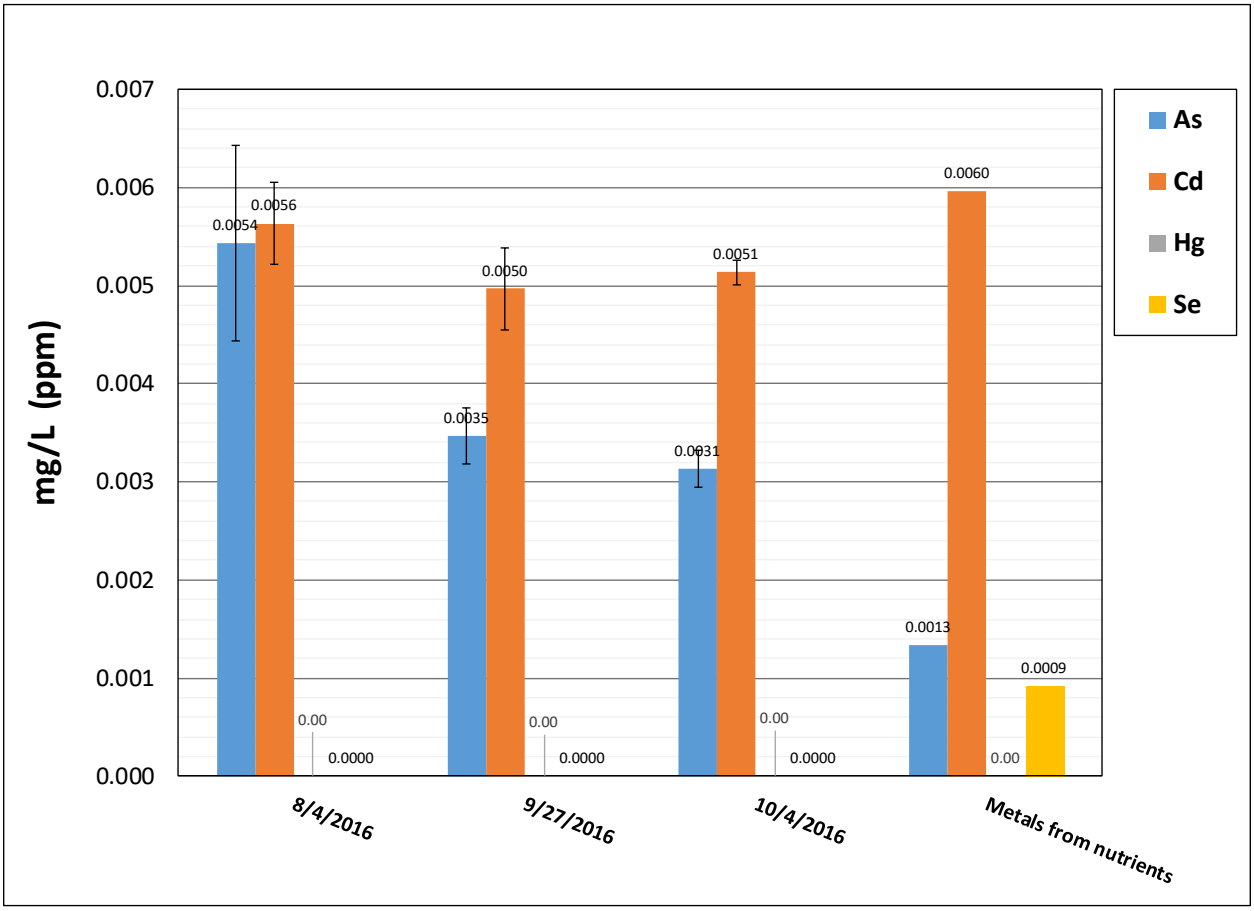

Figure 50. Analysis of liquid samples taken from the East Bend photobioreactor in 2016 on three separate occasions. Metals from Nutrients represents the expected concentrations of As, Cd, Hg and Se based on metal concentrations in the dry nutrients and their respective target concentrations in the culture medium. Error bars indicate standard deviations (n=3).

Table 8. Expected metal concentrations in culture medium based on target nutrient concentrations.

As	0.0013	mg/L
Cd	0.0060	mg/L
Hg	0.0000	mg/L
Se	0.0009	mg/L

Figure 51 illustrates the comparison of metal concentrations in solution (the same data shown in Figure 50) as compared with MCLs for As, Cd, Hg and Se in drinking water per the Safe Drinking Water Act of 1974 (SDWA). Concentrations of As, Se and Hg are well below limits for drinking water. Only one of the three Cd measurements is above the limit for drinking water with a statistically significant concentration of 0.0056±0.004 mg/L (ppm). Similar MCLs for wastewater exist in various forms for federal, state and local permitting. However, there is no standard federal guideline for the MCLs of these metals in wastewater.

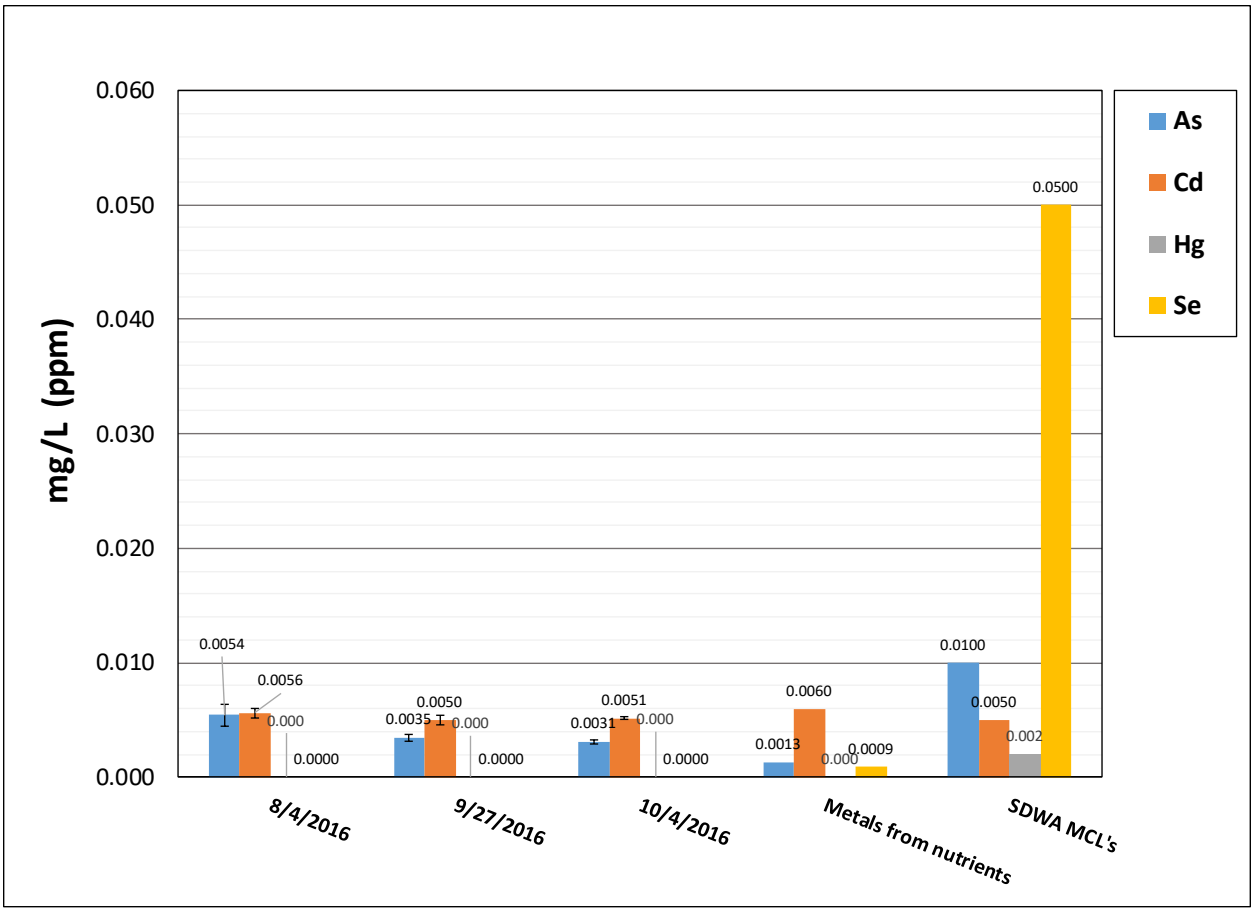

Figure 51. Analysis of liquid samples taken from the East Bend photobioreactor in 2016 on three separate occasions for As, Cd, Se and Hg (as for Fig. 50). Metals from Nutrients represents the expected concentrations of As, Cd, Hg and Se based on metal concentrations in the dry nutrients and their respective target concentrations in the culture medium. SDWA MCL's represent the Maximum Contaminant Levels (MCLs) for drinking water as regulated by the Safe Drinking Water Act of 1974. Error bars indicate standard deviations (n=3).

No selenium was detected in any liquid sample shown in Figure 50. However, calculated numbers for the contribution from nutrients, together with the presence of Se detected in dry algae samples, suggest that it is present in solution. Extremely low concentrations of around 0.0009 mg/L (0.9 ppb) were expected but were not detected due to the low minimum detection limit of Se in the ICP-MS instrument runs. Minimum detection limits for Se in the instrument runs shown in Figure 50 were 0.015 mg/L, well above the expected values of 0.0009 mg/L.

As shown in Figure 52, As, Cd, Hg and Se concentrations measured in dry algae harvested in 2015 and 2016 show similar values. The 2015 values correspond to the averages for 6 separate algae biomass samples, while the 2016 values represent the averages for 3 different samples. The individual values are reported in Tables 9 and 10.

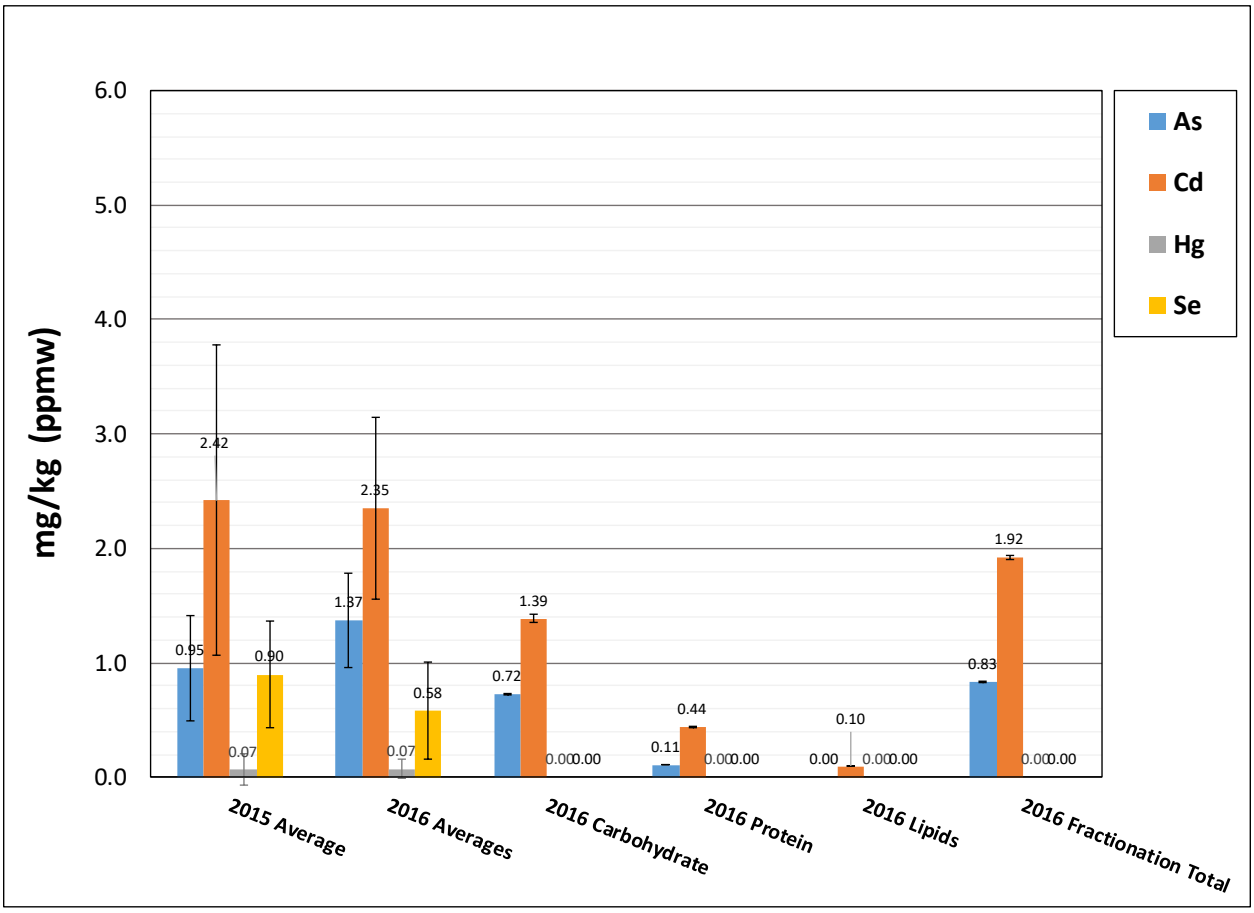

Figure 52. Analysis of dry algae and fractionated components for As, Cd, Hg and Se from samples of algae grown on flue gas at East Bend Station. 2015 Averages and 2016 Averages are measured concentrations of As, Cd, Hg and Se in samples of dry algae grown at East Bend Station in 2015 and 2016, respectively. 2016 Carbohydrates, 2016 Protein and 2016 Lipids are the measured concentrations of As, Cd, Hg and Se in fractionated algae biomass grown on flue gas at East Bend Station in 2016. 2016 Fractionation Total represents the calculated sum of metals present in the fractionated algae biomass. Error bars represent standard deviations.

Table 9. Metal concentrations measured in dry algae grown at East Bend Station in 2015.

	As	Cd	Hg	Se	
5/11/2015	1.17	1.91	0	0.76	mg/kg
5/29/2015	1.66	1.2	0.077	0.66	mg/kg
6/30/2015	1.06	1.07	0.067	0.34	mg/kg
8/3/2015	0.34	4.99	0	0.94	mg/kg
8/17/2015	0.51	3.1	0.24	0.99	mg/kg
8/27/2015	0.99	2.27	0.017	1.7	mg/kg
Average	0.95	2.42	0.067	0.9	mg/kg
Stdev	0.46	1.36	0.14	0.46	mg/kg

Table 10. Metal concentrations measured in dry algae grown at East Bend Station in 2016.

	As	Cd	Hg	Se	
8/4/2016	0.94	2.23	0.12	0	mg/kg
9/27/2016	1.76	2.86	0.0081	0.94	mg/kg
10/4/2016	1.42	1.96	0.091	0.81	mg/kg
Average	1.37	2.35	0.074	0.58	mg/kg
Stdev	0.41	0.79	0.08	0.43	mg/kg

One notable difference in the cultivation methods used in 2015 and 2016 was the use of fresh water after every harvest in 2016. In 2015, decanted “recycle” water from the flocculation process was re-used in the PBR whenever possible. Note that 2016 Carbohydrates, 2016 Protein and 2016 Lipids in Figures 52-54 refer to fractionated algae components and are listed as mg/kg on a dry basis. 2016 Protein refers to the proteinaceous residue obtained after lipid removal from the whole algae cells, which also results in the partial removal of carbohydrates.

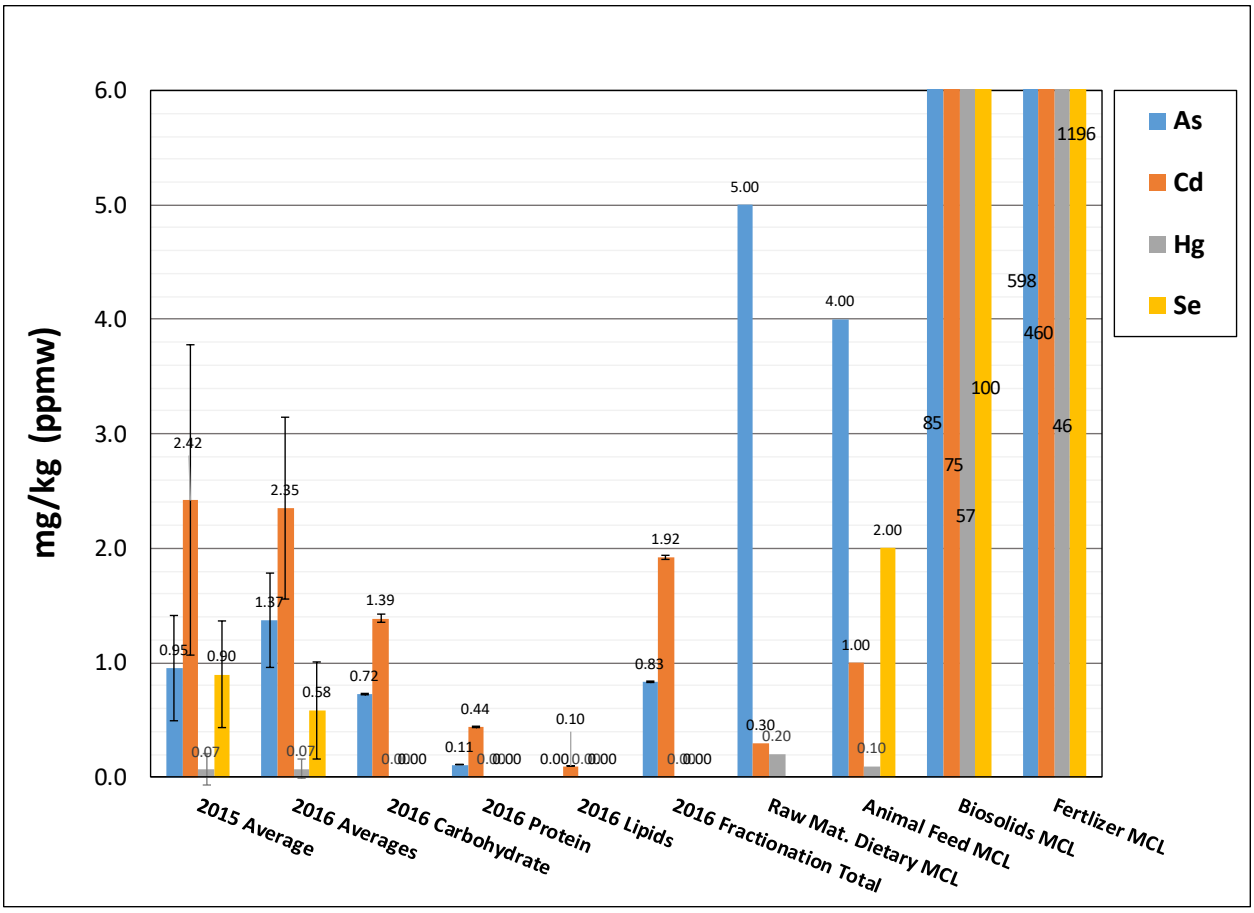

Figure 53. Analysis of dry algae and fractionated components for As, Cd, Hg and Se from samples taken at East Bend Station as well as Maximum Contaminant Levels (MCLs) for various industrial products. 2015 Averages and 2016 Averages are measured concentrations of As, Cd, Hg and Se in samples of dry algae grown on flue gas at East Bend Station in 2015 and 2016, respectively. 2016 Carbohydrates, 2016 Protein and 2016 Lipids are the measured concentrations of As, Cd, Hg and Se in fractionated algae biomass grown on flue gas at East Bend Station in 2016. 2016 Fractionation Total represents the calculated sum of metals present in the fractionated algae biomass. Raw Material Dietary MCL, Animal Feed MCL, Biosolids MCL, Fertilizer MCL represent MCL's for various industrial products. Error bars represent standard deviations.

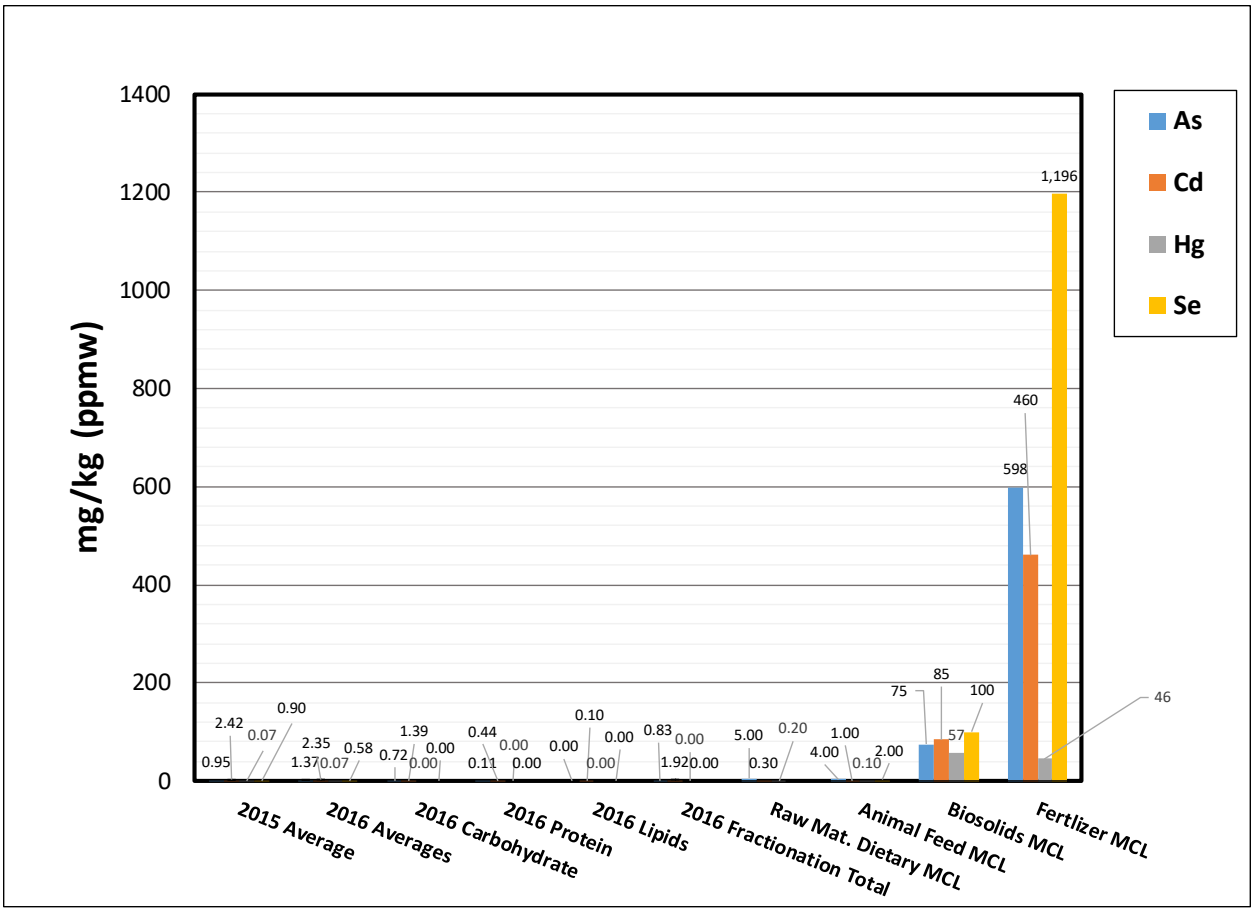

Figure 54. Analysis of dry algae and fractionated byproducts for As, Cd, Hg and Se from samples taken at East Bend Station as well as Maximum Contaminant Levels (MCLs) for various industrial products. 2015 Averages and 2016 Averages are measured concentrations of As, Cd, Hg and Se in samples of dry algae grown on flue gas at East Bend Station in 2015 and 2016, respectively. 2016 Carbohydrates, 2016 Protein and 2016 Lipids are the measured concentrations of As, Cd, Hg and Se in fractionated algae biomass grown on flue gas at East Bend Station in 2016. 2016 Fractionation Total represents the calculated sum of metals present in the fractionated algae biomass. Raw Material Dietary MCL, Animal Feed MCL, Biosolids MCL, Fertilizer MCL represent MCL's for various industrial products.

The MCLs for various industrial products shown in Figures 53 and 54 represent a metric for the potential use of algae and algae by-products. Figure 54 is identical to Figure 53 except for an increased range on the y axis in order to show the MCLs for Biosolids and Fertilizer. Often there are no statutory MCLs for As, Cd, Se and Hg from algae in various animal and human feed stocks, given that those levels are regulated by individual ingredient or follow industry standard guidelines.

All dry algae samples fall within acceptable levels for plastics used for food packaging that has an unregulated industry standard level of 60 mg/kg as outlined by the World Health Organization (Conti, 2008). Accordingly, this level is accepted as the legal limit in the European Union (EU Commission Directive 2002/72/ED, 2002).

Levels of As, Hg and Se present in dry algae and fractionated algae are below the MCLs for all of the listed industrial products in Figures 53 and 54. All samples have As, Cd, Hg and Se concentrations below the MCLs for biosolids and fertilizer MCLs (U.S.C.o.F., 2010b; A.o.A.P.F.C., 2017). "Biosolids" refers to the EPA statutory limits on solids, often sludge from wastewater treatment plants, that are applied as fertilizer. However, Cd levels in dry algae from 2015/2016, as well as carbohydrate and de-fatted algae fractionates, are too high for use in raw materials for dietary supplements and animal feed (NSF/ANSI, 2011; National Research Council, 2005). Finding a source of PO_4^- that has a lower Cd content should mitigate Cd levels within the final products.

If algae within the PBR at a culture density of 1 g/L were to uptake all of the Cd as contributed by the nutrient medium, the resulting concentration in dry algae would be ~6 mg/kg. By the same calculation, As levels would be ~1.3 mg/kg. Combined averages of the concentrations of As and Cd measured in samples from 2015 and 2016 were 1.16 ± 0.45 mg/kg and 2.39 ± 1.11 mg/kg, respectively. Figure 55 shows that, at a culture density of 1 g/L, the range of theoretical values for the concentrations of metals in dry algae are at or above the levels measured in actual samples. In reality, algae cultures that were analyzed for metals had an average culture density of 0.87 ± 0.22 g/L. Assuming total uptake, this average culture density would yield theoretical concentrations of 1.49 ± 0.51 mg/kg and 6.89 ± 2.34 mg/kg for As and Cd, respectively. That is to say, the concentrations of As and Cd in the nutrient medium are sufficient to supply the quantities of metals measured in the dry algae samples.

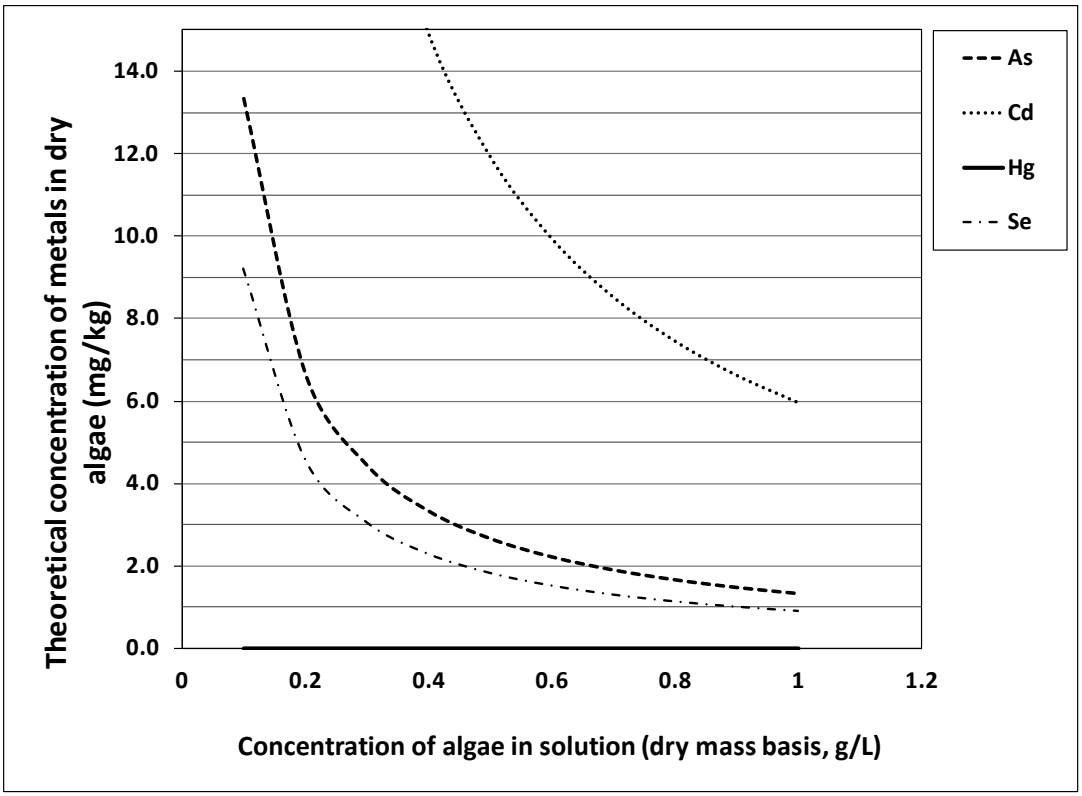

Figure 55. Dependence of theoretical concentrations of metals in dry algae on the concentration of algae in the culture (dry mass basis). Calculations reflect metals as contributed solely by nutrients. These calculations make the assumption that all metals contributed by the nutrients are taken up by the algae.

3.2.3. Dewatering System Design

Flocculation Study

In order to increase the efficiency and performance of the primary algal dewatering process, a number of polymeric cationic and anionic flocculants were tested. These flocculants, which were acquired from a commercial vendor, possess a range of molecular weights. Algae flocculation testing was conducted on harvested algae with a culture density of 0.456 g/l. This culture density is lower, and therefore more challenging, than typical harvest densities (~0.8 g/l). One liter of culture was conditioned for 1 minute after the addition of cationic flocculant (55 mole %) to promote coagulation of suspended cells. Several flocculants of varying molecular weight were evaluated in this initial series of setting tests. The flocculated suspension was then transferred to a 1 liter Imhoff Cone and allowed to settle for 10 minutes, after which a sample of the suspended solids was obtained from the 500 ml volume level of the Imhoff Cone. The dry mass concentration of the suspended solids was determined by UV-vis spectrophotometry and solids capture was calculated by the difference between the dry mass concentration of the feed and the clarified water after 10 minutes of settling. Results are summarized in Figure 56. Using the highest molecular weight cationic flocculant evaluated (9,000,000-11,000,000 Da, designated

as 9-11M), the objective of >90% solids capture was not achieved until the dosage was increased to 10 ppm.

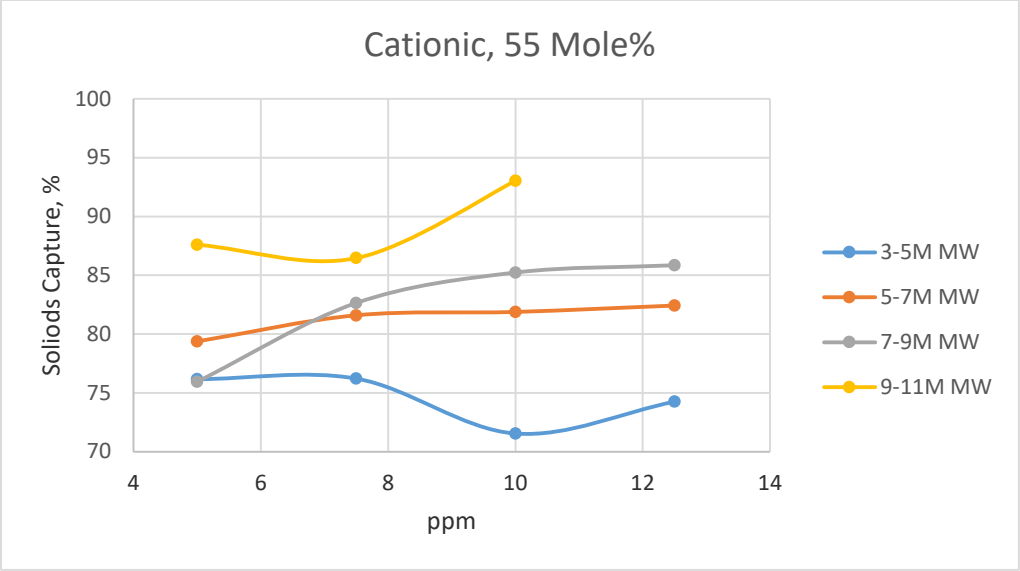

Figure 56. Effect of cationic flocculant dosage and molecular weight on solids capture of harvested algae.

In order to improve overall solids capture, another series of tests was conducted incorporating both cationic and anionic flocculants. In this approach, the harvest suspension was initially conditioned for 1 minute with 5 ppm cationic flocculant (6M molecular weight, 55 mole %) to promote coagulation of suspended cells. Varying dosages of anionic flocculant were then added to the coagulated suspension and conditioned for an additional minute prior to being transferred to the settling cones. Results are shown in Figure 57.

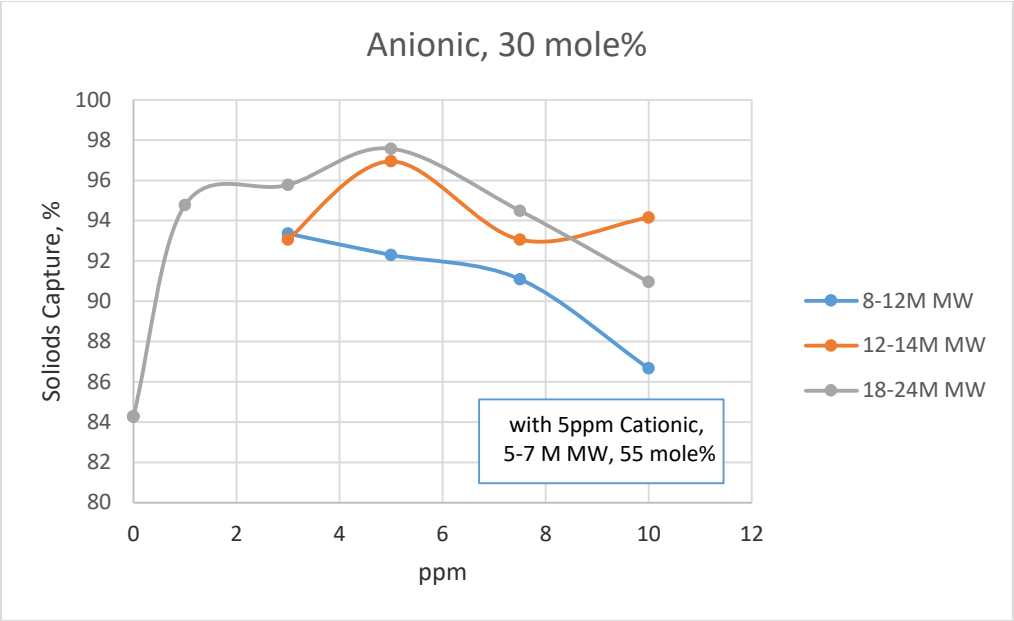

Figure 57. Effect of anionic flocculant dosage and molecular weight on solids capture of harvested algae pretreated with 5 ppm cationic flocculant.

Adding only 5 ppm cationic flocculant, 84% solids capture was achieved. When only 1 ppm of high molecular weight (12-24M) anionic flocculant was added after the cationic flocculant, solids capture increased to 95%. Solids capture improved to 98% as anionic flocculant addition increased to 5 ppm. Further increase of the dosage to 10 ppm resulted in decreased solids capture (91%). When using a lower molecular weight anionic flocculant (12-14M), similar results were obtained; a maximum of 97% solids capture was achieved at a dosage of 5 ppm, and solids capture decreased at higher dosages.

The lowest molecular weight anionic flocculant tested was 8-12M, which resulted in 93% solids capture at a dosage of 3 ppm. Increasing the dosage to as high as 10 ppm decreased solids capture to 86.6%.

When cationic flocculants are used as a coagulation step, solids capture is approximately 80 to 85%. However, when anionic flocculants are used to agglomerate algae coagulated with cationic flocculant, settling performance increased significantly. The addition of only 1 ppm high MW anionic flocculant after initial coagulation with 5 ppm cationic flocculant increased solids capture from 84% to 95%. Settling performance of >90% solids capture was readily achieved with several commercial products when using this dual flocculant approach. Results also showed that there is an optimum anionic flocculant dosage and results were diminished at higher (>5ppm) dosages.

Several conclusions can be drawn from these results pertaining to the flocculation treatment of harvested algae. First, cationic flocculants alone can provide >80% solids capture; however, dosage requirements are high. In general, solids capture at any dosage increases with cationic flocculant molecular weight. Second, anionic flocculant alone is not an effective approach. Several tests conducted with only anionic flocculant achieved <50% solids capture after 10

minutes of settling. This was not unexpected since it is well established that *Scendesmus acutus* at neutral pH is negatively charged. With a negative surface charge, the likely adsorption mechanism for anionic flocculants is polymer bridging, which results show is significantly less effective than the electrostatic attraction that results when cationic flocculants are used. As shown in the figure above, the addition of just 2 ppm anionic flocculant results in over 95% solids capture, showing the overall performance capable from the two flocculant system.

Development of a continuous algae dewatering unit

At the beginning of this project, algae harvesting operations were conducted in batch mode, whereby a volume of algae culture is collected, flocculated and allowed to settle. In this manner, a dilute algae culture is separated into two distinct components: a settled accumulation of biomass (>2% solids) and clarified water containing essentially no biomass. The clarified water is then decanted and sterilized using a UV filter and recycled back to the growth system, while the settled solids are removed for further dewatering via filtration. While this mode of operation is adequate for pilot-scale operations, commercial scale algae culturing operations would require harvesting and dewatering to be performed on a continuous basis.

Successful harvesting requires that algae cells be agglomerated to the extent that rapid settling can be achieved. Since the algae cells have a density of only slightly higher than 1.0 g/cm^3, it is imperative that individual cells be agglomerated to sufficient mass that settling will occur. This is typically accomplished with the addition of 5 to 10 ppm high molecular weight (4-6M MW) polyacrylamide flocculants. At this dosage, adequate settling and clarity are achieved in batch operation over approximately 2 hours. The objective of this study was therefore to develop a harvesting system capable of achieving similar, or improved performance in continuous operation.

In order to achieve rapid settling of flocculated biomass continuously, it is necessary to minimize turbulence within the flocculating vessel or thickener. Batch thickener operation clearly showed that flocs will settle under quiescent conditions, and the challenge is to design a system that will maintain quiescent conditions during continuous operation. Similar challenges are encountered in many water treating operations and are often remedied using lamella thickeners, which is the approach that was evaluated. The operating principle of lamella thickeners is to provide a flocculating chamber where floc growth can be promoted, thereby allowing most of the flocculated solids to settle from the moving fluid. Clarified water then migrates to the top of the settling vessel where it continuously overflows the thickener.

To minimize turbulence, overflowing clarified water must pass through an array of inclined lamella plates which serve two distinct purposes. First, the inclined plates minimize turbulence which prevents suspended solids from being entrained in the velocity profile of the overflowing liquid. Secondly, suspended solids in water migrating to the top of the vessel are provided with a surface on which to settle. This essentially means that suspended solids do not have to migrate independently to the bottom of the vessel to be removed. Rather, they only need to settle the short distance to the surface of lamella plates, where they accumulate. Since the lamella plate are inclined at 45^o, which is greater than the angle of repose of the biomass, accumulated biomass will slide along the plates and re-enter the settling zone, thereby minimizing entrainment in the overflow.

A small prototype lamella thickener was designed (Figure 58) and fabricated (Figure 59). The thickener was comprised of clear Plexiglas to allow visual observation of the settling process, with a total volume of 25 liters. Flocculated feed slurry is pumped into a cylindrical mixing chamber, from which flocculated biomass settles into a conical-shaped settling chamber in the lower portion of the vessel. The conical shape promotes compaction as the flocculated biomass settles to the base of the conical section where it is periodically removed through a ½ inch exit port by opening a discharge valve. The cylindrical section located just above the conical settling zone provides an area for further agglomeration of flocs to occur. As clarified water rises above the cylindrical section, it passes through an array of 11 lamella plates (each 6" x 6.5") inclined at 45^{o} to provide a settling surface for residual solids while minimizing turbulence. After rising through the lamella plates, clarified water overflows the device at a rate equivalent to the feed rate.

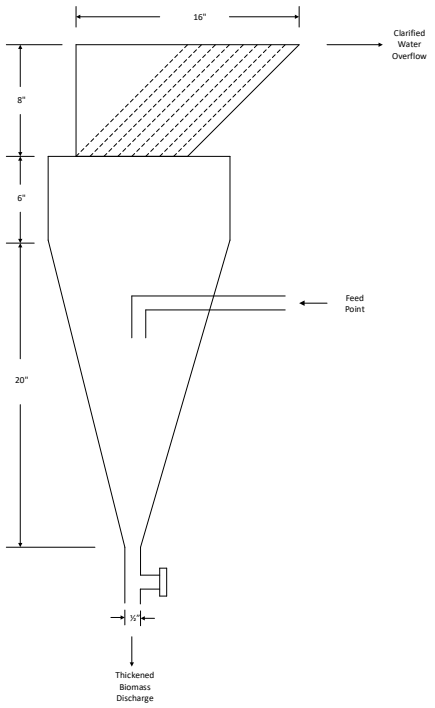

Figure 58. Schematic diagram of prototype lamella thickener

Figure 59. Prototype lamella thickener

Initial testing was conducted by pre-flocculating the algae culture and pumping it into the device to verify operational performance. The primary operating variable evaluated was feed rate in order to establish the required retention time to achieve acceptable underflow and overflow quality. Figure 60 shows thickener operation during the initial stage of operation where flocculated algae entering the device settles in the conical section. During the latter stages of operation (i.e., after 2 hours) water in the cylindrical mixing section is much more turbid; however, the water rising through the lamella plates remained clear, as shown in Figure 61.

Figure 60. Lamella thickener during initial stage of operation

Figure 61. Lamella thickener after 2 hours of operation.

The effect of feed rate on solids capture is shown in Figure 62. These tests were conducted using a constant dosage of 7 ppm commercial grade cationic flocculant (4650 VHM) supplied by SNF Flomin, Baytown TX. Solids capture was determined by mass balancing the difference between the feed suspension and overflow water quality using three different measuring techniques: dry mass, absorbance and cell counting, all done in triplicate and reported as an average. Samples of the pre-flocculated feed suspension were taken at the beginning of the test and samples of the overflow water were taken throughout the test. Dry mass was determined by filtering samples through 0.45 µm filter paper and weighing samples after drying. Absorbance was determined by measuring chlorophyll A absorbance using a spectrophotometer, while cell count was determined using a standard microscopy technique. Results using absorbance measurements showed solids capture increased from 95% to 99% as retention time increased from 42 minutes to 62 minutes. Similar results were obtained using cell count data. Dry mass results showed a decrease in solids capture as retention time increased, attributed to the difficulties associated with drying and weighing the very small quantity of solids present in the overflow water. From this experiment, it appears that absorbance measurements provide the most reliable and reproducible results.

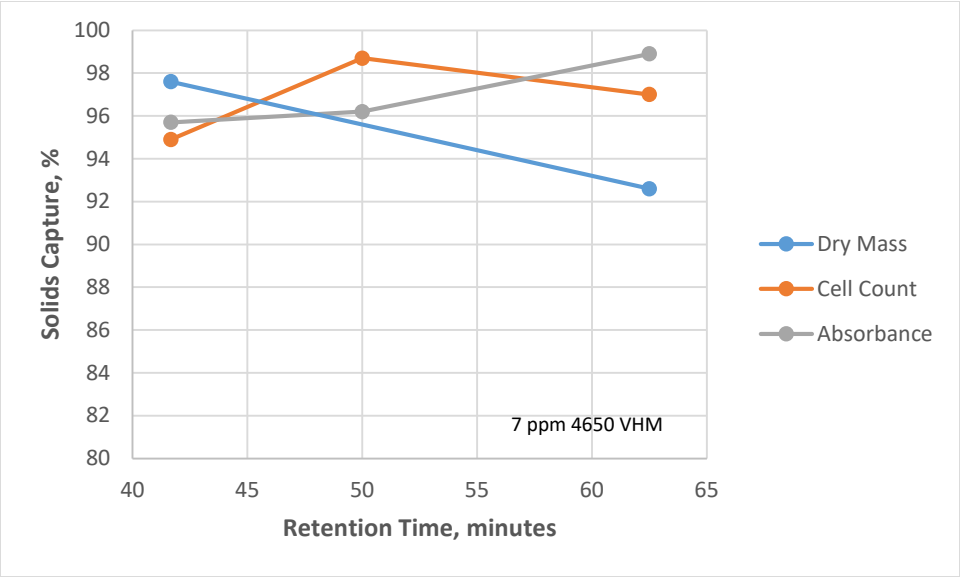

Figure 62. Effect of feed rate on solids capture for lamella thickener

Thickening tests were continued using the prototype lamella thickener to understand the effect of varying flocculent concentrations. Figure 63 shows the effect of flocculant dosage on solids capture from tests performed using fixed feed rate of pre-flocculated feed. As the flocculant dosage was increased from 2 to 7 ppm, solids capture determined by absorbance increased from 60% to 96%. Similar trends were observed when results were calculated based on cell count and dry mass, although the actual solids capture was different for each measurement technique. The important conclusions that can be drawn from these results are that with a retention time of 50 minutes, >90% solids capture is achieved on pre-flocculated algae using a dosage of >5 ppm cationic flocculant, as determined by absorbance and cell count measurement. Results using dry mass measurement were somewhat lower (i.e., >85%) although the same basic trend was observed.

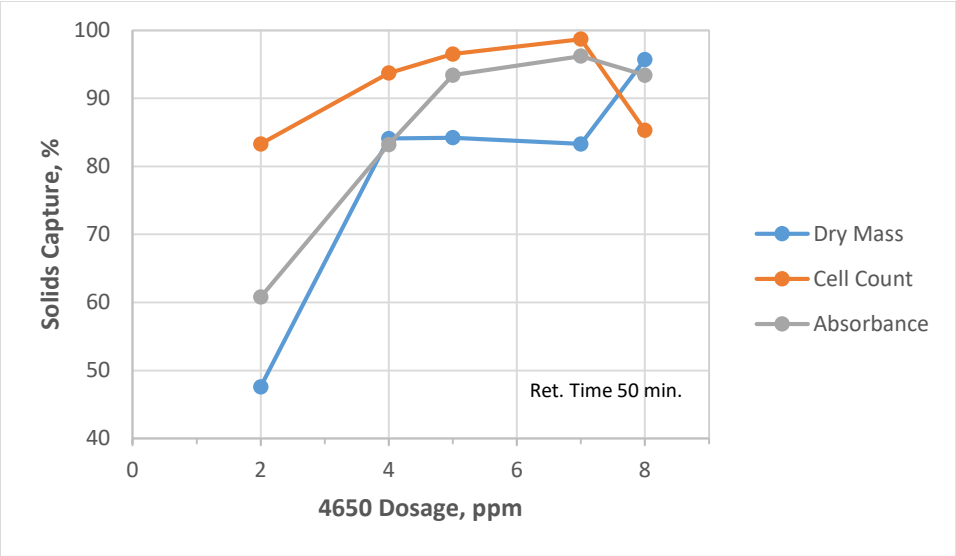

Figure 63. Effect of flocculant dosage on solids capture for lamella thickener performance using pre-flocculated feed

In order to demonstrate the viability of continuous operation, it was necessary to develop a feed arrangement that would allow the feed suspension and flocculant solution to be pumped separately and adequately mixed to promote floc formation prior to entry into the lamella thickener. This was accomplished by using a static mixer. Dilute flocculant solution was continuously pumped via a metering pump into the algae feed slurry prior to entry of both fluid streams into the static mixer. The mixed suspension then flowed immediately into the lamella thickener. Figure 64 summarizes the results of a longer duration test (i.e., 5 hours) with a fixed retention time (50 minutes) at a dosage of 8 ppm flocculant. Solids capture (by absorbance measurement) was 87% after 1 hour and increased to >90% after 3 hours. Similar results are shown for both cell count and dry mass measurement techniques.

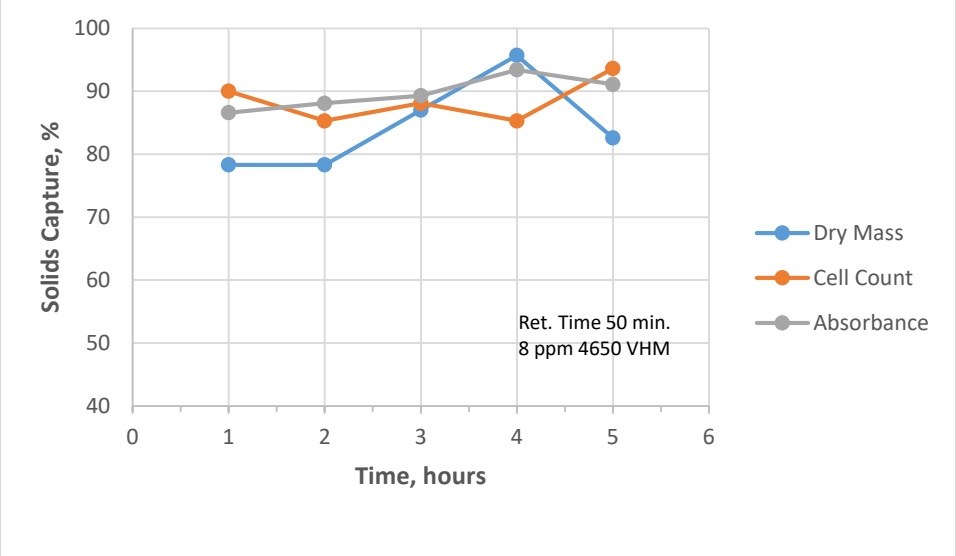

Figure 64. Results of continuous thickening tests

One limitation that was observed with continuous testing was that flocculated solids accumulated on the walls of the conical section, rather than settling to the compaction zone at the base of the device prior to discharge. As the test progressed, small bubbles were observed forming on the flocculated algae, and flotation of algal flocs occurred. While the mechanism of bubble formation is not known presently, if high solids capture is to be maintained, it is imperative that flocculated solids be removed from the walls of the thickener rather than accumulate. A simple mechanical scraper was designed and fabricated to be inserted into the conical section of the thickener. The scraper would be rotated periodically to dislodge settled flocs and minimize any build-up of settled solids.

Field testing of continuous dewatering unit:

Continuous thickening tests were conducted at East Bend Station using the 25 liter volume lamella clarifier described previously. Harvested algae slurry was continuously pumped into the device using a variable speed pump while a solution of cationic flocculant (VHM 4650) was metered into the slurry feed line. Mixing was accomplished as the two flow streams passed through an in-line static mixer. The feed slurry and clarifier overflow stream were sampled at regular time intervals, with solids capture being calculated based on the difference between the flow rate of algae cells into the clarifier and the flow rate of algae cells in the overflow. Retention time was changed by varying the slurry feed rate while flocculant dosage was changed by adjusting the flocculant solution metering pump. Results are summarized in Figure 65. At a flocculant dosage of 6 ppm, solids capture was only 50 to 60 % over a retention time range of 35 to 50 minutes. When the flocculant dosage was increased to 10 ppm, solids capture increased from 62% to 80% as the retention time increased from 39 minutes to 50 minutes. The low solids capture achieved in these tests is attributed to the low culture density of the harvested feed, which was only 0.37 g/liter.

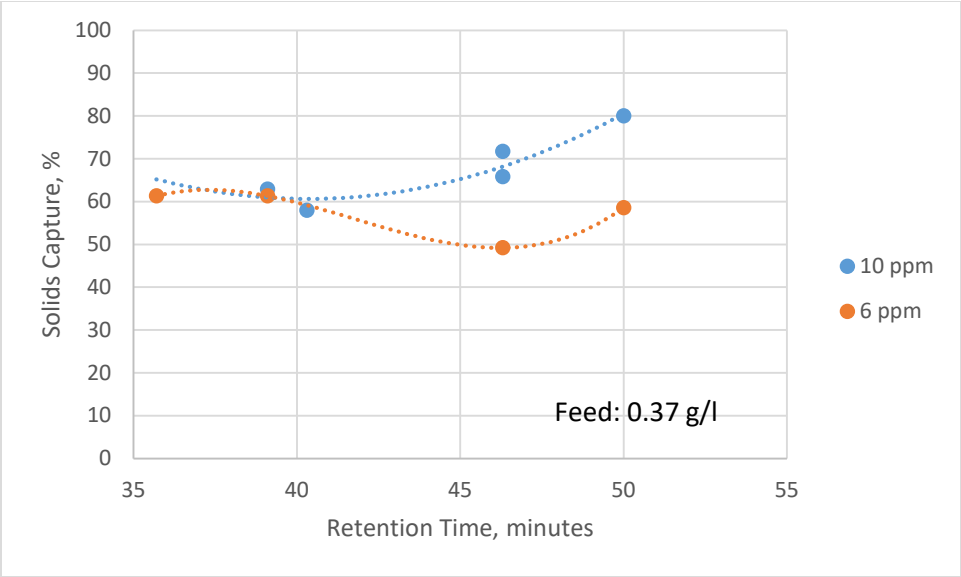

Figure 65. Effect of retention time and flocculant dosage on solids capture for harvested algae at East Bend using a lamella clarifier.

The effect of flocculant dosage was determined in previously reported testing using the same experimental conditions. Using a longer retention time (i.e. 90 to 120 min), solids capture improved from 61% to 98% as the flocculant dosage was increased from 2 ppm to 7 ppm, and the minimum flocculant dosage required to achieve the target objective of 90% solids capture was 5 ppm (Figure 66). However, these results were obtained using a higher feed culture density of 0.7 to 2.3 g/l dry mass.

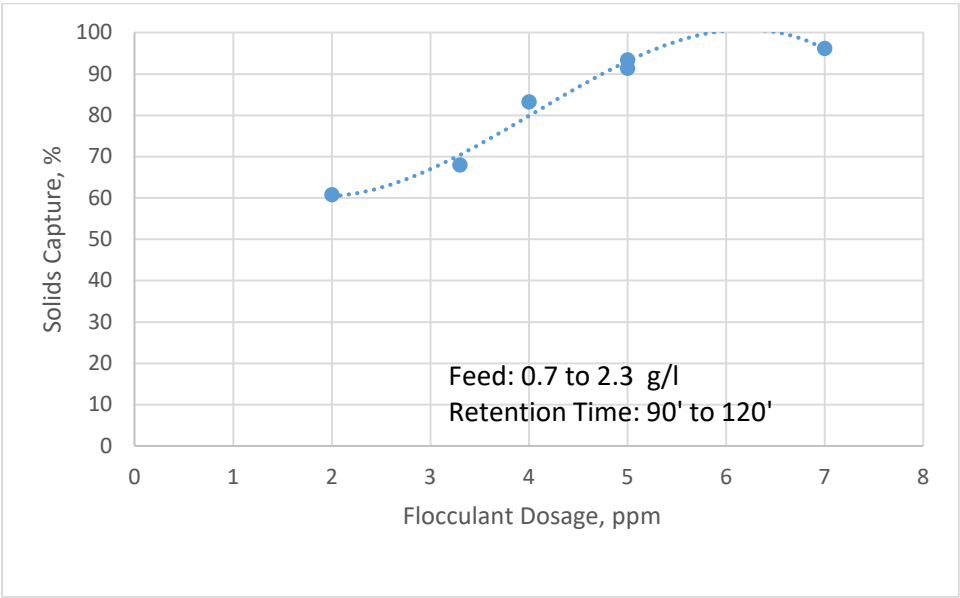

Figure 66. Effect of cationic flocculant dosage on solids capture on harvested algae using a lamella clarifier.

The importance of feed culture density is shown in Figure 67. At a retention time of 50 minutes and a flocculant dosage of 8 ppm, solids capture was maintained at 90% over a 5 hour duration. These results were obtained with a feed culture density of 0.74 g/liter. Repeating the test using a lower dosage of 4 ppm achieved much lower solids capture. These results illustrate the importance of flocculant dosage and suggest that a dosage of 8 ppm is sufficient to maintain 90% solids capture at a retention time of 50 minutes, provided that the feed culture is sufficiently dense. When the feed culture contained only 0.37 g/liter (Figure 65), a similar dosage provided only 80% solids capture at the same retention time. Hence, these results clearly show the importance of feed culture density on thickening performance. In order to achieve the target objective of 90% solids capture at a retention time of 50 minutes, a flocculant dosage of 5 ppm is sufficient, provided that the feed culture density is adequately high (i.e., >0.5 g/l). If the feed culture density is lower, a flocculant dosage greater than 10 ppm is required. While flocculating lower culture density feed is achievable with higher flocculant dosage and longer retention time, test results show that harvesting dense cultures (>0.5 g/l) is the preferred option. Floc formation, growth and settling is more effective at a given dosage when there are more cells present.

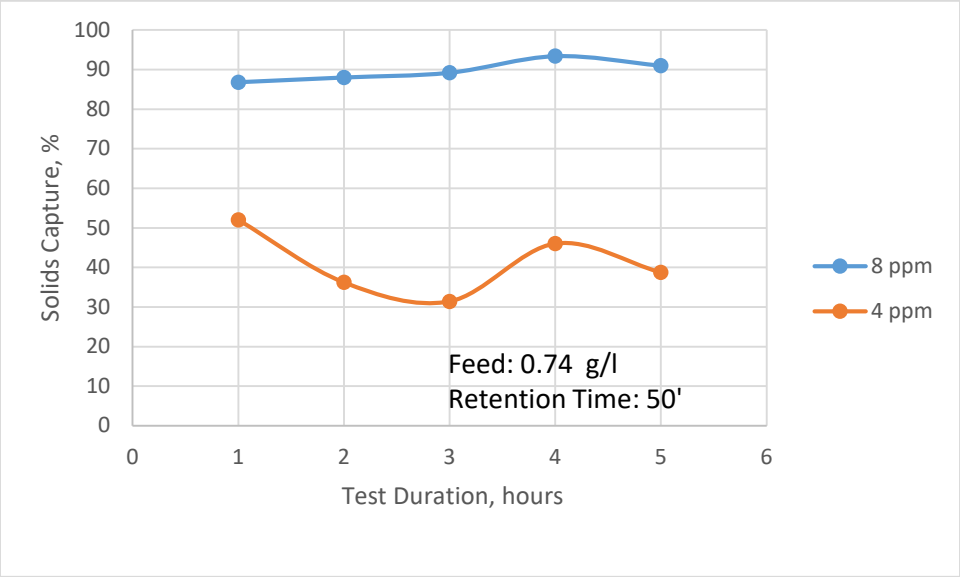

Figure 67. Effect of flocculant dosage on solids capture on high culture density harvested algae using a lamella clarifier.

Conclusions

A wide range of commercial flocculants were screened to gain a better understanding of the requirements of algae biomass dewatering. It was determined that a low dosage of high molecular weight cationic flocculant, combined with 1-2 ppm anionic flocculant yielded the best results.

A demonstration scale continuous dewatering system was designed, prototyped, and tested highlighting the effects of harvested culture density, retention time, and mixing on solids capture.

Under the appropriate conditions (typically, culture density of >0.5 g/L and retention time of 50 min), continuous dewatering was demonstrated with adequate solids capture performance.

3.2.4. Power Plant Heat Integration

Given the limited growing season in Kentucky and other states of similar latitude, a study was conducted to evaluate the possibility of using low grade waste heat as a way to elevate the temperatures of algae cultures during seasonally cool conditions, thereby extending the growing season. Several potential heat sources were examined using East Bend Station as a base case, and a heat transfer model for the cyclic flow PBR that includes calculated heat transfer coefficients was finalized. The most abundant and accessible heat source is a water stream that flows from the boiler structure to the cooling towers. This stream contains waste heat as water at a temperature range of 45-32 °C and flow rate of 910,000 L/min.

Initial calculations showed that heating the PBR via the flue gas feed is not practical given the low heat capacity of flue gas and its estimated flow rate into the system. A more feasible design was considered, in which algae culture temperatures are elevated through the use of a countercurrent heat exchanger during the liquid cycling process in the PBR (Figure 68).

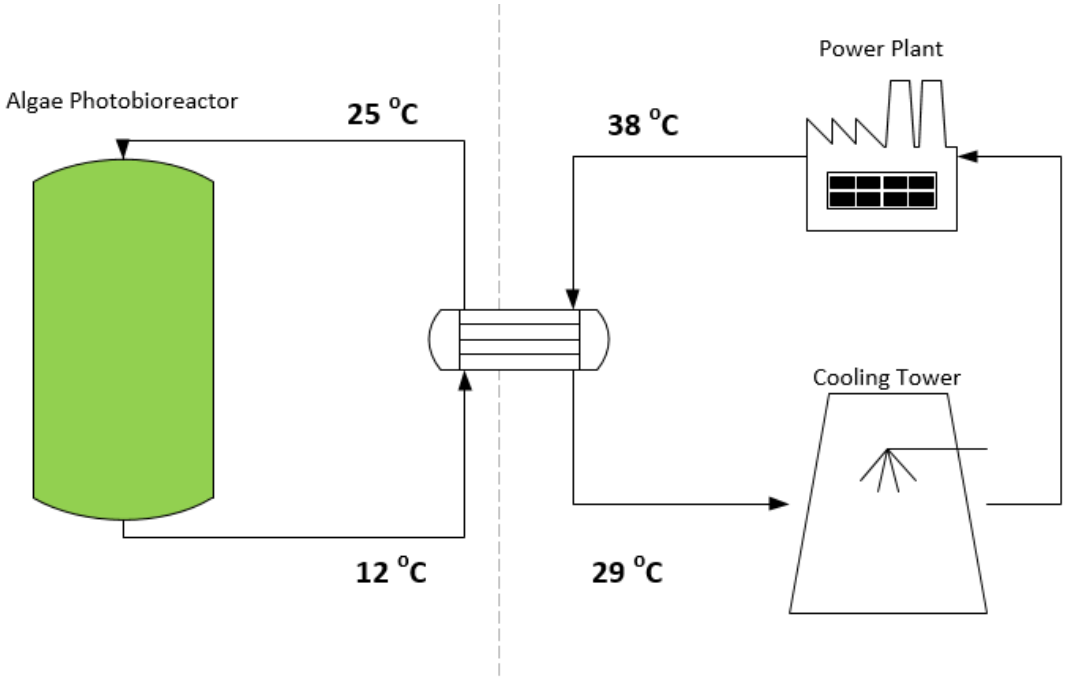

Figure 68. Process flow diagram for heat exchanger. Algae cultures are heated from 12 °C to 25 °C. A slipstream of water that circulates from the power plant to the cooling towers is cooled from 38 °C to 29 °C.

From previous experiments with *Scenedesmus* algae cultures conducted at the UK CAER, it was observed that photosynthesis begins as culture temperatures approach 12 °C, i.e., temperatures below 12 °C cannot sustain culture growth. This was ascertained by monitoring oxygen

evolution within cultures as a function of temperature. Data suggest a temperature of 25 °C as being optimal for algae culture growth. In order to determine how often the cyclic flow PBR would require heat injection in cold weather via cycling, a heat transfer model was constructed based on the cooling time from 25 °C to 12 °C within the cyclic flow PBR and overall heat transfer coefficients were derived and calculated using two different models.

The cyclic flow PBR currently cycles every 6 hours, using a pump to drain and fill the tube banks. Time-temperature charts (first model) and summary techniques (second model) were used to determine the reactor cooling times, from which the required frequency of cycling was calculated (required to maintain the reactor at a temperature of at least 12 °C). The energy cost associated with the increase in required cycling time was calculated for a hypothetical algae installation (sized for 1 MW power plant), the energy requirement being calculated according to an LCA previously performed at UK.

Initially, the injection of flue gas was considered as a heat transfer mechanism. This would have allowed for normal operation of the reactor with no increase in cycling frequency, incurring only the energy penalty associated with heating the injected gas. However, given its low heat capacity, around 1000 J kg^{-1} K^{-1}, calculations showed flue gas to be an inadequate carrier of heat to the reactor (Figure 69).

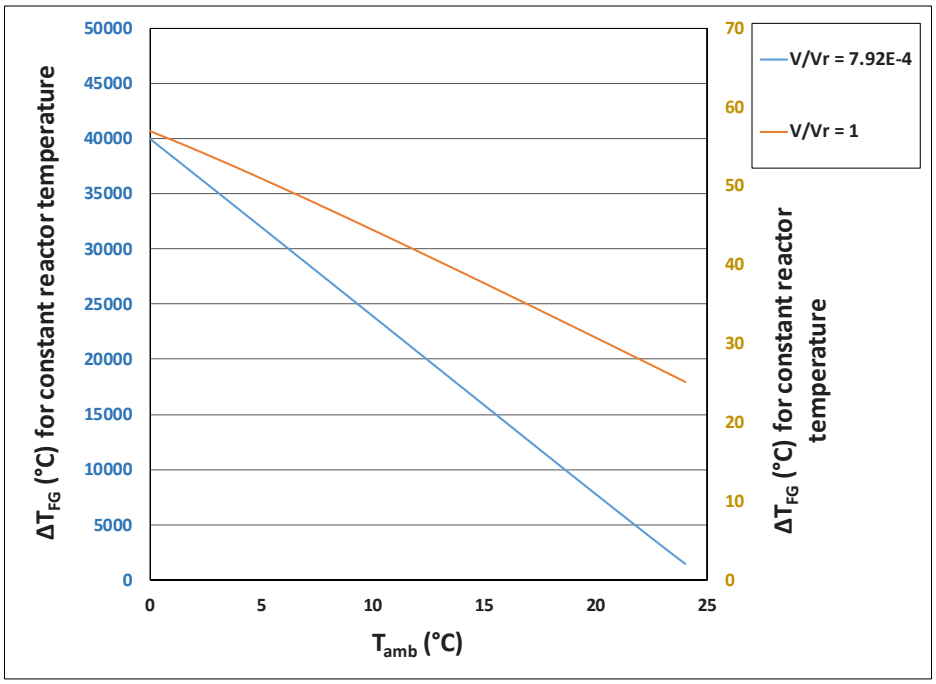

Figure 69. ΔT for flue gas injection at different flow rates vs. ambient temperature. The blue line represents the current $\dot{V}/V_R$ for the cyclic flow reactor (7.92E-4) and is correlated with the left y axis. The orange line represents a theoretical $\dot{V}/V_R$ of 1 for the cyclic flow reactor and is correlated with the right y axis. Calculations were based on the first heat transfer model with an average wind speed of 5 m/s and an overall heat transfer coefficient range of 28.1-30.8 W/m^2K. Units of $\dot{V}/V_R$ are s^{-1}.

Within Figure 69, the blue line represents $\dot{V}/V_R$ associated with the current estimated volumetric flow rate into the cyclic flow PBR of 0.9 L/s (reactor volume = 1136 L). Both y axes represent the associated change in flue gas temperature required to supply sufficient heat to maintain a constant reactor temperature of 25 °C at the given ambient temperature range. At current volumetric flow rates, the ΔT needed to keep the reactor at a constant 25 °C is in the range of 2500-60000 °C, a ludicrous range. The orange line and right y axis represent a volumetric flow rate of flue gas of 1136 L/s, or a V/V_r of 1 and has a reasonable ΔT range but an impossible volumetric flow rate. This gas injection quantity would displace all of the liquid within the reactor.

Within the cyclic flow reactor, each tube acts as an individual bubbling fluidized bed reactor. Flue gas is injected via compression-induced pressure-driven flow and bubbled through the columns (tubes). A basic model for heat transfer within a column is derived as follows:

$$q_r = q_U + q_{FG} + q_\lambda \tag{1}$$

where q_U is the conductive heat transfer at the reactor wall, q_{FG} is the heat supplied to the reactor by the injected flue gas, and q_λ is the heat contribution from the latent heat of water associated with the change in the state of the water contained in the gas entering and leaving the reactor.

For estimative calculations, a steady state model can be applied in the form of

$$-m_R Cp_R \left(\frac{dT_R}{dt}\right) = UA\,(T_R - T_\infty) + \dot{m}_{FG} Cp_{FG}(T_{in} - T_{out}) + \dot{m}_{FG}\lambda_{H_2O}\left(y_{H2O_{IN}} - y_{H2O_{OUT}}\right) + \mathcal{F}_{12} A\sigma({T_{wall}}^4 - {T_{sun}}^4) \tag{2}$$

Two models were created based on these equations. The first model was built using tabulated data as well as physical and material properties of the cyclic flow reactor. The model was constructed based on the cyclic flow PBR's material composition, geometry and position at East Bend Station. Initially the model was based on tabulated data for water, polyethylene terephthalate (PET) and air using correlations found in the literature, considering the surface area of the tubes to be the site of heat transfer.

In this model, the reactor was assumed to be filled with standing water, neglecting the effects of flue gas injection. Therefore, the first model attempted to provide an estimate of q_U. Forgoing flue gas calculations (q_{FG} and q_λ) allowed for an initial estimation of heating and cooling times for liquid in the reactor. This approach separated liquid and gas phase heat transfer calculations, allowing the model to determine the feasibility of one phase contributing heat to another.

Data also confirmed that the heat contributions of q_2 and q_3 (those contributed by flue gas injection and latent heat resulting from the change of the mass fraction of water in the gas phase) were negligible. Conduction, as represented by q_1, which is dominated by sunlight (solar gain) and wind speed, was the main heat transfer driving force as confirmed by data collected at East Bend (see Figure 70).

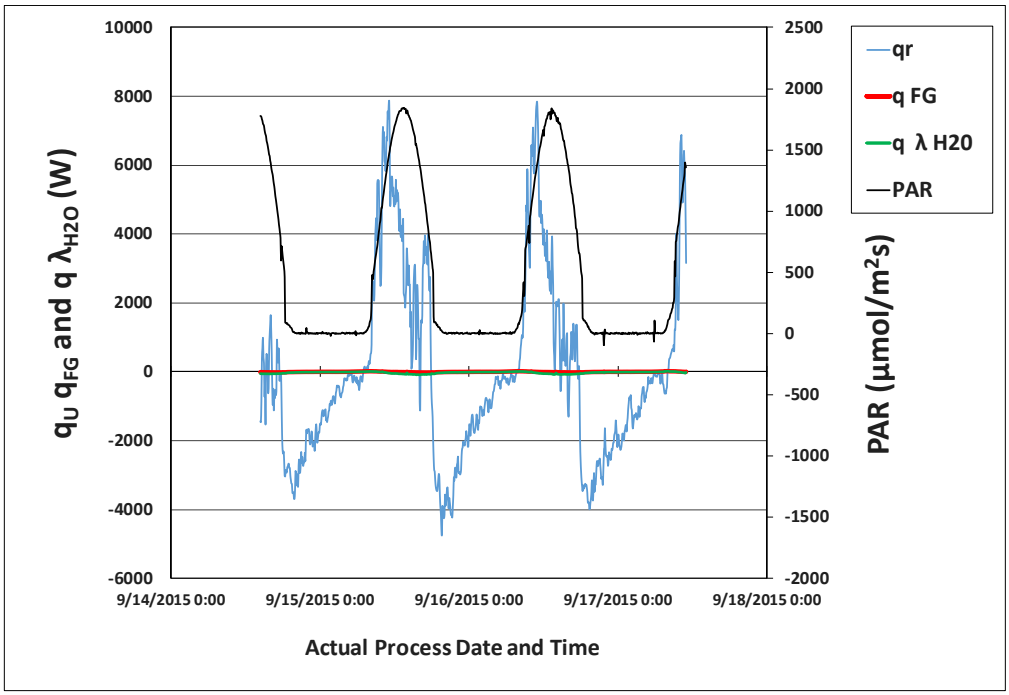

Figure 70. Heat contributions to the cyclic flow PBR and PAR (photosynthetically active radiation) vs. time. Reactor conduction, q_U, follows a pattern consistent the presence or absence of sunlight and is shown to be orders of magnitude larger than contributions from gas injection.

In order to estimate U for the first model (the overall heat transfer coefficient for the reactor) based on tabulated data and physical and material properties for the cyclic flow PBR, a model for a single tube was necessary. The steady-state heat transfer coefficient for a single tube in the cyclic flow PBR is defined as the inverse of the sum of convective and conductive resistances, modeled for a long cylinder:

$$U = \left[A_o\left[\left(\frac{1}{h_{H_2O}A_i}\right) + \left(\frac{\ln\left(\frac{r_o}{r_i}\right)}{2\pi K_{PET}L}\right) + \left(\frac{1}{h_{air}A_o}\right)\right]\right]^{-1} \quad (3)$$

This heat transfer coefficient is comprised of inverse resistances based on the natural convection of water within the reactor (assumed to be standing for estimative calculations), the conductive resistance of the PET wall material at its given thickness and the forced convection of air against the tubes in crossflow.

The forced convective heat transfer coefficient of air in crossflow with a single cylinder was also calculated using correlations from Churchill and Bernstein (Churchill and Bernstein, 1977):

$$\overline{Nu_{D^1}} = 0.3 + \left\{\frac{0.62 Re_D^{\frac{1}{2}} Pr^{\frac{1}{3}}}{\left[1 + (0.4/Pr)^{\frac{2}{3}}\right]^{\frac{1}{4}}}\right\}\left[1 + \left(\frac{Re_D}{282{,}000}\right)^{\frac{5}{8}}\right]^{\frac{4}{5}} \quad (5)$$

The Nusselt number calculated for a single tube ($\overline{Nu_{D^1}}$) served as a precursor to a more accurate Nusselt number based on the PBR's tube bank positioning. As they are positioned, the tubes act as a staggered tube bank heat exchanger with $N = 2\ (number\ of\ rows)$ (see Figure 71). Correlations used for the staggered tube bank Nusselt number were taken from Mills (Mills, 1999).

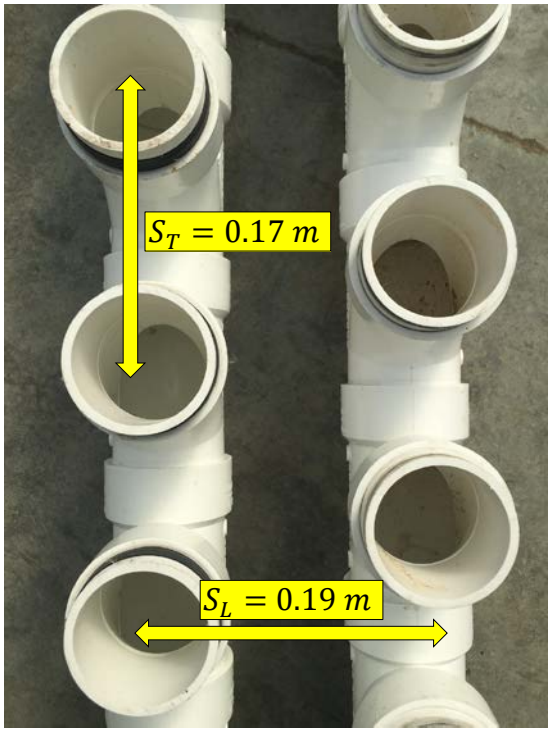

Figure 71. Top down view of the cyclic flow PBR tube bank. S_T and S_L are measured factors used in determining the forced convection heat transfer coefficient of a staggered tube bank heat exchanger.

Taking into account the staggered arrangement of the tubes provided for a final Nusselt number and forced convection heat transfer coefficient using the equations (Mills, 1999):

$$v_\infty = \frac{\bar{v}\left[S_T - \left(\frac{\pi D}{4}\right)\right]}{S_T} \tag{6}$$

And

$$\Phi = 1 + \frac{2}{3P_L} \tag{7}$$

Where

$$P_L = \frac{S_L}{D} \tag{8}$$

and

$$\overline{Nu_D} = 1 + \frac{(N-1)\,\Phi\,\overline{Nu_{D1}}}{N} \tag{9}$$

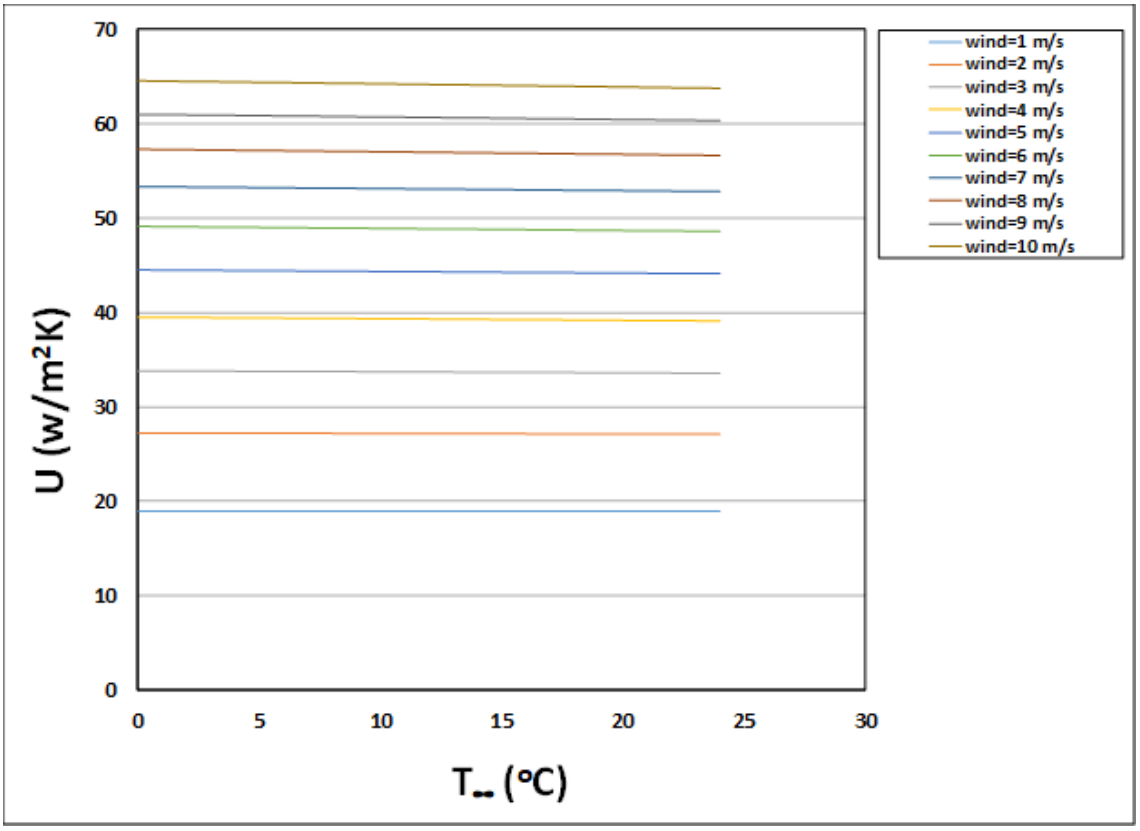

Figure 72. U (W/m^{2}K) vs. ambient temperature at a range of wind speeds.

Figure 72 demonstrates the dominance of the forced convection coefficient of air in a range of overall heat transfer coefficients. The range of U dictated by wind speed at a given temperature is large, with a given of range of ~19-64 W/m^{2}K. At an average wind speed of 2 m/s the range of values of the overall heat transfer coefficient for the cyclic flow PBR was calculated to be 27.0 W/m^{2}K from 0-11 ^{o}C.

The second model, based on empirical real-time data collected at East Bend station during the 2015 growing season, was constructed using a linearization of the initial heat transfer equations. Equation 2 is a steady state 'snapshot' estimation of Equation 1. With minimal algebraic rearrangement, Equation 2 becomes:

$$\left(\frac{\Delta T_R}{\Delta t}\right) = \frac{UA(T_R - T_\infty)}{m_R Cp_R} + \left[\frac{\dot{m_{FG}} Cp_{FG}(T_{in} - T_{out})}{m_R Cp_R} + \frac{\dot{m}_{FG}\lambda_{H_2O}(y_{H2O_{IN}} - y_{H2O_{OUT}})}{m_R Cp_R} + \frac{\mathcal{F}_{12}A\sigma\left({T_{wall}}^4 - {T_{sun}}^4\right)}{m_R Cp_R}\right] \quad (10)$$

And is linearized by:

$$y = \left(\frac{\Delta T_R}{\Delta t}\right) \quad (11)$$

$$x = (T_R - T_\infty) \quad (12)$$

$$m = \frac{UA}{m_R Cp_R} \quad (13)$$

$$b = \left[\frac{\dot{m_{FG}} Cp_{FG}(T_{in} - T_{out})}{m_R Cp_R} + \frac{\dot{m}_{FG}\lambda_{H_2O}(y_{H2O_{IN}} - y_{H2O_{OUT}})}{m_R Cp_R} + \frac{\mathcal{F}_{12}A\sigma({T_{wall}}^4 - {T_{sun}}^4)}{m_R Cp_R}\right] \quad (14)$$

Ambient temperature and reactor temperature were recorded for the 2015 growing season. The mass and heat capacity of the liquid within the reactor were estimated based on the PBR's known volume and the density and heat capacity of water. At any time the algae culture amounted to less than 0.1% of the total mass within the reactor and its contributions to density and heat capacity were considered negligible.

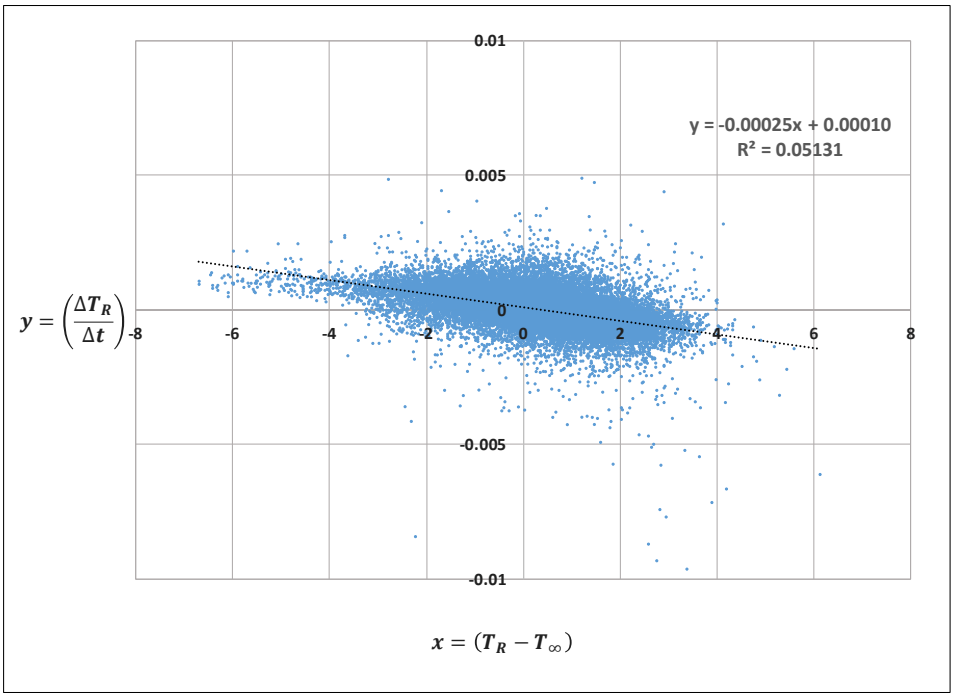

Figure 73. Linear correlation of change in temperature inside the PBR over time vs. temperature inside the PBR minus ambient temperature. Data were acquired during the 2015 East Bend growth season. Graph represents over 42,000 data points averaged every five minutes over a 5 month period in 2015.

Linearization of change in reactor temperature over change in time vs. reactor temperature minus ambient temperature data gives the equation:

$$\left(\frac{\Delta T_R}{\Delta t}\right) = -0.00025(T_R - T_\infty) + 0.0001 \qquad (15)$$

Based on the slope in Figure 73, Equation 15 can be used to back out an overall heat transfer coefficient of 24.8 W/m^{2}K. This value for U (W/m^{2}K) provided by the second model is well within the range of 19-64 W/m^{2}K supplied by the first model and is extremely close to the overall heat transfer coefficient provided by the first model at a wind speed of 1.7 m/s.

In order to determine the cooling time based on the empirical model, summary methods were used using the data-based linear correlation summation:

$$\Delta t_{cooling} = \sum_{i=(T_R=25^0C,T_R-1)}^{(T_R=12^0C)} \Delta t_i = \sum_{i=(T_R=25^0C,T_R-1)}^{(T_R=12^0C)} \frac{T_{R_i} - T_{R_{i-1}}}{m(T_{R_i} - T_\infty) + b} \qquad (16)$$

Time-temperature tables were used to interpolate cooling times for the cyclic flow PBR within a range of wind speeds as seen in Figure 74 and were calculated using both heat transfer models. Cooling times associated with the first model were calculated using ambient temperatures (T_∞) and wind speeds at ranges of respectively 0-12 ^oC and 2-8 m/s. Included in Figure 74 is a cooling time curve associated with the second data-based model, using the same ambient temperature range.

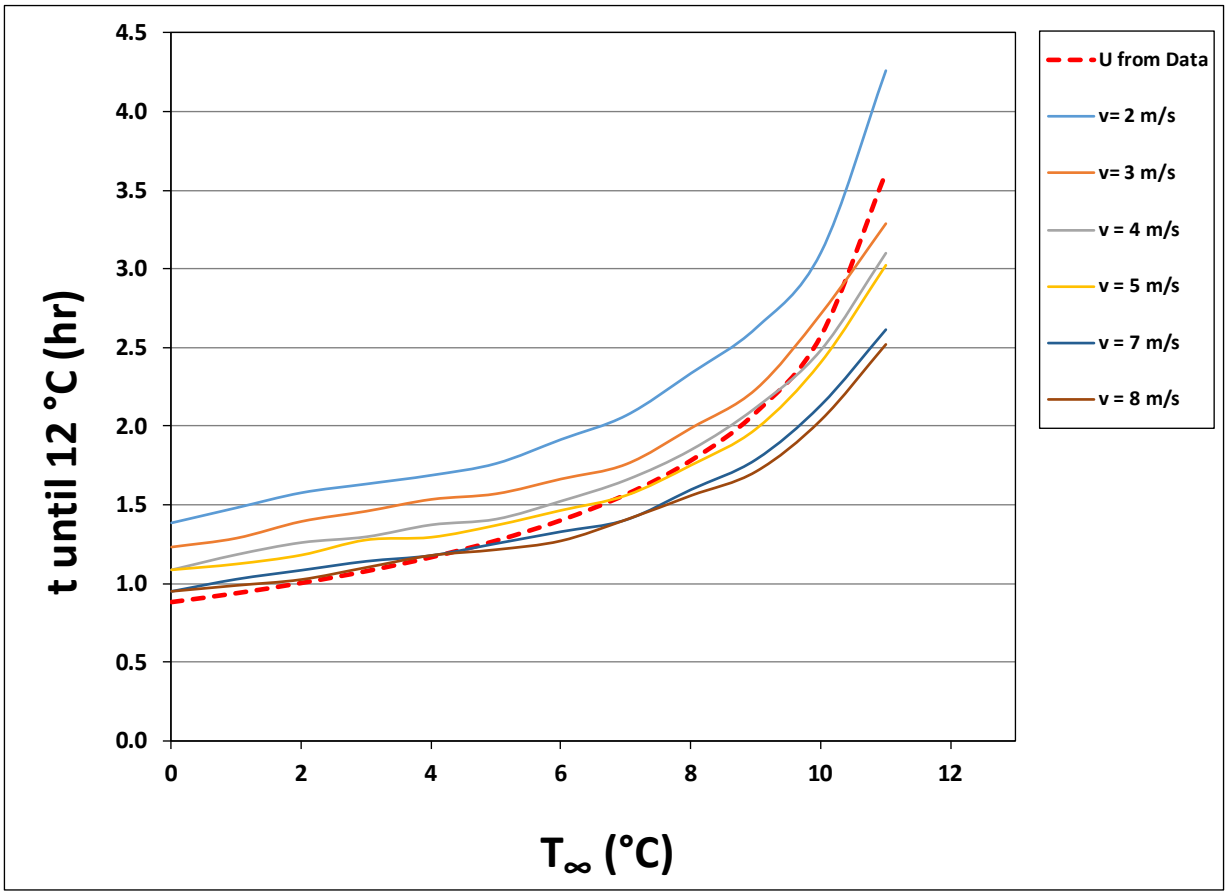

Figure 74. Reactor cooling times from the first model at various ambient temperatures and wind speeds as well as cooling times calculated using the second model (shown in red).

All of the calculated cooling times were less than the current cycle time of 6 h. The current feed pump work duty of 0.22 MWh/day, according to a recent LCA, was used as a basis of calculation in determining the energy penalty associated with the increase in cycling frequency. The new feed pump duty associated with this increase was calculated assuming that additional pump requirements would be fulfilled by the installation of multiple, identical pumps.

The pump duty associated with the transportation of circulating water from the heated water stream to the PBR was calculated assuming a stainless steel pipe with a pipe diameter of 0.15 m, traveling a distance of 100 m. The latter is a rough estimation of the current distance between the circulating water pipeline and the cyclic flow PBR at East Bend Station.

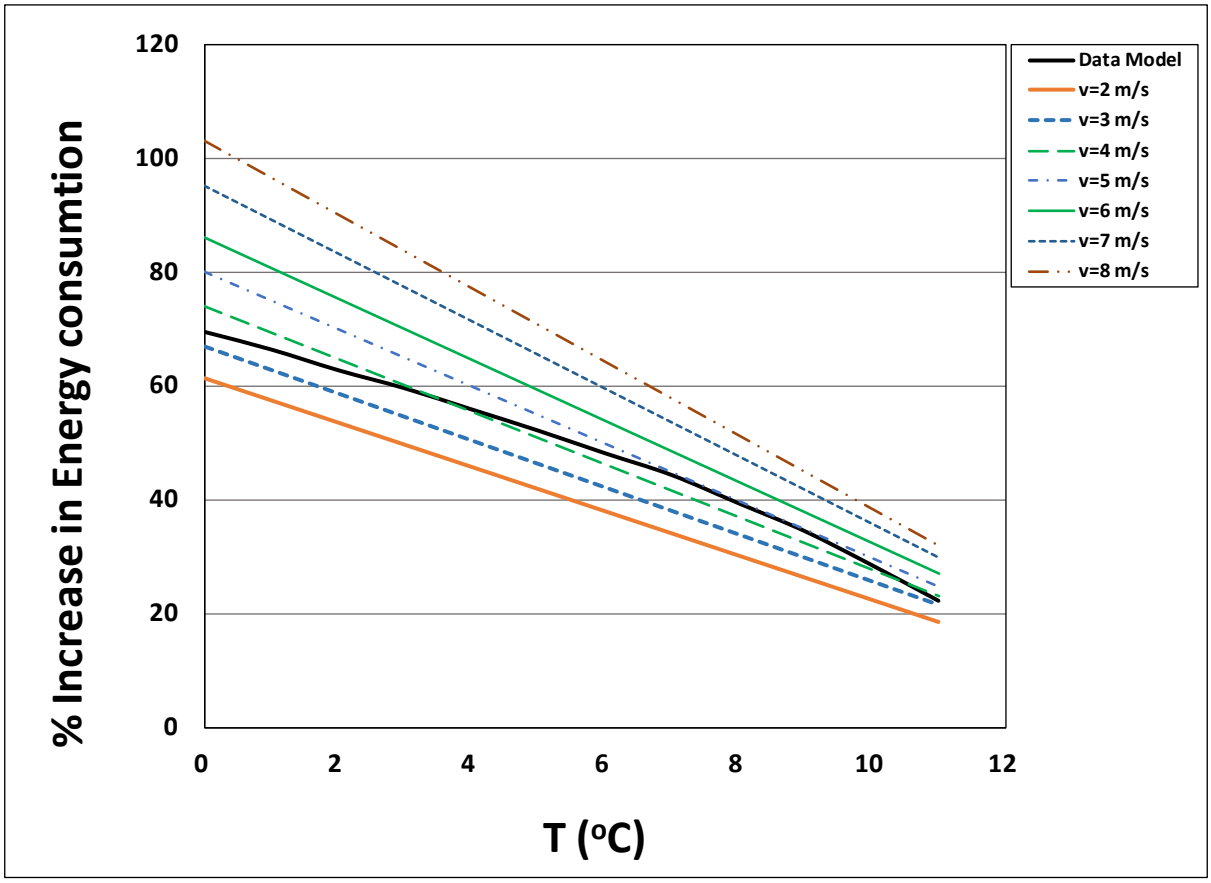

Figure 75. Energy increase requirement for operation with increased cycling for all pumps (additional feed pumps plus pumps used for transport of heated circulating water). Power requirements shown are based on cooling times calculated using various wind speeds from the theoretical model and from the heat transfer coefficient derived in the data-based model.

Percent increase in system energy consumption ranges from 18-103% at given wind speed and temperature. The above chart could prove quite useful for operative predictions for a PBR in cold climates. One important factor to note is that solar gain is not accounted for in the first model which is based on tabulated data. Actual solar gain is implicit in the data collected at East Bend Station used in creating the second model. Despite these stark differences in method, both models produced strikingly similar heat transfer coefficients. This implies that one could use the lines in Figure 75 contributed by the first model as a metric for increased energy use for any PBR in colder climates. If need be, a relatively small data set of PBR and ambient temperatures could be collected at potential site locations and used to determine the net transfer coefficient.

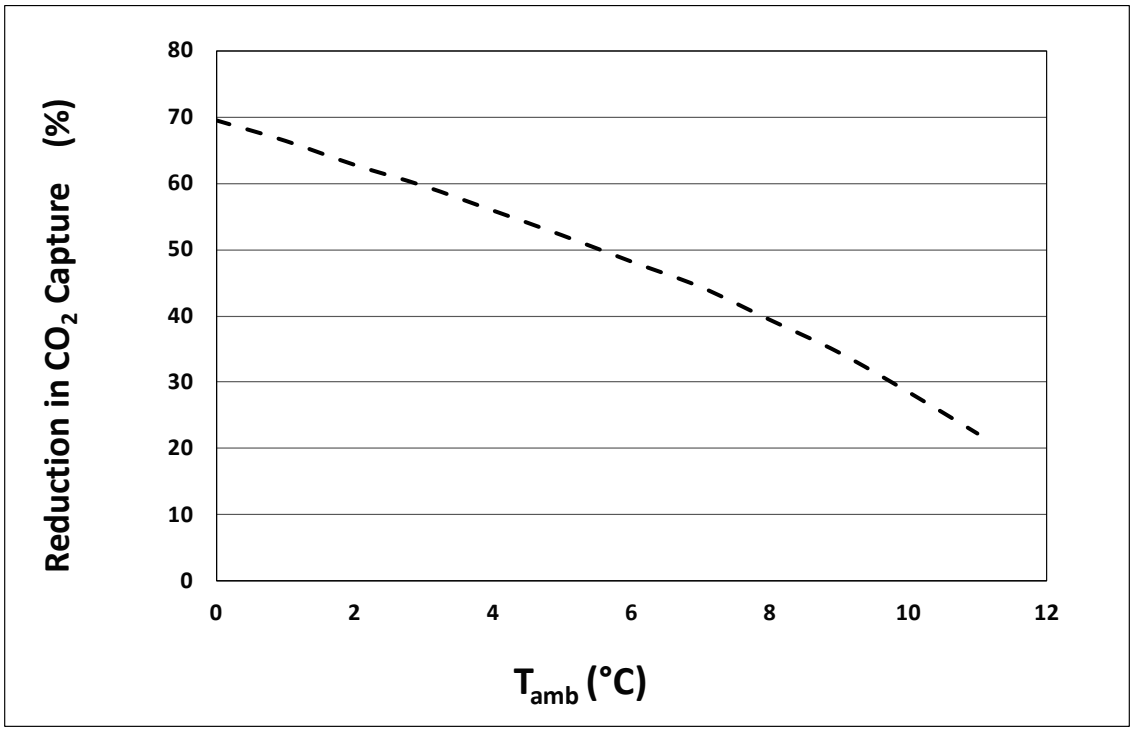

Figure 76. Reduction in overall CO_2 capture vs. ambient temperature for a photobioreactor with operating heat integration equipment. Reduction in CO_2 capture values are instantaneous energy penalties associated with the operation of heat integration equipment.

As shown in Figure 76, reduction of CO_2 capture occurs as a result of energy usage associated with increased liquid pumping both for algae cultures and circulating water. Instantaneous CO_2 capture penalties associated with heat integration operation are significant. During cold temperatures, keeping the algae culture at or above 12 °C has the potential to require 6 times the amount of liquid pumping as compared to the normal operation of the PBR without any heat integration. At ambient temperatures of 0-4 °C, reduction in CO_2 capture ranges from 55-70%. However, as temperatures approach freezing levels, reductions in CO_2 capture do not reach 100%, allowing for the overall process to remain carbon negative.

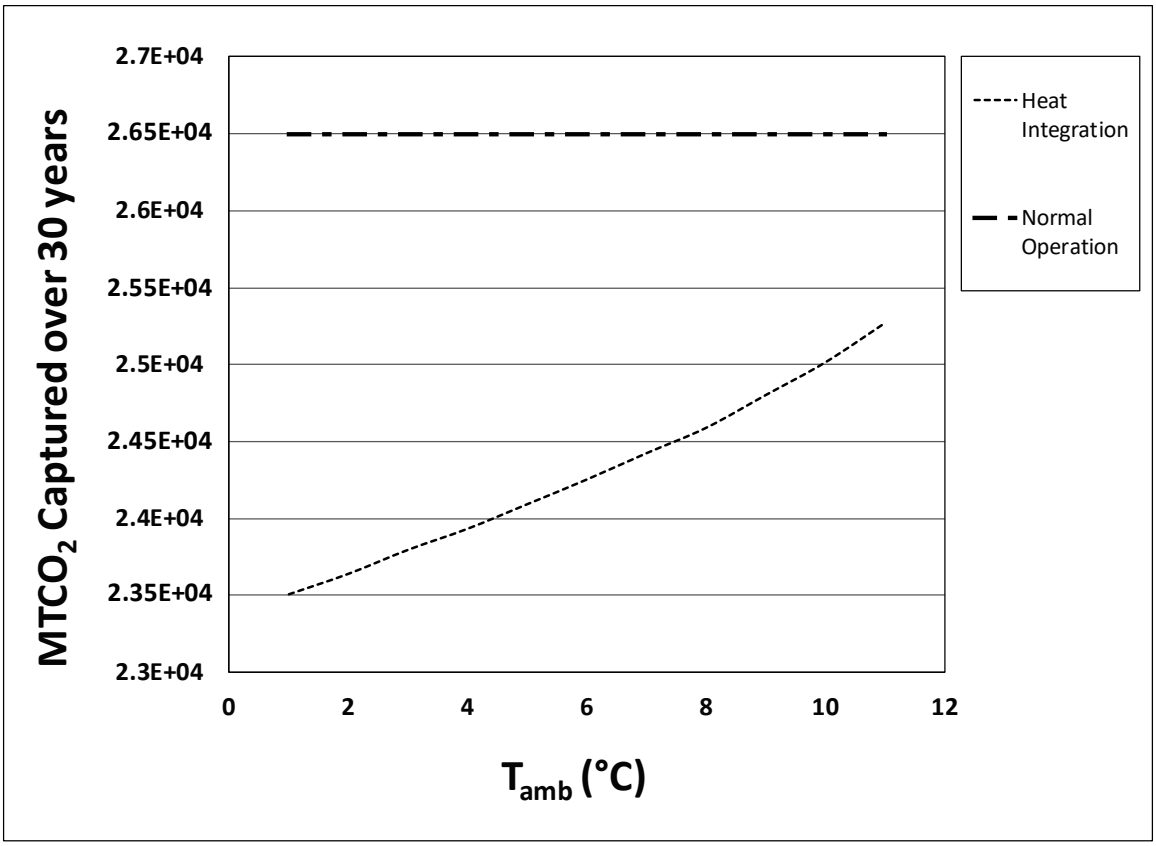

Figure 77. $MTCO_2$ captured over a 30-year period vs ambient temperature for two separate PBRs at a 1 MW power plant. Normal operation refers to a PBR system without heat integration equipment and a growing season of 240 operating days. Heat integration refers to a PBR system with heat integration equipment and a growing season of 300 operating days per year.

Penalties shown in Figure 77 were individually calculated assuming that heat integration equipment was in use for the 60-day growth season extension period and that temperatures during that period remained constant. This calculation was repeated for given temperatures in the range of 0-11^o C. Implementation of heat integration would not cause the system to become carbon positive and would only reduce CO_2 capture over the system lifetime by 2-12%.

Following extensive engineering calculations, life-cycle assessment and techno-economic analysis methods were implemented to assess the feasibility of this scenario. Table 11 summarizes the main assumptions made. For this study, a possible scenario was evaluated in which the growing season in Union, KY could be extended by 60 days by the installation and operation of equipment for utilizing waste heat from the power plant. The growing season was assumed to extend from 240 days to 300 days. 300 days is a likely number of operating days for a warmer climate similar to that of Florida.

Table 11. Inputs and assumptions used when calculating increases in CAPEX and OPEX due to heat integration

Input	**Value**	**Units / notes**
PBR flow rate	500	L/min
Circ. water flow rate	900	L/min
Plant capacity	1	MW
CO_2 capture efficiency	30	% (in-out)
Growth rate	25	g m^{-2} d^{-1}
Electricity price	0.02	$/KW-hr
Polypropylene cost	1,100	$/tonne
Pump cost	2,500	$/unit
Heat exchanger cost	33,000	$/unit
Heat exchanger cost (areal)	0.012	Unit/m^2

Heat exchangers were assumed to be in close proximity to the photobioreactor system. The pump duty associated with taking a slipstream of circulating water to the heat exchanger was calculated, assuming a stainless steel pipe material with an assumed pipe diameter of 0.15 m, the water traveling a distance of 100 m at flow rate of 900 L/min. This travel distance was a rough estimation of the current distance between the circulating water pipeline and the cyclic flow PBR at East Bend Station.

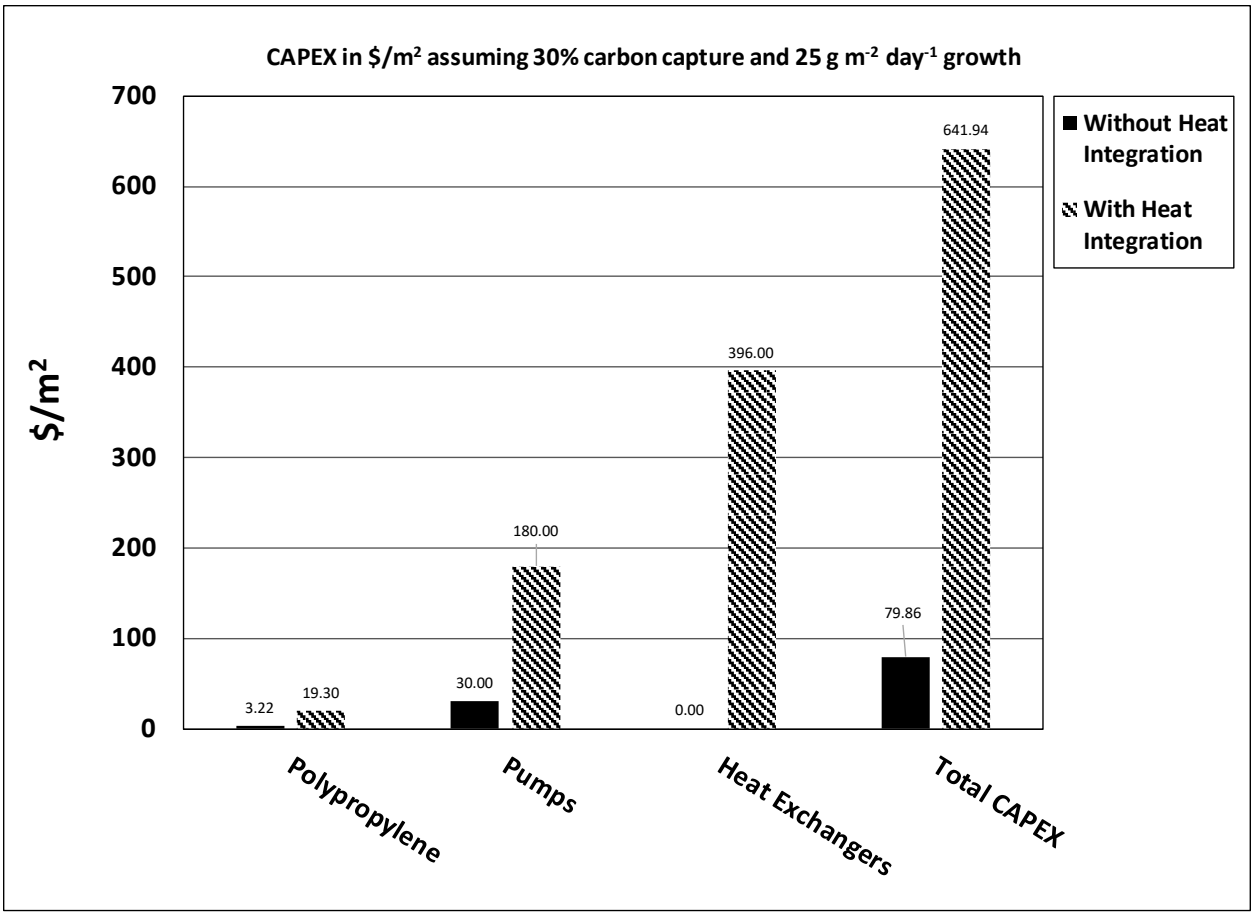

Figure 78. Capital expenditures (CAPEX) for a PBR system with and without installed heat integration equipment. Both PBR systems were sized for a 1 MW power plant. Capital costs ($/m^2) were calculated assuming a 30% CO_2 capture rate and a biomass productivity of 25 g m^{-2} day^{-1}.

As shown in Figure 78, there are dramatic increases in CAPEX associated with the purchase of the heat integration equipment, which includes extra polypropylene for feed tanks, additional pumps and shell tube heat exchangers. The majority of the increase in total CAPEX lies in the purchase of heat exchangers. Given the modular nature of the PBR system, heat integration would require purchasing and installing 6 times the number of liquid pumps normally required. The majority of these pumps, however, 5 out of 6, would sit idle for most of the year (240 days). Overall, the purchase of heat integration equipment alone increases total CAPEX by a factor of 8. If the cost of heat exchangers and pumps were cut in half, CAPEX would still be increased by a factor of 4.

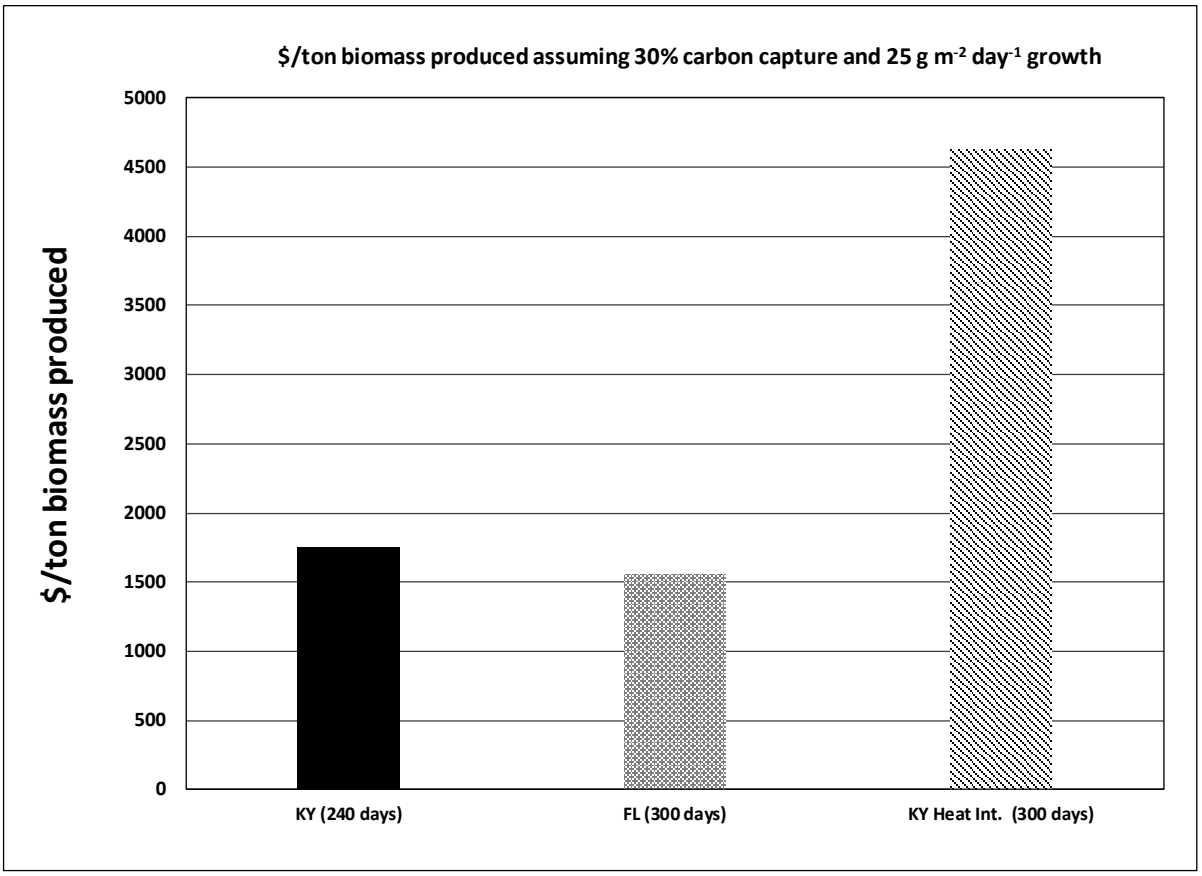

Figure 79. Cost of biomass production in $/ton for three separate PBRs, each at a 1 MW power plant. The first case corresponds to Kentucky, the second to Florida and the third to the same PBR in Kentucky with heat integration. Numbers include capital and operating cost over a 30-year amortization period assuming a 30% CO_2 capture rate and a biomass productivity of 25 g m^{-2} day^{-1}.

The production cost for one ton of biomass is reduced with a longer growing season. This is displayed in Figure 79, the production cost for the same system in Florida, being compared with the same system in Kentucky under the same carbon capture and growth assumptions. In Kentucky, however, this reduction in production cost is dwarfed by the rise in production cost incurred by heat integration.

In Kentucky and similar geographic locations, extending the growing season by 60 days using heat integration would almost triple the cost of biomass production, the majority of this increase in production cost being expenditures associated with the purchase of heat integration equipment. All of the OPEX increases associated with heat integration correspond to increases in energy costs due to extra liquid pumping and were found to be negligible in comparison to the increases in CAPEX.

It is important to note that numbers for heat integration in Figure 79 reflect an assumed productivity of 25 g m^{-2} day^{-1} during the 60-day extension to the growing season. In reality, the productivity would most likely be lower than this during colder months. That is to say, the numbers seen for heat integration in Figure 79 represent a best-case scenario, given that light limitations during the 60-day extension would likely limit the algae productivity to values less than 25 g m^{-2} day^{-1}. In conclusion, for this particular scenario, the increase in CAPEX associated with the purchase of heat integration equipment incurs an increase in biomass production cost that is untenable.

3.2.5. Techno-economic Analysis

An existing preliminary techno-economic model concerning the biological utilization of power plant emissions using microalgae was updated to better reflect design changes to the overall system, and to include more up to date data obtained from operations at East Bend Station. Microsoft Excel was chosen as the platform in order to accommodate the interconnectivity of the various parameters in the model and for ease of sharing among collaborators. Changes were also made to make the model more flexible towards factors such as fuel type, biomass composition, and location, the latter affecting the available sunlight (and hence system productivity) and the number of annual operating days possible. The algae species, and hence biomass composition, impacts the mass fraction of proteins, carbohydrates, and lipids produced, while also affecting the stoichiometry of CO_2 uptake by the biomass. The yields of the various fractions will in turn affect the utilization strategy, and processes, necessary for biomass valorization. Figure 80 shows the overall structure of the model.

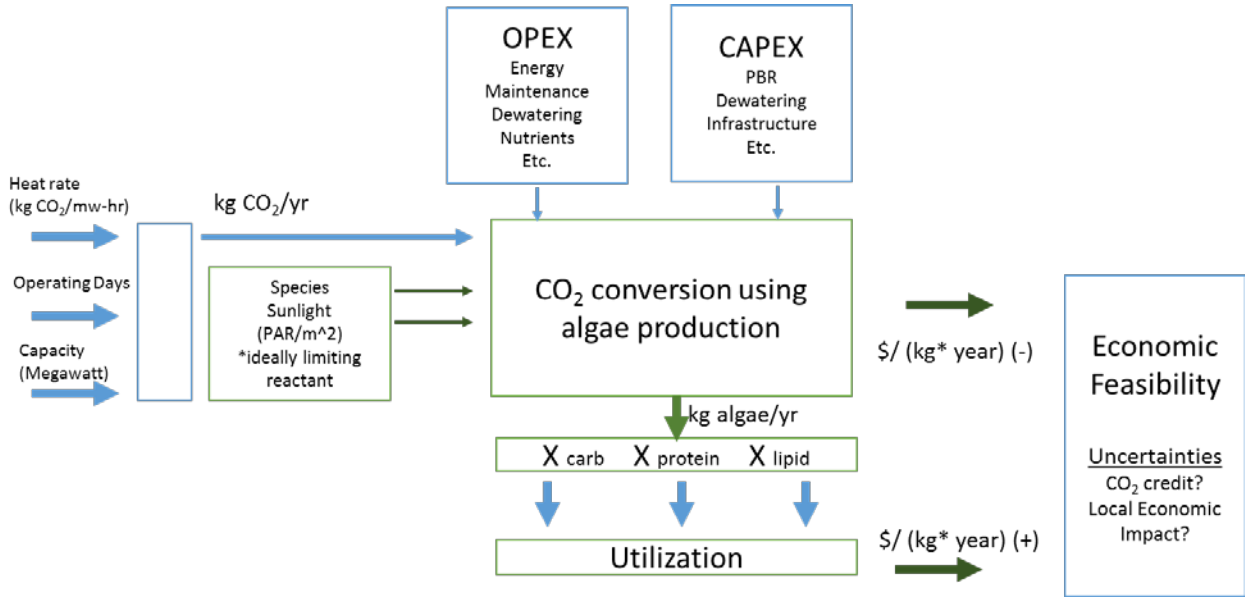

Figure 80. Techno-economic model

Operating expenses (opex) include the energy requirements of the overall system, maintenance, dewatering (flocculant and energy), and the nutrients necessary for algae production. Capital

expenses (capex), which include the photobioreactor, site preparation, infrastructure development and the dewatering system, are paid off over the operational lifetime of the facility (30 years) and are combined with the opex estimates to determine the annual cost associated with facility operation. Algae areal productivity is measured in g-algae/(m^2*day) and is treated as a yearly average. Photobioreactor prices are modeled using the current prices of raw materials and material requirements, and are comparable to current estimates from our Chinese partners, Lian Heng Hui. Our projected target, established in 2013, was a capital intensity of $69.44 per square meter of cultivation infrastructure (photobioreactor footprint). The cost of the mass produced photobioreactor components manufactured by Lian Heng Hui in Zhengzhou, China, was recently reported (May 2016) to be $70/$m^2$ for a 0.65 hectare photo bioreactor footprint. Operational expenses are based on modeled predictions also used in accompanying life cycle assessment calculations (see section 3.2.6), and are consistent with operational experience.

Once the model was completed, a baseline estimate was made of the cost of biomass production using the current state of the proposed technology. The reported case (Figure 81) is a best case scenario based on 75% conversion efficiency a stream of flue gas associated with 1 MW of coal-fired electric generating capacity, operating 300 days per year. The amount of CO_2 captured is a direct function of required capture efficiency and can be scaled appropriately. For example, for a 30% capture target of the total CO_2 emissions associated with the slipstream, the biomass production target can be effectively scaled, and matches the target of 3.9 tons of algae biomass per day used in the lifecycle assessment model. Table 12 highlights other important inputs to the model and assumptions.

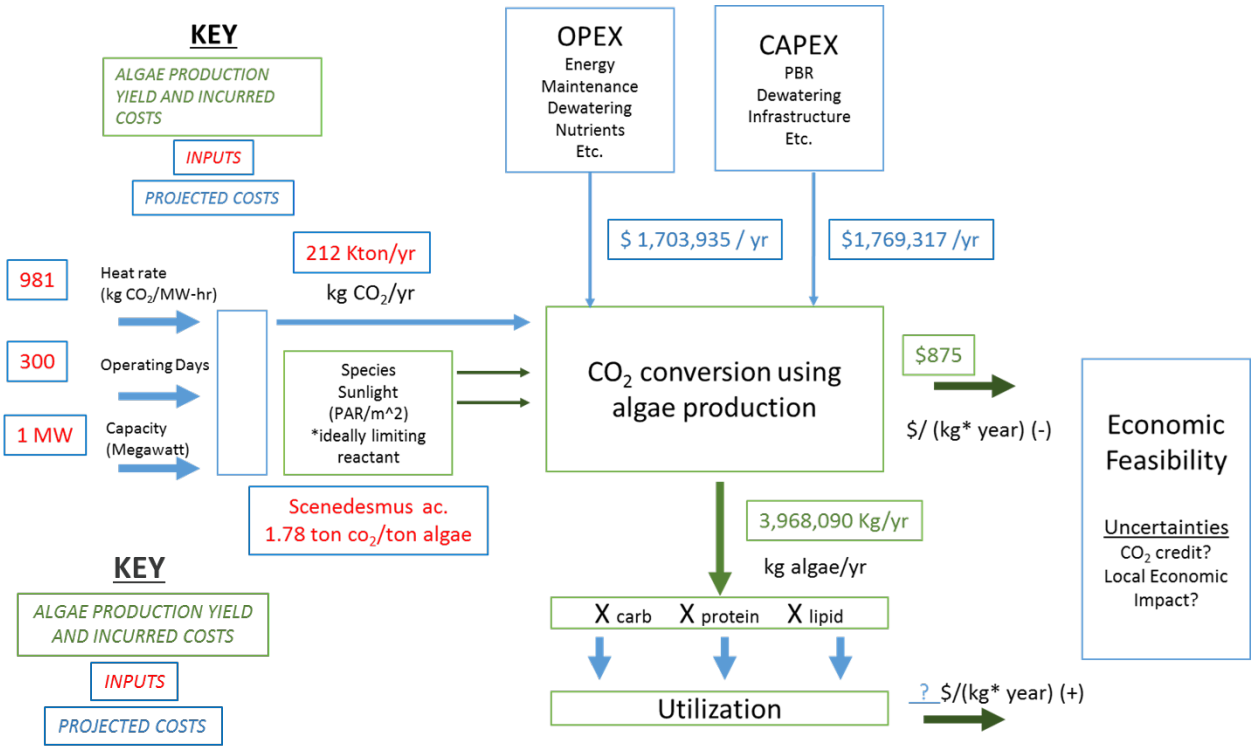

Figure 81. Current baseline (best case) scenario for operations in the United States

Table 12. Key inputs and assumptions used in the techno-economic analysis

Input	Value	Units / notes
Fuel Type	Sub-bituminous	eia.com
Heat Rate	981	kg CO_2 / MW-hr
Plant Capacity	1	MW
CO_2 capture efficiency	75%	Trade-off between growth, energy penalty, and capture efficiency
Electricity price	$0.02	$/KW-hr
Flocculant cost	$7.50	$/ton biomass harvested
Algae strain	*Scenedesmus actutus*	cultured since 2010
Growth rate	0.15	g/l
Culture Density	0.8	g/l at harvest
Operating days	300	per year
Nutrient Costs	$0.14/kg biomass produced	Current nutrient recipe utilizes bulk grade fertilizer

Scenedesmus acutus was chosen as the cultivation species so as to be able to leverage data collected in field and laboratory studies. Current results estimate the cost of producing biomass in our system to be $875/ton biomass, or $492/ton of CO_2 utilized/captured, for the best case scenario in the US market. In China, opportunities for lower cost biomass production exist based on lower costs associated with labor as well as manufacturing. It should be noted that the figure of $875/ton is the cost to produce the wet biomass and ***does not*** take into account the cost of capital or any expenses associated with subsequent utilization processes, and does not include any revenue generated. This is discussed in the next section. An interesting finding from this analysis is that operating costs are of approximately equal magnitude as compared to the annual capex contribution to the cost of CO_2 conversion.

Initial sensitivity analyses indicate that two of the most dominant factors in the cost of algae production are the capital cost of the biomass production infrastructure and the areal productivity of the production system. The faster the algae grow, the smaller the area of land required to convert the carbon dioxide, and therefore the lower the cost to produce the biomass. Figure 82 shows the comparison of two scenarios, corresponding to algae biomass production in the US and in the People's Republic of China (PRC). In both cases, the cost of production is shown as a function of the areal productivity.

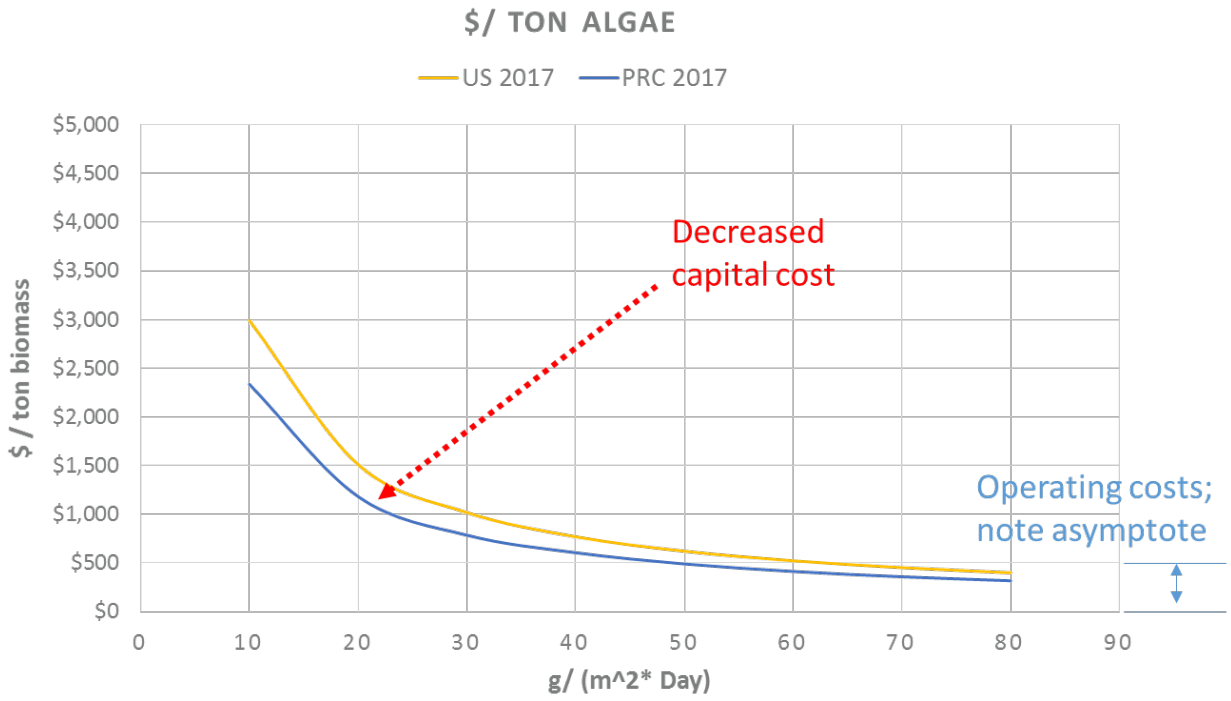

Figure 82. Effect of capital cost and areal productivity on the cost of biological carbon utilization.

The main difference between the US and PRC scenarios is the cost of labor for construction and operation of an appropriately sized algae system, which ultimately effects the capital intensity of the project. Overall, it can be seen that increasing the system productivity, though engineering or biological methods, would have the greatest effect on the overall economics. In addition, minimizing energy consumption, and hence operating costs, would move the cost curves downwards, providing another means of decreasing the production cost. The UK CAER sets a realistic target of 35 g/(m^2*day), which would result in a cost of $875/ton of produced biomass averaged over the lifetime of the project.

Utilization of whole algae biomass was compared to use of the individual components from a revenue potential projection. Table 13 shows the costing information used in the analysis. The value of raw carbohydrates was evaluated using bulk commodity pricing for lower grade sugars as well as raw sugar to determine the range of revenue potential. The worth of the proteins in the dried defatted biomass residue used for bioplastic production was assumed to be higher than the whole biomass based on data from Algix showing a higher protein content and lower concentration of volatile (odor-causing) compounds present in the feed. The value of the lipids in this case was determined using the price of crude oil and the improved potential revenue of biodiesel pricing. These low and high estimates were then averaged for future analysis.

Table 13. Commodity price ranges

Fraction	% of whole	Low Estimate ($/ton)	High Estimate ($/ton)	Average ($/ton)	Wtd Average ($/ton)
Carbohydrates	45	$300	$440	$370	$166.50
Proteins	40	$1,200	$2,000	$1,600	$640.00
Lipids	15	$75	$167	$121	$18.15
Whole algae	100	$800	$1,200	$1,000	$1,000.00

The weighted average can be equated to the maximum theoretical revenue potential of a ton of produced biomass, if fractioned into its basic components. This initial analysis, with the value of the lipids informed by the bulk prices for oil and biodiesel, indicates that the cumulative fractions ($824.65/ton) are worth less than if the whole biomass were used directly for bioplastics production (~$1,000/ton), without even considering the cost of processing the algae. It is apparent that if any further algae processing is required, the production of a high value product is essential to offset the costs.

The next step was to quantify the costs incurred when separating the biomass into its major fractions of lipids, carbohydrates, and proteins. In order to properly assess the feasibility of the biomass fractionation process developed as part of this project, data from bench-scale experiments were used to perform an engineering analysis. As before, a system designed to process the biomass required to beneficially re-use 30% of a 1 MW (electrical) CO_2 stream was used to better understand the economics and energetics associated with fractioning the biomass at commercial scale. This CO_2 stream is assumed to be from a coal fired unit equipped with modern emission controls and results in the beneficial re-use of 6.8 tons of CO_2 per day. A more detailed description of the process is presented in the following lifecycle assessment section below (section 3.2.6).

The main components that affect the cost of processing the biomass are the acquisition of the chemicals used (hydrochloric acid, methanol, and hexane), the electricity required for the various sub-processes, as well as the pay-off of the capital costs of the fractionation facility over its operational lifetime. Table 14 shows the projected costs per ton of biomass for the major components.

Table 14. Cost per ton of biomass processed

Expense	$ / ton biomass
HCl	$81.23
Methanol	$15.41
Hexane	$52.40
Electricity	$44.39
Capital	$68.38
Total	$261.80

The engineering analysis resulted in an overall cost of over $260 per ton to separate the biomass fractions for beneficiation. Bulk chemical prices (Alibaba.com) were used to harness the benefits of economy of scale and both methanol and hexane were recycled (>98%) to minimize expenses. The cost of chemicals used was over 56% of the overall cost, highlighting a potential area for improvement in future process development.

Once the minimum cost associated with fractionating the biomass was determined, it was integrated with the cost of produced biomass to perform an economic feasibility assessment based upon three scenarios. Table 15 compares the potential revenue for the utilization of whole biomass (with lower processing costs), the fractionation of biomass for the production of fuels, and a scenario where a portion of the lipids were used to generate high value co-products in addition to bioplastics and chemicals.

Table 15. Revenue potential of three potential strategies for biomass utilization

Cost/Revenue ($/ton)	% of whole	Fuels Only	High Value Case	Whole
Biomass Production	-	-$875.00	-$875.00	-$875.00
Fractionation	-	-$261.80	-$261.80	-$25.00
High Value Lipids	0 /4.5	$0.00	$1,327.50	$0.00
Lipids for Fuel	9 / 4.5	$72.43	$55.59	$0.00
Proteinacious solids	40	$713.85	$713.85	$1,000.00
Carbohydrates	45	$123.16	$123.16	$0.00
Total	-	-$227.37	$1,083.29	$100.00

To better understand the effect of the different kinds of lipids present in the algae biomass, it is important to consider the different components in the extracted lipids. Experimental data indicate that 40% of extracted lipids (6% of the whole algae) correspond to compounds that render the material unsuitable for use as fuels or high value chemicals (chlorophyll, phospholipids, etc.). In the two extraction case studies considered the remaining lipids (9% whole algae) were used to produce a) fuels only, as well as b) high value products such as polyunsaturated fatty acids (omega-3/6 oil). Again, bulk pricing was used to estimate the worth of the high value lipids ($2,900/ton, Alibaba.com) and a conservative (low end) value was selected for the analysis.

It is clear from this study that it is important to produce a high value co-product to justify the relatively high processing costs of algae fractionation. Another important result is the relatively

low value of the carbohydrate stream, highlighting a potential improvement in the lipid extraction process. If the extraction process were modified so that the carbohydrates remained in the solid phase, a higher fraction of the biomass could be used as a bioplastics feedstock. Also, it is edifying to note that a relatively modest portion of the biomass can drastically affect the economics of algal processing. Figure 83 compares the fractions of each component of the produced biomass, as well as the percentage of corresponding revenue potential.

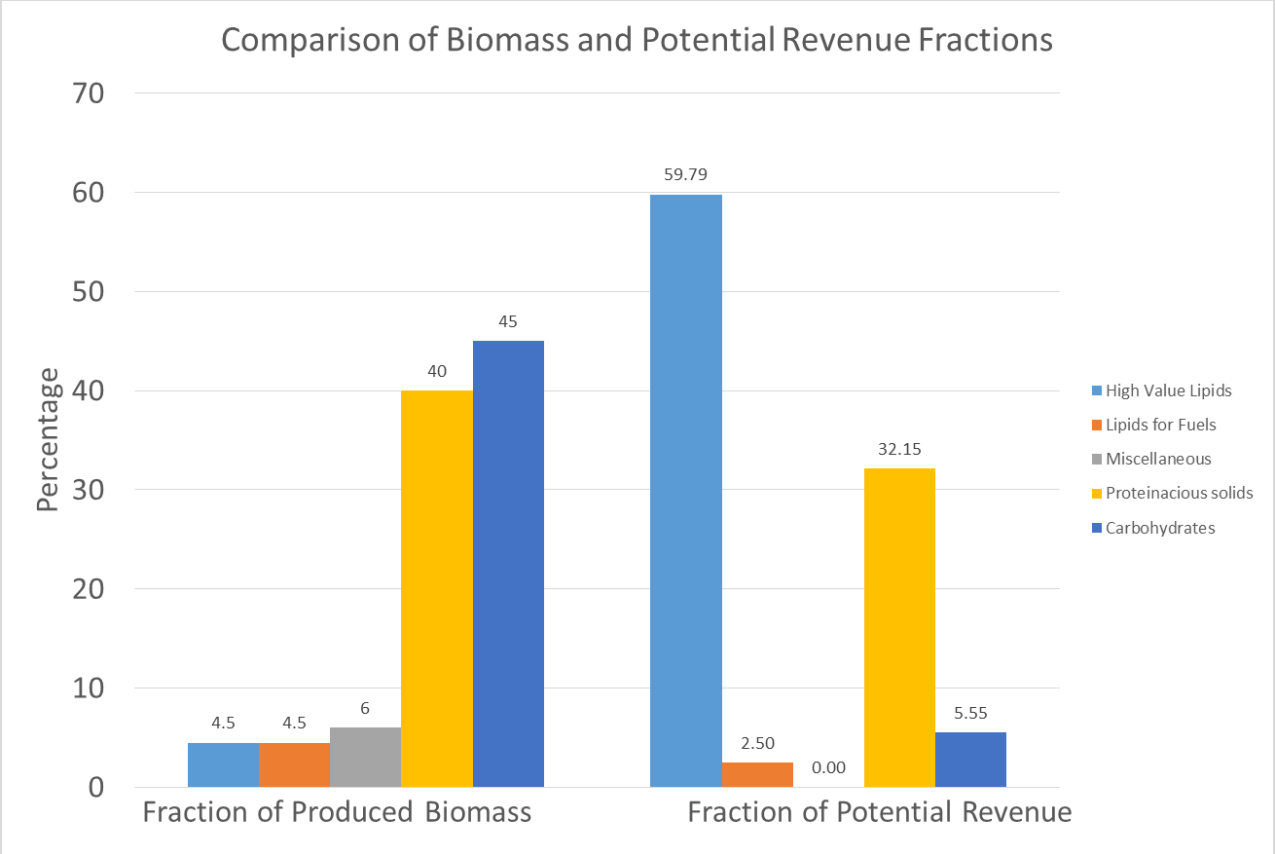

Figure 83. Comparison of Biomass Fractions and potential revenue streams.

This analysis affirms that future work needs to be focused on the production of high protein solids as well as chemical compounds that have a higher selling price than crude oil or biodiesel.

3.2.6. Lifecycle Assessment

Algae Production

Life cycle assessment (LCA) is a quantitative modeling tool used to evaluate the environmental impacts of a product or process throughout the life-time of all aspects of the product or process. The total energy produced/consumed and the energy content of raw materials used in production/construction, in addition to the energy required for plant operations, are evaluated in the model. Detailed LCA on various algae systems aimed at the production of biomass,

biodiesel, and/or biogas have been conducted (Lardon et al., 2009; Jorquera et al., 2010; Stephenson et al., 2010; Collet et al., 2011; Rogers et al., 2014). In comparison, very few LCAs have focused attention on the analysis of CO_2 mitigation from flue gas using algae. In this study, a LCA was developed to investigate the potential of using algae grown in a cyclic flow photobioreactor to mitigate 30% of the CO_2 emitted by a coal-fired power plant.

Method and Assumptions

A life cycle assessment was developed for an algae system capturing 30% of the CO_2 emitted by a representative 1 MW coal-fired power plant. Operation of the algae system included cumulative process/energy requirements associated with algae cultivation, harvesting, dewatering, nutrient recycling, and water treatment, and net greenhouse gas emissions. However, the analysis excluded the power plant infrastructure, power plant operation, fuel transportation costs, and labor requirements. The model was evaluated over thirty years of system operation (the expected lifespan of the equipment such as pumps and PVC piping).

The LCA was process specific and the system boundary was set up to enclose the algae-based system only. All relevant materials and energy consumption required in the production of algae were applied to the analysis, in addition to the assumptions given below.

Power Plant

The coal-fired power plant of 1 MW capacity was operated 300 days per year. The power plant capacity was limited to 1 MW to allow easy scale-up and analysis of any size of power plant. Coal was the power plant's only fuel source. Flue gas containing 10% CO_2 was compressed and introduced into the algae system. Conditioning of the flue gas was assumed to be unnecessary.

Cyclic Flow Photobioreactor (PBR)

The cyclic-flow PBR was assumed to operate 300 days per year with a CO_2 capture efficiency of 75%. The PBR modules did not require any temperature adjustment. Flue gas was compressed and introduced into PBR modules in periods of 5 seconds for every minute via compressors. Compressors (72% efficiency) operated 12 hours a day at an assumed inlet and outlet gas flowrate of 0.5 and 0.98 m^3/s, respectively, and the gas pressure was increased from 2 mbar to 10 mbar above atmospheric pressure before introduction into the PBR. The PBR was a closed system and CO_2 leakage from the PBR and intake of outside air into the PBR was neglected.

The PBRs were operated in a cyclic mode, draining and filling one row at a time, 4 times per day, via feed pumps. Each drain/fill cyclic sequence took 5.5 hours to complete, and thus each feed pump operated 22 hours per day. All feed pumps and compressors utilized in the algae system were powered by electricity.

Algae Culture/Media Preparation

Scenedesmus acutus (code name UTEX B72, The Culture Collection of Algae at the University of Texas at Austin) was the only fresh water strain cultured in the PBR. Media formulation was based on the elemental composition of *Scenedesmus acutus* (Table 16). Commercially available fertilizers were used to prepare the growth medium and all nutrients were assimilated and utilized by the algae. Greenhouse gas emissions (N_2O and CO_2) and energy consumption required for fertilizer manufacturing and water treatment were accounted for in the LCA.

Table 16. Elemental composition of *Scenedesmus acutus* (Crofcheck et al., 2012).

Carbon	50.02%
Oxygen	25.98%
Hydrogen	7.43%
Nitrogen	7.80%
Phosphorus	2.20%
Potassium	0.82%
Magnesium	0.39%
Sulfur	0.69%
Iron	0.43%
Calcium	1.30%
Manganese	0.002%
Copper	0.002%
Zinc	0.005%

Algae Harvesting and Dewatering

Harvested algae were dewatered via flocculation and sedimentation. Flocculated algae were settled and collected from the settling tanks with negligible energy consumption. Spent media/water contained insignificant nutrients (N, P, K) and was recycled back to PBR feed tanks after UV-sterilization.

System Design and Layout

The algae system included the operations of algae cultivation, harvesting and dewatering. Based on an algae specific growth rate of 0.15 g/L/day and a maximum culture density of 0.8 g/L (dry weight) (Wilson et al., 2016), 260 cyclic flow PBR modules are required to capture 30% of the CO_2 emission from a 1 MW power plant. Each PBR module was comprised of 5,760 PBR tubes (total culture volume of 100,000 L), a PBR tank, a PBR feed pump, and a compressor. The feed pump, operating at a flowrate of 600 L/min, circulated algae from the PBR feed tank to 5,760 PBR tubes in a closed loop system. The compressor compressed flue gas into the PBR module at an assumed inlet and outlet flowrate of 0.5 and 0.98 m^3/s respectively.

A total volume of 4105 m^3 fresh algae was harvested and combined with polyacrylamide flocculant (5 ppm) in various settling tanks on a daily basis. From the settling tanks, flocculated algae biomass at a concentration of 10 g/L (dry weight) was produced. The remaining spent media/water was transferred to holding tanks for sterilization and recycled back to the PBR feed tanks.

The system layout included PBR modules, settling tanks, holding tanks, and UV sterilizers. As mentioned above, one PBR feed pump, a PBR feed tank, and a gas compressor were included in each PBR module. For algae harvesting and media/water processing, one settling tank, holding tank, and UV sterilizer were allocated for each set of 13 PBR modules. The whole algae system was made up of 260 PBR modules (260 feed tanks, feed pumps, and compressors), and 20

settling tanks, holding tanks, and UV sterilizers. The system would cover approximately 82 acres of land (see Figures 84-86 for schematic and flow diagram of the system).

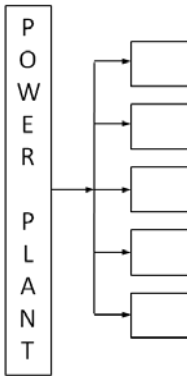

Figure 84. A schematic of the algae production system, consisting of a total of 260 PBR modules (260 individual feed tanks, feed pumps, and compressors) and 20 individual settling tanks, holding tanks, and UV sterilizers. An in-line pump was required for each settling tank and UV sterilizer. The whole algae system was divided into 5 sections. Each section was comprised of 52 PBR modules, 4 settling tanks, holding tanks, and UV sterilizers (see Figure 85). Flue gas was compressed and fed into each module via a compressor. (Note: figure was drawn for illustrative purposes and is not scaled to actual dimensions).

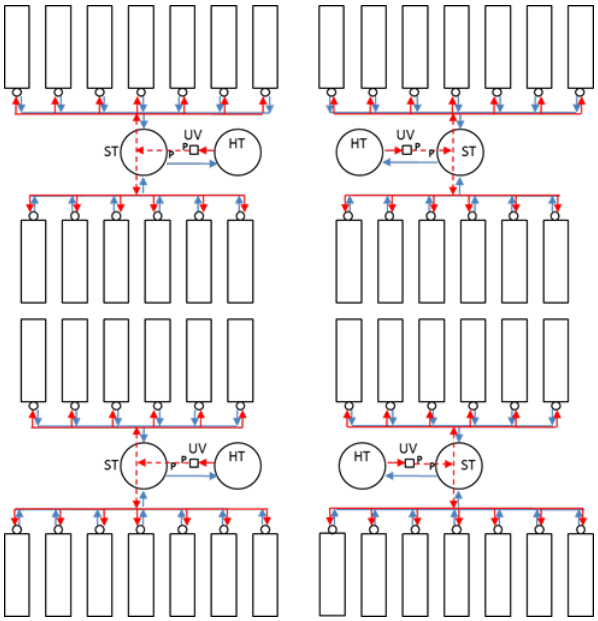

Figure 85. Schematic of a section of the algae system consisting of 52 PBR modules, 4 settling tanks (ST), holding tanks (HT), and UV sterilizers (UV). One settling tank, holding tank, and UV sterilizer was equipped to process algae and recycled spent media harvested from 13 PBR modules. For every 13 modules, algae were harvested, flocculated, and dewatered in the settling tank. Recovered water and nutrients were then sent to the holding tank and sterilized via the UV sterilizer, before recycle back into all 13 feed tanks. (Note: figure was drawn for illustrative purposes and is not scaled to actual dimensions.)

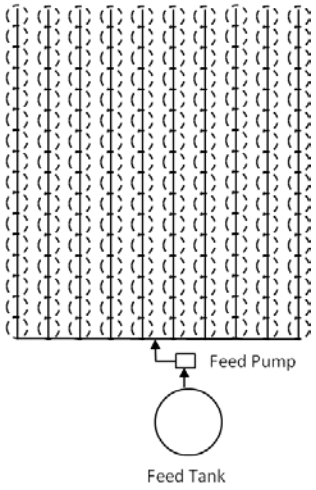

Figure 86. Schematic of a cyclic flow PBR module consisting of 5760 tubes (10 rows of tubes, 576 tubes/row), 1 feed tank, 1 feed pump, and 1 compressor (not shown in the figure). Flue gas was compressed by a compressor and introduced into the module through the feed manifold. Each row of PBR tubes was filled and drained (from/to the feed tank) 4 times a day in sequence via the PBR feed pump. (Note: figure is drawn for illustrative purposes and is not scaled to actual dimensions).

LCA Model

With the exception of the PBR feed pumps, all compressors, in-line pumps, and UV sterilizers were operated at full capacity for 12 hours a day (during daylight). The PBR feed pumps were designed to operate at various speeds in a cyclic motion, filling, and draining each row of PBR tubes in sequence 4 times a day. Thus the feed pumps operated a total of 22 hours per day with a maximum flowrate of 600 L/min. All PBR feed pumps, compressors, UV-sterilizers, and in-line pumps were powered by electricity. The compressor power requirement was calculated using Aspen. The equivalent CO_2 emissions related to nutrient manufacturing, PBR and tank construction, manufacturing of PVC pipes and fittings, water/media treatment, and all energy consumption were incorporated in the LCA (see Table 17 for process parameters utilized in the LCA).

Table 17. Key inputs and assumptions used in the LCA.

Power plant		
Capacity	1	MW
CO_2 emission	22.76	ton/day
CO_2 capture	30	%
CO_2 emission mitigated	6.83	ton/day
Operation	300	day/year
Algae		
Strain	*Scenedesmus acutus*	
Growth rate	0.15	g/L/day
Culture density at harvest	0.8	g/L (dry weight)
Algae required for 30% CO_2 capture	3.88	ton/day
Nutrients		
Wt. fraction of nitrogen in urea fertilizer	0.46	
Wt. fraction of potassium in potash fertilizer	0.5	
Wt. fraction of phosphorus in triple super phosphate fertilizer	0.26	
PBR module		
Number of modules	260	
CO_2 capture efficiency	75	%
PBR tube diameter	0.0889	m
PBR tube length	2.44	m
Equivalent tube length/module	25.25	m
PBR volume	100,000	L/module
Maximum tube flowrate	600	L/min
Operation	300	day/year
PBR feed pump		
Flowrate	varies due to cyclic flow pattern	
Efficiency	75	%
Operation	22	hour/day
Compressor		
Flue gas compression	5	sec every minute
Flue gas flowrate	4.72	L/s/module
Efficiency	72	%
Operation	12	h/day

Results and Discussion

A summary of the net CO_2 emissions of the algae system over a lifespan of 30 years is shown in Figure 87. As the figure shows, the amount of raw CO_2 captured was 6.14×10^4 metric tons. Notably, the CO_2 emission associated with the compressor (8.7×10^3 metric tons) was much

larger than the pump requirement (1.9 x 10^3 metric tons) showing the impact of the cyclic flow design on the overall energy consumption. The large emission associated with the compressor was a consequence of the large amount of flue gas (4422 m^3/h) being compressed at full capacity for 12 h per day. In comparison, feed pumps were not operating at full capacity the whole time due to the cyclic operation mode. Overall, the PBR system was able to capture 43% (2.6 x 10^4 metric tons) of the target CO_2 emission (6.1 x 10^4 metric tons). This result demonstrates that the PBR algae system can be considered as a CO_2 capture technology. In order to further reduce net CO_2 emissions, algal productivity should be maximized, while reducing the compressor and pump requirement if possible. An increase in productivity would reduce the number of PBR modules required to capture CO_2 and the corresponding greenhouse gas emissions associated with PET and PVC acquisition.

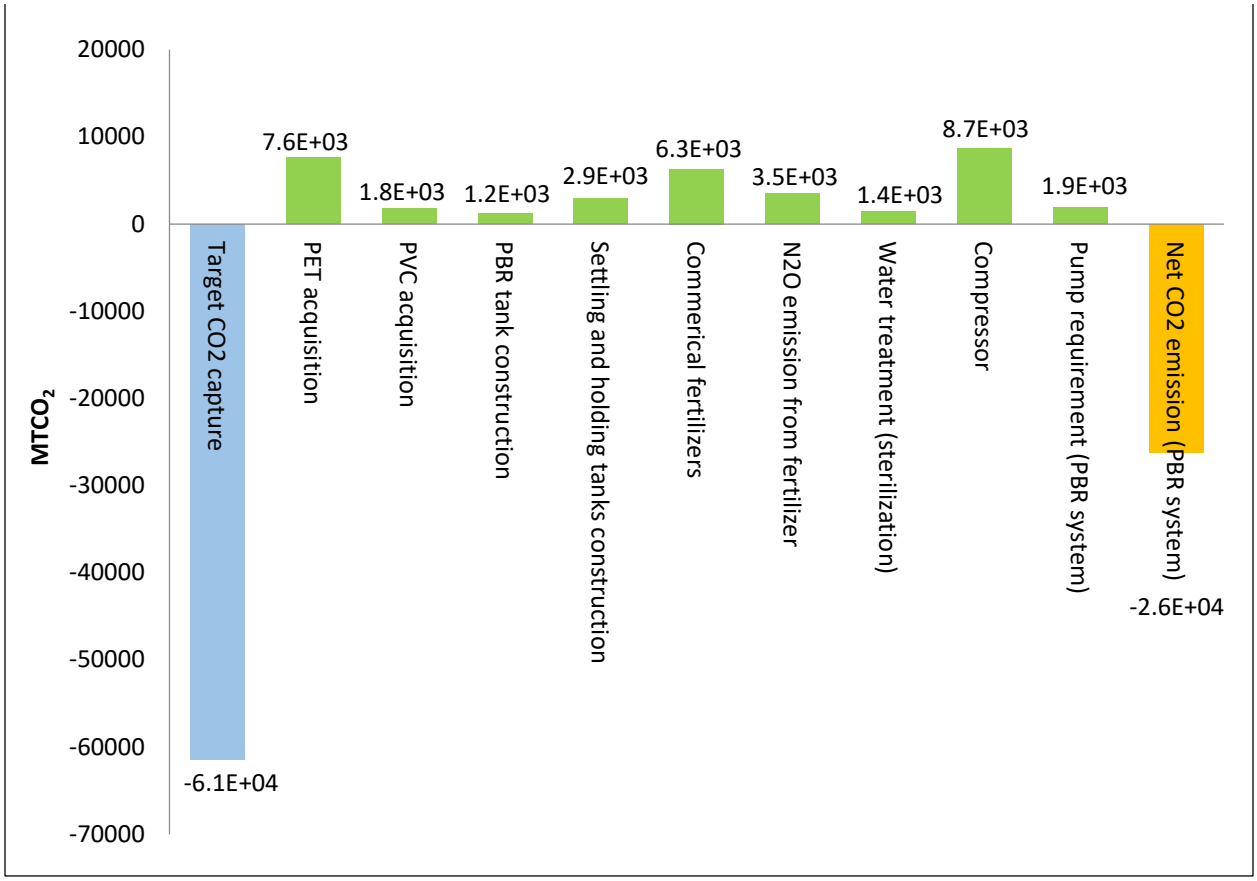

Figure 87. Summary of the CO_2 emissions for an algae system consisting of 260 modules of cyclic flow photobioreactors (including feed tanks, feed pumps, and compressors) and 20 settling tanks, holding tanks, and UV sterilizers, over a lifespan of 30 years. The liquid flowrate was 600 L/min (corresponding to the system operated at East Bend in 2015).

Life Cycle Assessment of Biomass Fractionation

In order to properly assess the feasibility of the biomass fractionation process developed as part of this project, data from bench-scale experiments were used to perform an engineering analysis. The results of these experiments were then integrated with the previous LCA of algae production to understand the interconnectivity of the two processes. As before, a system designed to process the biomass required to beneficially re-use 30% of a 1 MW (electrical) slip stream was used to better understand the economics and energetics associated with fractioning the biomass at commercial scale. This slipstream is assumed to be from a coal fired unit equipped with modern emission controls and results in the beneficial re-use of 6.8 tons of CO_2 per day. Figure 88 shows the layout of the photobioreactor and algae processing facility.

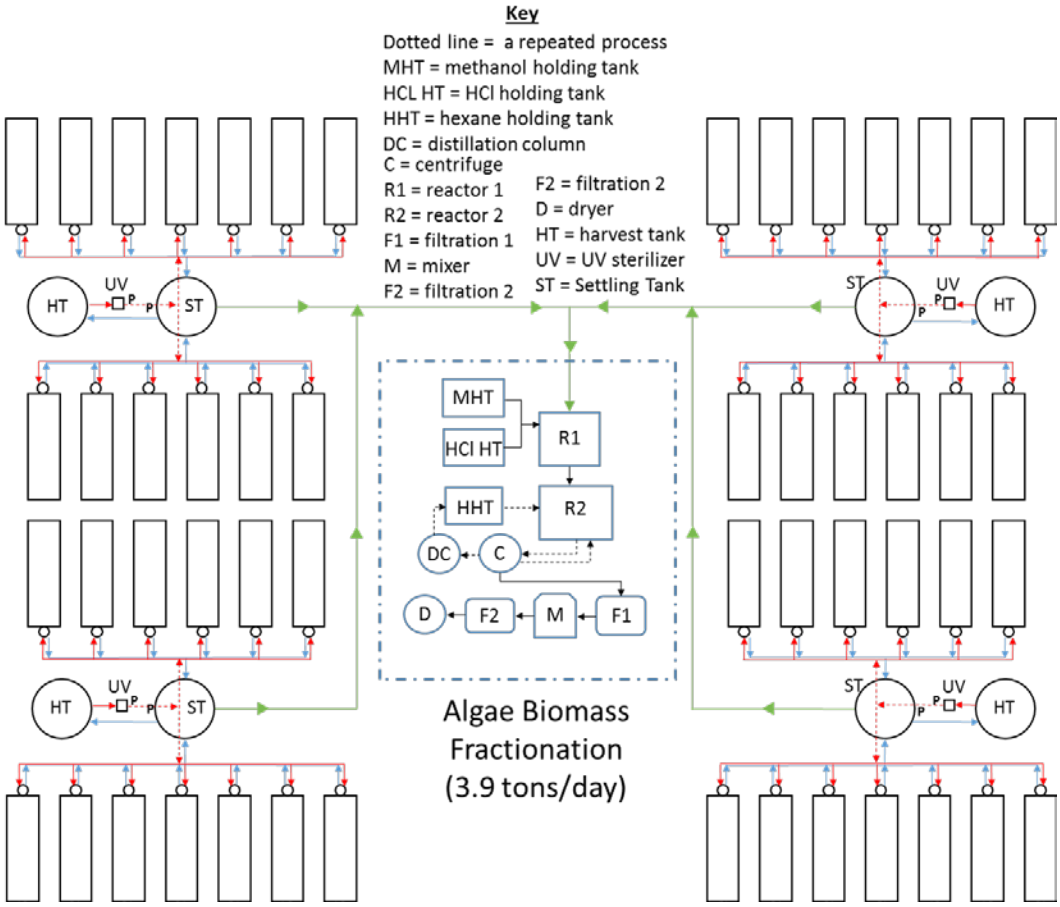

Figure 88. Layout of facility designed to beneficially re-use 30% of a 1 MW slip stream.

Leveraging the modularity of the cyclic flow photobioreactor (PBR), while also limiting the energy requirements of the system, resulted in the layout shown above (discussed previously for the algae production LCA). The site is divided into 5 clusters consisting of 13 individual PBR systems and equipped with its own harvesting/dewatering system and UV sterilizer to treat the water returning to the PBR. Each individual PBR module is 100,000 L, resulting in a total system volume of 5,200,000 L of culturing capacity, producing 3.9 tons of algae biomass per

day. The produced biomass is assumed to be dewatered using flocculation, sedimentation, and filtration, producing a fully dewatered biomass at 20 % solids supplied for further processing.

The approach taken by the UK CAER is to fractionate the produced biomass into its major components – proteins, carbohydrates, and lipids – in order to maximize the revenue potential of each fraction. This approach, as opposed to using whole biomass, enables the production of high value co-products such as pigments and nutritional supplements. The algae biomass used for this analysis was the traditional CAER baseline production strain, *Scenedesmus acutus*, and contains an overall breakdown of ~15% lipids, ~40% proteins, and ~45% carbohydrates based on typical analyses of our produced biomass. Figure 89 shows the fractionation approach designed during this project, as well as the breakdown of the products.

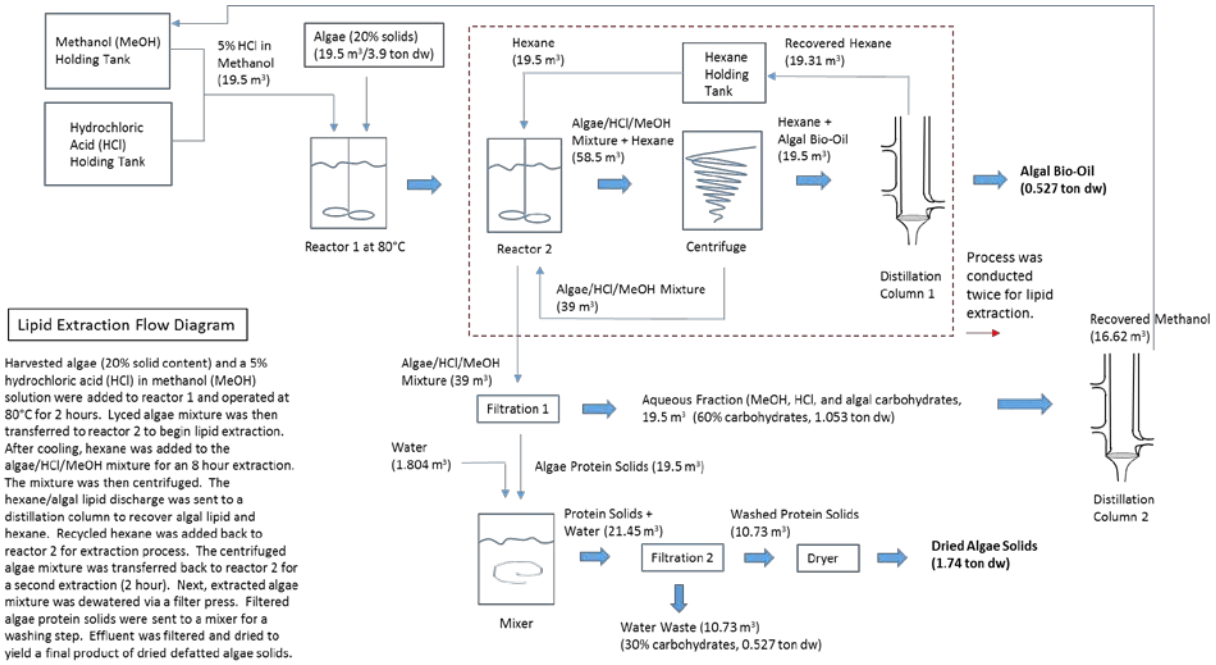

Figure 89. Process flow diagram for fractionation process.

A chemical pretreatment is used to lyse the cell walls of the algae and allow for recovery of the lipids via in situ transesterification and extraction into hexane. 5% HCl is added to methanol and mixed with the algae slurry for 2 h at 80 °C, after which the slurry is transferred to another reactor where it is allowed to cool before the addition of hexane for a series of extractions. The primary extraction removes approximately 60% of the extractable lipids in an 8 h period before the slurry is sent to a centrifuge to separate the hexane and aqueous fractions. The hexane layer, containing the extracted lipids, is sent to a flash distillation column to reclaim the hexane solvent and to concentrate the algae lipids. The 'aqueous fraction' – containing a mixture of algae biomass, methanol, and hydrochloric acid – is then returned to the reactor for an additional extraction to reclaim a further 30% of the extractable lipids. The centrifugation process is repeated with the hexane layer being sent to the distillation process and the remaining biomass solids sent to a filter press. The biomass solids are dewatered to approximately 50% solids, with

the permeate containing solubilized carbohydrates in addition to the water-methanol-hydrochloric acid mixture. This filtrate is sent to a second distillation in order to recycle the methanol used in the process.

During the extraction process, the carbohydrates are liberated in addition to the lipid fraction of the biomass. Initial characterization data provided by Algix showed that the presence of these free sugars can result in solids agglomeration during melt processing of bioplastic blends, affording a product with sub-optimal properties. In order to maximize the value of the produced bioplastics, and thereby the proteinaceous algae feed used for their production, a washing step was added to remove the free sugars. The addition of this washing step enables the near complete fractionation and recovery of the three main biomass components. The washed biomass is then dewatered again using a filter press to ~50% solids. These solids, containing mostly protein, are dried for storage and processing.

Once the overall process was sized, the energy required for system operation was calculated. The major energy inputs for this process are the pretreatment, centrifugation, and drying sub-processes, as shown in Table 18.

Table 18. Power requirements of fractionation process.

Equipment	Power requirement (MW-hr)
Reactor 1	1.008
Reactor 2	0.039
Centrifuge	0.160
Hexane Distillation Column	1.645
Methanol Distillation Column	4.588
Filtration 1	0.030
Mixer	0.001
Filtration 2	0.030
Dryer	1.156
Total	8.656

The main power requirements were associated with the recovery of the hexane and methanol via distillation, while other major contributors include drying the defatted biomass. While this fractionation process was adapted from the literature to minimize solvent use, further work is necessary to optimize and improve this system.

CO_2 Emission Summary

A summary of the CO_2 emissions from the algae production system and lipid extraction process over a lifespan of 30 years is shown in Figure 90.

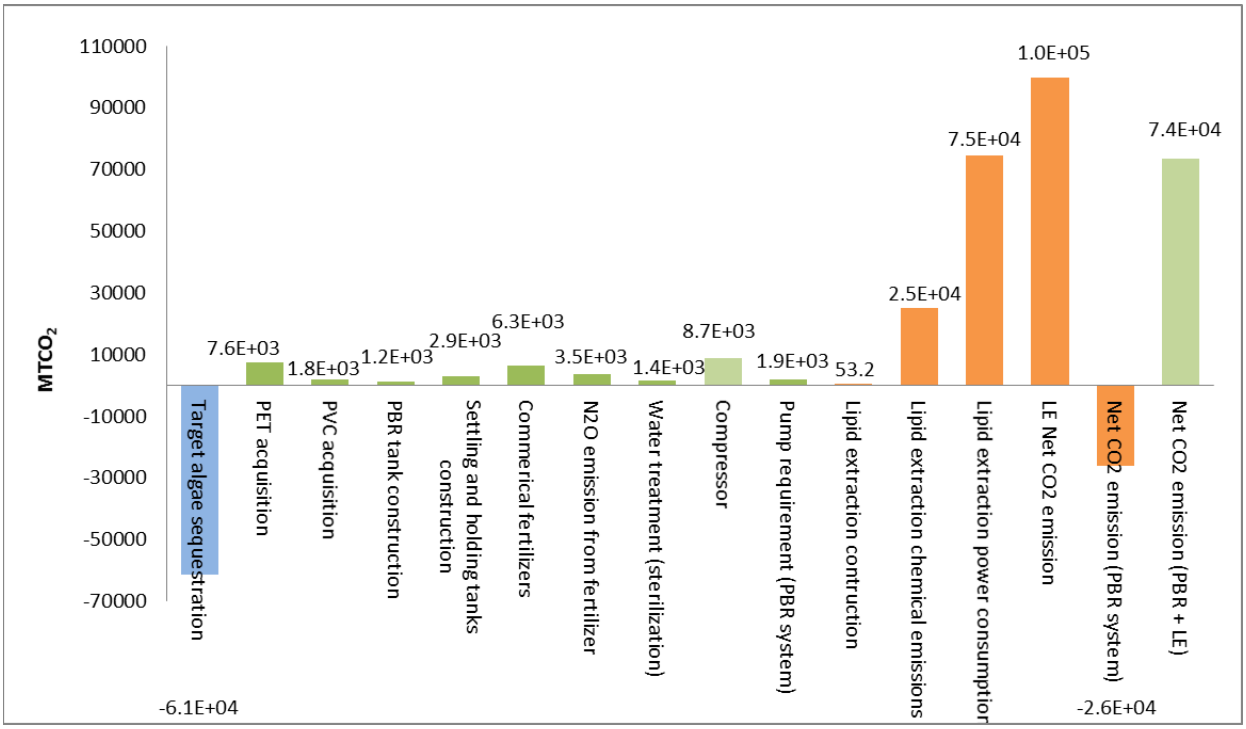

Figure 90. Summary of the CO_2 emission of an algae system capturing 30% CO_2 from a 1 MW coal-fired power plant and subsequent lipid extraction process over a lifespan of 30 years. NOTE: credits for utilization or offset of petroleum based products (plastics / fuels) were not considered.

As the figure shows, the amount of raw CO_2 captured was 6.14 x 10^4 metric tons. The largest CO_2 emission of 8.7 x 10^3 metric tons obtained in the algae (PBR) system was due to the flue gas compressor, operating and compressing 4422m^3/h of flue gas for 12 h/day. In comparison, the PBR feed pumps emitted significantly less CO_2 (1.9 x 10^3 metric tons) showing the impact and efficiency of the cyclic flow design on the overall energy consumption. As a whole, the PBR system was able to capture 43% (2.6 x 10^4 metric tons) of the target CO_2 emission (6.1 x 10^4 metric tons). In contrast, lipid extraction yielded a larger than expected amount of 1.6 x 10^5 metric ton of CO_2. *It is important to note that this analysis does not include any offsets or credits associated with the production and use of the products (bio-crude, bioplastics, etc.) from this process*. The largest CO_2 emissions were due to the relatively large power consumption associated with recovering and recycling chemicals, followed by the manufacturing of chemicals used in the extraction. The LCA results show that the biomass fractionation developed over the course of this project is net CO_2 positive, contributing to greenhouse gas emissions as opposed to reducing it. Future research and development of low energy biomass extraction techniques will be required to make fractionation a viable approach from a life cycle perspective. Efforts should

be focused on minimizing the amount of chemicals required as well as process development that could yield step change improvements. Future analyses will have to be extended to include the utilization and offset of produced products to better understand the overall impact.

LCA Summary

According to the foregoing LCA, algae cultivation based on the use of a cyclic flow photobioreactor is capable of lowering the net carbon emissions of a given slipstream of flue gas. In order to further minimize CO_2 emissions, algal productivity must be maximized in parallel with reducing the compressor and pump requirements, as well as improving the reactor design (if possible) to minimize use of raw materials.

The fractionation of the biomass, while attractive from a theoretical and techno-economic outlook, does not meet expectations from an overall emissions perspective at this time. However, two important caveats must be added. First, the fractionation process modeled does not represent an optimized process. Indeed, areas for process improvement are clearly indicated in the above analysis. Specifically, future efforts should focus on the optimization of the pretreatment step, hexane/lipid separations, and dewatering/drying steps to reduce the overall energetics of the system. Second, the LCA ends at the biomass fractionation stage, and takes no account of any GHG credits associated with downstream applications of the biomass. In other words, this analysis does not include any offsets or credits associated with the production and use of the products (bio-crude, bioplastics, etc.). In the case of bioplastic production, algal biomass is used to displace a certain fraction of petroleum derived base resin (up to 50% by weight), thereby generating a CO_2 credit. Consequently, in future work the boundary of the LCA should be extended to include the production and use of these products so as to arrive at a complete picture.

3.3. Biomass Utilization

3.3.1. Extraction, Characterization and Upgrading of Lipids

Baseline Characterization of Production Biomass

Algal biomass grown at East Bend Station during September 2015 was analyzed for elemental analysis and ash content (CHN analysis and ICP-OES). Results are summarized in Figure 91. According to the results, carbon accounts for ~50% of the algae by mass. This is consistent with previous elemental data obtained on samples grown at East Bend Station in 2014, which showed consistent carbon mass percentages of ~51-52%.

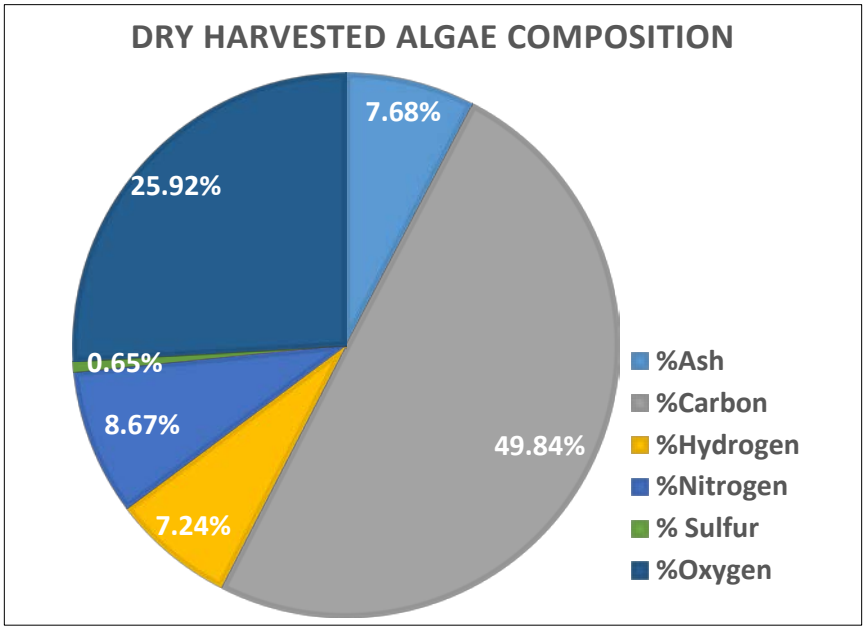

Figure 91. Elemental analysis (dry basis, mass %) of algae grown at East Bend Station during September 2015. Note that %Oxygen was determined by difference and also includes trace elements (<0.5 mass%) and phosphorus (*ca*. 1 mass%).

Note that the ash content of harvested algal biomass tends to be somewhat variable, depending as it does on a number of factors such the nutrient content of the broth at the time of harvest and the degree to which the biomass is dewatered prior to drying. A low ash content is a benefit when using algae in the production of bioplastics.

Using an industry standard conversion factor of 4.78 g anhydrous amino acid to 1 g nitrogen (Lourence *et al*., 2004), a protein content of ~41.4% was calculated for the biomass. Overall, these results indicate a low ash content and high protein content of *Scenedesmus* algae produced at East Bend in 2015.

Lipid Extraction

In initial work lipid extraction from wet algal biomass using hexane was examined under the action of sonication or bead milling, the latter method being particularly effective according to a literature

report (Shen *et al*., 2009). However, results with *Scenedesmus acutus* were disappointing, the maximum yields of crude lipid not exceeding 3-4 wt% compared to the theoretical maximum of ca. 14 wt% total lipids. This is due to the extremely tough cell wall of this particular alga, which renders physical lysing of the wet cells challenging. Consequently, an alternative method was examined, based on chemical lysing of the cells (under the action of an HCl/methanol mixture) and simultaneous *in situ* transesterification (Laurens *et al*., 2012).

In an effort to minimize the required solvent to algae ratio, numerous experiments were performed to determine the minimum amount of solvent necessary to substantially defat wet *Scenedesmus* algae while also allowing high throughput production of defatted algal solids for use in bioplastic formulation. In the course of these experiments, timely separation of aqueous and lipid layers could not be achieved via gravity separation with reduced quantities of solvent. This was determined to be a result of concentration of the chemical flocculent used during algae harvesting. As water is removed from the algae the flocculent is concentrated in the biomass, leading to undesirable effects during subsequent lipid extraction, such as flotation of solids and emulsion formation. Given the cost of utilizing the large quantity of solvent necessary to achieve desirable separation, a modified procedure was developed which streamlines the extraction process and employs centrifugation to overcome the difficulties in achieving separation. In this procedure, 1 L of 5% HCl in methanol was added to 1 kg of wet algae at approximately 15% solids. The mixture was then heated and stirred for 2 h at 70 °C. After cooling, the extraction mixture was added to centrifuge tubes along with an equal volume of hexane (1 L) to extract the esterified lipids. This mixture was shaken vigorously and stirred for 1 h before being centrifuged at 2500 rpm for 10 min. The hexane layer was then decanted and the extraction process was repeated two more times. This procedure typically yields total lipids at 10.2 ± 1.6 wt% of the total algal biomass (dry mass basis; n = 3), the corresponding yield of esterifiable lipids being ~6.5 wt%. This figure is very close to the value previously reported by us for esterifiable lipids extracted from dry *Scenedesmus acutus* (Santillan-Jimenez *et al*., 2016). The boiling point distribution plot of these lipids is presented below (Figure 92) and confirms the absence of high boiling triglycerides.

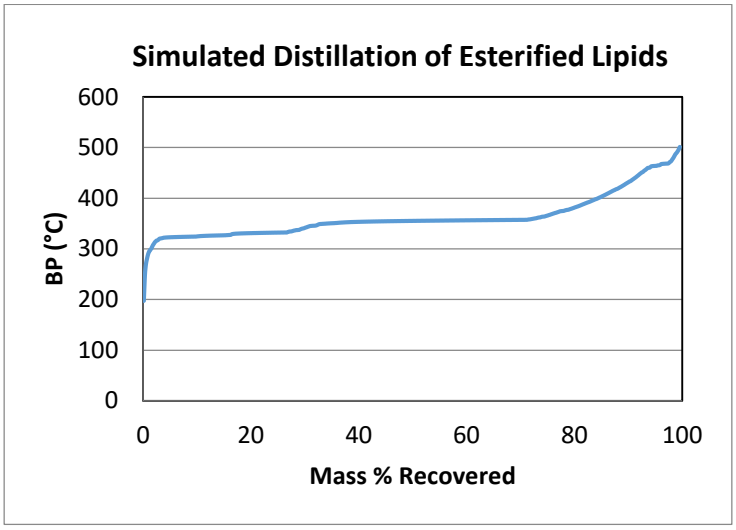

Figure 92. Boiling point distribution of algal fatty acid methyl esters extracted from wet *Scenedesmus acutus*.

Subsequently, this extraction method was scaled up to produce sufficient defatted biomass for bioplastic compounding studies. Lipid extractions were performed by combining 1 kg of dewatered algae at approximately 19 wt% solids with 1 L of 5% HCl in methanol. This mixture was then heated to 85 °C for 1 h with vigorous stirring. Finally, the lipids were separated by adding 2 L of hexane to the mixture before agitating and centrifuging the resulting emulsion to yield a lipid layer which was then decanted. In order to maximize lipid recovery, the separation step was then repeated an additional two times. The hexane was recovered by rotary evaporation and recycled, with the resulting aqueous layer being air dried. The yields from this process are presented in Table 19 in which raw algae slurry refers to the mass of algae + water, recovered solids refers to the mass of dry, defatted biomass obtained, and recovered mass % is the amount of recovered solids + lipids divided by the initial mass of raw algae used on a dry basis.

Table 19. Gravimetric yields of lipid extraction/*in situ* transesterification experiments (data represent the average +/- st. dev. from 6 experiments)

Raw algae slurry (g)	Recovered solids (g)	Recovered lipids (g)	Recovered mass %
1027.3 (+/-10.1)	156.2 (+/-10.2)	12.7 (+/-0.2)	84.0 (+/-4.7)

The mass percentage not accounted for (16%) is assumed to be lost during filtration of the aqueous layer and consists mainly of soluble carbohydrates (e.g., simple sugars) together with lesser amounts of protein. This procedure was repeated until 5 kg of dried, defatted algal solids were obtained. The resulting biomass was supplied to Algix in 2016 for use in bioplastic compounding trials. Elemental analysis of the algae feed ("2016 algae") and the products (defatted algae and algal lipids) was also performed, the results being presented in Figure 93. The low ash and high nitrogen content of the defatted algal solids suggest that they should be suitable for use as bioplastic feedstock.

In 2017, a second batch of biomass (2.2 kg) was supplied to Algix. This material was prepared according to the procedure described above, with the addition of a washing step. Specifically, the defatted algal biomass was stirred with deionized water (1 L per ~100 g biomass) for 1 h, after which the biomass was isolated by filtration. This additional step was included in order to remove free sugars from the biomass, formed by acid-catalyzed hydrolysis of polysaccharides during cell lysing. The presence of these simple sugars is believed to contribute to the formation of agglomerates during bioplastic melt processing, this being detrimental to the physical properties of the final bioplastic. The defatted and washed biomass is referred hereafter as defatted & sugar extracted biomass. Elemental analysis data for this material are given in Table 20, while the results of protein and ash analyses on both sets of biomass supplied to Algix are included in Section 3.3.2 below. Note that the data in Table 20 are consistent with increased protein content in the defatted and "desugared" biomass, the concentrations of both N and S increasing relative to the whole biomass (see Figure 93). Moreover, the concentration of P decreased after lipid extraction and washing from ca. 1% in the whole biomass to 927 ppm, indicating that phospholipids were largely removed.

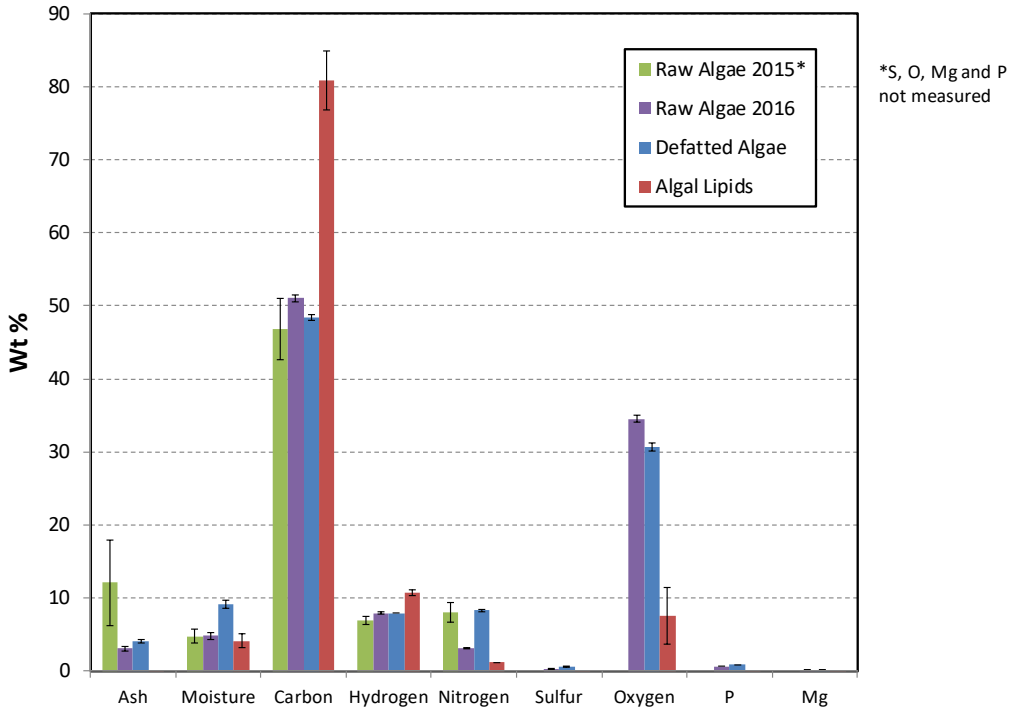

Figure 93. Elemental analysis of raw algal biomass used for extraction experiments, defatted biomass and extracted lipids. Error bars represent the standard deviations for the analyses (n = 16 for 2015 raw algae; n = 3 for 2016 raw algae, defatted algae and lipids).

Table 20. Elemental analysis of defatted & sugar extracted biomass

Ash (%)	H (%)	C (%)	N (%)	S (%)	P (ppm)
1.08	7.53	53.92	9.53	0.75	927

Characterization of Extracted Lipids

Typically, lipid profiling by gas chromatography (GC) is carried out using an HP-88 (mid-range polarity) column and a flame ionization detector (FID), with peak identification and quantitative calibrations relying on the information gathered from the injection of Supelco's 37 FAME standard mixture. Unfortunately, the FID is limited in its ability to identify components that do not line up exactly with the retentions times associated with the components in the standard mixture, which can lead to peaks being either unidentified or misidentified.

The recent commissioning of a GC with dual detection capabilities at the University of Kentucky – i.e., equipped with both FID and Mass Spectrometer (MS) detectors – made it possible both to identify previously unidentified peaks as well as to corroborate ambiguous identifications. The new instrument is equipped with a VF-5HT (non-polar) column which alters the elution order of the constituents; however, the MS detector significantly increases the confidence in the

identification both of compounds present in the 37 FAME mixture and of previously unidentified components in algal lipids, particularly those compounds giving rise to peaks present in the 25-27 min retention time window.

Thus, algal lipids obtained by simultaneous *in situ* esterification and extraction from *Scenedesmus acutus* were analyzed by both the traditional method and by the dual detection method. Analysis via the dual detection method showed 3 significant differences including: 1) identification of several polyunsaturated FAMEs such as C16:4, as shown in Figure 94; 2) improved resolution of the linolelaidic and both the α- and γ-linolenic FAMEs which tend to co-elute in the traditional method; and 3) refuted the identification of nervonic FAME in favor of bis(2-ethylhexyl)phthalate (DEHP) – a common constituent of algae oil.

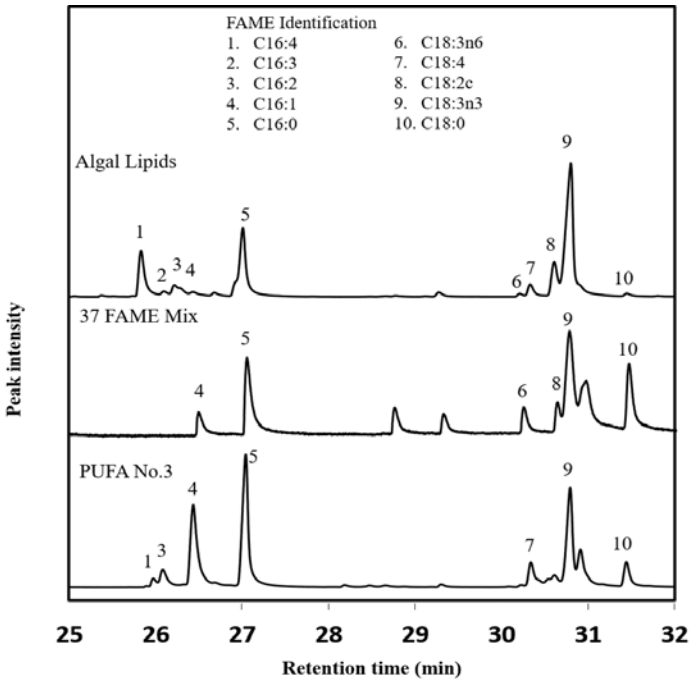

Figure 94. Gas chromatograms of lipids extracted from *Scenedesmus acutus*, and two different standard mixtures.

While the quality of the NIST Library identifications was ≥ 90% in all cases, an analytical standard containing the polyunsaturated FAMEs – PUFA No.3 (from menhaden oil) – was purchased from Sigma Aldrich and used to confirm the aforementioned findings. Table 21 summarizes the data obtained using the traditional method and compares it with that obtained using the more comprehensive dual detection method. Notably, the new analysis method shows the algal lipids to be significantly more unsaturated than previously thought, the major FAME component being derived from α-linolenic acid (18:3n3), a valuable ω-3 unsaturated fatty acid.

Table 21. Algal lipid profile as determined via GC traditional analysis and dual detection analysis.

Fatty acid chain (X:Y)[a]	Traditional Analysis	Dual Detection Analysis
Myristic (14:0)	2.6	0.3
Palmitic (16:0)	37.0	18.3
Palmitoleic (16:1)	9.9	2.9
(16:2)	-	4.1
Hiragonic (16:3)	-	1.2
(16:4)	-	10.5
Stearic (18:0)	-	0.7
Linolelaidic (18:2t)	24.0	-
Linoleic (18:2c)	13.7	9.6
α-Linolenic (18:3n3)	-	46.8
γ-Linolenic (18:3n6)	5.2	0.6
Stearidonic (18:4)	-	3.5
Gadoleic (20:1)	-	0.5
cis-docosadienoic (22:2)	3.8	0.5
Nervonic (24:1)	3.9	-
DEHP	-	0.6

Catalytic Upgrading of Algal Lipids to Fuel-like Hydrocarbons

In order to demonstrate that lipids derived from *Scenedesmus* acutus can be readily upgraded into hydrocarbon type-fuels, an upgrading experiment was performed. Lipids extracted using the *in situ* transesterification process (which affords FAMEs) were first purified – using activated carbon as a low cost, high surface area adsorbent – to remove chlorophyll, a known catalyst poison. The resulting purified algal FAMEs were catalytically deoxygenated in a continuous (fixed bed) reactor using a low cost nickel catalyst developed in house (Loe *et al*., 2016). Notably, conversion was observed to be quantitative at all reaction times sampled, >94% of reaction products comprising fully deoxygenated hydrocarbons – the vast majority of which were diesel-like hydrocarbons – irrespective of time on stream (Figure 95).

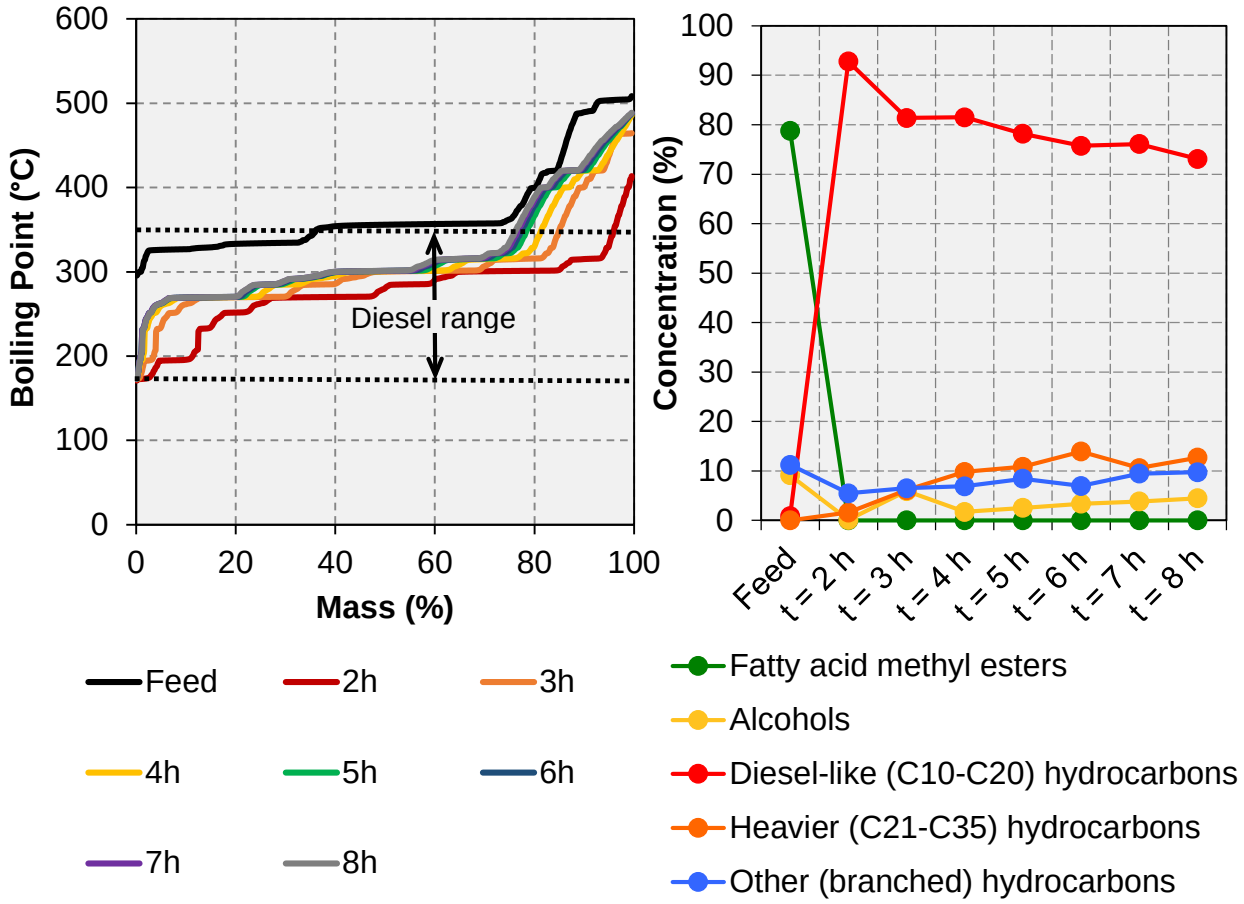

Figure 95. Simulated distillation boiling point distribution plot (left) of 75 wt% algal FAMEs in dodecane (feed) and the products collected after 1-8 h of time of stream and GC-MS data (right) showing the evolution of different compounds during the catalytic upgrading of the feed over 20% Ni-5% Cu/Al_2O_3 at 375 °C and a weight hour space velocity of 2 h^{-1}.

The analysis of the incondensable gases recovered during the catalytic deoxygenation of the algal FAMEs revealed the presence of methane (Figure 96), which is produced by cracking (loss of terminal carbons) as well as by the hydrogenation of the CO_x evolved during the feed deoxygenation via decarboxylation/decarbonylation. Overall these findings are similar to results recently reported by us for a variety of other concentrated, unsaturated lipid feeds, such as waste cooking oil and hemp oil (Santillan-Jimenez *et al.*, 2017).

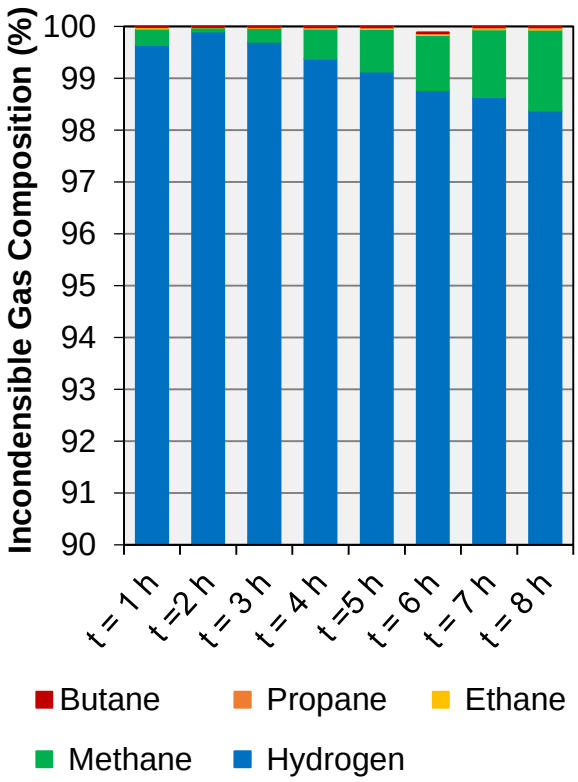

Figure 96. Composition of incondensable gases collected after 1-8 h of time of stream during the catalytic upgrading of 75 wt% algal FAMEs in dodecane over 20% Ni-5% Cu/Al_2O_3 at 375 °C (weight hour space velocity = 2 h^{-1}).

3.3.2. Bioplastic Compounding and Evaluation

Analysis of Raw Algae

The biomass received from UK CAER was analyzed to determine its viability for use in bioplastic compounds. Protein content, being one of the more important characteristics needed for successful bioplastic convergence, was found to increase as lipids and sugars were removed from the biomass. Ash did not seem to follow the same trend. The Defatted UK CAER algae seemingly increases in ash content while also increasing in moisture content. Defatted & Sugar Extracted UK CAER Algae decreased in moisture content and maintained consistent ash content with the Raw UK CAER Algae. All samples had noticeably different total peak counts analyzed via GC/MS amounting to differing numbers of compounds in each. Nitrogen containing compounds, sulfur compounds, and furans were counted separately as their own total at a lower temperature in the headspace. These compounds are attributed to rotting biomass or protein rich biomass, unpleasant smells, and burnt biomass respectively. Most samples of algae that are used in bioplastic production have a total of less than 20 of these specific compounds. See Table 22 for raw material results.

Table 22. Algae analyses

Name of Sample	Moisture	Protein	Ash	Nitrogen, Sulfur, and Furan Volatiles	Total Compound Count
Raw UK-CAER algae	7.45%	44.29%	11.30%	16	141
Defatted UK-CAER Algae	11.85%	50.57%	20.50%	12	121
Defatted & Sugar Extracted UK-CAER Algae	4.95%	58.73%	16.18%	18	154

Compounding Results

Before processing, the raw material needed to be pulverized down to a smaller size by hammer milling large chunks through a small mesh. Particle size results are taken before compounding on the Labtech twin screw extruder (see Table 23).

Table 23. Particle distribution data

	Particle Distribution (um)		
Name of Sample	**D99**	**D90**	**average**
Raw UK-CAER algae	147.34	80.50	37.34
Defatted UK-CAER Algae	160.05	92.33	43.50
Defatted & Sugar Extracted UK-CAER Algae	171.47	98.96	42.48

Processing conditions for each formulation are shown in Table 26 and Table 27. Temperature profiles were changed to accommodate differing base resins. Compounding formulations are labeled as K1-K7, see Table 24. It should be noted, however, that the final formulations are used in all mechanical property testing; see Table 25 for the Final Formulations.

Table 24. Compounding formulations

Material	K1 wt%	K2 wt%	K3 wt%	K4 wt%	K5 wt%	K6 wt%	K7 wt%
Ethylene Vinyl-Acetate (EVA)	65			63	63	65	53
Linear Low Density Polyethylene (LLDPE)		70					
Polylactic acid (PLA)			70				
compatibilizer				2	2		2
Raw UK-CAER algae					35	35	
Defatted UK-CAER algae	35	30	30	35			
Defatted & sugar extracted UK-CAER algae							45
Algix algae							

Table 25. Final formulations via injection molding

Material	F1 wt%	F2 wt%	F3 wt%	F4 wt%	F5 wt%	F6 wt%	F7 wt%
Ethylene Vinyl-Acetate (EVA)	70			68	68	70	68
Linear Low Density Polyethylene (LLDPE)		70					
Polylactic acid (PLA)			85				
compatibilizer				2	2		2
Raw UK-CAER algae					30	30	
Defatted UK-CAER algae	30	30	15	30			
Defatted & sugar extracted UK-CAER algae							30
Algix algae							

Table 26. Temperature profiles used for each formulation

Formulation	Feed Zone (°C)	Zone 1 (°C)	Zone 2 (°C)	Zone 3 (°C)	Zone 4 (°C)	Zone 5 (°C)	Zone 6 (°C)	Zone 7 (°C)	Zone 8 (°C)	Zone 9 (°C)	Die (°C)
K1	180	175	170	150	130	120	100	90	90	100	120
K2	80	170	170	160	150	140	135	135	140	145	155
K3	210	205	205	185	175	165	160	155	150	165	170
K4	180	175	170	150	130	120	100	90	90	100	120
K5	180	175	170	150	130	120	100	90	90	100	120
K6	180	175	170	150	130	120	100	90	90	100	120
K7	80	175	170	150	130	120	100	90	90	100	125

Table 27. Processing output data

Formulation	Screw RPM	Torque (%)	Pressure (psi)	Melt Temperature (°C)
K1	125	55	820	87
K2	125	52	80	NA
K3	150	44	100	156
K4	125	55	820	87
K5	125	48	750	89
K6	125	54	850	88
K7	140	55	700	103

Viscosity was measured on a Tinius Olsen MP1200 Extrusion Plastometer according to ASTM D1238, see Table 28. Those formulations containing ethylene-vinyl acetate (EVA) but less algae than K7 were shown to be higher in melt flow index (MFI) than FB (Bloom Product) shown in Figure 97. When algae are less abundant, as in K7, the MFI becomes relatively closer to the EVA baseline master batches (FB) in terms of viscosity. The presence or absence of a compatibilizer did not seem to have significant impact on the MFI between formulations of the same algae. K2 and Alga have similar MFI but do not contain the related plastics. K3 was not tested.

Table 28. Testing conditions and results of Melt Flow Index

Formulation	Temperature (°C)	Weight (Kg)	g/10min
K1	190	2.16	3.62
K2	190	2.16	11.1
K4	190	2.16	2.95
K5	190	2.16	2.99
K6	190	2.16	2.81
K7	190	2.16	1.75
Alga	210	2.16	11.29
Bloom	190	2.16	1.94

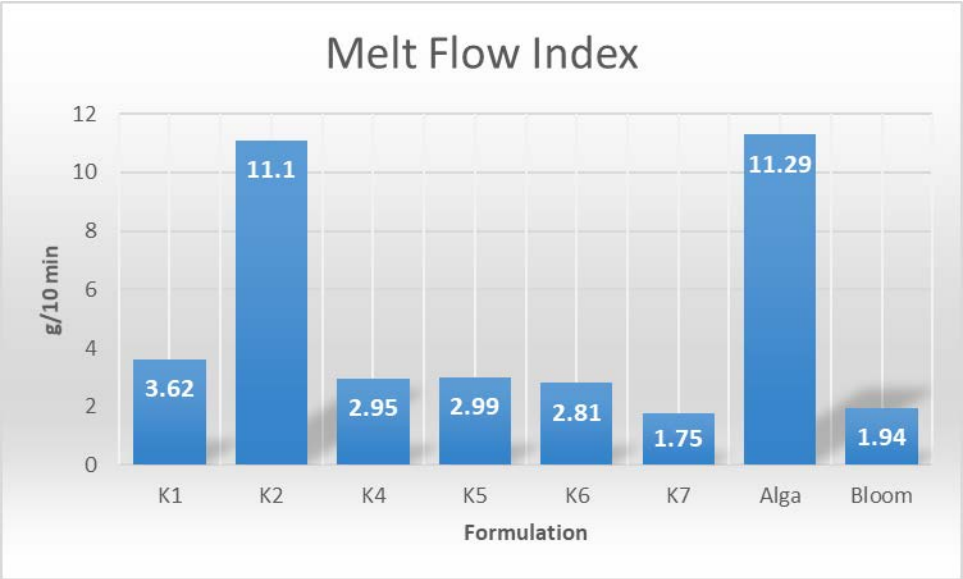

Figure 97. Comparison chart of MFI results

A Carver Press was used on the raw material to produce thin films of each formulation. The uniform thickness of the thin film allowed for a visual representation of agglomeration by the algae within the resin. The UK CAER algae formulations can be seen to have relatively high numbers of agglomerates as compared to the standard ALGIX product, (Figures 98-105). The weight percent of algae in the UK CAER formulations also did not seem to make a significant impact on the presence of agglomerates. The presence or absence of agglomerates, tiny globs of concentrated algae in the matrix, may be due to the particle size of the algae when incorporated with plastic.

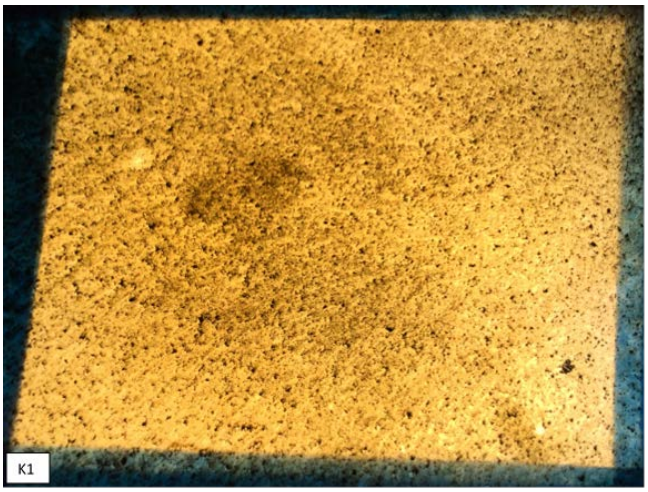

Figure 98. K1 press

Figure 99. K2 press

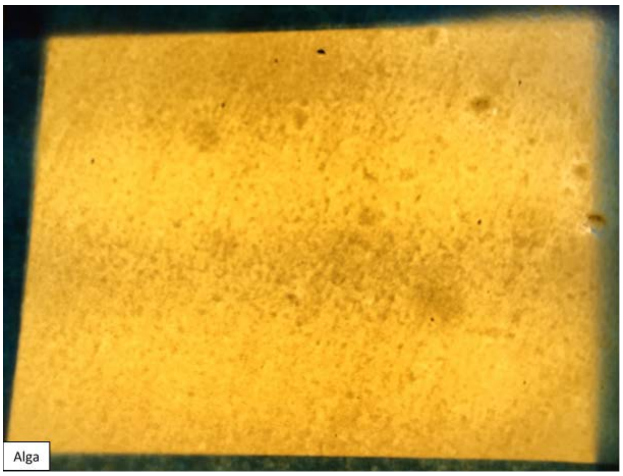

Figure 100. K4

Figure 101. K5

Figure 102. K6

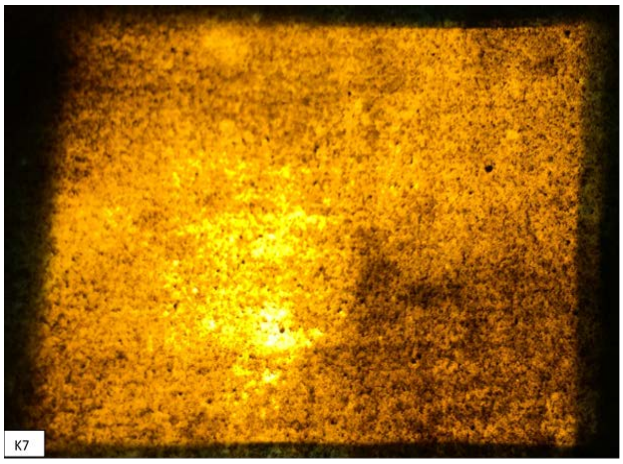

Figure 103. K7

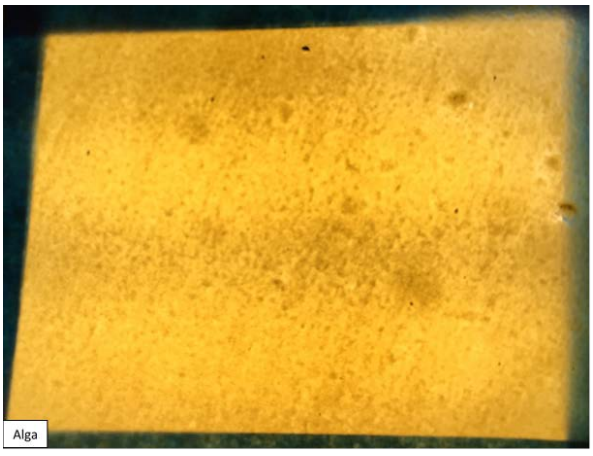

Figure 104. Alga

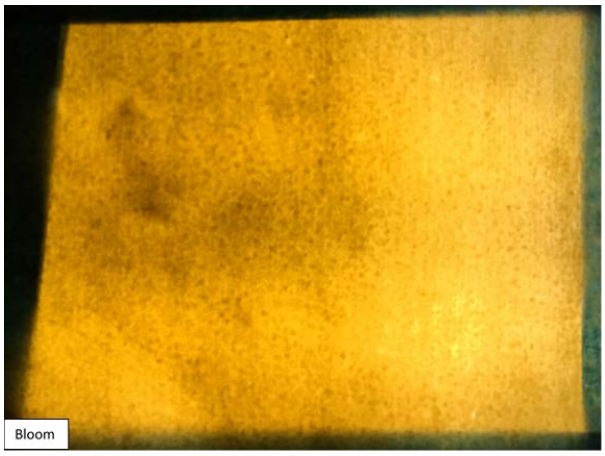

Figure 105. Bloom

Injection Molding

Injection molding was implemented on the bioplastic material to mold the pellets into usable and testable parts. A type 1 mold was used in accordance with ASTM D638-02a. These bars were molded with the same conditions for F1, F2, F4, F5, F6, F7, and Bloom (FB), found in Table 29. All formulations injection molded were made to contain 30% algae by weight by means of letting down with each formulation's base resin as shown in Table 25.

Table 29. Injection molding conditions

Zone	Temperature (°C)
Feed zone	37.8
Compression Zone	154.4
Metering Zone	160
Nozzle	165.6
Mold	42.2

Post Injection Molding Material Properties

An Instron instrument was used to test pull strength of the injection molded parts and filament shown in Figures 106-110. Final Formulation 3 (F3) is put into comparison to the Alga (FA) standard both consisting of 15% algae content by weight in final formulation. All other formulations were tested at 30% algae content by weight, see Table 25. All final formulation tensile results were plotted on the same graph for extension, load, and Young's modulus.

Table 30. Reference of final formulations table

Formulation	Base Resin	Compatibilized	Algae
F1	EVA	0%	Defatted UK-CAER algae
F2	LLDPE	0%	Defatted UK-CAER algae
F3	PLA	0%	Defatted UK-CAER algae
F4	EVA	2%	Defatted UK-CAER algae
F5	EVA	2%	Raw UK-CAER algae
F6	EVA	0%	Raw UK-CAER algae
F7	EVA	2%	Defatted & sugar extracted UK-CAER algae
FA	PLA	0%	Algix algae
FB	EVA	2%	Algix algae

Extension of the EVA containing formulations F1, F4, F5, F6, F7, and FB was drastically different depending on the type of algae used. However, in all algae cases the extension was less than half of the EVA control. It can be assumed from the data shown in Figures 106 and 107 that the addition of algae to EVA reduces the elongating properties of the final product. The poorest extension at machine peak load was demonstrated to be with the Algix Bloom (FB)

which was comparable to the Defatted UK CAER algae, see Figure 106. The Defatted UK CAER algae had a lower extension at peak load when compatibilized (F4) vs not compatibilized (F1). The opposite held true for the Raw UK CAER algae F5 & F6. The Raw UK CAER algae in EVA tested very similar to the Defatted & sugar extracted UK CAER algae (F7), see Figures 106-109. Both formulations containing PLA broke after a very small amount of extension compared to the other formulations, see Figure 107.

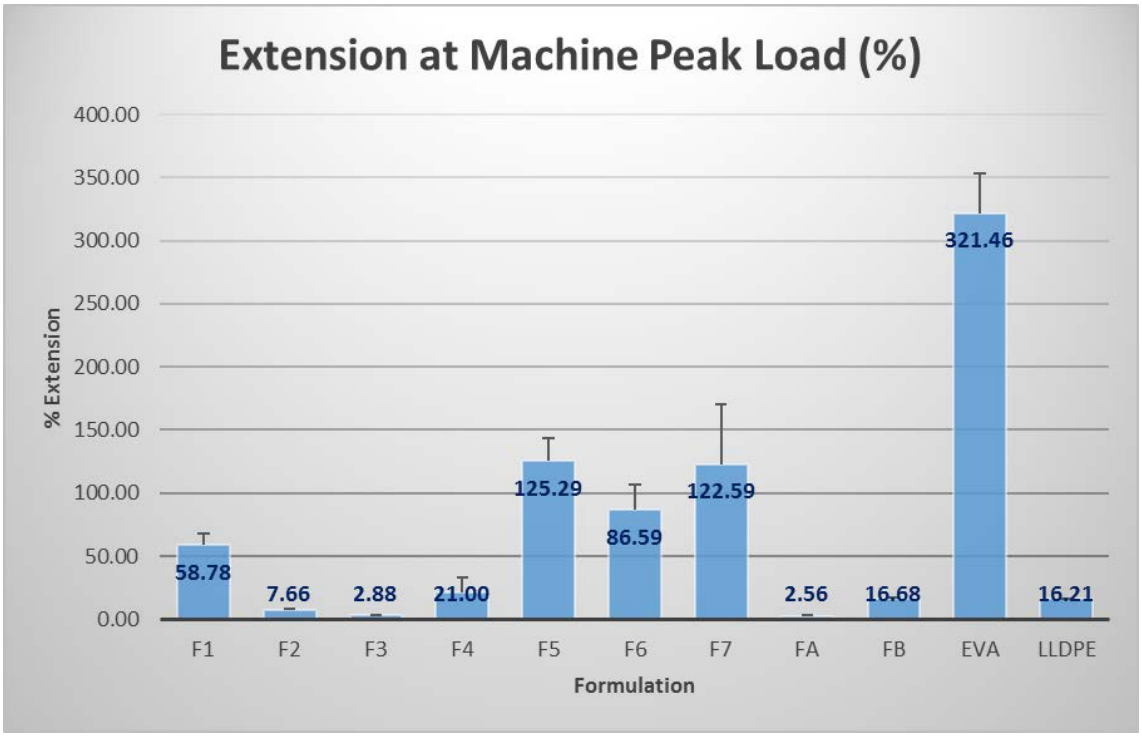

Figure 106. Extension at machine peak load

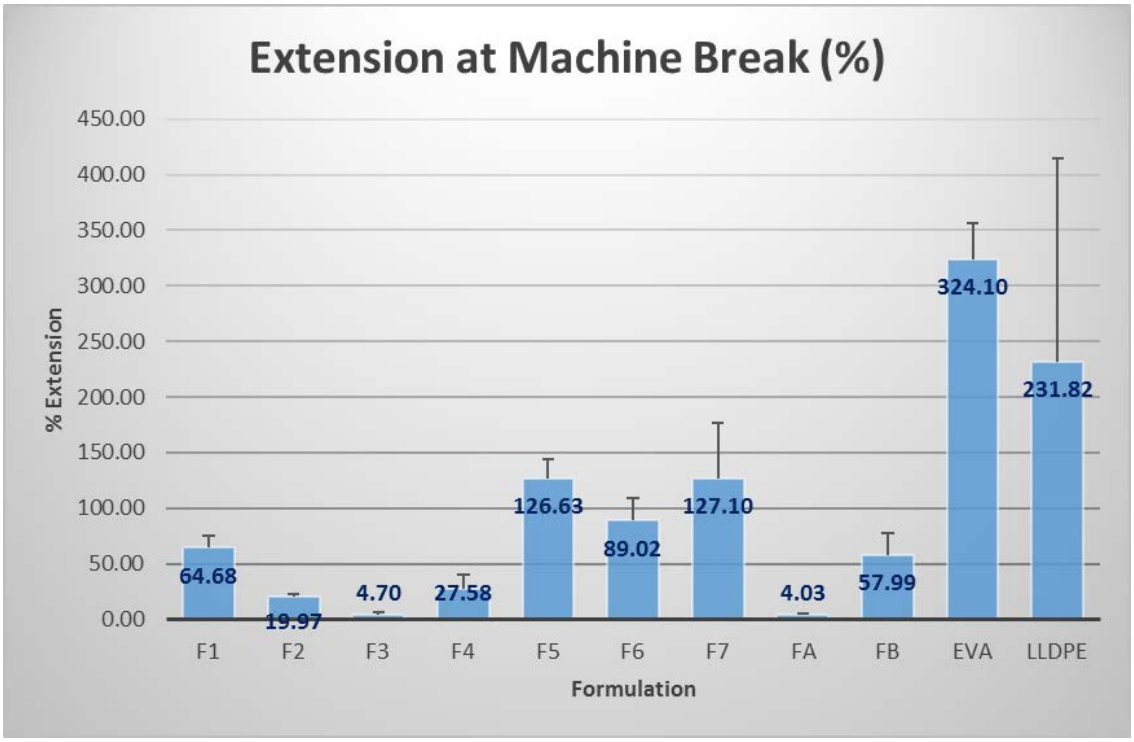

Figure 107. Extension at machine break

Force or tensile strength was also plotted, as shown in Figures 108 and 109. The algae formulation containing linear low-density polyethylene (LLDPE) (F2) had the highest peak in strength when pulled followed by Bloom product (FB) and lowest pull strength was measured in the PLA formulations (F3 and FA) as shown in Figure 108. Even though neat EVA and LLDPE have practically identical peak loads, according to Figure 108, LLDPE maintained a higher peak load after being compounded with algae than EVA did. Even Algix's Bloom product (FB) did not come close to the strength of the Defatted UK CAER algae LLDPE formulation (F2) in strength. It was found that all the UK CAER formulations tested very similarly to each other for load at machine peak. Compatibilizer addition to the formulations did not produce consistent properties across Defatted UK CAER algae and Raw UK CAER algae. Formulations containing the same algae and base resin that only differed from each other by the presence of a compatibilizer showed two different trends, the first trend being that the Defatted UK CAER formulation F4 with compatibilizer showed superiority to F1 without compatibilizer in terms of strength at break and peak strength. The opposite was true for the two Raw UK CAER algae formulations. The formulation without compatibilizer, F6, had higher strength in both categories. The improvement of strength through compatibilization for the Defatted UK CAER algae formulation with EVA (F4) did not seem to have the same effect on the Raw UK CAER algae. However, with the comparable strength results of the Defatted & sugar extracted UK CAER algae formulation F7 and F4 the compatibilizer may have helped increase F7's strength based on the data presented in Figure 108.

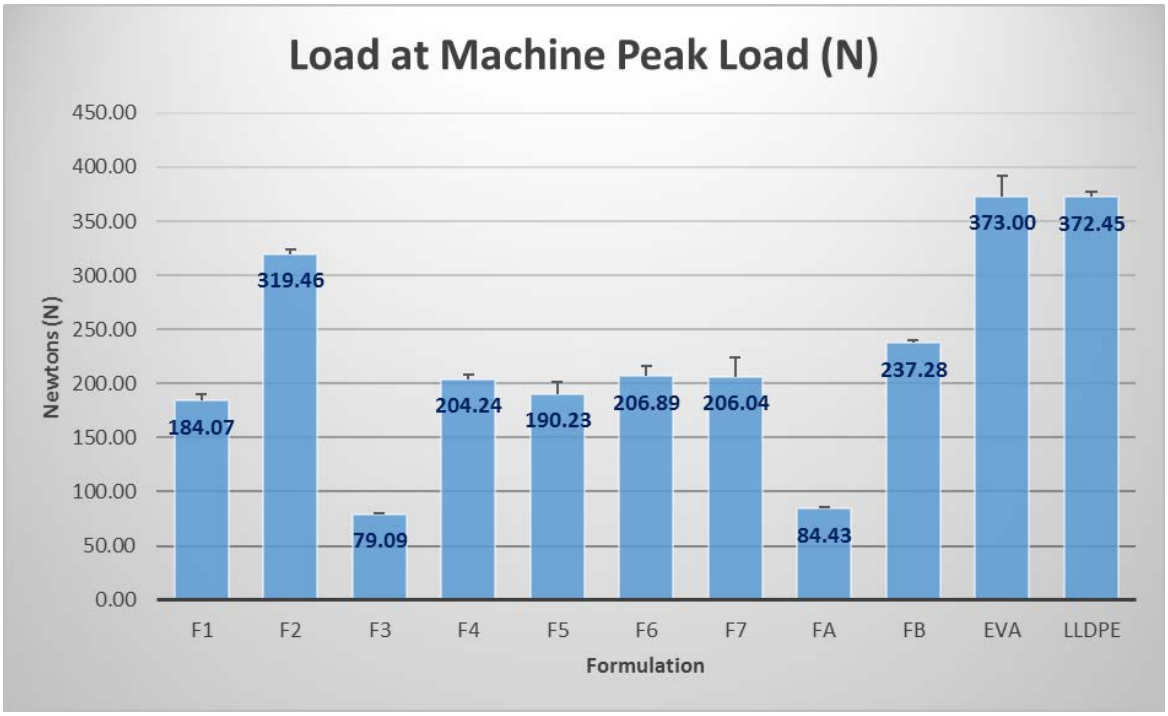

Figure 108. Load at machine peak load

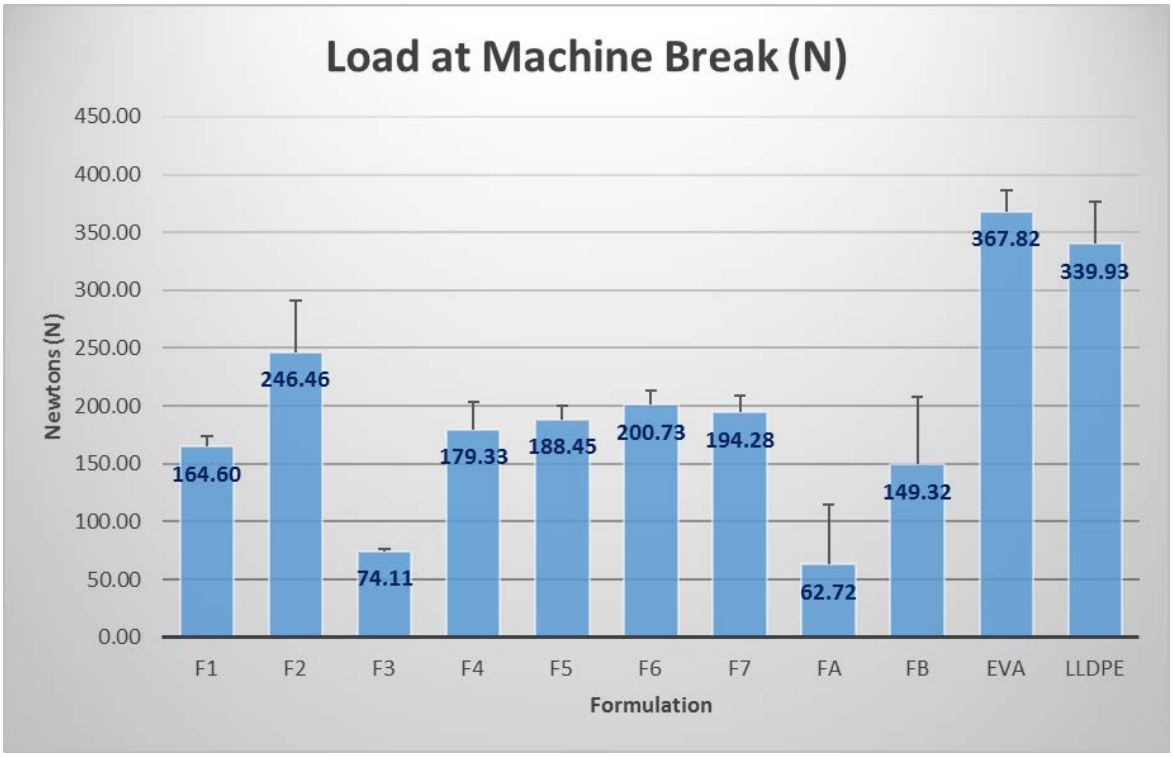

Figure 109. Load at machine break

Young's modulus or elastic modulus was measured for all final formulations. The stress/strain results are plotted in Figure 110. The most rigid material of the base resin selection, PLA, produced the highest modulus values for both of its formulations. F3 produced a lower modulus than the Alga product that Algix produces. This could coincide with once again algae property differences interfacing with the polymer matrix, producing different mechanical property relationships within the part. All the final formulations containing EVA were consistent within modulus results except F7. It is possible that this comes from the removal of the sugar content of the algae, making it lose the factor that would increase rigidity in the final product. Only a small difference was detected between the Raw UK CAER algae formulations, in which compatibilizer addition seemed to slightly increase rigidity. Young's modulus of the LLDPE and EVA formulations were increased by the addition of algae when compared to the neat polymers. Both EVA and LLDPE neat have lower moduli than any of their respective compounded formulations. From the data presented in Figure 110 the addition of algae clearly increases **rigidity** of the product in these two materials.

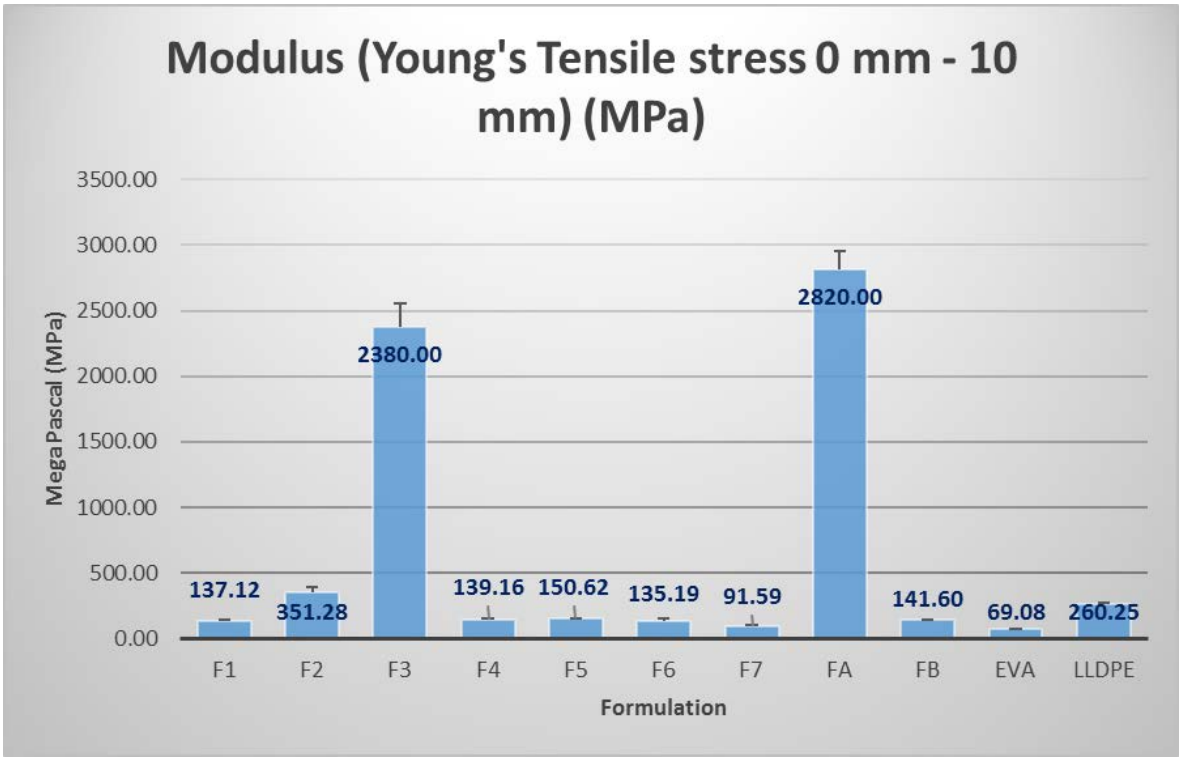

Figure 110. Young's modulus

Conclusions

Initial studies on the algae biomass provided by the University of Kentucky Center for Applied Energy Research provided that the algae would be a good candidate for bioplastic compounding. Being rich in protein, low in ash content, and having an acceptable volatile count all made for promising results. Before compounding the Defatted UK CAER algae and Defatted & sugar extracted UK CAER algae were subjected to a milling process using the same size mesh to

produce roughly identical particle sizes as reported in Table 23. Extrusion was performed using three types of polymers and the three batches of algae from UK CAER in various combinations. Compounding created a processable thermal melt through heat and shear to form bioplastic products which were tested via melt flow rate and thermal pressing. The temperatures were kept within small windows of each other to produce similar product by base resin. Melt flow rate or melt flow index (MFI) showed a similarity between Raw UK CAER algae and Defatted UK CAER algae on how they affect the melt properties of their base resins. K7, in this respect, showed similar properties to Algix's product known as Bloom. Heat presses of the different bioplastic products revealed that the compounding process produced large amounts of visible agglomerations in each of the UK CAER supplied algae regardless of base resin used. Since all the particle sizes used tested similarly to each other it may be noted that the ideal particle size for algae-plastic integration may need to be further researched.

EVA and LLDPE containing bioplastics were injection molded via a 35-ton injection molder at a similar algae content for further study. The conditions for injection molding each formulation were kept the same. Once complete parts were made a series of tensile tests were conducted after conditioning the parts. It was found that while some properties of the newly formed bioplastic products improved upon the neat material properties, other properties lessened. Overall, the potential for the UK CAER supplied algae to become a viable and processable bioplastic with adequate mechanical properties has been clearly shown. The best candidate for further review was the sugar and fat extracted material, which showed the highest extension values with comparable load values to other UK CAER EVA materials. It demonstrated extension benefits against the Algix Bloom product (currently offered commercially), even though it had quite a few agglomerates which generally act as a mechanical property reducing phenomenon. This leads to speculation that with enhanced milling that exists on the commercial scale, the sugar and fat extracted product may be even more competitive. Compared to raw UK CAER material the sugar and fat extracted samples were better but not substantially. However, compared to the Defatted algae, the agglomerate counts were much better and properties show a significant improvement. This indicates that if fat extraction is going to be conducted for biodiesel processing, then the resulting sugars must also be extracted to maintain product properties. Overall photobioreactor algal biomass grown from flue gas appears to have significant mechanical advantages over commercially available algal sources for applications with higher toughness and elasticity demands compared to the more rigid commercially available options used today. Additionally, if the algae are extracted for fat recovery it appears clear that sugar recovery is also necessary to maintain the utility of the algal biomass in plastic applications. For applications that demand higher resiliency, the algae meal derived from photobioreactor grown algae may be able to demand price premiums in the market. Hence, if the extracted sugars can also be valorized this would represent a promising opportunity to enhance biodiesel economics through the fractionation methodology demonstrated in this project.

4. Environmental Health and Safety Analysis

From available information, no significant EH&S risks were identified that would adversely affect the implementation of an algae facility design to capture point source CO_2 emissions. In this context it is pertinent to note that commercial-scale algae cultivation (typically using bottled CO_2) has been practiced since the early 1960s, in regions such as California, Hawaii, Japan and Israel (in the latter case, the CO_2 was supplied as flue gas from Israel Electric Corporation's Ashkelon coal-fired power plant). However, for full-scale operation at a power plant, an EH&S impact study would need to be conducted.

5. Technology Gap Analysis

Please refer to Appendix B, which contains the complete technology gap analysis for this project.

6. Training and Professional Development

In the first year of the project several undergraduate students were involved, as detailed below:

A female non-traditional student from the University of Kentucky who was involved in this project was encouraged to apply and supported in her successful application to the Research Scholars Program of the Kentucky National Science Foundation Experimental Program to Stimulate Competitive Research (KY NSF EPSCoR). The KY NSF EPSCoR support allowed her to work towards "Removing roadblocks to make the conversion of CO_2 emissions to diesel and jet fuel using algae an industrially viable process", this being the title of her funded proposal. The student successfully extracted algal lipids from wet algae via direct transesterification, and removed all traces of chlorophyll from the resulting crude algal lipids using activated carbon as a low-cost adsorbent. The resulting purified algal lipids were then catalytically upgraded via decarboxylation/ decarbonylation to afford hydrocarbons boiling in the diesel fuel range.

A female African-American student from Kentucky State University (KSU), the only Historically Black College or University (HBCU) in Kentucky, laid the ground work for the aforementioned upgrading work, since she ran a number of preliminary experiments to identify the best and most industrially relevant set of reaction conditions to upgrade lipids to diesel-range hydrocarbons. The student performed this work with support from KSU and thus, her involvement in this project incurred no cost to the sponsor.

Another KSU student was trained to assist with the algae-based CO_2 utilization demonstration at East Bend Power Station in Boone County, Kentucky. He took an interest in the chemical flocculation technique used to harvest and dewater the algae grown in the cyclic flow PBR. As a result of inconsistent results, he proposed and conducted experiments to fine tune the procedure by testing three cationic flocculants at varying concentrations and at differing temperatures and culture densities. These experiments shed light on possible improvements to the process that could improve harvest yields.

A male non-traditional student was trained to assist with the demonstration at East Bend Power Station. He quickly familiarized himself with the reactor system and recognized an area in the harvest process that could be improved upon to increase efficiency. By learning solid modeling techniques, the student designed and integrated a customized eductor injection system,

eliminating the need for hand mixing of flocculant into the culture and greatly decreasing the risk of culture contamination.

Another non-traditional chemical engineering student volunteered to work on the project in order to gain experience in energy research. He helped in the day to day execution of research activities as well as leading his own research associated with power plant integration.

In the second year of the project, student participation involved five undergraduates selected through a $38,000 Sustainability Challenge Grant funded by the University of Kentucky to enhance student development. The main goal of this award is to create a novel interdisciplinary research program for undergraduate students which combines a broad range of disciplines and provides unique opportunities for educational and professional development.

The five students chosen to participate in this project were chosen not only for their mix of backgrounds and high GPAs, but also for their enthusiasm for working in interdisciplinary groups. In addition to being directly involved in the day-to-day execution of research, these students were exposed to regular scientific seminars, in-depth lab tours, design thinking/iteration, and professional development opportunities, including resume formatting and interview etiquette.

7. Work Products

7.1. Publications, Conference Papers and Presentations

1. M. Wilson, J. Groppo, D. Mohler, S. Kesner, M. Crocker, “Algae Based Beneficial Re-use of Industrial Carbon Emissions: Demonstration Update and Mass Balance”, Algae Biomass Summit, Washington, D.C., September 29-October 2, 2015.
2. J. Groppo, “University of KY CAER - Duke Energy East Bend Algae Demonstration Project”, National Coal Council, 2015 Annual Fall Meeting, Nov 4-5, Pittsburgh PA.
3. M. Wilson, M. Carr, N. Deich, T. Jensen, L. Harmon, M. Allen, “Panel Discussion: Using Nature’s CO_2 Sink to Convert Carbon from Challenge to Economic Opportunity: Are Biological Capture and Utilization Technologies Ready to Deliver?”, Carbon Management Technology Conference, Houston, TX, November 17-19, 2015.
4. C. McKelphin, E. Santillan-Jimenez, M. Crocker, “Improving the Economics of Algae Biofuels through Optimized Extractions from Wet Algae”, 5th Annual Sustainability Forum, Lexington, KY, December 1, 2015.
5. M. Crocker, “Beneficial re-use of industrial CO_2 emissions using microalgae”, DOE 2015 CO_2 Utilization Workshop, December 2, Washington, DC.
6. C. McKelphin, R. Loe, E. Santillan-Jimenez, M. Crocker, “Kinetic Study of the Decarboxylation/Decarbonylation for the Upgrading of Triglycerides to Fuels”, Annual Convention of the National Society of Black Engineers. Boston, MA, March 25, 2016.
7. C. McKelphin, E. Santillan-Jimenez, M. Crocker, “Optimization of Algal Extracts for the Production of Fuels”, 243rd American Chemical Society National Meeting, San Diego, CA, March 14, 2016.

8. A. Zeller, “Using Algae as a Source for Renewable Bioproducts”, MBRE 2016, International Conference on Marine Biomass as Renewable Energy, Glasgow, Scotland, March 3-4, 2016.
9. C. McKelphin, E. Santillan-Jimenez, M. Crocker, “Optimization of Algal Extracts for the Production of Fuels”, 15th Annual Poster's at the Capital. Frankfurt, KY, February 25, 2016.
10. C. McKelphin, E. Santillan-Jimenez, M. Crocker, “Optimization of Algal Extracts for the Production of Fuels”, 25th Anniversary of the Louis-Stokes Alliance for Minority Participation in STEM, Washington, DC, February 23, 2016.
11. M.H. Wilson, D.T. Mohler, J.G. Groppo, T. Grubbs, S. Kesner, E.M. Frazar, A. Shea, C. Crofcheck, M. Crocker, “Capture and Recycle of Industrial CO_2 Emissions using Microalgae”, *Appl. Petrochem. Res.*, 6(3) (2016) 279.
12. M.H. Wilson, A. Shea, J. Groppo, D. Mohler, S. Kesner, C. Crofcheck, M. Crocker, “Lifecycle assessment of algae-based beneficial re-use of industrial carbon emissions”, 6th International Conference on Algae Biomass, Biofuels & Bioproducts, San Diego, CA, June 26-29, 2016
13. D. Mohler, “Algae Based Beneficial Re-use of Industrial Carbon Emissions: Demonstration and Heat Integration Assessment”, oral presentation at the Algae Biomass Organization’s annual Algae Biomass Summit, October 23-26, Phoenix, AZ.
14. M. Wilson, “Beneficial Re-use of Carbon Dioxide Emissions Using Algae”, U.S. DOE BETO Algae Cultivation for Carbon Capture and Utilization Workshop, Orlando, FL, May 23-24, 2017.
15. M. Crocker, “CO_2 to Fuels, Chemicals and Bioproducts: Recent Advances in (i) CO_2 Capture and Recycle using Microalgae and (ii) Oxidative Lignin Depolymerization”, National Renewable Energy Laboratory, Golden, CO, June 8.
16. R. Pace, E. Santillan-Jimenez, M.H. Wilson, J.G. Groppo, S. Kesner, E. Frazar, A. Zeller, M. Crocker, “Processing of algae biomass for the production of fuels and bioplastics”, oral presentation 6A.2, 7th Int. Conference on Algal Biomass, Biofuels and Bioproducts, Miami, FL, June 18-21, 2017.
17. M. Crocker, “CO_2 Capture and Recycle Using Microalgae”, Bioeconomy 2017, Washington, DC, July 11-12, 2017.
18. M. Crocker, “A Microalgae-based Platform for the Beneficial Reuse of CO_2 Emissions from Power Plants”, 2017 NETL CO_2 Capture Technology Project Review Meeting, Pittsburgh, PA, August 21-25, 2017.

7.2. Technologies or Techniques

Not applicable.

7.3. Inventions, Patent Applications and/or Licenses

Not applicable.

8. Conclusions

This project sought to address the technical and economic barriers to carbon dioxide (CO_2) capture and utilization using microalgae. A key finding was that harvested algae grown using flue gas as the CO_2 source contained very low heavy metal concentrations (As, Cd, Hg, Se), consistent with heavy metals incorporation from the supplied nutrients. This indicates that algal biomass produced from coal-derived flue gas should be suitable for use as animal feed or fertilizer.

A lifecycle assessment showed that the UK-designed cyclic flow PBR employed in this work qualifies as a net CO_2 capture technology. Indeed, over a 30-year period, net CO_2 capture would equate to 43% of the targeted amount, i.e., the amount captured from the supplied flue gas. A techno-economic analysis indicated that the minimum production cost of *Scenedesmus acutus* biomass in the US is in the order of $875/ton, excluding the cost of capital. While this figure is not too dissimilar to values reported for open raceway ponds in similar scenarios, it emphasizes that for current cultivation technology any pathway to economic viability will require applications for which algal boimass can be sold at prices in excess of $1,000/ton. Currently, such applications represent relatively small markets, such as pigments (e.g., astaxanthin) and nutraceuticals (ω-3 unsaturated fatty acids), as well as nutritional supplements (whole algae) for human consumption and for use in pet food. Consequently, the commercialization of large-scale algae-based CO_2 capture and utilization will require the development of new technologies to reduce the cost of algae production and/or the development of new, high-value applications for algal biomass.

One of the more promising applications for algal biomass is in the production of bioplastics. According to Algix, the potential for the algae grown in the East Bend PBR for the production of bioplastic with adequate mechanical properties was clearly shown. Positive features of the produced biomass include a high protein content and a composition that is generally more homogeneous than biomass grown in open ponds (in which many species may be present). The best candidate for further review, after incorporation into ethylene-vinyl acetate, was a lipid and sugar extracted material, which showed the highest extension values with comparable load values to other UK-derived samples. It also demonstrated extension benefits against the Algix Bloom product (currently offered commercially), even though it contained agglomerates which generally exert a negative effect on mechanical properties. This leads to speculation that with enhanced milling that exists on the commercial scale, the sugar and fat extracted product may be even more competitive. This, in turn, points to the need for additional work in order to assess the properties of such optimized algae-based plastics and the price point they can command.

9. References

A.o.A.P.F.C. 2017. Statement of Uniform Interpretation and Policy (SUIP) #25 - The "Heavy Metal Rule". Available from: http://www.aapfco.org/rules.html.

Carney L T, Lane T W. 2014. Parasites in algae mass culture. *Front. Microbiol.* 5: 278

Chen, Y, Li X, Sun Z, Zhou Z. 2017. Isolation and identification of *Choricystis minor* Fott and mass cultivation for oil production. *Algal Research* 25: 142-148

Churchill S W, Bernstein M. 1977. A Correlating Equation for Forced Convection From Gases and Liquids to a Circular Cylinder in Crossflow". *Journal of Heat Transfer, 99*(2): 300-306.

Collet P, Helias A, Lardon L, Ras M, Goy R-A, Steyer J-P. 2011. Life-cycle assessment of microalgae culture coupled to biogas production. *Bioresource Technology* 102(1): 207-214.

Conti M E. 2008. World Health Organization. Heavy Metals in Food Packagings, The State of the Art.

Crofcheck C, E X, Shea A, Montross M, Crocker M, Andrews R. 2012. Influence of media composition on the growth rate of *Chlorella vulgaris* and *Scenedesmus acutus* utilized for CO_2 mitigation. *Journal of Biochemical Technology* 4(2): 589–594.

EU Commission Directive 2002/72/EC of 6 August 2002 relating to plastic materials and articles intended to come into contact with foodstuffs. 2002.

Gardner R D, Cooksey K E, Mus F, Macur R, Moll K, Eustance E, Carlson R P, Gerlach R, Fields MW, Peyton B M. 2012. Use of sodium bicarbonate to stimulate triacylglycerol accumulation in the chlorophyte Scenedesmus sp. and the diatom Phaeodactylum tricornutum. *Journal of Applied Phycology* 24(5): 1311-1320.

Gardner R D, Lohman E J, Cooksey K E, Gerlach R, Peyton B M. 2013. Cellular cycling, carbon utilization, and photosynthetic oxygen production during bicarbonate-induced triacylglycerol accumulation in a *Scenedesmus* sp. *Energies* 6: 6060-6076.

Gardner R D, Lohman E, Gerlach R, Cooksey K E, Peyton B M. 2013. Comparison of CO_2 and bicarbonate as inorganic carbon sources for triacylglycerol and starch accumulation in *Chlamydomonas reinhardtii. Biotechnol. Bioeng*. 110(1): 87-96.

Gehl K A, Colman B. 1985. Effect of external pH on the internal pH of *Chlorella saccharophila*. *Plant Physiol*. 77: 917-921.

Gerloff-Elias A, Spijkerman E, Proschold T. 2005. Effect of external pH on the growth, photosynthesis and photosynthetic electron transport of *Chlamydomonas acidophila* Negoro, isolated from an extremely acidic lake (pH 2.6). *Plant, Cell and Environment* 28: 1218-1229.

Goldman J C, Azov Y, Riley C B, Dennett M R. 1982. The effect of pH in intensive microalgal cultures. I. Biomass regulation. *Journal of Experimental Marine Biology and Ecology* 57(1): 1-13.

Gonzalez L E, Bashan Y. 2000. Increased growth of the microalga *Chlorella vulgaris* when coimmobilized and cocultured in alginate beads with the plant-growth-promoting bacterium *Azospirillum brasilense*. *Appl. Environ. Microbiol*. 66(4): 1527-1531.

Hanagata N, Takeuchi T, Fukuju Y. 1992. Tolerance of microalgae to high CO_2 and high temperature. *Phytochemistry* 31(10): 3345-3348.

Hannon M, Gimpel J, Miller T, Rasala B, Mayfield S. 2011. Biofuels from algae: challenges and potential. *Biofuels* 1(5): 763-784.

Hawarti T U, Willke T, Vorlop K D. Characterization of the lipid accumulation in a tropical freshwater microalgae *Chlorococcum* sp. Bioresource Technology. 121: 54-60.

Huang G, Wang J, Kuang Y, He H. Effects of SO_2 and NO_2 in flue gas on CO_2 sequestration and intracellular microstructures analysis of *Chlorella* sp. *Research and Reviews: Journal of Microbiology and Biotechnology* 5(3): 60-67.

Ilkov G. 1975. Population dynamic relationships during *Phlyctidium scenedesmi* development in *Scenedesmus acutus* cultures. *Appl. Microbiol.* 6: 104-110.

Ji M, Yun H, Hwang J, Salama E, Jeon B, Choi J. 2017. Effect of flue gas CO_2 on the growth, carbohydrate and fatty acid composition of a green microalga *Scenedesmus obliquus* for biofuel production. *Environmental Technology* 38(16): 2085-2092.

Jiang, Y, Zhang W, Wang J, Chen Y, Shen S, Liu T. 2013. Utilization of simulated flue gas for cultivation of *Scenedesmus dimorphus*. *Bioresource Technology* 128: 359-364.

Jorquera O, Kiperstock A, Sales E A, Embirucu M, Ghirardi M L. 2010. Comparative energy life-cycle analyses of microalgal biomass production in open ponds and bioreactors. *Bioresource Technology* 101(4): 1406-1413.

Juneja A, Ceballos R M, Murthy G S. 2013. Effects of environmental factors and nutrient availability on the biochemical composition of algae for biofuels production: a review. *Energies* 6: 4607-4638.

Karpov S A, Mamkaeva M A, Aleoshin V V, Nassonova E, Lilije O, Gleason F H. Morphology, phylogeny, and ecology of the aphelids (Aphelidea, Opisthokonta) and proposal for the new superphylum Opisthosporidia. *Front. Microbiol.* 5: 112.

Lane A E, Burris J E. Effects of environmental pH on the internal pH of *Chlorella pyrenoidosa*, *Scenedesmus quadricauda*, and *Euglena mutabilis*. *Plant Physiol*. 68: 439-442.

Lardon L, Helias A, Sialve B, Steyer J-P, Bernard O. 2009. Life-cycle assessment of biodiesel production from microalgae. *Environmental Science and Technology* 43(17): 6475-6481.

Laurens L M L, Nagle N, Davis R, Sweeney N, Van Wychen S, Lowell A, Pienkos P T. 2015. Acid-catalyzed algal biomass pretreatment for integrated lipid and carbohydrate-based biofuels production. *Green Chemistry*, 17: 1145.

Laurens L M L, Quinn M, Van Wychen S, Templeton D W, Wolfrum E J. 2012. Accurate and reliable quantification of total microalgal fuel potential as fatty acid methyl esters by in situ transesterification. *Anal. Bioanal. Chem*., 403: 167-178.

Lee J S, Kim D K, Lee J P, Park S C, Koh J H, Cho H S, Kim S W. 2002. Effects of SO_2 and NO on growth of *Chlorella* sp. KR-1. *Bioresource Technology,* 82: 1-4.

Letcher PM *et al*. 2013. Characterization of *Amoeboaphelidium protococcarum*, an algal Parasite New to the Cryptomycota Isolated from an Outdoor Algal Pond used for the Production of Biofuel. *PLoS One* 8(2): e56232.

Loe R, Santillan-Jimenez E, Morgan T, Sewell L, Ji Y, Jones S, Isaacs M A, Lee A F, Crocker M. 2016. Effect of Cu and Sn promotion on the catalytic deoxygenation of model and algal lipids to fuel-like hydrocarbons over supported Ni catalysts. *Appl. Catal. B*, 191: 147-156.

Lohman E J, Gardner R D, Pedersen T, Peyton B M, Cooksey K E, Gerlach R. 2015. Optimized inorganic carbon regime for enhanced growth and lipid accumulation in *Chlorella vulgaris*. *Biotechnology for Biofuel*s 8(1): 82.

Lourence S O, Barbarino E, Lavin P L, Lanfer Marquez U M, Aidar E. 2004. Distribution of intracellular nitrogen in marine microalgae: calculation of new nitrogen-to-protein conversion factors. *European J. Phycol*., 39: 17-32.

Maeda K, Owada M, Kimura N, Omata K, Karube I. 1995. CO_2 fixation from the flue gas on coal-fired thermal power plant by microalgae. *Energy Conversion and Management* 36(6-9): 717-720.

Matsumoto H, Hamasaki A, Sioji N, Ikuta Y. 1997. Influence of CO_2, SO_2, and NO in flue gas on microalgae productivity. *J. Chem. Eng. Jpn*. 30:620-624.

Mendoza L, Taylor J W, Ajello L. 2002. The class mesomycetozoea: A heterogeneous group of microorganisms at the animal-fungal boundary. *Annual Review of Microbiology* 56: 315-344.

Mills A F. Heat Transfer, 2d ed., Prentice-Hall, 1999, p. 348.

Mortensen L M, Gislerød H R. The growth of *Chlorella sorokiniana* as influenced by CO_2, light, and flue gas. *J. Appl. Phycol*. 28: 813-820.

Mudimu O, Rybalka N, Bauersachs T, Friedl T, Schulz R. 2015. Influence of different CO_2 concentrations on microalgae growth, α-tocopherol content and fatty acid composition. *Geomicrobiology Journal* 32: 291-303.

Nagase H, Yoshihara K I, Eguchi K, Yokota Y, Matsui R, Hirata K, Miyamoto K. 1997. Characteristics of biological NOx removal from flue gas in a *Dunaliella tertiolecta* culture system. *Journal of Fermentation and Bioengineering* 83(5): 461-465.

National Research Council. 2005. Mineral Tolerance of Animals. National Academies Press: Washington, D.C.

NSF/ANSI, 173-2010 *Dietary Supplements*. 2011.

Ota M, Kato Y, Watanage H, Watanabe M, Sato Y, Smith RL Jr, Inomata H. 2009. Effect of inorganic carbon on photoautotrophic growth of microalga *Chlorococcum littorale*. 25(2): 492-498.

Papazi A, Makridis P, Divanach P, Kotzabasis K. 2008. Bioenergetic changes in the microalgal photosynthetic apparatus by extremely high CO_2 concentrations induce an intense biomass production. *Physiologia Planatrum* 132: 338-349.

Rebolloso Fuentes M M, García Sánchez J L, Fernández Sevilla J M, Acién Fernández F G, Sánchez Pérez J A, Molina Grima E. 1999. Outdoor continuous culture of Porphyridium cruentum in a tubular photobioreactor: quantitative analysis of the daily cyclic variation of culture parameters. *Journal of Biotechnology, 70*(1–3):271-288.

Rogers J N, Rosenberg J N, Guzman B J, Oh V H, Mimbela L E, Ghassemi A, Betenbaugh M J, Oyler G A, Donohue M D. 2014. A critical analysis of paddlewheel-driven raceway production at commercial scales. *Algal Research* 4: 76-88.

Santillan-Jimenez E, Loe R, Garrett M, Morgan T, Crocker M. 2017. Effect of Cu promotion on cracking and methanation during the Ni-catalyzed deoxygenation of waste lipids and hemp seed oil to fuel-like hydrocarbons. *Catal. Today*, http://dx.doi.org/10.1016/j.cattod.2017.03.025.

Santillan-Jimenez E, Pace R, Marques S, Morgan T, McKelphin C, Mobley J, Crocker M. 2016. Extraction, characterization, purification and catalytic upgrading of algae lipids to fuel-like hydrocarbons. *Fuel*, 180: 668-678.

Sarat CT, Deepak RS, Maneesh KM, Mukherji S, Chauhan VS, Sarada R, Mudliar SN. 2016. Evaluation of indigenous fresh water microalga Scenedesmus obtusus for feed and fuel applications: Effect of carbon dioxide, light and nutrient sources on growth and biochemical characteristics. *Bioresource Technology* 207:430-439.

Schwenk D, Nohynek L, Rischer H. 2014. Algae-bacteria association inferred by 16S rDNA similarity in established microalgae cultures. *Microbiology Open* 3(3): 356-368

Shen Y, Pei Z, Yuan W, Mao E. 2009. Effect of nitrogen and extraction method on algae lipid yield. *Int. J. Agric. Biol. Eng*., 2(1): 51-57.

Sobczuk T M, Camacho F G, Rubio F C, Fernandez F, Grima E M. 2000. Carbon dioxide uptake efficiency by outdoor microalgal cultures in tubular airlift photobioreactors. *Biotechnology and Bioengineering, 67*(4): 465-475.

Solovchenko A, Khozin-Goldberg I. High-CO_2 tolerance in microalgae: possible mechanisms and implication for biotechnology and bioremediation. *Biotechnology Letters* 35: 1745-1752.

Stephenson A L, Kazamia E, Dennis J S, Howe C J, Scott S A, Smith A G. 2010. Life-cycle assessment of potential algal biodiesel production in the United Kingdom: A comparison of raceways and air-lift tubular bioreactors. *Energy Fuels* 24(7): 2062-4077.

Taylor AR, Brownlee C, Wheeler GL. 2012. Proton channels in algae: reasons to be excited. *Trends in Plant Science* 17(11): 675-684.

U.S.C.o.F., Regulations, *Maximum contaminant level goals for inorganic contaminants*, in *40 C.F.R. 141.51*. 2010a.

U.S.C.o.F., Regulations, *Pollutant Limits*. 2010b.

Wang B, Li Y, Wu N, Lan C Q. 2008. CO_2 bio-mitigation using microalgae. *Appl. Microbiol. Biotechnol.* 79(5):707-718.

Wilson M H, Mohler D, Groppo J, Grubbs T, Kesner S, Frazar E M, Shea A, Crofcheck C, Crocker M. 2016. Capture and recycle of industrial CO_2 emission using microalgae. *Applied Petrochemical Research* 6(3): 279-293.

Yang Y, Gao K. 2003. Effects of CO_2 concentrations on the freshwater microalgae, *Chlamydomonas reinhardtii, Chlorella pyrenoidosa* and *Scenedesmus obliquus* (Chlorophyta). *J. Appl. Phycol.* 00:1-11.

Yen HW, Ho SH, Chen CY, Chang JS. 2015. CO_2, NOx and SOx removal from flue gas via microalgae cultivation: a critical review. *Biotechnol. J.* 10(6): 829-839.

Appendix A – Acronyms

CAER	Center for Applied Energy Research
EVA	Ethylene-vinyl acetate
GC-MS	Gas chromatography-mass spectrometry
ICP-OES	Inductively coupled plasma – optical emission spectroscopy
LCA	Lifecycle assessment
LLDPE	Linear low-density polyethylene
MCL	Minimum contaminant level
MFI	Melt flow index
PBR	Photobioreactor
PET	Polyethylene terephthalate
PSII	Photosystem II
PVC	Polyvinyl chloride
TEA	Techno-economic analysis
UD	University of Delaware
UK	University of Kentucky

Appendix B – Technology Gap Analysis

Technology Gap Analysis

A Microalgae-Based Platform for the Beneficial Re-use of Carbon Dioxide Emissions from Power Plants

Principal Author
Mark Crocker
University of Kentucky, Lexington KY

Contributing Co-authors
Jack Groppo, Stephanie Kesner, Daniel Mohler, Eduardo Santillan-Jimenez, Michael Wilson
University of Kentucky, Lexington, KY

Submission Date
December 2017

Work Performed Under Award Number
DE-FE0026396

Submitted By
University of Kentucky Research Foundation
109 Kinkead Hall
Lexington, KY 40506-0057

Principal Investigator
Mark Crocker
(859) 257 0295
mark.crocker@uky.edu

DOE Program Manager
Isaac 'Andy' Aurelio
304-285-0244
Isaac.Aurelio@NETL.DOE.GOV

Submitted To
U.S. Department of Energy, National Energy Technology Laboratory

Executive Summary

Production-scale cultivation of microalgae has been practiced for over 50 years. Through this work, it has been determined that algae production economics depend strongly on cultivation productivity, significant penalties being encountered if areal productivity is lower than 25 $g/m^2/day$. Notably, current best-case scenario estimates for algal biomass productivity range from 33 to 42 $g/m^2/day$, productivities demonstrated to date ranging from 13 to 21 $g/m^2/day$. In view of these values, it is clear that algae production economics can be greatly improved if the productivities demonstrated to date are further increased and start approaching current best-case scenarios.

Research and development (R&D) efforts since 2010 have resulted in reductions in the cost of algae-based biocrude of up to two orders of magnitude, from a starting baseline of $240/gallon to $7.50/gallon. These biocrude prices can be employed as a useful proxy for algae production costs, although an exclusive focus on less valuable biofuels has been abandoned in favor of a model in which algae-derived fuels are economically enabled by higher value co-products. Additional cost reductions could be achieved by focusing on innovations in four main aspects of the algae production and utilization process, namely, algae strain development, improved cultivation, low energy harvesting, and high yield extraction-conversion technology. Techno-economic modeling of a number of processes suggests that mechanisms exist to reduce costs further through the aggressive recycling of streams. In short, although the commercial production of algae-derived biofuels is not economically viable at the present time, models predict that with improvements in the four main aspects mentioned above, economic viability can be attained.

One of the main challenges faced by the large scale cultivation of algae is the fact that CO_2 availability can limit photosynthesis and the associated fixation of carbon into biomass, which makes the prospect of beneficially reusing emission streams such as combustion flue gases interesting as these constitute CO_2-rich streams. In order for the carbon present in the flue gas to be used by the algae, it needs to be made available to the individual cells suspended in the growth medium. Carbon dioxide can be separated from the flue gas to provide an almost pure CO_2 source, or introduced directly to the algae culture as a portion of the whole flue gas stream, the latter option avoiding the additional capital and operating costs associated with chemical CO_2 capture. There are essentially two options to use flue gas directly in an algae cultivation system: 1) compression and subsequent bubbling of the CO_2-rich gas directly into the algae growth system; and 2) producing a concentrated aqueous stream saturated or supersaturated with dissolved carbon. While the former method represents a tried and tested method for the carbon supplementation of algae cultures, the latter approach represents a nascent technology showing potential for lowering operating costs and increasing the viable distance between an algae farm and a point source of emissions. In fact, novel processes involving membranes and/or carbon adsorbers may represent the next step in the integration of algae cultivation systems with CO_2 point sources.

Two main technologies are currently used for large-scale algae cultivation: outdoor open pond systems and indoor or outdoor photobioreactor (PBR) systems. Each of these approaches offers a number of advantages and disadvantages. On the one hand, open ponds consume less energy,

however, they also display lower productivity. On the other hand, PBRs minimize both water evaporation and the risk of culture contamination, although they incur higher capital costs. Researchers at the University of Kentucky (UK) Center for Applied Energy Research (CAER) have designed a next generation 'cyclic flow' PBR, which includes a host of cost- and energy-saving features, which directly address and assuage a number of issues typically associated with PBRs. Although there are at this time no significant technological hurdles to overcome in order for these technologies to be used for large-scale cultivation of algae biomass, neither method has proved to be economically viable as a method of biofuel production. Therefore, most work in this area is focused on attaining the dramatic reductions (on the order of 80-90%) in capital and/or operating costs necessary to enable economic success. This work is complemented with efforts to maximize biomass productivity and to diversify algal biomass utilization focusing on the extraction of specialty products, which represent two methods to render large-scale algae cultivation more economically feasible (the use of industrial wastewater as a nutrient source being another option to reduce operating costs). Moreover, the combination of the two main cultivation systems (ponds and PBRs) represents an underexplored area of research that could increase areal productivity by respectively harnessing and remediating the advantages and disadvantages of each of these systems.

UK's harvesting and dewatering strategy employs a proven low-cost approach based on flocculation-sedimentation followed by gravity filtration, yielding algae containing 10-15 wt% solids. Initially this process was performed batch-wise, however, as part of the current DOE-sponsored project, the process has been modified to operate in continuous mode, as would be required at significant scale. Periodic harvesting allows recovering algae for utilization (maintaining culture density in a range suitable for optimal growth) and for process water containing unused nutrients to be recycled. With large-scale operations, multiple banks of PBRs would be at various stages of the growth cycle, those approaching a maximum culture density being diverted to a centralized harvest system to provide a continuous harvest feed. An assessment of current harvesting and dewatering technology readiness shows that while centrifuges are the industry state of the art for harvesting algae, this approach is energy intensive and has high capital and operating costs. A reasonable alternative would be to utilize the methods employed by other applications that separate solids from dilute suspensions, such as municipal wastewater treatment or mineral processing. In these applications, effective thickening is employed to concentrate suspended solids while producing clarified water, significantly reducing the volume of solids suspension for further dewatering. A number of flocculants including chitosan and $AlCl_3$ have been evaluated, UK CAER testing having shown that operating costs for a combination of cationic and anionic flocculants are lower than chitosan or $AlCl_3$ with >95% solids capture. In addition, this UK CAER approach has been demonstrated in continuous operation using a static thickener with lamella plates to minimize the suspended solids entrained with the clarified water. Alternative technologies such as membrane filtration, dissolved air flotation and spiral plate separation as well as electrolytic and ultrasonic harvesting can significantly reduce harvesting operating costs relative to centrifugation; however, they have yet to be demonstrated in continuous operation at significant scale.

As mentioned above, attention has shifted away from an exclusive focus on less valuable biofuels to focus on a model in which algae-derived fuels are economically enabled by higher value co-products. This new paradigm implies that algal biomass fractionation approaches may need to be employed, the fractionation scheme of choice depending on the end use of the biomass. In terms of algal lipid extraction, the commercial processes developed by Valicor represent the state of the art and it is hard to see how significant improvement of these processes is possible. Other approaches for lipid extraction from algae have been reported, including the use of sonication, pulsed electric field (PEF) technology and microwave irradiation; however, few of these methods have been commercialized, which is mainly due to their elevated cost. In contrast to lipid extraction – where at least some processes have been commercialized – full algal biomass fractionation has not been commercially developed.

In terms of their use, whole algae, algae fractions and individual algae-derived compounds have applications that are as numerous as they are varied, the aquaculture, animal feed and fertilizer, bioplastics, nutraceuticals, dyes and pigments, and cosmetics industries capturing most of the market share. Notably, technology gaps exist in most industries in which algal biomass finds its end uses. For instance, there are considerable gaps regarding the integration of large-scale microalgal biomass production with aquaculture, particularly in terms of co-locating aquaculture facilities at microalgae production sites and reclaiming and recycling a significant fraction of the nutrients excreted by fish. Moreover, the promise of much higher available quantities of algal biomass in the future is prompting evaluation of algae as a major ingredient in formulated animal feeds and as a soil fertilizer. Furthermore, the effect of algae processing on the quality and properties of bioplastics comprising algal biomass remains a topic in need of additional research. Finally, albeit several compounds found in algae are used as nutraceuticals, pigments and other high value products, these compounds tend to be produced from sources other than microalgae, which implies that additional work is required to determine if sourcing these compounds from algae could have technological, economical or environmental advantages.

Last but certainly not least, it is important to note that there are several companies with ongoing large-scale algae cultivation operations and/or with demonstration-scale projects in the area of microalgae removal of CO_2 from flue gas. Some salient examples include Pond Technologies (Ontario, Canada), Genesis Biofuels Inc. (Boulder, Colorado), Cellana, Inc. (Kona, Hawaii), and Global Algae Innovations, Inc. (San Diego, California). Pond Technologies is investigating the use of algae for the reduction of greenhouse gas emissions from industrial point sources, aiming to ultimately convert these emissions into valuable bioproducts such as biofuel, fertilizer and animal feed. Similarly, Genesis Biofuels Inc. is in the business of building algae-based refineries that sequester CO_2 emissions from cement plans to produce renewable energy products. Cellana, Inc. is investigating the use of microalgae to sequester the CO_2 in the flue gas from on-site diesel generators, while Global Algae Innovations, Inc. claims to have the world's only large-scale open raceway utilizing power plant flue gas as its only CO_2 source for the production of algal protein along with biofuel and high value commodities.

Disclaimer

Acknowledgement

This material is based upon work supported by the Department of Energy under Award Number DE-FE0026396.

Table of Contents

List of Tables

List of Figures

1. Overview of the Proposed Algae-Based Platform for the Beneficial Capture and Utilization of Carbon Dioxide Emissions from Power Plants

1.1.Process Description

1.1.1. Background

The impetus behind algae-based carbon capture and utilization technology dates back to the U.S. DOE's Aquatic Species Program (ASP), which from 1978 to 1996 funded research and development efforts to produce biodiesel from algae grown in ponds using waste CO_2 emissions from coal-fired power plants [1]. This program, funded by the DOE Office of Fuels Development, made possible noteworthy advances not only in the science of algal biology (with the objective of increasing lipid content in microalgae) but also in the engineering of microalgae production systems (with the goal of maximizing algal biomass productivity at reasonable cost). More recently, the ASP – which was focused mostly on upstream (algal biomass production) processes – has been complemented by a more comprehensive research and development program. Indeed, between 2010 and 2013, the National Alliance for Advanced Biofuels and Bioproducts (NAABB) – which was managed through the Bioenergy Technologies Office of the U.S. Department of Energy – supported research efforts spread more evenly across upstream and downstream (algal biomass harvesting, fractionation and utilization) processes [1], resulting in a number of innovations with the potential to considerable improve the technological and economic viability of algae-based carbon capture and utilization. More recently, testbed networks funded in part by the Bioenergy Technologies Office of the U.S. Department of Energy – including the Algae Testbed Public-Private Partnership (ATP^3) and the Regional Algal Feedstock Testbeds (RAFT) – have been established to accelerate R&D for the sustainable and cost-effective production of algal biomass (and algae-derived fuels and chemicals) mainly through gathering, standardizing, analyzing and disseminating long-term cultivation data [2].

1.1.2. State of technology

A recent report – published in 2017 by IEA Bioenergy and authored by Lieve Laurens *et al*. – provides a thorough and up-to-date review of the state of the technology related to algae-based bioenergy [3]. In addition, another relatively recent report – published in 2015 by the IEA Clean Coal Center and authored by Xing Zhang – represents an excellent survey and analysis of published literature in the area of microalgae removal of CO_2 from flue gas [4]. Other noteworthy reviews have summarized the status and challenges faced by microalgae-based carbon capture [5] and provided a perspective on microalgal CO_2 emission mitigation systems [6]. The algal biomass productivity and CO_2 consumption data in these contributions provide an excellent snapshot of the state of the technology in the form of specific benchmarks to be improved upon by current and future projects. Indeed, the aforementioned reviews compiled and compared algal biomass productivity and CO_2 fixation performance values reported in the literature, arranging the data as a function of the microalgal species and the type of reactor and/or growth strategy employed. In short, the microalgae species that have been most widely used for CO_2 capture include *Botryococcus braunii*, *Chlorella sp.* (including *Chlorella vulgaris* and *Chlorella kessleri*), *Chlorocuccum littorale*, *Chlamydomonas reinhardtii*, *Scenedesmus sp.* (including *Scenedesmus obliquus*), *M. minutum*, *Tetraselmis sp.*, and *Spirulina sp.* [4-7]. Most saliently, algal biomass productivity values ranging from 40 to 1,000 mg/L/day and CO_2 consumption values ranging from

20 to 5,345 mg/L/day have been reported, the average value being 370 mg/L/day for algal biomass productivity and 775 mg/L/day for CO_2 consumption rates [6]. A more recent NAABB report published in 2014 reports somewhat higher productivity values ranging from 560 to 1,000 mg/L/day, the average being 767 mg/L/day [8]. Expressed in terms of areal productivity, other publications have reported maximum theoretical algal biomass productivity to be 196 g/m^2/day [9], best-case scenario estimates to range from 33 to 42 g/m^2/day [10], and demonstrated productivities in closed photobioreactors and open ponds to average 20.7 and 13 g/m^2/day, respectively [11,12]. Obviously, algae production economics are strongly dependent on cultivation productivity, dramatic penalties being encountered if areal productivity is lower than 25 g/m^2/day [3]. Fortunately, the latter value falls within the best-scenario estimates above, meaning that the economics can be greatly improved if the productivities demonstrated to date are further improved and start approaching current best-case scenarios.

1.1.3. Cost

The work performed by the NAABB between 2010 and 2013 resulted in reductions in the cost of algae-based biocrude of up to two orders of magnitude, from a starting baseline of $240/gallon to $7.50/gallon [13]. Admittedly, an exclusive focus on less valuable biofuels has been abandoned in favor of a model in which algae-derived fuels are economically enabled by higher value co-products (as is discussed below in more detail); however, biocrude prices can still be employed as a useful proxy for algae production costs. According to the NAABB, the greatest cost reductions could be achieved by focusing on innovations in four main aspects of the process, namely, algae strain development, improved cultivation, low energy harvesting, and high yield extraction-conversion technology [13]. Indeed, the techno-economic modeling of a number of processes suggested that mechanisms exist to reduce costs to below $4 per gallon through the aggressive recycling of streams [8]. Notably, the NAABB determined that cost reductions are closely tied to the capital costs (CAPEX) and the operating costs (OPEX) of an algae farm. Indeed, according to cost simulations performed by the NAABB, positive net present values are attained if CAPEX and OPEX are reduced by 50%, additional reductions rendering the algae farm even more profitable. In fact, there is a 98% probability of economic success when an algae farm reduces its OPEX and CAPEX by 80% and 70%, respectively, as these reductions result in a total cost of $2.10/gallon of crude oil [8]. In turn, the cost of biomass is calculated at $1,033/ton, $395/ton and $205/ton if CAPEX and OPEX are not reduced, reduced 50% and reduced 70%, respectively. In short, although the commercial production of algae-derived biofuels is not economically viable at the present time, models predict that with improvements in algae strains, cultivation, harvesting and extraction, economic viability can be attained.

More recent calculations performed applying techno-economic analysis (TEA) models to algae productivity values achieved at different locations have estimated a cost of algae biomass production ranging from 3.1 to 11 €/kg (see Figure 1). These calculated costs are 6-10-fold higher than the price point considered to be economically viable for fuel production, although a future projection for a flat panel photobioreactor (PBR) sited in Southern Spain has shown the potential to achieve biomass production costs of 0.5 €/kg [3].

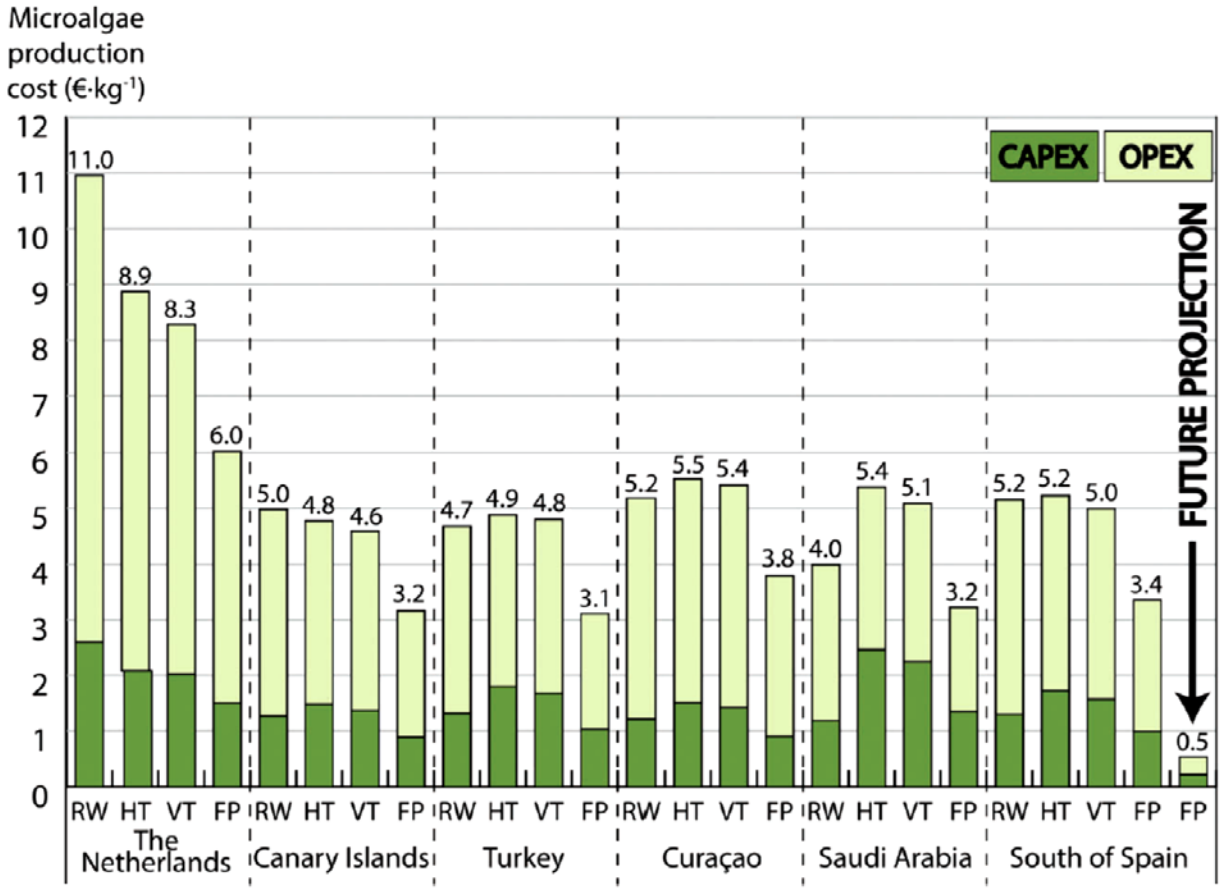

Figure 1. Projected biomass production costs (cultivation and harvesting) as a function of location and cultivation technology (RW: raceway pond; HT: horizontal tubular PBR; VT: vertically stacked horizontal tubular PBR; FP: flat panel PBR) [14].

Notably, this value is in overall agreement with the conclusions of another recent study performed to estimate the costs of algal biomass production in open ponds. Indeed, this study calculated an average cost of $0.54/kg for *Scenedesmus acutus* grown at a rate of 25 g m^{-2} day^{-1} and showing a lipid content of 27% [15].

1.2.Major and Critical Components

1.2.1. Power Plant Flue Gas as a Source of CO_2 for Algae Cultivation Systems

One of the main challenges faced by the large scale cultivation of algae is the fact that CO_2 availability can limit photosynthesis and the associated fixation of carbon into biomass. Carbon constitutes ca. 50% by weight of the elemental composition of algal biomass [3], with CO_2 representing the most significant nutrient requirement and a significant contributor to operational expenses. This is mainly because traditionally, compressed cylinders of lab or food grade carbon dioxide gas are purchased and used to increase the yield of algal biomass through carbon supplementation. While this is an effective way to boost the productivity of algal cultivation systems, it negatively impacts the overall life cycle analysis of the process due to the fact that this approach significantly increases both energy requirements and CO_2 emissions.

Some large scale facility designs have considered co-locating algae cultivation with CO_2 pipelines traditionally used for enhanced oil recovery (EOR) in the tertiary production from developed oil fields [16]. While promising in principle, most attempts to integrate with this infrastructure have proved difficult to negotiate. Additionally, most of the carbon dioxide used to supply the network of pipelines for EOR applications comes from natural sources such as mined CO_2 deposits, which represent an additional source of greenhouse gas emissions.

Encouragingly, this important challenge faced by large-scale algaculture also represents an opportunity to beneficially reuse CO_2-rich emission streams such as combustion flue gases. One of the inherent benefits of working with coal flue gas is the high percentage of CO_2 (10-15%) in this stream compared to the atmospheric CO_2 concentration (400 ppm). Indeed, in view of their elevated concentration of CO_2, these waste streams can be used as an input to an industrial photosynthetic process, eliminating carbon limitation, and enabling faster algae growth [4].

In order for the carbon present in the flue gas to be used by algae, it needs to be made available to the individual cells suspended in the growth medium. The carbon dioxide can be separated from the flue gas through chemical or physical means to provide an almost pure CO_2 source, or introduced directly to the algae culture as a portion of the whole flue gas stream. The concept developed at the University of Kentucky Center for Applied Energy Research (UK CAER) involves using flue gas directly – as opposed to separating the CO_2 from the flue gas in a separate process – in order to avoid additional capital and operating expenses associated with chemical CO_2 capture [17]. Currently, the flue gas is delivered to the PBR and mildly compressed (10-15 psi gauge) before being introduced to the algae culture via a gas line at the bottom of each reactor manifold. Rather than continuously bubbling gas into the reactor, a duty cycle is used not only to increase CO_2 utilization efficiency, but also to minimize the energy required to appropriately mix the culture [18]. The flue gas used for algae growth studies at East Bend Station – obtained after all emission control units – is delivered to the PBR site via a 1” stainless steel pipe, being driven to the reactor at 10-15 psi gauge by a diaphragm vacuum pump. The flue gas is then delivered to the individual PBR modules via a simple network of electronic solenoid valves (to enable automated operation) and introduced as bubbles to provide CO_2 for photosynthesis, limit oxygen inhibition [19], and provide mixing for the culture.

1.2.2. Algae Cultivation System

Two main technologies are currently used for large-scale algae cultivation: (i) outdoor open pond systems; and (ii) indoor or outdoor photobioreactor (PBR) systems. Each of these approaches offers a number of advantages and disadvantages. On the one hand, open ponds consume less energy; however, they also display lower productivity. On the other hand, PBRs minimize both water evaporation and the risk of culture contamination, although they incur higher capital costs. System selection is made taking into account the economics of the target products and the availability of algae strains capable not only of affording the desired products, but also of thriving in the chosen environment.

(i) Ponds:

Open ponds have been used for large-scale algae cultivation for over 60 years, the most commonly used system being open raceway ponds (ORP). Raceway ponds are most often oval-shaped (resembling a race track), have a typical depth of 10-50 cm, and circulate in a closed loop to achieve continuous production. A paddle wheel operates to constantly facilitate culture and growth media flow through the system, in addition to gas-to-liquid contact and mixing. Nutrients are added after the paddlewheel and harvesting takes place in line before the paddlewheel [20]. Unsurprisingly, the main advantages of open pond systems over PBRs are much lower capital costs and lower operating costs. Indeed, ponds typically display much lower energy consumption [21].

Nevertheless, open pond systems are not free of drawbacks. Indeed, they render the algae culture highly susceptible to contamination from other microorganisms and have higher water requirements to compensate for evaporation-related losses. In addition, they require large amounts of land and display lower algal biomass yields relative to PBRs. The fact that ponds are less productive than PBRs for algal biomass production can be attributed to several factors, including insufficient mixing, light limitations, evaporative losses and CO_2 deficiency [22]. In particular, CO_2 deficiency – caused mainly by atmospheric diffusion limitations and poor mixing – can lead to dramatic reductions in biomass productivity due to a less efficient utilization of CO_2 and poor CO_2 mass transfer rates [23].

(ii) Photobioreactors:

Photobioreactors are designed to circumvent some of the major drawbacks associated with open pond systems. First and foremost, closed PBRs are more amenable to growing a single algal species for prolonged periods of time as this configuration minimizes the risk of external contamination. Tubular, flat panel and column PBRs are among the most common designs, all usually consisting of an array of plastic or glass tubes or panels wherein algae growth is facilitated by the addition of various nutrients. Each of the aforementioned PBR designs offers certain specific advantages. Flat panel PBRs display high photosynthetic efficiencies, whereas tubular PBRs are suitable for outdoor cultivation due to their large surface area and column PBRs have the highest volumetric mass transfer, the best mixing and the most controllable internal conditions [20].

By leveraging years of experience acquired working in the field, researchers at the UK CAER have designed the next generation ‘cyclic flow’ PBR used in the present study. This improved PBR consists of clear vertical tubes – designed and positioned to maximize sunlight exposure – each of which is sparged periodically with flue gas, making it a form of column PBR. The tubes are filled with the algae culture by means of a pump, however, the pump is not operated continuously; rather, it is used to periodically fill and drain the tubes. In this manner, energy requirements associated with pumping are significantly reduced relative to conventional PBR systems [18].

The PBR body consists of a system of vertical tubes made of clear PET (polyethylene terephthalate) tubes (8.9 cm in diameter and 244 cm high) connected with schedule 40 PVC (polyvinyl chloride) pipe (7.5 cm in diameter). To increase individual tube access to solar radiation and minimize shading, reactor tubes are arranged in two parallel manifold lines, offset so that each

tube is centered between the empty spaces of the other row (Figure 2). Figure 3 depicts a computer-generated image of the PBR tube arrangement along with a photograph of an installed pilot-scale system [18].

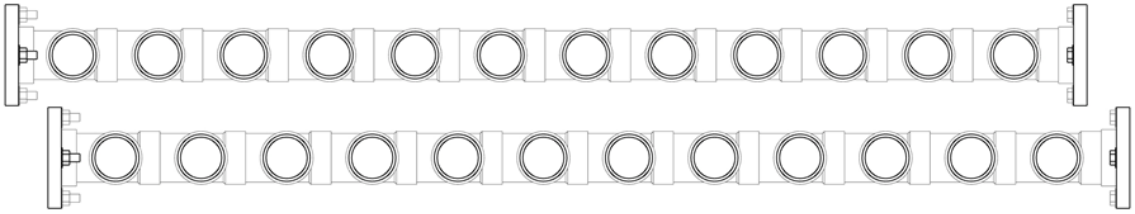

Figure 2. Overhead view of parallel manifolds showing alignment of tubes to minimize shading [18].

Figure 3. Computer generated image showing PBR tube arrangement and photograph of an installed pilot-scale PBR [18].

The ‘cyclic flow’ reactor is designed to operate differently than other PBR designs, due to the fact that – in addition to the high energy penalty associated with the continuous circulation of large volumes of algae culture – other issues must also be addressed. For instance, fully developed flow in a pipe results in a ‘no slip’ condition at the pipe wall, which provides excellent conditions for algae cells to accumulate on the internal surface of the tube. Given time, these cells will establish colonies and ultimately form a biofilm, biofilm formation being a major technical hurdle in the deployment and scale up of photobioreactors. To avoid this issue, the culture does not flow continuously in the novel reactor design. Instead, the tubes in the photoarray drain and fill in a cyclic manner multiple times per day. Consequently, the liquid flow is never fully developed and

biofilm formation is minimized. In the cyclic flow PBR, biofilm mitigation is additionally controlled by the introduction of gas bubbles in the PET tubes to create multi-dimensional fluid mixing, and through the use of a buoyant pipe pig (one per PET tube) to clean the reactor walls as flow is cycled. Each time the reactor is filled and drained the pipe pigs, which are equipped with rubber gaskets, travel the length of the clear PET tubes, mechanically removing any attached algae [18].

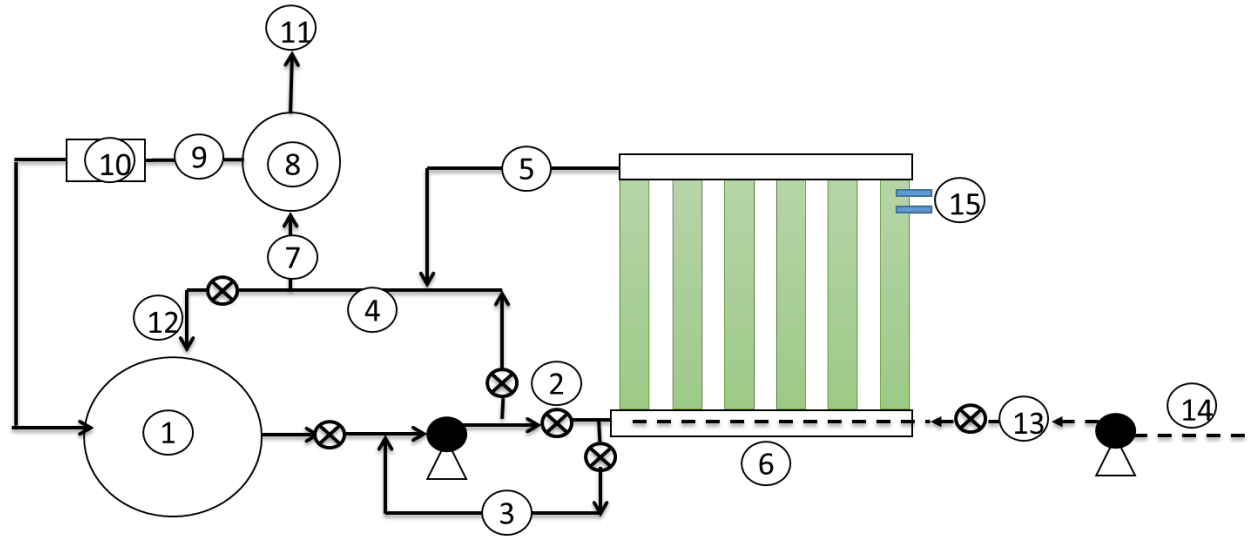

1	Main Process Tank	9	Supernate/ Nutrient Return
2	Tube Fill Line	10	UV Sterilization
3	Tube Drain Line	11	Concentrated Biomass Removal
4	Recycle / Return Line	12	Process Return to Tank
5	Overflow / Gas Exchange	13	Flue Gas / CO_2 Introduction
6	Phototube Array	14	Flue Gas From Stack
7	Harvest Port	15	pH and dO_2 probes
8	Harvest Tank		

Figure 4. Process flow diagram of photobioreactor. Figure taken from [18].

Energy savings are also realized by avoiding sparging gas and/or circulating the culture continuously and by instead duty cycling these operations based on the needs of the algae culture for mixing, ensuring suspension of the culture, and providing adequate CO_2. A schematic flow diagram of the system is shown in Figure 4. A main process tank (1) is sized to be equal or greater to the volume of one phototube array, which consists of two parallel manifold lines. A centrifugal pump and valving system is used to move algae slurry from the process tank to the phototube arrays (2), from the phototube arrays back to the tank for mixing and/or harvesting (3), and to mix the culture via a recycle line (4). An overflow line (5) enables gas, originally in the empty tubes, to be transferred to the tank during fill cycles and for the same volume of gas to be transferred back to the phototube array during draining cycles to prevent suction from damaging the semi-

rigid PET tubes. Flue gas is periodically added directly to the phototubes via perforated tubing (13) to mix the culture and add CO_2. Algae are harvested via a harvest port (7) and sent to a primary dewatering system to separate the algae from the nutrient medium (8). Clarified water (containing any unused nutrients) is returned (9) to the process tank via a UV sterilizer (10) to prevent contamination of the system. The feed and drain valves (2 & 3) are repeated for each additional tube array to accommodate a series of parallel reactors, which operate separately. Labview software is used to control the actuation of the process valves, start and stop the pump, actuate solenoid valves to control the injection of flue gas to the system, and monitor process parameters such as photosynthetically active radiation, pH, dissolved oxygen, and temperature [18].

1.2.3. Harvesting and Dewatering of Algal Biomass

UK's harvesting and dewatering strategy employs a proven low-cost approach based on flocculation-sedimentation followed by gravity filtration, an approach commonly used in the mining, industrial and municipal water treating industries [18,24]. When harvesting occurs, a portion of the culture volume is diverted from the growth system into the harvest system during the mixing phase of growth system operation. Moderate molecular weight cationic polyacrylamide flocculant is added at a dosage of 5 to 7 ppm, dependent upon harvest culture density, and mixed using a recirculating centrifugal pump. The flocculated system is allowed to settle for approximately 1 h, after which settled biomass (20 to 30 g/L) is removed from the thickener and clarified water is pumped back into the feed tank to recycle water along with remaining soluble nutrients. As water is recycled, it is passed through a UV sterilizer. The concentrated algae slurry is then transferred to a horizontal gravity filter dryer and allowed to drain on a multifilament filter fabric. Initially this process was performed batch-wise, however, as part of the current DOE-sponsored project, the process has been modified to operate in continuous mode, as would be required at significant scale. Gravity filtration typically yields algae containing 10-15 wt% solids. This can be increased to ca. 25 wt% solids by brief application of a vacuum, at which point more than 95% of the external water has been removed (the remaining water being intracellular). Alternatively, a plate and frame press or centrifuge can be used to achieve similar results. After filtration, dewatered biomass is dried in an oven at 60 °C for storage or utilization. Once dried, biomass flakes are homogenized and stored in sealed plastic bags and stored in a freezer to prevent degradation. If wet utilization is warranted, no drying is necessary and wet biomass is directly placed in sealed plastic bags and stored in a freezer.

Periodic algae harvesting is necessary for three specific reasons. The first is to recover algal biomass for utilization. Since culture density in the growth system is dilute (ca. 1 g/liter), it is necessary to concentrate biomass into a more usable concentration by removal of free water. The second is to maintain culture density in a range suitable for optimal growth. As culture density increases, light inhibition occurs, which inevitably results in limited productivity. Effective harvesting enables dilution of the culture in the growth system to remedy light inhibition. The third reason is to enable recycling of process water. One obvious benefit is minimization of water consumption, however, just as important is that reusing soluble nutrients in recycled process water significantly reduces nutrient consumption. An additional benefit is realized as clarified process

water is sterilized to control bacteria and rotifer populations, allowing the system to maintain a healthy culture environment.

Harvest time and volume is currently determined by tracking growth rate through sampling. Representative composite samples are periodically collected and analyzed for dry mass concentration, from which the culture density of the entire system is calculated. The appropriate harvest volume is then calculated to ensure that when recycled process water is added to the growth system after harvesting, the culture density will be in the appropriate range (i.e., ~0.2 g/liter). When the growth system achieves a culture density of ca. 1 g/liter, the harvesting cycle is repeated.

With large-scale operations, a similar strategy would apply. Since multiple banks of PBRs would be at various stages of the growth cycle, those approaching a maximum culture density would be systematically diverted to a centralized harvest system, thus providing a continuous harvest feed.

1.2.4. Algal Biomass Fractionation

The type of algal biomass fractionation scheme employed in any production process will depend on the end use of the biomass. For some applications, such as animal feed and bioplastics, fractionation is not required, the biomass being used as whole cells (albeit subject to additional processing). For other uses extraction of the lipids is required, while others may require further fractionation of the biomass into protein and carbohydrates. The following provides a brief summary of the main (commercially relevant) processes that have been developed for this purpose.

(i) Lipid extraction (dry solid):

Solvent extraction of lipids from microalgae is an area of research that has been the subject of much recent attention; an excellent review on this topic has recently appeared [25]. Lipid extraction from as harvested (wet) algae poses a problem since traditional extraction procedures typically require a completely dehydrated and well ground feed stock (typically obtained by bead milling) [25]. If the goal is to produce a low value product such as liquid fuel from the algae, it is desirable that the lowest possible amount of energy be used. While a variety of concentration techniques are available, evaporative dehydration is required to obtain a completely dry feedstock, making dry extraction far too energy intensive for most applications [20,26]. However, for high value applications (such as nutraceuticals), solvent-based extraction of dry biomass may be preferable, suitable solvents including supercritical CO_2 and ethanol.

(ii) Lipid extraction (wet solid):

Wet extractions, in which algae feed stocks are only partially dewatered [26-29], can be much more energy efficient, and have efficiencies that are potentially less dependent on mechanical cell disruption than dry solvent extractions. The method used at the UK CAER for lipid extraction from wet algal solids represents a modification of a method reported by Laurens *et al*. for the analytical-scale quantification of esterifiable lipids in microalgae [30]. Treatment of the wet algae (10-20 wt%) with sufficient 5% HCl/MeOH so as to decrease the pH to 1, followed by addition of hexane and stirring at 85 °C for 2 h, results in lysing of the cell walls, with concomitant acid-catalyzed esterification/transesterification and extraction of the lipids present. The products are fatty acid methyl esters (FAMES) obtained in amounts that are close to values achieved for

solvent-based extraction from dry algae. The other products, which are isolated by means of settling and subsequent filtration, are a solid ("defatted" algae), and an aqueous MeOH stream that contains carbohydrates. In this scheme the acid serves two purposes, *viz.*: (i) chemical lysing of the algae cells and (ii) acid catalyst for esterification reactions.

A similar approach has been developed by Valicor, Inc. in their commercial "AlgaFrac™" process (see Figure 5 below) [31]. Wet algae biomass is first subjected to "conditioning", involving the addition of acid to the biomass to pH 1-2 and heating for ca. 60 min at 80-150 °C. Hexane is then added, with vigorous mixing, to extract the lipids. Separation of the hexane and aqueous layers is achieved by centrifugation. According to Valicor's patent, analysis of the aqueous layer shows the presence of algal solids, while the aqueous solution contains sugars, phosphate, organic acids, and a relatively small amount of protein products, in addition to some unidentified compounds. A variant of this approach uses hexane and methanol for the extraction instead of simply hexane, in which case the extracted lipids are obtained in the form of fatty acid methyl esters.

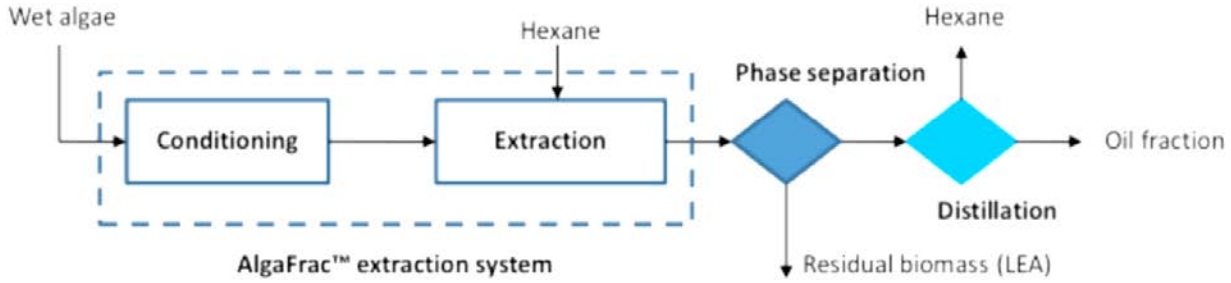

Figure 5. Schematic of Valicor AlgaFrac™ lipid extraction process.

Valicor have also patented a method involving lipid extraction using ethanol from algae biomass that has been dried to 45-55 wt% solids [32]. This is a far milder approach than the one described above (acid addition is not required) and is suitable for the extraction of high value products for human consumption, such as omega-3 unsaturated fatty acids. However, the requirement that the biomass is first dried to 45-55 wt% solids renders this method prohibitively expensive for the extraction of less valuable lipids.

In this context it should be noted that researchers at NREL have recently described an approach to full algae biomass fractionation. In NREL's Combined Algal Processing (CAP) approach [33], the algal slurry is subjected to acid pre-treatment into order to hydrolyze carbohydrates into sugars, which are directly used for fermentation to ethanol. The ethanol and microalgal lipids can be sequentially recovered from the fermentation broth by thermal treatment and solvent extraction. In this manner, almost all the fermentable sugars can be used for ethanol production without compromising lipid recovery, leaving behind a protein-rich solid. In terms of the ultimate product slate, CAP is somewhat similar to the above UK and Valicor lipid extraction processes, the main difference being that the more severe conditions used in CAP result in greater release of fermentable sugars. Indeed, the NREL process requires pre-treating the wet, concentrated biomass in an autoclave, using 2% acid loading (w/w), a temperature of 155 °C, reaction time of 10 minutes and solids loading of 25% (w/w) [34].

1.2.5. Utilization of Algal Biomass Fractions

Whole algae, algae fractions and individual algae-derived compounds have applications that are as numerous as they are varied. However, most end uses given to algal biomass are concentrated in a handful of industries, which are discussed below.

(i) Aquaculture:

Aquaculture now provides more than 50% of all fish consumed by humans, i.e., more than wild harvested fish. Currently, aquaculture is a $97 billion global business, growing at 9% per year [35]. 30% of world algae production is reportedly sold for aquatic and animal feed applications, and over 50% of *Spirulina* production is used as a feed supplement [36]. In aquaculture, microalgae are used as a feed additive or as a sole feed component, and for coloring the flesh of fish such as salmon. The most frequently used species include *Chlorella*, *Tetraselmis*, *Isochrysis*, *Pavlova*, *Phaeodactylum*, *Chaetoceros*, *Nannochloropsis*, *Skeletonema* and *Thalassiosira* [22,37]. In order to be suitable for aquaculture, a microalgal strain has to meet certain criteria, which include being non-toxic, the correct size and shape for easy ingestion, possessing favorable nutritional qualities and possessing a digestible cell wall so that the nutrients are readily available. Protein content is the single most important parameter determining the nutritional value of the algae [36]. Currently, dry fish feed sells for between $850 and $1,200/ton, based on a protein content of 60 wt% [37]. Lower protein content equates to a lower selling price. Hence, for green algae with a typical protein content of ~30%, the value of the algae as (dry) fish feed will be in the order of $425-600/ton.

(ii) Animal feed and fertilizer:

The suitability of algal biomass as a feed supplement has been well documented [22,36,38,39]. Consequently, microalgae are applied in pet food (mainly for cats, dogs, aquarium fish and ornamental birds) and in farm animals (horses, cows and poultry). Algae provide a broad profile of natural vitamins, minerals and essential fatty acids, benefitting animal health, and are rich in protein. The main microalgae grown for this purpose belong to the genera *Chlorella*, *Spirulina* and *Scenedesmus* [22]. The value of microalgae as a feed supplement depends on the application; as a simple protein replacement/supplement, the value is probably not more than $800/ton [38], whereas as a nutritional supplement (e.g., in pet food) its value may be significantly greater.

The relatively high N and P content of microalgae suggest that they should function as an excellent fertilizer. Several studies have indeed shown this to be the case [40-44]. To date most studies have been performed with blue-green algae, although there is no reason to think that green algae should behave any differently. In principle, microalgae can be applied as an organic solid for soil amendment, or in the form of an organic liquid fertilizer.

(iii) Bioplastics:

While the protein-rich solid resulting from the fractionation process could potentially be used as animal feed, bioplastics represent a more valuable application. Currently, the polymer marketplace is dominated by products composed primarily of polyolefins derived from crude oil derivatives; as of 2011, only 10-15% of the market was occupied by bioplastics. The majority of the bioplastics in this market are made with food products. Hence, utilization of the proteinaceous algal fraction

in this market provides a means to improve overall biofuel economics, while decreasing the utilization of petroleum and food crops for polymer production. A recent study reports that the global bioplastics market will grow at an annual compounded growth rate of 29.3% over the next five years from 2016-2020 [45]. The European Bioplastics Organization reports that over 2 million tonnes of bioplastics will be produced in the year 2016, where approximately 40% of that volume represents biodegradable formulations, and 60% represents durable formulations of bio-based polymers [46].

Notably, the value of whole algae for bioplastics production is typically in the order of $0.30-$0.40/lb (i.e., $660 - $880/ton), depending on the protein content (ideally, >40 wt%) and ash content (which should be <15 wt%). When algae biomass or algae protein isolate is used in a bioplastic composite, the algae replaces a percentage of the base resin. Depending on the specific application, the algae bioplastics could be used for durable, biodegradable or engineered applications. The most common durable applications would be using the algae to displace commodity thermoplastics such as polyethylene, polypropylene, and polystyrene, where these resins are valued between $0.70 - $1.00/ lb ($1,540 – $2,200/ ton) depending on grade. The biodegradable resins, such as PLA, PBAT, PHA and PBS, are valued between $1.20 - $2.50/lb ($2,640 - $5,500/ton) depending on the grade. Engineered resins such as polycarbonate, ABS, polyamide (nylon), and thermoplastic elastomers values can range from $1.00 to $4.00/lb ($1,540 - $8,800/ton) depending on grade and the use of functional fillers, such as carbon fiber, graphene, minerals or glass. The inclusion of algae biomass into any of these systems requires processing costs associated with thermoplastic compounding to incorporate the algae biomass into the polymer matrix, but displacement of these resins offers opportunities for margin as algae biomass costs should be lower than premium thermoplastic base resins.

The main player in the area of algae-derived bioplastics is ALGIX, a clean technology company dedicated in part to the production of algae biomass to ultimately service the demand for low-cost, bio-based feedstock for the renewable plastics industry [47]. ALGIX developed the process for thermoplastic co-processing of algae biomass for algae-blended thermoplastic compositions via commercial collaboration with Kimberly Clark Corporation, where ALGIX is the exclusive world-wide licensee of this patented technology. In addition, ALGIX has expanded its intellectual property portfolio to include compositional patents on closed cell foaming of algae blended thermoplastics, algae blends in thermoset polyurethane composites, and compounding of algae extracts for antimicrobial properties in finished articles.

An overview of the algae bioplastic production process for thermoplastics is shown below (Figure 6). The process starts with careful drying of algae biomass to prevent the creation of odiferous volatiles, such as sulfur, nitrogen and furan containing compounds, in the dry material. The algae feedstock is then micronized to reduce the particle size distribution to a target range depending on the end-use application. By using a fluidized bed jet milling system, the maximum particle size (D100 or D99) can be tailored to prevent the presence of large particles in the fine powder by controlling classifier wheel speed.

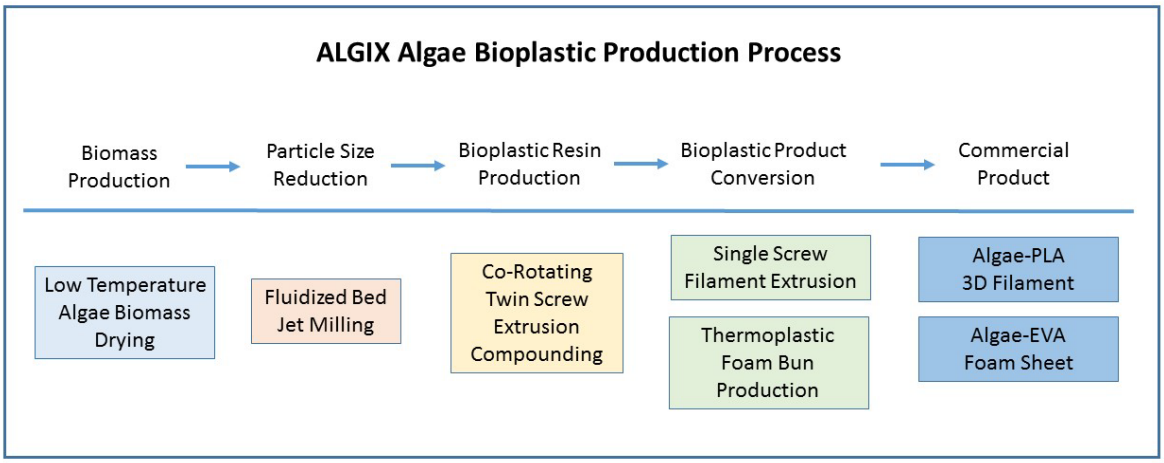

Figure 6. Block diagram of ALGIX algae bioplastic production process.

The micronized algae powder is pneumatically conveyed to gravimetric feeders. The algae powder is then fed into a co-rotating twin screw extruder at a feeding rate to achieve a 45-50% loading level by weight. The extrusion system comprises the majority of the proprietary process which includes custom screw designs and specially designed mixing elements, custom de-volatilization/moisture removal equipment, proprietary thermal recipe for heating zones, screw speed ratio, and proprietary compatibilizers/coupling agents for enhanced biomass incorporation with the carrier resin. The precise use of heat and pressure in specific zones of the extruder assists in the denaturation of algal proteins, which allows their unfolding and incorporation into a thermoplastic polymer matrix due to dispersive and distributive mixing.

The algae bioplastic resin is then ready for product conversion via a number of thermoplastic conversion routes. ALGIX owns and operates its own 3D filament production company, ALGIX 3D, which comprises four individual 45 mm single screw extruders for the precise profile extrusion of 1.75 mm and 2.85 mm filament for use in FDM-style 3D printers. In this process, the algae bioplastic pellets are blended with additional ingredients, such as pigments and odor treatment additives and are extruded, measured for dimensional accuracy via Statistical Process Control (SPC) and wound onto a spool to produce the finished commercial product (Figure 7).

Figure 7. Left to right: algae blended thermoplastic resins pellets using different polymer carrier resins under the Solaplast™ brand; ALGIX 3D™ Algae-PLA filament for FDM-style 3D printers; BLOOM™ flexible foam sheets for footwear, luggage, flooring, sports, and other applications.

ALGIX has also partnered with two flexible foam manufacturers to produce algae bioplastic closed cell flexible foam sheets. The foam sheet process uses algae bioplastics pellets, which are thermally melted and blended with additional ingredients, including pigments, blowing agents, and specialty additives. The molten blend is extruded into thin sheets which are inserted into special compression ovens where heat and pressure are applied to induce the foam expansion and create the finished foamed bun or sheet. ALGIX sells the foam sheets to 3rd party customers under the brand BLOOM™ foams that use die cutting techniques to create products such as shoe insoles, midsoles, and other flexible foam products (Figure 8).

Property	Test Standard	Units	BLOOM EVA	Closed Cell EVA	BLOOM Advantage
Hardness	JIS K6253	Asker C	27	20-30	Adjustable Hardness
Density	ASTM D297	g/cm^3 lbs/ft^3(PCF)	0.12 7.6	0.13-0.17 8.0-10.5	**25%** Lighter Weight
Tensile Strength	ASTM D412	Kg/cm^2 lbs/in^2(PSI)	12.1 172.3	7.5 107	**61%** Stronger Tensile Strength
Tear Strength	ASTM D624	Kg/cm lbs/in	7.4 41.3	3.5	**111%** Improved Tear Strength
Elongation	ASTM D412	%	220	180	**22%** Increased Elongation
Compression Set	ASTM D3575-00	%	11.6	10	**16%** Improved Compression Set
Compression Deflection (25%)	ASTM D3575-00	Kg/cm^2 lbs/in^2(PSI)	0.68	0.45 6.5	**51%** Improved Compression Deflection
Resilience	ASTM D2632	%	53.8	45±5	**20%** Increased Resilience

Figure 8. Comparison of BLOOM™ foam's algae bioplastic sheets vs conventional virgin ethylene vinyl acetate (EVA).

One of the early and primary target markets for ALGIX bioplastics is the flexible foam market for sustainable footwear (flexible foam insole and midsoles). This has the potential for over 1 billion pairs of shoes annually, representing approximately 100 million pounds of algae bioplastic resin requiring 50 million pounds of algae biomass. These two components represent a $115 million opportunity annually for the sale of algae bioplastic resins for use in flexible foams for footwear.

In addition, fibers and films markets would be attainable for higher value applications. The enhanced profitability is best demonstrated by the example of synthetic fibers that mimic a natural fiber feel. This has been achieved with plant proteins from agricultural commodity crops such as soy. A protein-rich meal from algae without agglomeration risk would be anticipated to produce a similar natural feel and might represent a higher value market opportunity. In the film sector, agricultural protein meals have been demonstrated to provide improved oxygen barrier properties for food packaging films leading to reduced rotting and enhanced produce taste. In the agricultural sector, ALGIX has produced agricultural products such as mulch films which enhance plant growth significantly through slow release fertilization from protein degradation. Food packaging films represent a sizable market of 1.76 million metric tonnes as of 2014. These films represent some of the most contested areas for plastic end of life concerns. These high value niche and moderate value but huge volume market opportunities are largely unavailable to whole algae meal usage due to the combined impact of odor and agglomerates. Hence, fractionation of algal biomass represents a significant opportunity for this market.

As noted above, market predictions for bioplastic production in 2016 exceeded 2 million tonnes per year corresponding to a market value of *ca*. 1.6 billion dollars. This translates into the potential to utilize 1.8 million tonnes tons of CO_2 per year (at 50% algae content) or 0.13% of the 1,364 million metric tons of coal-derived CO_2 emissions in the US [48].

(iv) Other high value products from algae:

Commercial large-scale production of algae started in the early 1960's in Japan with the culture of *Chlorella* as a nutritional supplement. Today, there are numerous commercial applications of microalgae, including use as a supplement to increase the nutritional value of food and animal feed, use in cosmetics, as a source of polyunsaturated fatty acids (particularly omega-3 fatty acids), as a source of additives for food coloring, and for the production of antioxidants. World production of microalgae was reported to be 5000 t of dry matter/year in 2006, generating a turnover of $1.25 billion/year (processed products are not included in this figure) [36]. For detailed information, the reader is referred to several reviews which have appeared on this subject [20,22,36,38,49]. The following provides a brief overview, emphasis being placed on those products which appear to have the greatest commercial potential.

Whole microalgae as nutritional supplements: Microalgae contain polyunsaturated fatty acids (PUFAs), the consumption of which is linked to several health benefits, as well as other biologically active compounds, such as carotenoids and phycocyanin, which possess antioxidant properties. Consequently, whole microalgae such as *Spirulina* and *Chlorella* are sold in health stores as nutritional supplements. Typically these take the form of tablets, capsules or liquids, although microalgae are also incorporated into snack foods, candy bars, pasta, beverages, etc. [36].

Omega-3 fatty acids: this term refers to a group of three polyunsaturated fatty acids, *viz*., ALA (α-linolenic acid, found in plant oils), EPA (eicosapentaenoic acid) and DHA (docosahexaenoic acid), EPA and DHA both being commonly found in marine oils [50]. Omega-3 fatty acids are vital for normal metabolism, although some of the potential health benefits of supplementation are controversial. However, a growing body of literature suggests that higher intakes of ALA, EPA, and DHA may afford some degree of protection against coronary disease [50]. Certain algae strains produce omega-3 fatty acids in significant amounts; moreover, fatty acids produced from microalgae have advantages over fish oils, such as the lack of unpleasant odor. Indeed, Martek (USA) and Nutrinova (a Germany company) have commercialized the production of DHA from microalgae for human and other applications [36], while Qualitas Health (Israel) and Valicor Renewables (USA) have partnered to commercialize an algae-derived omega-3 oil that is high in EPA [51].

Food-coloring products: In addition to chlorophyll as the primary photosynthetic pigment, microalgae contain many other pigments. These compounds improve the efficiency of light energy utilization and protect them (in the case of carotenoids) from solar radiation. Carotenoids extracted from algae are commercially important: β-carotene from *Dunaliella* is used in health foods as a

vitamin A precursor, while astaxanthin from *Haematococcus* is used in aquaculture for coloring the flesh of fish (mainly salmon).

Cosmetics: Various other algae-derived compounds have found applications in cosmetics, a well-known example being the Algenist skin care range produced by Solazyme (a San Francisco algae fuel startup), which uses microalgae as a main ingredient [52]. Several other companies in Europe also incorporate microalgae extracts in their skin care products [36].

Phycobiliproteins: Phycobiliproteins (specifically, phycoerythrin and phycocyanin) extracted from microalgae are used as natural dyes in food production and in cosmetics. They are also widely used in research laboratories as fluorescent dyes. The global market was estimated at $50 million in 1997 [36]. Commercially they are produced from *Spirulina*, a cyanobacterium, and *Porphyridium*, a rhodophyte (red alga); i.e., they are not produced from chlorophytes (green algae).

Most of the aforementioned high value algae-derived products are recapitulated in Table 1 below, along with the strain of algae from which they are extracted, their concentration in those algae strains, their commercialization stage and their selling price.

Table 1. Select high value compounds produced by microalgae [20,22,36,38].

Product/extract	Algae	Comment / selling price	Wt.% in algae
Whole microalgae	*Spirulina, Chlorella, Dunaliella salina, Aphanizomenon flos-aquae*	Commercialized since 1960's; ~$40/kg	100%
β-carotene	*Dunaliella*	Commercialized; $300-3000/kg	14%
Astaxanthin	*Haematococcus*	Commercialized; $2500-7150/kg	3%
DHA	*Crypthecodinium, Schizochytrium*	Commercialized; ~$25-75/kg	7.8%[a]
EPA	*Nannochloropsis, Phaeodactylum, Nitzschia*	Commercialized; ~$25-90/kg	4%[b]
Other PUFAs	*Spirulina* *Porphyridum*	α-linolenic acid; commercialized? Arachidonic acid; commercialized	1.35%[c] 2%[d]
Lutein	*Scenedesmus almeriensis* *Chlorella protothecoides* *Chlorella zofingensis* *Muriellopsis* sp. *Dunaliella*	Not yet commercialized from microalgae; ~$500/kg	7%[e]
Phycobiliproteins	*Spirulina* *Porphyridium*	Commercialized; $250-12,000/kg	2%[f]

[a] See ref. [53]. [b] See refs. [54,55]. [c] See ref. [56]. [d] See ref. [57]. [e] See ref. [58]. [f] See ref. [59].

These data clearly illustrate that although most of these compounds are present in algae in relatively low concentrations, they can command a considerable selling price. Therefore, their commercialization along with less valuable but more abundant products – such as algae-derived fuels – has great potential to significantly improve the economic viability of algae-based technology.

2. Technology Gap Analysis of the Proposed Algae-Based Platform for the Beneficial Capture and Utilization of Carbon Dioxide Emissions from Power Plants

2.1. Technology Gap Identification Method

In order to identify and evaluate the main technology gaps separating algae-based CO_2 capture and utilization technologies at an intermediate stage – i.e., a Technology Readiness Level (TRL) of 5/6 – from those at the commercialization level (TRL of 8/9) several criteria must be considered. First, the status of algae-based CO_2 capture and utilization research worldwide is used as a baseline to estimate technology maturity. Secondly, the targets and requirements put forward by DOE – such as a projected cost target for algal biomass production of $491/tonne by 2022 for a design based

on 10-acre ponds [15] – are used as the goalposts for commercialization at scale, specific advances to key technologies that can make the overall approach more commercially viable (including those achieved through the current DOE-sponsored project) being taken into account. In addition, the effect of equipping a commercial power plant with an algae-based carbon capture and utilization system in terms of input (energy, land, water, etc.) requirements as well as the effect on power plant performance and cost of electricity, are also considered to assess the viability of different technologies. Moreover, lessons learned through UK CAER's demonstration unit regarding the impact of an algae-based carbon capture and utilization system on mass transfer, heat transfer, balance between heat and mass transfer, as well as the cost of supplies (e.g., PBR construction materials and nutrients), all of which are major factors determining capital and operating costs, are also examined. Lastly, critical sub-processes and components (or technologies) are individually considered in order to identify desirable and undesirable attributes that should be respectively pursued and avoided in order to meet the application requirements.

2.2. Status of Research on Algae-Based CO_2 Capture and Utilization Systems

2.2.1. Ongoing Algae-Based CO_2 Capture and Utilization Projects at the Pilot Scale and Above

While the recent report published in 2017 by IEA Bioenergy authored by Lieve Laurens *et al*. includes an up-to-date overview of companies and research groups with ongoing large-scale algae cultivation operations [3], the 2015 report published by IEA Clean Coal Center authored by Xing Zhang offers a thorough account of demonstration-scale projects in the area of microalgae removal of CO_2 from flue gas, including the current DOE-sponsored project [4]. However, relevant information regarding commercial projects in this area is also given in section 3.2 of this report.

2.2.2. Key Component Development for Algae-Based CO_2 Capture and Utilization

2.3. Technology Understanding and Criteria for Future Application and Commercialization

2.3.1. Introduction of Power Plant Flue Gas to Algae Cultivation System

If an initial step to concentrate CO_2 is to be avoided in favor of using flue gas directly in an algae cultivation system, there are essentially two options: 1) compression and subsequent bubbling of the CO_2 rich gas directly into the algae growth system; and 2) producing a concentrated aqueous stream saturated or supersaturated with dissolved carbon.

Bubbling compressed carbon dioxide is a tried and tested method for the carbon supplementation of algae cultures that has been proven effective with both photobioreactors and raceway ponds. A wide variety of materials to introduce CO_2 into algae cultures – from laser-cut silicon tubing to porous ceramic disks have been used, albeit most materials have advantages and disadvantages in terms of capital (material cost) and operating (pressure drop) expenses. For example, a material that produces smaller bubbles – which would increase mass transfer efficiency – may prove undesirable from an overall life cycle assessment standpoint due to the energy penalty associated with overcoming the associated pressure drop.

The alternative method mentioned above, in which an aqueous stream is pre-saturated with carbon, shows some potential for lowering operating costs and increasing the viable distance between an

algae farm and a point source of emissions. An additional benefit of these systems is that the exhaust gas can be returned to the main emissions stack, potentially making air permits easier to obtain. Global Algae Innovations, a company located in Kauai, Hawaii, is at the forefront of utilizing this flue gas introduction approach [60]. Indeed, this company employs both an absorber process integrated with a power plant and a carbonate solution to transfer the carbon contained in the flue gas to open raceway ponds for algae production. The engineering team at Global Algae Innovations claims a 1 psi pressure drop across the absorption tower, which in all likelihood ignores the operational expenses associated with circulating the carbonate solution through the system and overcoming the height of the absorber.

A few technologies currently under development also show promise from a life cycle perspective for the overall reduction of carbon emissions. For instance, one interesting technology being researched at Arizona State University represents a potential route for decoupling carbon utilization from point sources of emissions. In this approach, direct air capture technology [61,62] is used to produce a concentrated stream of dissolved carbon, which is then introduced to algal systems using selective hollow fiber membranes to improve mass transfer efficiency and carbon utilization [63]. While at a low TRL, this concept shows promise and highlights the potential of integrating technologies from different industries and fields.

Another emerging approach is the combination of technologies developed with the support of the NETL carbon capture program with technologies developed through the support of the Bioenergy Technologies Office of DOE. An example of this approach would be the combined use of an upstream membrane to increase CO_2 concentration [64] and a countercurrent carbon absorber, which could reduce both capital and operating costs and may represent the next step in the integration of algae cultivation systems with CO_2 point sources [65].

2.3.2. Algae Cultivation System

Large-scale cultivation of algae has been proven in open pond systems and to a lesser extent in PBRs. There are at this time no significant technological hurdles to overcome in order for these technologies to be used for large-scale cultivation of algae biomass. For example, as a means of biofuels production, both technologies have been proven to give a net-positive energy return on investment (EROI), brackish saltwater ponds and PBRs having higher EROIs than their respective freshwater counterparts [66]. However, there is considerable uncertainty regarding the climate change impacts of PBR systems due to the significant variance of different systems vis-à-vis greenhouse gas (GHG) emissions [67], some systems being net-emitters of GHGs and some being net-sequesters [66].

Neither method has proved to be economically viable as a method of biofuel production. One study found that the total cost of lipid production was $12.74/gal and $32.57/gal for open ponds and PBRs, respectively. Based on information available in 2012, this particular scenario gave a 100% probability of a negative present value of ending net worth, meaning that any investor trying to gain profit from production of algal biofuels would garner negative gains on their original investment. Only dramatic reductions on the order of an 80-90% reduction in capital and/or operating costs can provide for a chance of economic success [21]. According to one study, the

only current economically viable scenario is one in which certain algae are cultivated for the extraction of specialty products [68].

In view of the foregoing, the majority of academic and industrial research has focused on the reduction of capital and operating costs for algae cultivation systems in order to make large-scale production of biofuels economically feasible. The UK CAER is making efforts to compensate for these high costs by diversifying methods for by-product utilization. Fractionating biomass into multiple, valuable products and product intermediates including lipids, carbohydrates and proteins may be a viable way to offset the high costs associated with the construction and operation of both PBRs and open ponds. The UK CAER is also making efforts to maximize biomass productivity, which also constitutes an effective means of cost reduction.

2.3.3. Harvesting and Dewatering of Algal Biomass

It has been well established that algae harvesting and lipid extraction comprise a significant proportion of the cost associated with biofuel production [69,70]. It is essential that harvesting and dewatering technologies adopted for large-scale operations have low capital, operating and maintenance costs, be compatible with a broad range of species, allow for recycling water, have a low environmental impact and carbon footprint [8]. With these considerations in mind, this Technology Gap Analysis provides an assessment of current harvesting and dewatering technology readiness. Table 2 below summarizes operating costs reported by the NAABB for several harvesting technologies [8]. While centrifuges are the industry state of the art for harvesting algae, this approach clearly has the highest OPEX. Alternative technologies such as dissolved air flotation and spiral plate separation have lower OPEX, but are less commonly employed as the extent of dewatering achieved with these technologies is lower than that achieved with centrifugation. NAABB evaluated electrolytic, membrane filtration, and ultrasonic harvesting based on their total economic feasibility. While these approaches significantly reduced harvesting OPEX, they have yet to be demonstrated in continuous operation at reasonable scale.

Table 2. Baseline feasibility assessment of harvesting technologies

Technology	Energy Input (kWh/kg)	Chemical Cost (US$/kg)	Electricity Cost (US$/kg)	OPEX (US$/kg)	OPEX (US$/gal)
Baseline Harvesting Technologies					
Centrifuge Baseline	3.300	0.000	0.264	0.264	1.799
Dissolved Air Flotation	0.250	0.008	0.020	0.028	0.191
Spiral Plate Separation	1.418	0.000	0.113	0.113	0.773
NAABB Harvesting Technologies					
Chitosan Flocculation	0.005	0.055	0.000	0.055	0.377
$AlCl_3$ Flocculation	0.120	0.048	0.010	0.056	0.383
Electrolyte Harvesting	0.039	0.004	0.003	0.007	0.049
Membrane Filtration	0.046	0.000	0.004	0.004	0.025
Ultrasonic Harvesting	0.078	0.000	0.006	0.006	0.043

While this evaluation compares the operating costs of harvesting technologies, it does not provide any means to compare performance on an equivalent basis, which is an important consideration since the extent of dewatering that can be achieved with each technology varies significantly. In order to make direct comparisons between harvesting technologies, it is necessary to compare technologies on an equivalent performance basis – such as OPEX – to achieve a specific product moisture. This type of comparison is essential for comparing dewatering approaches.

Chitosan and $AlCl_3$ were evaluated as flocculants in this study, but polymeric flocculants were not. As polymeric flocculants are commonly used in commercial water treatment, some consideration for algae dewatering is warranted. As stated above, the NAABB Harvesting Technologies compares OPEX for different flocculating, harvesting and dewatering approaches without including reference to either dosage or the performance each approach achieved. UK CAER testing has shown that OPEX for using a combination of cationic (5 ppm) and anionic (1-2 ppm) flocculants is significantly lower than chitosan or $AlCl_3$ (0.031 $/kg) with >95% solids capture.

As previously stated, NAABB reports that centrifugation is the industry state of the art for harvesting algae for the production of high value products [8]. This report also states that while centrifugation is time-tested and effective, it is energy intensive and has high capital and maintenance costs. A principal reason for these high costs is the dilute nature of the harvest suspension, with algal cells often comprising <0.1% of the culture volume. Given the high costs associated with centrifugation, a reasonable approach would be to utilize the approach employed by other industries that require solid/liquid separation of dilute suspensions. Examples are municipal wastewater treatment, where suspended solids concentrations are typically in the range of 250 to 600 g/m^3 [71], or the mineral processing industry where the suspended solids range is typically 2 to 5%. In these applications, effective thickening is employed to concentrate suspended solids while producing clarified water, significantly reducing the volume of solids suspension for

further dewatering. In the case for algae, thickening a harvest culture density of 1 g/L (0.1% solids) to 40 g/L (4% solids) would reduce the feed capacity of the subsequent dewatering process by a factor of 40. Since dewatering processes such as centrifugation and filtration are significantly more expensive unit processes than thickening, thickening prior to dewatering is common practice for many commercial applications that require dewatering of dilute feedstocks, and should be considered as a prerequisite for algae harvesting.

The fact that membranes display pore sizes ranging from angstroms to microns imply that they can be used in a number of separations relevant to algae cultivation – including solid-liquid (e.g., algal biomass concentration and dewatering through cell retention), solute-liquid (e.g., water purification, feedstock preparation, effluent recycling and bioproduct recovery) and even gas-liquid (e.g., gas delivery and removal) – that are either challenging or impossible with other technologies [72]. In view of this, membranes have long been used in microalgae cultivation and processing, the membrane materials and processes used for these applications having been thoroughly reviewed [72,73]. However, it is also recognized that considerable advances are necessary for membrane technology to be applied in the bulk-production of algal biomass, biofuels and bioproducts, as important challenges related to the reduction of energy requirements, fouling and costs still need to be overcome. Nevertheless, it is widely recognized that membranes have great potential to substantially advance algae-based technology, as is clearly illustrated by the considerable amount of work currently being performed in the area to address the aforementioned challenges [74-91].

2.3.4. Algal Biomass Fractionation

Given the hydrophobic characteristic of lipids, combined with the necessity of a water-miscible solvent for wet extraction, the process of solvent selection for wet extraction becomes quite complex. The considerably larger amount of water present in algae relative to lipids indicates that polar solvents are necessary for extraction; moreover, the presence of a polar solvent is necessary to release lipids bound in protein and sugar complexes [92,93]. Mixed solvent systems with both polar and non-polar solvents can provide higher extraction efficiencies, but in the interest of solvent recovery on a more industrial scale, a single solvent system is more desirable [93].

Against this background, the commercial processes developed by Valicor represent the state of the art. Indeed, it is hard to see how significant improvement of these processes is possible, assuming that the goal is simple lipid extraction, as opposed to full biomass fractionation. Given that the Valicor processes are commercial, a TRL of 10 can be assigned. That said, it is worth noting that differences between algae species/strains (e.g., strength of the cell wall) mean that some optimization of the process conditions may be required for specific algae.

It should also be noted that a variety of other approaches for lipid extraction from algae have been reported in the literature, including the use of sonication, pulsed electric field (PEF) technology and microwave irradiation [25]. However, few of these methods have been commercialized. OriginOil has developed a process in which a combination of ultrasound and electromagnetic pulses are used to disrupt algal cell walls. CO_2 is then injected into the resulting slurry of algal biomass to lower the pH, which facilitates separation as the oil rises to the top and the biomass

sinks to the bottom of the aqueous layer [94]. However, specific cost data for this process do not appear to be available in the literature, although the National Alliance for Advanced Biofuels and Bio-products (NAABB) reports a very high cost for the pulsed electric method for cell lysing [8], and the technology has not been widely adopted. Table 3 below summarizes operating costs reported by the NAABB for several extraction methods [8], from which it may be concluded that wet hexane extraction is the most cost effective.

Table 3. Operating costs for several wet lipid extraction methods [8].

Technology	Energy input (kWh/kg)	Chemical cost ($/kg)	Electricity cost ($/kg)	OPEX ($/kg)	OPEX ($/Gal)
Pulsed electric field	11.52	0.00	0.922	0.922	6.28
Wet hexane extraction	0.11	0.001	0.009	0.010	0.068
Ultrasonic extraction	0.384	0.00	0.031	0.031	0.209
Supercritical	1.174	0.00	0.094	0.094	0.64

In contrast to lipid extraction, full algal biomass fractionation has not been commercially developed. However, it should be a relatively simple step to increase the severity of the pre-treatment or conditioning step used in the Valicor AlgaFrac^{TM} process, such that the carbohydrates present are fully hydrolyzed, resulting in their removal as sugars in the aqueous stream. Whether this is in fact desirable depends on the value of the resulting product streams (protein-rich solid and aqueous sugar stream) as compared to the defatted algae. Given that the value of the sugar stream is rather low, in the context of bioplastics manufacture, the determining factor will be the properties of the defatted/“desugared” biomass versus the defatted biomass, i.e., whether the former offers superior properties in bioplastics applications. Similarly, lipid extraction will only be of commercial interest if the defatted biomass outperforms the whole biomass in terms of bioplastics manufacture, or, if the extracted lipids are of significant value, e.g., as nutraceuticals or pigments.

2.3.5. Utilization of Algal Biomass Fractions

Technology gaps in the utilization of whole algae, algae fractions and individual algae-derived compounds exists in most industries in which algal biomass finds its end uses.

(i) Aquaculture:

An alternative to the use as microalgae in dry fish feed is the use of live algae as food for molluscs, peneid shrimp or indirectly as food for the live prey fed to small fish larvae (i.e., algae are fed to zooplanktons, which in turn are fed to fish larvae). Although microalgae are reported to exhibit many benefits in these applications in terms of improving the health of dense fish populations [22,36], the high cost of producing, concentrating and storing live microalgae represents a significant drawback [36]. Typically, the production of live microalgal biomass for this purpose is performed locally and often represents the major cost item in aquacultural production [22].

One approach to improve the economics of microalgae utilization in aquaculture would be to integrate large-scale microalgal biomass production with aquaculture. While this would necessitate the establishment of aquaculture facilities at microalgae production sites (i.e., where CO_2 is available, in the case of autotrophically cultured algae), potential benefits would include the avoidance of having to dry the harvested algae (in the case that live algae are utilized), and the ability to reclaim a significant fraction of the nutrients in the biomass, i.e., N and P. Typically, fish excrete 80% of the nutrients in the feed; in principle, these nutrients can be captured using bead filters, which accomplish both solids capture and biofiltration. Assuming that the resulting matter can be processed into a form suitable for utilization by microalgae, the opportunity exists to recycle the N and P, thereby reducing the nutrient costs associated with microalgae production. However, given the relative modest nutrient costs associated with algae cultivation, as compared to the capital costs involved, the ability to recycle nutrients is unlikely to constitute a principal economic driver with respect to the preferred algal biomass utilization route; rather, the value of the biomass must be maximized.

(ii) Animal feed and fertilizer:

As indicated above, to date commercial applications have mainly focused on algae as a micro-feed ingredient, imparting specific beneficial properties rather than gross nutrients to the recipient animal. However, finite supplies of premium raw materials (particularly fish meal and fish oil) and the promise of much higher available quantities of algal biomass in the future are prompting evaluation of algal biomass as a major ingredient in formulated animal feeds, especially for aquaculture. Several companies are said to be currently evaluating microalgae for this purpose, including OriginOil [95,96]. Whether algal biomass will be adopted in future as a bulk feedstuff to supply protein and energy in animal feeds, or will remain only as a supplement, will depend on biomass availability, composition and cost. There is currently a large discrepancy in the global supply and purchase cost of algal biomass versus existing commodity animal feedstuffs, even for those categories of algal product that are produced at the largest scale. Hence, until supplies increase and costs decrease, algal biomass and biomass extracts will continue to occupy niche markets within the animal feed sector [97].

Historically, while the use of macroalgae as soil fertilizer has been practiced by coastal communities all over the world, the use of microalgae for this purpose is much less well established and appears to be confined to rice cultivation in tropical and sub-tropical regions [22]. However, based on current prices for high quality organic fertilizers, the value of microalgae for this application has been estimated to be as high as $800-1200/ton [98]; consequently, this appears to be an interesting application for algae produced in high volumes. This has been recognized by Accelergy Corporation, which has commercialized an algae-based biofertilizer technology called TerraSync®. This technology isolates, cultivates and incorporates algae strains into a proprietary bio-fertilizer, which replaces conventional nitrogen fertilizers. Once applied, the biofertilizer biologically extracts and fixes both nitrogen and CO_2 from the atmosphere and releases into the soil simple nitrogen and carbon containing compounds that can be used by crops [99].

(iii) Bioplastics:

The value of whole algae for bioplastics production is typically in the order of $0.30-$0.40/lb (i.e., $660 - $880/ton), depending on the protein content (ideally, >40 wt%) and ash content (which should be <15 wt%). Based on a minimum of cost of production of, say, ~$1,000/ton for algal biomass, and a typical cost of $120/ton for drying and micronization of the biomass ($20/ton for solar drying + $20-$100/ton for micronization, depending on the application), the required selling price (RSP) of the biomass for bioplastic applications must be in excess of $1,120/ton. From this it follows that it is necessary both to minimize algae production costs and realize the maximum value of the biomass by producing a high quality product (high protein, low ash content). Importantly, defatting the algae may actually increase its value by producing a feedstock with a higher protein content. Algae that has a protein content over 50% and an ash content below 10% is considered premium material for thermoplastic conversion into algae biocomposites. The higher protein content in the whole algae biomass with low levels of ash provides a more polymeric substrate that yields superior product properties. These enhanced properties impact the value of the biomass due to a larger variety of viable end-use applications of the bioresin formulation.

In addition, the removal of lipids and sugars to achieve these higher protein contents is anticipated to confer several technical advantages. Lipid-extracted algal biomass has already been used to demonstrate improved odor characteristics of the finished algae-based plastics, but it also contained a large fraction of short chain polysaccharides and monosaccharides. The lipid extracted meal suffered in performance compared with raw algae due to the formation of large agglomerates (which weaken the material and favor charring that confers the plastic an unpleasant smell), a common occurrence seen in other similar materials with high short-chain polysaccharide or monosaccharide contents. The low molecular weight polysaccharides are believed to interact with proteins through Maillard reactions, and each other through caramelization reactions to produce irreversible bound masses in the polymer system identified as agglomerates. This agglomerate formation is very restrictive to the market opportunities available, and therefore an additional sugar extraction included into the biomass fractionation is proposed to improve the material's suitability for market implementation and prospects in higher value markets. These include film and fiber markets which are extremely sensitive to agglomerate formation and are high value commodities.

(iv) High value products from algae:

Recently, several smaller producers of algae-derived omega-3 fatty acids such as DHA and EPA have commenced production in the U.S. as the market for these nutraceuticals continues to expand. Moreover, various other compounds are reported to be in development for applications in cosmetics, as nutritional supplements and pharmaceuticals [36].

Notably, several compounds found in algae – including lutein, zeaxantin and canthaxantin – are used for chicken skin coloration, although currently these compounds tend to be produced from sources other than microalgae. Lutein (IUPAC name β,ε-carotene-3,3'-diol) appears to be a particularly promising target product for algae cultivation. Lutein is used in chicken feed to provide the yellow color of broiler chicken skin (polled consumers view yellow chicken skin more favorably than white chicken skin). Such lutein fortification also results in a darker yellow egg yolk. Today the coloring of the egg yolk has become the primary reason for feed fortification.

Lutein is typically not used as a colorant in other foods due to its limited stability, especially in the presence of other dyes [100]. Lutein is an anti-oxidant and is found the macula, a small area of the retina responsible for central vision. Consequently, the suggestion has been made that lutein may be of benefit in retarding macular degeneration, although to date only one study has shown a benefit for lutein in this regard [101].

The lutein market is segmented into pharmaceutical, nutraceutical, food, pet foods, and animal and fish feed. The pharmaceutical market is estimated to be about $190 million, while nutraceutical and food applications are estimated to be about $110 million. Pet foods and other applications are estimated at $175 million annually. Apart from the customary age-related macular degeneration applications, newer applications are emerging in cosmetics and as an antioxidant; indeed, it is one of the fastest growing areas of the $2 billion carotenoid market [102]. Currently lutein is produced commercially by extraction from marigold flowers; however, the lutein content of marigolds is low (0.03% dry wt.) which renders alternative lutein sources, such as algae, of interest [103]. Indeed, several algae strains have been shown to produce lutein in commercially interesting amounts (see Table 1). Currently, this approach to lutein production does not appear to have been commercialized, although several companies are thought to be interested.

3. Identified Technology Gaps

3.1. UK-CAER's Approach and Methodology to Address the Technology Gaps Identified

3.1.1. Introduction of Power Plant Flue Gas to Algae Cultivation System

As discussed in Section 2.3.1, there are no significant technology gaps pertaining to the handling flue gas or the transfer of the carbon in flue gas to an algae culturing system. Notably, although the technology currently employed to handle carbon dioxide – specifically in the food or chemical industry – could be harnessed in the algae-based capture and utilization of CO_2, much of it is protected by trademark or industrial secrets. A current challenge is the evaluation of the options already available in the open market to introduce the carbon contained in point source emissions to algae cultivation systems. While individual technologies are typically well understood at a fundamental level, most research to date has ignored the practical and life cycle implications of integrating different technologies into an algae-based process that could serve as a carbon sink for CO_2 point sources. A study that compared the economics and energetics of the various technologies would be an extremely valuable asset moving forward.

3.1.2. Algae Cultivation System

As was previously mentioned, there are no significant technology gaps for algae cultivation on a large scale. However, capital and operating cost reduction remains the main focus of current research. Cultivation has many facets and stages that can be optimized in an effort to minimize cost. Table 4 gives a breakdown of these costs.

Table 4. Percentage of costs for cultivation of algae for production of algae crude and percentage of total CAPEX and OPEX for open raceway ponds and photobioreactors.

Algae cultivation system	**ORP**	**PBR**	**ORP**	**PBR**
CAPEX ($ gal^{-1})				
Cultivation	*% of cultivation*		*% of total CAPEX*	
Reactor Cost	98.36%	99.72%	81.96%	94.50%
Land cost	1.64%	0.28%	1.37%	0.27%
OPEX ($ gal^{-1})				
Cultivation	*% of cultivation*		*% of total OPEX*	
Electricity	3.60%	11.86%	1.15%	3.87%
Nutrients	0.76%	0.47%	0.24%	0.15
CO_2	8.04%	5.28%	2.58%	1.72%
Water	0.48%	0.35%	0.15%	0.11%
Wastewater treatment	1.24%	0.91%	0.40%	0.30%
Chemicals for cleaning/disinfection	0.01%	0.02%	0.00%	0.01%
Chemicals for crop protection/disinfection	0.41%	0.03%	0.13%	0.01%
Maintenance	51.38%	65.55%	16.47%	21.38%
Labor	34.09%	15.53%	10.93%	5.07%

Taken from [104].

Reductions in capital cost are unlikely to be dramatically affected by anything other than market forces. The cost of materials, labor and construction will vary slightly from one region to another, but the cost of reactor construction will remain the largest capital expense. Given the physical nature of algae cultivation systems, it is unlikely that massive reductions in CAPEX can be attained by technological advancement. However, the development of new technologies and their integration with existing methods may have the potential to significantly reduce OPEX.

Electricity remains a significant cost in algae cultivation, especially for photobioreactors. UK CAER's "cyclic flow" reactor design offers dramatic reductions in energy cost vs. PBR systems that need liquid constant circulation as shown in Figure 9 [18].

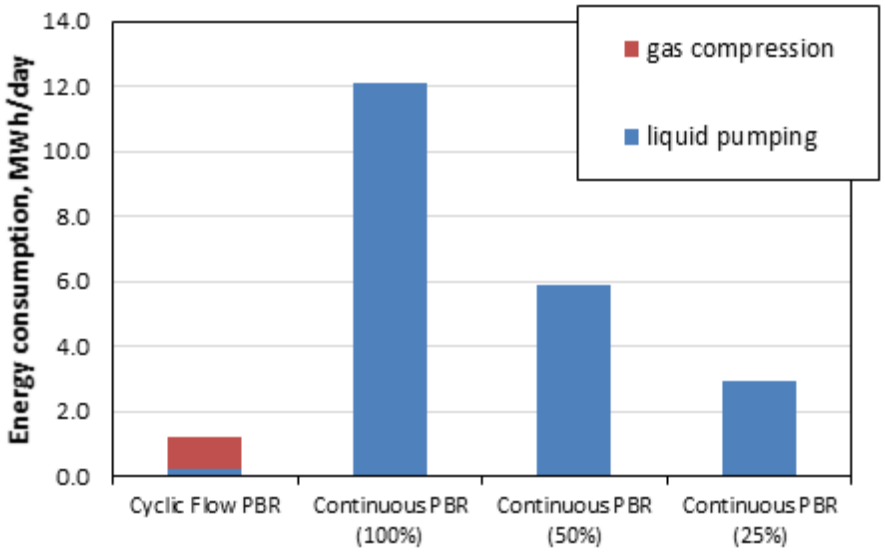

Figure 9. Comparison of energy consumption for cyclic flow and continuous flow PBRs (1 MW coal-fired power plant, 30% CO_2 capture). Values for the continuous flow PBR are shown at 100%, 50% and 25% of the design liquid velocity in the PBR.

Although gas compression represents the majority of the "cyclic flow" reactor's energy consumption, Figure 9 shows that innovative design in PBR construction and operation can help to significantly lower energy costs.

The "cyclic flow" reactor has been demonstrated to cultivate algae using flue gas fed from a coal combustion power plant. This gas serves as the CO_2 source for the algae, thus eliminating the expense of CO_2 in the cultivation process. The only penalty associated with using CO_2 from flue gas is the cost of gas compression in the form of electricity cost. A limited number of proof-of-concept studies have been performed using flue gas from combustion sources as a source of CO_2 for algae feed [3,18].

A smaller number of studies have actually used flue gas from a power plant [4,105]. However, to date there have been very few studies published concerning large-scale demonstrations of flue gas CO_2 capture by algae. One company, Seambiotic, has utilized flue gas from a coal burning power station for algae cultivation. Flue gas from Israel Electric Corporation's Ashkelon power station was fed to algae ponds, the produced algae being sold as a food additive [106]. In addition, demonstrations are in progress at power plants in such geographically diverse regions as Australia, Germany, China, Taiwan, South Africa and the USA [3,4].

The use of industrial wastewater as a nutrient source is another possible method of OPEX reduction. A recent study showed that it is possible to cultivate algae using wastewater concentrate as the sole nutrient source [107]. Unpublished work performed at the UK CAER in 2015 also demonstrated that municipal effluent wastewater was a more than suitable habitat for algae cultivation, thus conceivably reducing or even eliminating the cost of water supply for cultivation.

Increasing biomass productivity has recently become an area of interest for researchers, given that an increase in areal or volumetric productivity will inherently result in cost reduction. The UK CAER has recently been working on a techno-economic analysis (TEA) in order to understand the quantitative effect of cost reduction due to increases in biomass productivity.

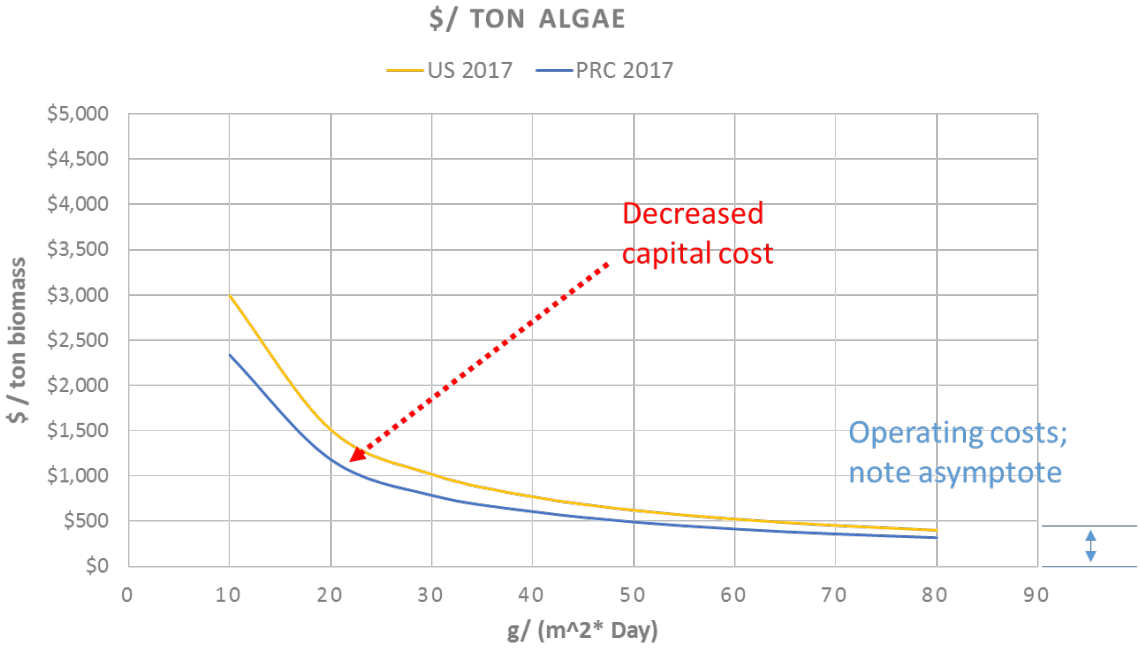

Figure 10. Cost per ton of biomass produced vs. areal productivity (g/(m^{2}day)). Blue line represents cost analysis done for the United States, red line represents same analysis done for People's Republic of China. This material is based upon work supported by the U.S. Department of Energy's National Energy Technology Lab and the Office of Fossil Energy (DE-FE0026396).

Figure 10 depicts the reduction in CAPEX as biomass productivity rises (note the asymptote in the graph representing OPEX). It is also important to note that this analysis was conducted for the UK CAER "cyclic flow" PBR. Similar analyses for other systems will differ but presumably follow the same trend.

An underexplored area of research lies in the combination of the two main cultivation systems, ponds and PBRs. In an effort to increase areal productivity, these systems could be made to serve one another, the PBR acting as an inoculum source for the ponds. This will presumably offer some remediation of each system's respective disadvantages. Since the PBR would need to hold only a small portion of the liquid in the system, the higher CAPEX and OPEX of PBRs could be mitigated. The PBR may also serve to mitigate the susceptibility of the culture in the ponds to contamination, by producing a strong monoculture for inoculation and supplementation.

3.1.3. Harvesting and Dewatering of Algal Biomass

Several technology gaps are evident with respect to the harvesting and dewatering algal biomass. While it is generally accepted that effective thickening prior to dewatering would significantly

improve both the performance and cost of harvesting operations, the use of polymeric flocculants to enhance dewatering is largely ignored as a treatment option. The current UK CAER project identified the use of low dosages of cationic (5 ppm) and anionic (1 to 2 ppm) flocculants to thicken harvested biomass while achieving >90% solids capture to generate clarified water and nutrients for recycling. No detailed performance comparison with chitosan or inorganic coagulants such as $AlCl_3$ was attempted since the dosage of these additives was inordinate by comparison, and the coagulated biomass settling rate was poor. The UK CAER approach has been demonstrated in continuous operation using a static thickener with lamella plates to minimize the suspended solids entrained with the clarified water.

UK CAER practice is to filter thickened biomass on commercial multifilament filter media, which produces a 20% solids product by gravity drainage. The thickened biomass would also be amenable to further dewatering by other means, such as centrifugation or pressure filtration.

3.1.4. Algal Biomass Fractionation

As discussed above, no technology gaps are evident for lipid extraction from wet algal biomass. On the other hand, full algal biomass fractionation has not been commercially developed. Indeed, given current fuel prices, there seems to be little impetus to do so.

In the context of the current project, the UK procedure for lipid extraction has been shown to work well, recovering close to the theoretical maximum yield of lipids, albeit the process parameters (pH, temperature and conditioning time) have not been completely optimized. One goal of future work should be to optimize the processing conditions with the goal of maximizing both the lipid and sugar yields. Simply increasing the severity of the conditioning step, so as to ensure complete carbohydrate hydrolysis, should be sufficient in this regard. This would result in the isolation of an extremely protein-rich solid, which would be of interest for the production of bioplastics. Whether such a defatted/desugared solid would offer significant advantages in bioplastic properties over whole algae or defatted algae is presently unknown, but could potentially provide a means of increasing the value of algal biomass.

3.1.5. Utilization of Algal Biomass Fractions

Due to the challenges posed by the various environments in which they grow, algae have adapted to thrive under an incredibly diverse set of conditions. As a result of these diverse systemic influences, algae cells produce a variety of complex and valuable compounds that can be isolated, extracted and utilized through various means. The following products provide economical potential for further avenues of research in market value.

(i) Bioplastics:

As mentioned above, the production of algae-derived bioplastics can be greatly improved through the use of a high quality feedstock displaying a high protein and a low ash content. Indeed, algae with a protein content over 50% and an ash content below 10% are considered premium material for thermoplastic conversion into algae biocomposites, as these characteristics result in a more polymeric substrate that yields superior product properties. Albeit defatting algae can increase its value by producing a feedstock with a higher protein content, defatted algae can also contain a

large amount of short chain polysaccharides and monosaccharides. The latter is problematic, since low molecular weight polysaccharides are believed to interact with proteins and with each other – through Maillard and caramelization reactions, respectively – to produce irreversible bound masses in the polymer system identified as agglomerates, which negatively impact bioplastic performance. Notably, films and fibers – both very high value commodities – are extremely sensitive to agglomerate formation, meaning that agglomerate formation is very restrictive to the market opportunities available. Therefore, an additional sugar extraction must be included into the biomass fractionation process to improve the material's suitability for market implementation and prospects in higher value markets. Against this backdrop, research is necessary to further fractionate the algae biomass into an algae protein isolate fraction that will have the highest polymeric potential for use in more valuable end-use applications such as films, fibers, flexible foams and coatings. The value of an algae protein isolate for use in bioplastics may increase to over $0.50/lb (i.e., $1,100/ton). The algae protein isolate fraction will constitute roughly half of the biomass yield per ton of algae produced compared to the whole algae biomass approach. However, the increased value generated from the protein isolate fraction for specialty applications, along with the additional value created through fermentation co-products during the fractionation process – which would also enable the recycle of nutrients in general and of phosphate in particular – could provide a higher value per ton of biomass.

(ii) Omega-3 fatty acids:

These compounds are essential throughout the food chain, but originate within the algae cells themselves. In the wake of increasing awareness of the importance of omega-3 fatty acids to the human diet, algae have come to play an important role, given their ability to synthesize these essential compounds. The ω-3 long chain polyunsaturated fatty acids (LC-PUFAs) are well studied bioactive molecules with important health benefits. Animals, including humans, do not carry the required genes necessary for the formation of ω-3 fatty acids these must be obtained from other natural sources. The current natural source of ω-3 PUFAs is fatty fishes, which accumulate these fatty acids in their oil due to their alga rich diet. Excessive harvesting of sea fishes for health benefits have put greater strain on fish hatcheries, making it important to explore alternate sustainable ω-3 PUFA sources. There are several popular strains of algae marketed for their high content of ω-3 fatty acids such as *Nannochloropsis*, *Chlorella* and *Scenedesmus*. The current market value for each fatty acid is ~$35 per kilogram for 100% ALA [108], ~$53 per kilogram for DHA [109], and ~$88 per kilogram for EPA [55]. Table 5 illustrates the polyunsaturated fatty acid content of different algae species.

Table 5. Polyunsaturated fatty acid content extracted from different microalgae species [110].

Species	Product	Yield	Extraction/Purification method	Reference
Arthrospira platensis	Total lipids	13.2% DW	Chloroform–methanol 1:1 (%v/v)	Ryckebosch and colleagues (2011)
Chlorella vulgaris		19.9% DW		
Chlorella vulgaris Green cells	ALA	661 mg/100 g	Acid digestion of biomass with 4 N HCl. Soxhlet method with petroleum ether for 6 h	Batista and colleagues (2013)
	EPA	19 mg/100 g		
	DHA	16 mg/100 g		
	GLA	112 mg/100 g		
Chlorella vulgaris Orange cells	ALA	3665 mg/100 g		
	EPA	39 mg/100 g		
	DHA	80 mg/100 g		
	GLA	23 mg/100 g		
Crypthecodinium cohnii	DHA	99.2% purity	Purification by saponification, winterization and urea complexation	Mendes and colleagues (2007)
Diacronema vlkianum	ALA	14 mg/100 g	Acid digestion of biomass with 4 N HCl. Soxhlet method with petroleum ether for 6 h	Batista and colleagues (2013)
	EPA	3212 mg/100 g		
	DHA	836 mg/100 g		
	GLA	112 mg/100 g		
H. pluvialis	ALA	3981 mg/100 g		
	EPA	579 mg/100 g		
	GLA	472 mg/100 g		
Isochrysis galbana	ALA	421 mg/100 g		
	EPA	4875 mg/100 g		
	DHA	1156 mg/100 g		
Scenedesmus obliquus	Total Lipids	29.7% DW	Chloroform–methanol 1:1 (%v/v)	Ryckebosch and colleagues (2011)
Spirulina maxima	ALA	40 mg/100 g	Acid digestion of biomass with 4 N HCl. Soxhlet method with petroleum ether for 6 h	Batista and colleagues (2013)
	GLA	452 mg/100 g		
Nannochloropsis salina	Total Lipids	34.4% DW	Chloroform–methanol 1:1 (%v/v)	Ryckebosch and colleagues (2011)
Nannochloropsis gaditana	EPA	3.7 g/100 g DW	Dichloromethane-ethanol (1:1)	Ryckebosch and colleagues (2013)
Parietochloris incise	ARA	9.1% DW	Methanol (10%DMSO) at 40°C for 5 min. Diethyl ether, hexane and water 1:1:1 (v/v/v)	Bigogno and colleagues (2002)
Phaeodactylum tricornutum	EPA	9.3% DW of total fatty acids (39%)	Chloroform–methanol 1:1 (%v/v)	Ryckebosch and colleagues (2011)
Porphyridium cruentum	EPA	50.8% recovery, 97% purity	Purification by saponification and urea complexation	Guil-Guerrero and colleagues (2000)
Tetraselmis sp.	EPA	10.41% of phospholipid fraction	Chloroform-methanol 2:1 (%v/v). Extract was washed with 0.88% w/v KCl to remove non-lipids	Makri and colleagues (2011)

(iii) Pigments:

Figure 11 highlights the many forms of bio-produced pigments and their origins. All photosynthesizing organisms produce chlorophyll A, whereas the green algae, red algae and cyanobacteria produce a broader range of pigments than terrestrial plants and other eukaryotes. The cyanobacteria, otherwise known as “blue-green algae”, are unique in that they possess the widest variety of chloroplasts that are one of the few sources of chlorophyll d and f. Due to the nature of their function, some of these pigments poses potential for utilization and application in number of markets. An excellent example is that of marennine – a water-soluble blue pigment derived from blue diatoms – with a number of biological (e.g., antioxidant, antibacterial, antiviral, etc.) functions and potential for commercial application in the aquaculture, cosmetics, food and health industries [111]. However, the commercial production of algae-derived pigments seems to

be underexplored, a noteworthy exception being phycocyanin, a blue pigment marketed as Spirulysat ® [112] by AlgoSource, a French company specialized in producing microalgae and bringing microalgae-derived products to market [113].

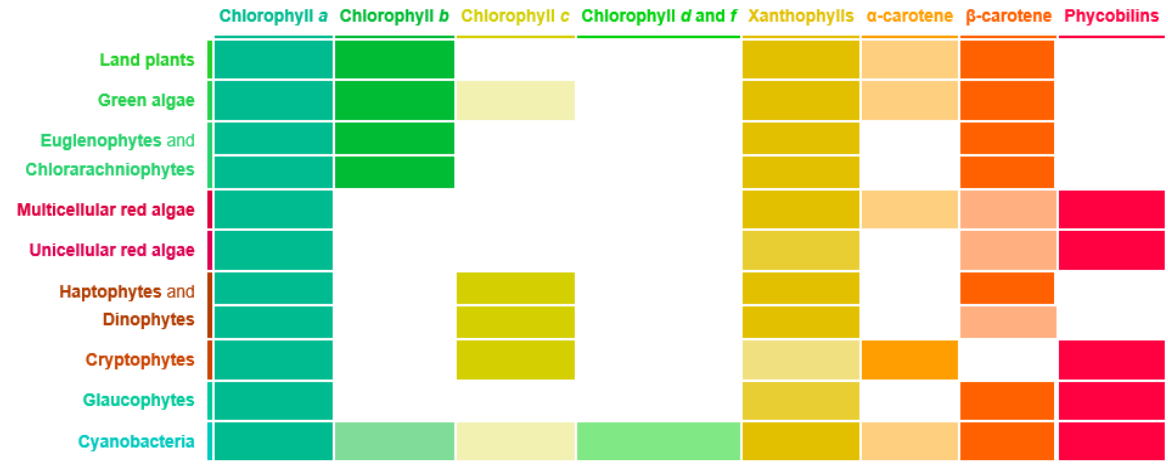

Figure 11. Presence of various pigments across chloroplast groups [114].

3.1.6. Summary of the R&D Gaps and Approach to Close the Gaps in Future Research

In the synopsis of its 2014 final report, the NAABB concluded that in order to reduce the cost of algae production, additional productivity and cultivation improvements would be needed; specifically, the NAABB suggested that new developments in the construction of algal farms and in the utilization of resources would be needed to respectively reduce CAPEX and OPEX by ~50% [13]. Additional recommendations in the synopsis included the implementation of algae strains and cultivation methods capable of maximizing biomass productivity year-round, along with techniques leading to the minimal and most efficient utilization of major resources including water and nutrients [13]. The latter is in overall agreement with a 2012 National Research Council (NRC) report on the sustainable development of algal fuels [115]. Indeed, according to this report a number of advances were required, including algal strains showing improved productivity, reactor strategies using either wastewater or water recycled during algae harvesting (particularly if freshwater is used), and nutrient recycling, all in addition to a land requirement assessment taking into account land prices, climatic conditions, sources of CO_2, as well as water resources in the form of fresh, waste, and saline (either inland or coastal) water.

Considerable research in the area of algal biology has been performed with the goal of increasing algal biomass productivity by identifying and improving naturally productive strains or by developing new high productivity strains through genetic modification. However, further research is needed on the genomic sequencing of algae in order to garner the knowledge needed for future strain enhancement efforts. Indeed, additional strains that are both productive and robust are needed so algae can be grown in diverse environments, including strains for fresh and impaired water, as well as strains for saltwater to be grown in coastal regions [13].

In terms of cultivation, it should be noted that microalgae cultivation in open raceway ponds has been practiced over the past fifty years for the production of nutritional products [13], which implies that this technology is mature and makes additional gains in terms of productivity and/or cost reduction hard to realize. Indeed, important advances have been achieved for a number of challenges associated with cultivation, including identifying robust and productive algae strains capable of growing reliably outdoors in various geographical locations, cultivating algae in low-cost media based on wastewater and recyclable agricultural-grade nutrients, as well as utilizing construction and operation materials and methods that improve productivity while reducing costs [13]. Along these lines, a noteworthy innovation achieved by the NAABB was the development of the Aquaculture Raceway Integrated Design (ARID) pond culturing system in which improved water temperature management keeps a given algae strain in the optimum range throughout the year, resulting in higher productivities and lower energy requirements and operating costs (the latter being achieved with the help of solar powered pumping and mixing systems) [13]. Nevertheless, one of the most promising approaches has been that of large-scale cultivation "hybrid" systems involving both PBRs and open ponds – such as Cellana's ALDUO™ [116] – in which a selected algae strain is grown first in a PBR to ensure the production of a monoculture free of contamination that is then used to inoculate open ponds where algae are grown rapidly and inexpensively. In this way, the advantages of PBRs (a closed system offering protection from contamination resulting in a monoculture) and open ponds (a low cost way to achieve high productivity) are synergized to address the disadvantages of each of these systems, namely, the relatively high cost of PBRs and the low productivity and contamination issues associated with open ponds. In fact, this approach – in which a PBR is used to produce a quality-controlled inoculum for open raceway ponds – has also been identified as a most promising approach by the NAABB [8]. Nevertheless, additional work focused on this approach is necessary, particularly in terms of PBR design, construction and operation, as the latter represent a critical aspect in which additional advancements and innovations can result in reduced costs and productivity enhancements [3]. Alternatively, it has been reported that growing several algae species in polycultures comprising four or more species can double the productivity and make cultures more resistant to contamination [8]. Notably, the importance of expanding the current understanding of how managing algal biomass production units as complex bioengineered systems can reduce algal biomass losses attributed to pathogens and grazers was highlighted in the 2012 NRC report on the sustainable development of algal fuels [1,115]. In fact, this report concluded that improvements in algae cultivation methods including the processes used to harvest, dewater and utilize algal biomass are as important as enhancements in algae strains [1].

Prior to their utilization, cultivated algae must be harvested and dewatered. Given that these processes involve recovering relatively small amounts of algal biomass from very large volumes of water, the associated costs are significant. However, several advances have been made to reduce the costs and energy requirements associated with harvesting and dewatering algae. Indeed, several technologies – such as ultrasonic harvesting, cross-flow membrane filtration and electrocoagulation – have been essayed in an effort to identify an approach showing a number of desirable characteristics, including low pumping and power requirements, limited environmental impact, and the capacity to process high volumes in an acceptable timeframe [13]. Notably, the

aforementioned technologies displayed considerable energy savings at scale relative to centrifugation (the baseline technology). Nevertheless, additional work is needed to test if the use of technologies in combination can result in a more complete water removal and/or higher throughputs, if consistent and high performance can be maintained over long periods, and if satisfactory results can be obtained with various algal feedstocks of different quality [13].

Regarding the issue of algae utilization, advances have also been made with the ultimate goals of improving the yield of valuable products obtained from algal biomass and of combining extraction and conversion steps to simplify unit operation, albeit the conversion of whole algal biomass into a bio-crude that can be upgraded to fuels has also been investigated [13]. Through this work, valuable information has been gained vis-à-vis the characterization of both algal biomass and its constituent fractions, albeit ample room for improvement exists regarding the cost, ease of use and versatility of the analytical instrumentation and methods employed to this end. Most work related to the conversion of algal lipids to fuels has been done utilizing UOP's Ecofining™ process, a commercial catalytic hydrotreatment process to obtain fuel-like hydrocarbons. However, the alternative Centia™ process – based on catalytic decarboxylation – has also been employed for the production of jet fuel and diesel [117-119]. Notably, decarboxylation-based processes are still in the research and development stage and additional work is needed to further asses the economic viability of this technology relative to the hydrotreatment route, which is technologically mature. It should also be noted that wet whole algae biomass has been directly converted to bio-oil through hydrothermal liquefaction, which has the potential to lead to gains in carbon and energy efficiency (as whole biomass is utilized and a drying step is obviated), while also allowing for water and nutrient recycling. In addition, capital and operating costs can also be reduced by enabling the use of infrastructure and catalytic technology already available in existing petroleum refineries, which can be leveraged to co-process the resulting bio-oil with petroleum derived feedstocks. However, additional research is also necessary on this approach, particularly regarding long-term catalyst performance and on the characterization and purification of the algae-derived oleaginous intermediates [3,13].

Given that is widely recognized that every part of algal biomass must be effectively utilized for algae-based technology to be sustainable from an economic and environmental standpoint, the use of lipid extracted algae (LEA or defatted algae) as animal feed and fertilizer has also been investigated [8,13]. However, the NAABB concluded that since the value of the LEA extracted from these applications did not offset the cost associated with defatting algae, further research in this particular area was not warranted [13]. Nevertheless, additional work focused on valorizing the LEA showed that value-added products – such as ethanolamines – can indeed be obtained from amino acids derived from the proteinaceous fraction of defatted algae [8]. The latter point illustrates that additional work is needed to identify and/or develop alternative utilization approaches showing more favorable economics. In other words, the production of high value compounds through cost effective fractionation approaches capable of separating whole biomass into several streams – each containing valuable compounds in a form and/or purity amenable to further processing or commercialization – represents an important technology gap that must be addressed through additional research and development efforts [3].

In conclusion, a number of critical parameters must be improved to ensure the viability of algae-based carbon capture and utilization technology. Foremost among these is the issue of productivity [1], robust growth throughout the entire year being more important that peak growth to overcome low winter productivity [13]. In principle, productivity increases can be achieved through improvements in cultivation, which in turn can be attained via enhancements to the biology and/or the cultivation system. The effect that other critical aspects have on productivity, such as the recycling of water, carbon and debris as well as photosynthetic efficiency and how the latter is modified through genetic engineering, also require further study. In addition, research and development work to achieve increases in productivity will need to be coupled with additional efforts designed to further reduce CAPEX and OPEX – including developing methods to minimize the need for using (and pumping) large amounts of water and optimizing nutrient utilization – to render algae-based carbon capture and utilization technology economically viable.

Finally, it is widely recognized that both techno-economic and life-cycle analyses should continue to be performed, revised, updated and harmonized as new data are made available by additional work in this area [3,13].

3.2. Other R&D Programs and Gap Closing of Algae-Based CO_2 Capture and Utilization Systems

Pond Technologies, a company based in Ontario, Canada, has partnered with the National Research Council of Canada to investigate the use of algae for the reduction of greenhouse gas emissions from industrial point sources, aiming to ultimately convert these emissions into valuable bioproducts such as biofuel, fertilizer and animal feed [3,120]. This company's technology is based on an enclosed PBR system, which is illuminated using both LED lights and sunlight. Notably, Pond Technologies claims to have achieved algae harvest rates >20x of those achieved in open ponds using their custom designed and built PBR, gas management, illumination, continuous harvest and control systems [121]. In addition, this company has tested its technology to grow algae using the raw, untreated flue gas from various industrial point sources, including a cement plant, and integrated steel mill, and a natural gas cogeneration plant. These tests have led the company to conclude that their technology is a cost effective carbon sequestration and utilization technology, particularly because algal biomass is produced in large amounts and provides several downstream processing options – such as biofuels, biolubricants, bioplastics and high value chemicals – for revenue generation [121]. Moreover, Pond Technologies has also concluded that their technology constitutes a cost effective air pollution scrubber, since CO_2, NO_x and SO_2 are all removed once exhaust gas flows through their system [122].

Unfortunately, no data have been published to date by Pond Technologies vis-à-vis the cost of producing algae using their approach. However, the high cost of LEDs and the tanks constituting this company's PBRs – as well as the fact that the latter must be housed indoors – imply that the cost of producing algae using this particular CO_2 capture and utilization technology will likely be too high as for it to be commercially viable at significant scale. Admittedly, developing downstream processing pathways focused on the production of high value products – such as nutraceuticals – could improve the economics of this approach, albeit regulatory hurdles associated

with the use of industrial emissions in the synthesis of a product suitable for human consumption would have to be overcome.

Genesis Biofuels Inc. (Boulder, Colorado) is a company dedicated to building algae-based refineries that sequester CO_2 emissions from cement plans to produce renewable energy products [123]. The refineries sold by Genesis Biofuels Inc. to cement companies as a method of pollution control have two end products, namely, biomass and biodiesel; while the former reduces the intake of coal, the latter fuels trucks and heavy equipment at the cement plants [124]. Genesis Biofuels Inc. grows algae in PBRs (as opposed to doing so in open ponds) to ensure a clean and controlled environment, centrifugation and ultrasound being used to remove most of the water and to extract the algal oils, respectively. While the resulting defatted algae is used as a low carbon fuel substituent for the coal needed by cement plants, the extracted lipids are transesterified to biodiesel, which is used to offset the fuel requirements of cements plants, any surplus being sold in the open market [125]. Notably, this company makes use of a continuous rate adjustable harvester – which allows all the water used in the process to be recycled – and the refining process runs on heat from a concentrated solar thermal system, which renders the refinery entirely carbon negative [126].

Cellana, Inc. has also investigated the use of microalgae to sequester the CO_2 in the flue gas from on-site diesel generators at their demonstration facility in Kona, Hawaii (Cellana uses diesel generators to power their facility, which is operated off the local electrical grid) [127]. The work of Cellana in this regard focused mostly on the capture, treatment and delivery of flue gas to open algae ponds dedicated to large-scale microalgae production. Indeed, in addition to testing the viability of replacing pure CO_2 with flue gas, Cellana researchers strived to satisfy a number of criteria with their flue gas capture, treatment and delivery system, including avoiding backpressure on the generator exhaust piping, reducing the soot in the flue gas, reducing flue gas temperature to <200 °C, ensuring resistance to H_2SO_4 that may form in the piping, monitoring and recording process parameters, and addressing safety concerns through gas monitoring and alarms. Cellana achieved all the aforementioned goals by implementing a number of innovations, including a blower preceded by an air filter to pull the flue gas through a process tank equipped with a seawater spray system, which reduced the temperature of the flue gas to <40 °C, significantly reducing the soot and slightly reducing both NO_x and SO_2. In addition, all materials were selected to withstand high temperatures as well as the potential for acid precipitation, and air quality monitoring equipment was installed both at the process tank and at the test pond, no CO, NO_2 or SO_2 being detected during flue gas operation. Finally, systems were employed to control the flue gas delivery based on the pH of the pond and the temperature of the process tank.

Using the system described above, Cellana successfully grew more than 100 kg of a strain of *Nannochloropsis oceanica* using treated flue gas from their onsite diesel generators. Notably, no differences in growth rate, nutrient uptake rate or biomass productivity were observed when using flue gas as opposed to pure CO_2. Moreover, the algal biomass grown with these different sources of CO_2 showed no differences in their lipid, carbohydrate and protein content, or in their lipid profile. Admittedly, heavy metals – including cadmium, arsenic and led – were slightly higher in

the algae grown using flue gas; however, the levels observed were below the single cell protein guidelines published by the International Union for Pure and Applied Chemistry (IUPAC).

Global Algae Innovations, Inc. is another company with operations in Lihue, Hawaii (and headquarters in San Diego, California), which claims to have the world's only large-scale open raceway utilizing power plant flue gas as its only CO_2 source [128]. This company focuses on developing and leveraging "radical advances" throughout the entire algae production process – including raceway design, harvest and dewatering, CO_2 supply, inoculation and drying – to enable the economical and sustainable production of algal protein for human and animal consumption along with biofuel and high value commodities such as astaxanthin, pigments, and omega-3 oils. Although Global Algae Innovations is purportedly demonstrating these advances in the aforementioned open raceway facility using power plant flue gas as its sole CO_2 source, no details are publicly available regarding the outcome of this demonstration or about the products targeted or obtained when flue gas is employed.

In Taiwan, Far East Bio-Tec. Co. [129] has partnered with China Steel Co. to investigate reducing emissions by fixing flue gas using algae [3], albeit almost no information related to this venture is publicly available. Similarly, Accelergy Corporation claims that TerraSync® – its proprietary carbon capture and utilization process affording a biofertilizer – begins with the CO_2 produced from point sources including fossil fuel-based electricity generation or refining operations [99]. However, other than stating that the CO_2 is used as feedstock in the cultivation of algae that are integral to the aforementioned biofertilizer, the only technical information publicly available is that the algae are actually cyanobacteria and are grown using a photobioreactor [130].

4. Commercially Available Equipment

4.1. Introduction of Power Plant Flue Gas to Algae Cultivation System

There are a multitude of commercial options for handling flue gas and dissolving carbon dioxide to afford aqueous solutions to support algae growth. A wide range of manufacturers and styles of pumps, blowers, and compressors are available, as the use of this equipment is widespread in a host of industries in addition to being commonly integrated in algae-based processes. Given that the ultimate goal of this technology is the beneficial re-use and overall the reduction of carbon emissions, approaching the selection of equipment from an overall lifecycle perspective is critical. Indeed, although some systems are well understood and wholly satisfactory from a technological and economic perspective, they may fall short of addressing the overall goal of reducing emissions.

The handling of bi-phasic (gas and liquid) flows has broad application in the aquaculture, food and beverage, pulp and paper industries, and a host of other chemical and manufacturing processes. One of the main providers of this type of technology is the Linde Group, which specializes in the engineering of gas handling. Aquaculture equipment producers, such as Pentair (US) and Aquatic Ecosystems (US), typically focus on maintaining high levels of dissolved oxygen in production systems, although these could be retrofitted to increase dissolved carbon dioxide loading in algal production systems.

Although most technology providers offer a wide range of traditional technologies that could be applied to large scale algaculture, there are a few emerging applications that specifically target algae producers. An example of a company adapting traditional aquaculture and water treatment technologies to provide solutions for algae producers is Searen, Inc. (Cincinnati, OH), which offers a gas-liquid contactor that simultaneously strips produced oxygen, saturates the algae culture with carbon dioxide, and provides a continuous harvesting potential. This certainly appears to be an area of growth moving forward.

4.2. Algae Cultivation System

Commercial PBRs are available from several vendors, albeit they are typically very expensive. Subitec (Germany) is a leading supplier of flat-panel PBRs. Microalghe Camporosso (Italy) has demonstrated flat panel photobioreactor construction and operation on a 1 hectare scale [68]. Varicon (UK) manufactures a variety of tubular and column photobioreactors.

Open pond systems are commercially available from a variety of companies like MicroBio and Commercial Algae Professionals. Commercial Algae Professionals sell systems that are furnished with a wide variety of analytical instrumentation.

Automated sensing and control systems needed for monitoring production-scale ponds are also available. Indeed, NAABB has developed a number of sensors, including an algae optical density (OD) sensor for measuring biomass concentration, a neutral algal lipid sensor based on Nile Red-staining-and-fluorescence, a sensor based on near-infrared (NIR) and Fourier-transform-infrared (FTIR) analysis to characterize algal biomass composition, and an algal lipid sensor based on thin-film infrared-attenuated total reflectance (IR-ATR) [8].

There is a suite of emerging technology providers supporting entrepreneurs in the algae field. Monitoring the performance of algae cultures in both ponds and photobioreactors is an area of particular focus, with solutions available from Mettler-Toledo, Hach, Algae Lab Systems, Neptune Aquatics, and YSI.

4.3. Harvesting and Dewatering of Algal Biomass

Commercial flocculants are available through a number of suppliers; however, SNF Floerger has a complete product line that is diversified and has been demonstrated to be effective. Thickeners are widely available from commercial suppliers such as WesTech Engineering (SuperSettler™), MAK Water (Lamella) and Parkson (EcoFlow®). For dewatering thickened biomass, horizontal belt filters are also widely available from numerous suppliers such as FLSmidth, WesTech Engineering, and Phoenix Process Equipment Company. These companies also provide pressure filters if production of drier biomass cake is warranted. All of these suppliers provide comprehensive services to the mining, municipal, and industrial water treating industries.

Recently, Global Algae Innovations, Inc. has developed the Zobi Harvester®, a new algae harvesting system using advanced membranes to achieve 100% harvest efficiency and obviate secondary dewatering, as the system produces a 15-20% algae concentrate with an exceptionally low energy use [131]. Notably, in addition to having been validated for several classes of algae – including diatoms, green algae, cyanobacteria and red algae – the system is both easy to operate

and it avoids exposing algae to elevated pressures, centrifugal forces or shear. Moreover, according to Global Algae Innovations, Inc. the system is scalable in sizes ranging from 5 gpm to 200,000 gpm.

4.4. Algal Biomass Fractionation

Lipid extraction services are already offered on a commercial basis by several companies (typically for dry algal biomass), although Valicor processes wet biomass using their patented procedures. Industry-standard equipment is used (tanks, stirrers, separation vessels, etc.).

4.5. Utilization of Algal Biomass Fractions

Fermentation and catalytic upgrading technology for the conversion of algae-derived sugars and oils to transportation fuels is widely available. In addition, equipment employed in the synthesis of bioplastics incorporating algae biomass can also be found in the market, albeit certain companies – such as ALGIX [47] – are exclusive world-wide licensees of patented technology for thermoplastic co-processing of algae biomass to afford algae-blended thermoplastic compositions. This technology comprises fluidized bed jet milling systems, pneumatic conveyors, and co-rotating twin screw extruders. As mentioned above, in the case of ALGIX the extrusion system comprises the majority of the proprietary process, which includes custom screw designs and specially designed mixing elements, custom de-volatilization/moisture removal equipment, proprietary thermal recipe for heating zones, screw speed ratio, and proprietary compatibilizers/coupling agents for enhanced biomass incorporation with the carrier resin. Once algae-derived bioplastic resin is obtained, additional commercially available equipment is employed for the thermoplastic production of the finished commercial product. For instance, single screw extruders are employed for the precise profile extrusion of filaments to be used in FDM-style 3D printers. Alternatively, bioplastics pellets can be thermally melted and blended with additional ingredients to afford a molten blend that is extruded into thin sheets, which are inserted into special compression ovens where heat and pressure are applied to induce the foam expansion and create the finished foamed bun or sheet. Die cutting techniques are finally applied to foam sheets to yield products such as shoe insoles, midsoles, and other flexible foam products.

5. Conclusions

Algae-based technology has long been considered a promising way to beneficially capture and utilize carbon dioxide emissions from power plants and other point sources, algae production economics being strongly dependent on cultivation productivity. Notably, current best-scenario areal productivity estimates already fall within ranges which have been deemed economically viable, meaning that as productivities demonstrated to date are increased further and start approaching current best-case scenarios, algae production economics can be greatly improved. Similarly, although the commercial production of algae-derived biofuels is not economically viable at the present time, models predict that with improvements in algae strains, cultivation, harvesting and extraction, economic viability can be attained.

Of the two main technologies currently used for large-scale algae cultivation, namely, outdoor open pond systems and indoor or outdoor photobioreactor (PBR) systems, PBRs are designed to circumvent some of the major drawbacks associated with open pond systems, as they are more

amenable to growing a single algal species for prolonged periods of time by minimizing the risk of external contamination. Recently, PBR design has been greatly improved through work performed at the UK CAER to develop the next generation 'cyclic flow' PBR. The latter includes a host of cost and energy saving features that address and assuage a number of issues typically associated with PBRs, including self-shading, biofilm formation and prohibitive pumping requirements. This is in line with the fact that neither ponds nor PBRs have proved to be economically viable as a method of biofuel production, so most work in this area is focused on the development of new algae strains (e.g., via mutagenesis, genetic engineering or directed evolution approaches) possessing improved productivity.

UK's harvesting and dewatering strategy employs a proven low-cost process – based on flocculation-sedimentation followed by gravity filtration – that has been adapted to operate in continuous mode. This approach further reduces the energy requirements and the overall cost of algae production. Indeed, while centrifuges are the industry state of the art for harvesting algae, this approach is energy intensive and has high capital and operating costs. Thus, methods employed by other applications that separate solids from dilute suspensions – such as municipal wastewater treatment or mineral processing (where effective thickening is employed to concentrate suspended solids while producing clarified water) – represent a reasonable alternative. Alternative technologies including dissolved air flotation and spiral plate separation as well as electrolytic and ultrasonic harvesting can also reduce harvesting operating costs relative to centrifugation; however, they have yet to be demonstrated in continuous operation at reasonable scale.

Whether algal biomass fractionation is needed depends on the end use of the biomass. For some applications, such as animal feed and bioplastics, fractionation is not required and the biomass is used as whole cells. For other uses, lipid extraction is required and further fractionation into protein and carbohydrates may also be needed. Fortunately, there are several commercially relevant processes that have been developed for this purpose. In fact, the commercial processes developed by Valicor represent the state of the art for algal lipid extraction and it is hard to see how significant improvement of these processes is possible. Albeit other approaches for lipid extraction from algae have been reported, their elevated cost has caused few of these methods to be commercialized. However, in contrast to lipid extraction – where at least some processes have been commercialized – full algal biomass fractionation has not been commercially developed.

Whole algae, algae fractions and individual algae-derived compounds have applications that are as numerous as they are varied. However, most end uses given to algal biomass are concentrated in a handful of industries, including aquaculture, animal feed and fertilizer, bioplastics, nutraceuticals, dyes and pigments, and cosmetics. Notably, technology gaps exist in most industries in which algal biomass finds its end uses. Indeed, there are considerable gaps regarding the integration of large-scale microalgal biomass production with aquaculture, particularly in terms of co-locating aquaculture facilities at microalgae production sites and of reclaiming and recycling a significant fraction of the nutrients excreted by fish. Moreover, the promise of much higher available quantities of algal biomass in the future is prompting evaluation of algae as a major ingredient in formulated animal feeds and as a soil fertilizer. Furthermore, the effect of algae processing on the quality and properties of bioplastics comprising algal biomass remains a topic

requiring additional research. Finally, albeit several compounds found in algae are used as nutraceuticals, pigments and other high value products, these compounds tend to be produced from sources other than microalgae, which implies that additional work is required to determine if sourcing these compounds from algae could have technological, economical or environmental advantages.

In short, a number of critical parameters must be addressed to ensure the viability of algae-based carbon capture and utilization technology. Foremost among these is the issue of system productivity, increases in which can potentially be achieved through improvements in strain productivity and cultivation practices. However, other factors affecting productivity, such as the recycling of water and cell debris, also require further study. In addition, R&D work to achieve increases in productivity needs to be coupled with efforts designed to reduce CAPEX and OPEX in order to render algae-based carbon capture and utilization technology economically viable. Finally, both techno-economic and life-cycle analyses should continue to be revised, updated and harmonized as new data become available in order to inform further advancements in algae culturing and processing technology.

References

1. Olivares, J. National Alliance for Advanced Biofuels and Bioproducts (NAABB) Final Report Section 1. US DOE-EERE Biotechnologies Office, 2014. https://energy.gov/eere/bioenergy/downloads/national-alliance-advanced-biofuels-and-bioproducts-synopsis-naabb-final

2. McGowen, J.; Knoshaug, E. P.; Laurens, L. M. L.; Dempster, T. A.; Pienkos, P. T.; Wolfrum, E.; Harmon, V. L., The Algae Testbed Public-Private Partnership (ATP3) framework; establishment of a national network of testbed sites to support sustainable algae production. *Algal Research Vol. 25 pp. 168-177*, 2017. http://www.sciencedirect.com/science/article/pii/S2211926417300875.

3. Laurens, L. M. State of Technology Review – Algae Bioenergy. IEA Bioenergy, 2017. http://www.ieabioenergy.com/wp-content/uploads/2017/01/IEA-Bioenergy-Algae-report-update-20170114.pdf.

4. Zhang, X. Microalgae removal of CO_2 from flue gas. IEA Clean Coal Centre, UK, 2015. https://www.usea.org/sites/default/files/042015_Microalgae%20removal%20of%20CO2%20from%20flue%20gas_ccc250.pdf.

5. Lam, M. K.; Lee, K. T.; Mohamed, A. R., Current status and challenges on microalgae-based carbon capture. *International Journal of Greenhouse Gas Control Vol. 10 pp. 456-469*, 2012.

6. Ho, S.-H.; Chen, C.-Y.; Lee, D.-J.; Chang, J.-S., Perspectives on microalgal CO 2-emission mitigation systems—a review. *Biotechnology advances Vol. 29 (2), pp. 189-198*, 2011.

7. Kumar, K.; Banerjee, D.; Das, D., Carbon dioxide sequestration from industrial flue gas by Chlorella sorokiniana. *Bioresource technology Vol. 152 pp. 225-233*, 2014.

8. Olivares, J. National Alliance for Advanced Biofuels and Bioproducts (NAABB) Final Report Section 2. US DOE-EERE Biotechnologies Office 2014. https://energy.gov/eere/bioenergy/downloads/national-alliance-advanced-biofuels-and-bioproducts-synopsis-naabb-final

9. Weyer, K. M.; Bush, D. R.; Darzins, A.; Willson, B. D., Theoretical maximum algal oil production. *Bioenergy Research Vol. 3 (2), pp. 204-213*, 2010.

10. Darzins, A.; Pienkos, P. T.; Edye, L. Current Status and Potential for Algal Biofuels Production. IEA Bioenergy, 2010. http://www.globalbioenergy.org/uploads/media/1008_IEA_Bioenergy_Task_39_-_Current_status_and_potential_for_algal_biofuels_production.pdf.

11. Fernandez, F.; Camacho, F. G.; Perez, J.; Sevilla, J.; Grima, E. M., Modeling of biomass productivity in tubular photobioreactors for microalgal cultures: effects of dilution rate, tube diameter, and solar irradiance. *Biotechnology and bioengineering Vol. 58 (6), pp. 605-616*, 1998.

12. Moheimani, N. R.; Borowitzka, M. A., The long-term culture of the coccolithophore Pleurochrysis carterae (Haptophyta) in outdoor raceway ponds. *Journal of Applied Phycology Vol. 18 (6), pp. 703-712*, 2006.

13. Olivares, J. National Alliance for Advanced Biofuels and Bioproducts (NAABB) Synopsis Report. US DOE-EERE Biotechnologies Office, 2014. https://energy.gov/eere/bioenergy/downloads/national-alliance-advanced-biofuels-and-bioproducts-synopsis-naabb-final

14. Ruiz, J.; Olivieri, G.; de Vree, J.; Bosma, R.; Willems, P.; Reith, J. H.; Eppink, M. H.; Kleinegris, D. M.; Wijffels, R. H.; Barbosa, M. J., Towards industrial products from microalgae. *Energy & Environmental Science Vol. 9 (10), pp. 3036-3043*, 2016.

15. Davis, R.; Markham, J.; Kinchin, C.; Grundl, N.; Tan, E. C.; Humbird, D. Process design and economics for the production of algal biomass: algal biomass production in open pond systems and processing through dewatering for downstream conversion (Technical Report No. NREL/TP-5100-64772). National Renewable Energy Laboratory (NREL), Golden, CO, United States, 2016. http://www.nrel.gov/docs/fy16osti/64772.pdf.

16. Martin, D. F.; Taber, J., Carbon dioxide flooding. *Journal of Petroleum Technology Vol. 44 (04), pp. 396-400*, 1992.

17. Wilson, M.; Groppo, J.; Placido, A.; Graham, S.; Morton, S.; Santillan-Jimenez, E.; Shea, A.; Crocker, M.; Crofcheck, C.; Andrews, R., CO_2 recycling using microalgae for the production of fuels. *Applied Petrochemical Research Vol. 4 (1), pp. 41-53*, 2014.

18. Wilson, M. H.; Mohler, D. T.; Groppo, J. G.; Grubbs, T.; Kesner, S.; Frazar, E. M.; Shea, A.; Crofcheck, C.; Crocker, M., Capture and recycle of industrial CO2 emissions using microalgae. *Applied Petrochemical Research Vol. 6 (3), pp. 279-293*, 2016. http://dx.doi.org/10.1007/s13203-016-0162-1.

19. Stewart, W. D.; Pearson, H., Effects of aerobic and anaerobic conditions on growth and metabolism of blue-green algae. *Proceedings of the Royal Society of London B: Biological Sciences Vol. 175 (1040), pp. 293-311*, 1970.

20. Brennan, L.; Owende, P., Biofuels from microalgae—a review of technologies for production, processing, and extractions of biofuels and co-products. *Renewable and Sustainable Energy Reviews Vol. 14 (2), pp. 557-577*, 2010.

21. Richardson, J. W.; Johnson, M. D.; Outlaw, J. L., Economic comparison of open pond raceways to photo bio-reactors for profitable production of algae for transportation fuels in the Southwest. *Algal Research Vol. 1 (1), pp. 93-100*, 2012. http://www.sciencedirect.com/science/article/pii/S2211926412000100.

22. Pulz, O.; Gross, W., Valuable products from biotechnology of microalgae. *Appl Microbiol Biotechnol Vol. 65 (6), pp. 635-48*, 2004. https://www.ncbi.nlm.nih.gov/pubmed/15300417.

23. Ugwu, C. U.; Aoyagi, H.; Uchiyama, H., Photobioreactors for mass cultivation of algae. *Bioresource Technology Vol. 99 (10), pp. 4021-4028*, 2008. http://www.sciencedirect.com/science/article/pii/S0960852407001368.

24. Groppo, J.; Rhea, N.; Shin, H. Y.; Mills, L. C.; Santillan-Jimenez, E.; Morgan, T.; Wilson, M.; Crofcheck, C.; Crocker, M. Microalgae Processing for the Production of Fuels. *4th International Conference on Algal Biomass, Biofuels & Bioproducts*, Santa Fe, NM, June 15-18, 2014.

25. Mercer, P.; Armenta, R. E., Developments in oil extraction from microalgae. *European Journal of Lipid Science and Technology Vol. 113 (5), pp. 539-547*, 2011.

26. Vandamme, D.; Foubert, I.; Meesschaert, B.; Muylaert, K., Flocculation of microalgae using cationic starch. *Journal of Applied Phycology Vol. 22 (4), pp. 525-530*, 2010.

27. Cooney, M.; Young, G.; Nagle, N., Extraction of bio-oils from microalgae. *Separation & Purification Reviews Vol. 38 (4), pp. 291-325*, 2009.

28. Prabakaran, P.; Ravindran, A. D., A comparative study on effective cell disruption methods for lipid extraction from microalgae. *Lett Appl Microbiol Vol. 53 (2), pp. 150-4*, 2011. https://www.ncbi.nlm.nih.gov/pubmed/21575021.

29. Bligh, E. G.; Dyer, W. J., A rapid method of total lipid extraction and purification. *Canadian Journal of Biochemistry and Physiology Vol. 37 (8), pp. 911-917*, 1959.

30. Laurens, L. M.; Quinn, M.; Van Wychen, S.; Templeton, D. W.; Wolfrum, E. J., Accurate and reliable quantification of total microalgal fuel potential as fatty acid methyl esters by in situ transesterification. *Analytical and bioanalytical chemistry Vol. 403 (1), pp. 167-178*, 2012.

31. Czartoski, T. J.; Perkins, R.; Villanueva, J. L.; Richards, G., Algae biomass fractionation. U.S. Patent 9,296,985: 2016.

32. Kadam, K. L.; Goodall, B. L., Algae extraction process. U.S. Patent 8,591,912: 2013.

33. Dong, T.; Knoshaug, E. P.; Davis, R.; Laurens, L. M. L.; Van Wychen, S.; Pienkos, P. T.; Nagle, N., Combined algal processing: A novel integrated biorefinery process to produce algal biofuels and bioproducts. *Algal Research Vol. 19 pp. 316-323*, 2016.

34. Laurens, L.; Nagle, N.; Davis, R.; Sweeney, N.; Van Wychen, S.; Lowell, A.; Pienkos, P., Acid-catalyzed algal biomass pretreatment for integrated lipid and carbohydrate-based biofuels production. *Green Chemistry Vol. 17 (2), pp. 1145-1158*, 2015.

35. http://www.biodieselmagazine.com/articles/8153/usda-lead-scientist-explains-aquacultures-need-for-algae (accessed July 2017).

36. Spolaore, P.; Joannis-Cassan, C.; Duran, E.; Isambert, A., Commercial applications of microalgae. *Journal of Bioscience and Bioengineering Vol. 101 (2), pp. 87-96*, 2006. https://www.ncbi.nlm.nih.gov/pubmed/16569602.

37. Tidwell, J., Personal Communication (Crocker, M., recipient), June 2013.

38. Borowitzka, M. A., Algal biotechnology products and processes—matching science and economics. *Journal of Applied Phycology Vol. 4 (3), pp. 267-279*, 1992.

39. http://www.algae4feed.org/brief/microalgae-in-feeds/57 (accessed July 2017).

40. Benemann, J. R., Production of nitrogen fertilizer with nitrogen-fixing blue-green algae. *Enzyme and Microbial Technology Vol. 1 (2), pp. 83-90*, 1979.

41. Singh, A.; Singh, P., Comparative effects ofAzolla and blue-green algae in combination with chemical N fertilizer on rice crop. *Proceedings: Plant Sciences Vol. 96 (2), pp. 147-152*, 1986.

42. Mulbry, W.; Westhead, E. K.; Pizarro, C.; Sikora, L., Recycling of manure nutrients: use of algal biomass from dairy manure treatment as a slow release fertilizer. *Bioresource technology Vol. 96 (4), pp. 451-458*, 2005.

43. Singh, P.; Panigrahi, B.; Satapathy, K., Comparative efficiency of Azolla, blue-green algae and other organic manures in relation to N and P availability in a flooded rice soil. *Plant and Soil Vol. 62 (1), pp. 35-44*, 1981.

44. Huang, C.-Y., Comparative efficiency of Azolla, Blue-green Algae and other organic manures in relation to N and P availability in a flooded rice soil. *Bot. Bull. Academia Sinica Vol. 19 pp. 41-52*, 1977.

45. http://www.marketwatch.com/story/world-bioplastics-market-growing-at-293-cagr-to-2020-2016-07-11-2220311 (accessed July 2017).

46. http://www.european-bioplastics.org/market/ (accessed July 2017).

47. http://algix.com/ (accessed July 2017).

48. http://www.eia.gov/tools/faqs/faq.cfm?id=77&t=11 (accessed July 2014).

49. Cohen, Z., Chemicals from Microalgae, Tylor & Francis Ltd, London, UK, 1999.

50. https://en.wikipedia.org/wiki/Omega-3_fatty_acid (accessed July 2017).

51. http://www.algaeindustrymagazine.com/qualitas-and-valicor-partner-to-commercialize-algal-omega-3/ (accessed August 2017).

52. https://www.algenist.com/ (accessed July 2017).

53. Jiang, Y.; Chen, F.; Liang, S.-Z., Production potential of docosahexaenoic acid by the heterotrophic marine dinoflagellate Crypthecodinium cohnii. *Process Biochemistry Vol. 34 (6), pp. 633-637*, 1999.

54. Zittelli, G. C.; Lavista, F.; Bastianini, A.; Rodolfi, L.; Vincenzini, M.; Tredici, M., Production of eicosapentaenoic acid by Nannochloropsis sp. cultures in outdoor tubular photobioreactors. *Journal of Biotechnology Vol. 70 (1), pp. 299-312*, 1999.

55. https://www.alibaba.com/product-detail/High-purity-Eicosapentaenoic-acid-10417-94_60491622770.html?spm=a2700.7724838.2017115.10.V2fytI (accessed July 2017).

56. Mahajan, G.; Kamat, M., γ-Linolenic acid production from Spirulina platensis. *Applied Microbiology and Biotechnology Vol. 43 (3), pp. 466-469*, 1995.

57. Ward, O. P.; Singh, A., Omega-3/6 fatty acids: alternative sources of production. *Process Biochemistry Vol. 40 (12), pp. 3627-3652*, 2005.

58. Del Campo, J. A.; Moreno, J.; Rodríguez, H.; Vargas, M. A.; Rivas, J. n.; Guerrero, M. G., Carotenoid content of chlorophycean microalgae: factors determining lutein accumulation in Muriellopsis sp.(Chlorophyta). *Journal of Biotechnology Vol. 76 (1), pp. 51-59*, 2000.

59. Román, R. B.; Alvarez-Pez, J.; Fernández, F. A.; Grima, E. M., Recovery of pure B-phycoerythrin from the microalga Porphyridium cruentum. *Journal of Biotechnology Vol. 93 (1), pp. 73-85*, 2002.

60. http://www.globalgae.com/ (accessed August 2017).

61. Lackner, K. S., Capture of carbon dioxide from ambient air. *The European physical journal-special topics Vol. 176 (1), pp. 93-106*, 2009.

62. Wright, A. B.; Lackner, K. S.; Ginster, U., Method and apparatus for extracting carbon dioxide from air. U.S. Patent 9,266,052: 2016.

63. Rittmann, B.; Lackner, K.; Wright, A.; Flory, J.; Patel, M., Systems and methods of atmospheric carbon dioxide enrichment and delivery to photobioreactors via membrane carbonation. WO Patent 2016164563 A1: 2016.

64. Merkel, T. C.; Lin, H.; Wei, X.; Baker, R., Power plant post-combustion carbon dioxide capture: an opportunity for membranes. *Journal of Membrane Science Vol. 359 (1), pp. 126-139*, 2010.

65. Yeon, S.-H.; Lee, K.-S.; Sea, B.; Park, Y.-I.; Lee, K.-H., Application of pilot-scale membrane contactor hybrid system for removal of carbon dioxide from flue gas. *Journal of Membrane Science Vol. 257 (1), pp. 156-160*, 2005.

66. Resurreccion, E. P.; Colosi, L. M.; White, M. A.; Clarens, A. F., Comparison of algae cultivation methods for bioenergy production using a combined life cycle assessment and life cycle costing approach. *Bioresource Technology Vol. 126 pp. 298-306*, 2012. http://www.sciencedirect.com/science/article/pii/S0960852412013831.

67. Soratana, K.; Landis, A. E., Evaluating industrial symbiosis and algae cultivation from a life cycle perspective. *Bioresource Technology Vol. 102 (13), pp. 6892-6901*, 2011. http://www.sciencedirect.com/science/article/pii/S0960852411005104.

68. Tredici, M. R.; Rodolfi, L.; Biondi, N.; Bassi, N.; Sampietro, G., Techno-economic analysis of microalgal biomass production in a 1-ha Green Wall Panel (GWP®) plant. *Algal Research Vol. 19 pp. 253-263*, 2016. http://www.sciencedirect.com/science/article/pii/S2211926416303320.

69. Schenk, P. M.; Thomas-Hall, S. R.; Stephens, E.; Marx, U. C.; Mussgnug, J. H.; Posten, C.; Kruse, O.; Hankamer, B., Second generation biofuels: high-efficiency microalgae for biodiesel production. *Bioenergy Research Vol. 1 (1), pp. 20-43*, 2008.

70. Lundquist, T. J.; Woertz, I. C.; Quinn, N.; Benemann, J. R., A realistic technology and engineering assessment of algae biofuel production. *Energy Biosciences Institute Vol. pp. 1*, 2010.

71. Henze, M.; Comeau, Y., Wastewater characterization. *Biological Wastewater Treatment: Principles, Modelling and Design. London: IWA Publishing Vol. pp. 33-53*, 2008.

72. Drexler, I. L. C.; Yeh, D. H., Membrane applications for microalgae cultivation and harvesting: a review. *Reviews in Environmental Science and Biotechnology Vol. 13 (4),*

pp. 487-504, 2014. https://www.scopus.com/inward/record.uri?eid=2-s2.0-84919915606&doi=10.1007%2fs11157-014-9350-6&partnerID=40&md5=81f4d5d82feabb51b67c0d097540cd24.

73. Bilad, M. R.; Arafat, H. A.; Vankelecom, I. F., Membrane technology in microalgae cultivation and harvesting: a review. *Biotechnology advances Vol. 32 (7), pp. 1283-1300*, 2014. https://www.scopus.com/inward/record.uri?eid=2-s2.0-84921969246&doi=10.1016%2fj.biotechadv.2014.07.008&partnerID=40&md5=6013bb5bbe9ec4c9f80756fd8722ba9e.

74. Chu, H.; Zhao, F.; Tan, X.; Yang, L.; Zhou, X.; Zhao, J.; Zhang, Y., The impact of temperature on membrane fouling in algae harvesting. *Algal Research Vol. 16 pp. 458-464*, 2016. https://www.scopus.com/inward/record.uri?eid=2-s2.0-84963951600&doi=10.1016%2fj.algal.2016.04.012&partnerID=40&md5=81ef928947f48a3752576295a0048619.

75. Discart, V.; Bilad, M. R.; Moorkens, R.; Arafat, H.; Vankelecom, I. F. J., Decreasing membrane fouling during Chlorella vulgaris broth filtration via membrane development and coagulant assisted filtration. *Algal Research Vol. 9 pp. 55-64*, 2015. https://www.scopus.com/inward/record.uri?eid=2-s2.0-84928672666&doi=10.1016%2fj.algal.2015.02.029&partnerID=40&md5=b32ebb01a462dd37637e31b60f0e42e4.

76. Sá, M.; Monte, J.; Brazinha, C.; Galinha, C. F.; Crespo, J. G., 2D Fluorescence spectroscopy for monitoring Dunaliella salina concentration and integrity during membrane harvesting. *Algal Research Vol. 24 pp. 325-332*, 2017. https://www.scopus.com/inward/record.uri?eid=2-s2.0-85018364229&doi=10.1016%2fj.algal.2017.04.013&partnerID=40&md5=811884f97d20f6daad548193ed945c8e.

77. Eliseus, A.; Bilad, M. R.; Nordin, N. A. H. M.; Putra, Z. A.; Wirzal, M. D. H., Tilted membrane panel: A new module concept to maximize the impact of air bubbles for membrane fouling control in microalgae harvesting. *Bioresource Technology Vol. 241 pp. 661-668*, 2017. https://www.scopus.com/inward/record.uri?eid=2-s2.0-85020481270&doi=10.1016%2fj.biortech.2017.05.175&partnerID=40&md5=545eb5a9794f220cd8858d057f8922e1.

78. Hwang, T.; Oh, Y. K.; Kim, B.; Han, J. I., Dramatic improvement of membrane performance for microalgae harvesting with a simple bubble-generator plate. *Bioresource Technology Vol. 186 pp. 343-347*, 2015. https://www.scopus.com/inward/record.uri?eid=2-s2.0-84937763332&doi=10.1016%2fj.biortech.2015.03.111&partnerID=40&md5=8c11d4ac449573ea37ba40288c39b1ef.

79. Kanchanatip, E.; Su, B. R.; Tulaphol, S.; Den, W.; Grisdanurak, N.; Kuo, C. C., Fouling characterization and control for harvesting microalgae Arthrospira (Spirulina) maxima using a submerged, disc-type ultrafiltration membrane. *Bioresource Technology Vol. 209*

pp. 23-30, 2016. https://www.scopus.com/inward/record.uri?eid=2-s2.0-84959422113&doi=10.1016%2fj.biortech.2016.02.081&partnerID=40&md5=5beb15547a2a7c39c048433d48e333af.

80. Safi, C.; Olivieri, G.; Campos, R. P.; Engelen-Smit, N.; Mulder, W. J.; van den Broek, L. A. M.; Sijtsma, L., Biorefinery of microalgal soluble proteins by sequential processing and membrane filtration. *Bioresource Technology Vol. 225 pp. 151-158*, 2017. https://www.scopus.com/inward/record.uri?eid=2-s2.0-84997080475&doi=10.1016%2fj.biortech.2016.11.068&partnerID=40&md5=c6506eae416f2495022e5302d1fcfce4.

81. Zhao, F.; Chu, H.; Tan, X.; Zhang, Y.; Yang, L.; Zhou, X.; Zhao, J., Comparison of axial vibration membrane and submerged aeration membrane in microalgae harvesting. *Bioresource Technology Vol. 208 pp. 178-183*, 2016. https://www.scopus.com/inward/record.uri?eid=2-s2.0-84959324079&doi=10.1016%2fj.biortech.2016.02.099&partnerID=40&md5=2f63b011f84921a023e09f96d031ed3a.

82. Venault, A.; Ballad, M. R. B.; Huang, Y. T.; Liu, Y. H.; Kao, C. H.; Chang, Y., Antifouling PVDF membrane prepared by VIPS for microalgae harvesting. *Chemical Engineering Science Vol. 142 pp. 97-111*, 2016. https://www.scopus.com/inward/record.uri?eid=2-s2.0-84951102991&doi=10.1016%2fj.ces.2015.11.041&partnerID=40&md5=42f4a0965d85d6c9fd6b95df982cc909.

83. Elcik, H.; Cakmakci, M.; Ozkaya, B., Preparation and characterisation of novel polysulfone membranes modified with Pluronic F-127 for reducing microalgal fouling. *Chemical Papers Vol. 71 (7), pp. 1271-1290*, 2017. https://www.scopus.com/inward/record.uri?eid=2-s2.0-85010781759&doi=10.1007%2fs11696-016-0120-5&partnerID=40&md5=4c286a489d480a3ee1b7ecaf48e9361f.

84. Kim, S. B.; Paudel, S.; Seo, G. T., Forward osmosis membrane filtration for microalgae harvesting cultivated in sewage effluent. *Environmental Engineering Research Vol. 20 (1), pp. 99-104*, 2015. https://www.scopus.com/inward/record.uri?eid=2-s2.0-84926339940&doi=10.4491%2feer.2015.005&partnerID=40&md5=21dc2446d62f8132759b664df08783bc.

85. Elcik, H.; Cakmakci, M., Harvesting microalgal biomass using crossflow membrane filtration: critical flux, filtration performance, and fouling characterization. *Environmental Technology (United Kingdom) Vol. 38 (12), pp. 1585-1596*, 2017. https://www.scopus.com/inward/record.uri?eid=2-s2.0-84989245472&doi=10.1080%2f09593330.2016.1237560&partnerID=40&md5=e994b9c85b59d0c038de36705fdf869c.

86. Chu, H.; Zhao, Y.; Zhang, Y.; Yang, L., Dewatering of chlorella pyrenoidosa using a diatomite dynamic membrane: Characteristics of a long-term operation. *Journal of*

Membrane Science Vol. 492 pp. 340-347, 2015. https://www.scopus.com/inward/record.uri?eid=2-s2.0-84935009088&doi=10.1016%2fj.memsci.2015.05.069&partnerID=40&md5=5329147aa22e0471afe2fcbaaef91447.

87. Zhao, F.; Chu, H.; Su, Y.; Tan, X.; Zhang, Y.; Yang, L.; Zhou, X., Microalgae harvesting by an axial vibration membrane: The mechanism of mitigating membrane fouling. *Journal of Membrane Science Vol. 508 pp. 127-135*, 2016. https://www.scopus.com/inward/record.uri?eid=2-s2.0-84959128327&doi=10.1016%2fj.memsci.2016.02.007&partnerID=40&md5=30e40cb2b4eac4f6f4e40029a375bb57.

88. Zhao, F.; Chu, H.; Tan, X.; Yang, L.; Su, Y.; Zhou, X.; Zhao, J.; Zhang, Y., Using axial vibration membrane process to mitigate membrane fouling and reject extracellular organic matter in microalgae harvesting. *Journal of Membrane Science Vol. 517 pp. 30-38*, 2016. https://www.scopus.com/inward/record.uri?eid=2-s2.0-84976574209&doi=10.1016%2fj.memsci.2016.06.022&partnerID=40&md5=2a59bb95f804cf07f8582a0bbebec6cd.

89. Zhao, F.; Chu, H.; Zhang, Y.; Jiang, S.; Yu, Z.; Zhou, X.; Zhao, J., Increasing the vibration frequency to mitigate reversible and irreversible membrane fouling using an axial vibration membrane in microalgae harvesting. *Journal of Membrane Science Vol. 529 pp. 215-223*, 2017. https://www.scopus.com/inward/record.uri?eid=2-s2.0-85012110545&doi=10.1016%2fj.memsci.2017.01.039&partnerID=40&md5=2b0f0e46cef63408606656350dd976f4.

90. Nedzarek, A.; Drost, A.; Harasimiuk, F.; Tórz, A.; Bonisławska, M., Application of ceramic membranes for microalgal biomass accumulation and recovery of the permeate to be reused in algae cultivation. *Journal of Photochemistry and Photobiology B: Biology Vol. 153 pp. 367-372*, 2015. https://www.scopus.com/inward/record.uri?eid=2-s2.0-84946423175&doi=10.1016%2fj.jphotobiol.2015.09.009&partnerID=40&md5=c94b004fcc8cc304f34af82eee28ab5d.

91. Hwang, T.; Kotte, M. R.; Han, J. I.; Oh, Y. K.; Diallo, M. S., Microalgae recovery by ultrafiltration using novel fouling-resistant PVDF membranes with in situ PEGylated polyethyleneimine particles. *Water Research Vol. 73 pp. 181-192*, 2015. https://www.scopus.com/inward/record.uri?eid=2-s2.0-84922362598&doi=10.1016%2fj.watres.2014.12.002&partnerID=40&md5=5ee6097275cf1eb3f6d6fb3de676eb8b.

92. Long, R. D.; Abdelkader, E., Mixed-polarity azeotropic solvents for efficient extraction of lipids from Nannochloropsis microalgae. *Am J Biochem Biotechnol Vol. 7 (2), pp. 70-73*, 2011.

93. Ryckebosch, E.; Muylaert, K.; Foubert, I., Optimization of an analytical procedure for extraction of lipids from microalgae. *Journal of the American Oil Chemists' Society Vol. 89 (2), pp. 189-198*, 2012.

94. Heger, M., A New Processing Scheme for Algae Biofuels. *MIT Technology Review Vol. pp.* 2009. https://www.technologyreview.com/s/413325/a-new-processing-scheme-for-algae-biofuels/.

95. http://www.originclear.com/pdf/Feed-The-World-With-Algae.pdf (accessed July 2017).

96. http://www.originclear.com/pdf/OriginOil-White-Paper-Algae-As-Aquafeed.pdf (accessed July 2017).

97. Shields, R. J.; Lupatsch, I., Algae for aquaculture and animal feeds. *J Anim Sci Vol. 21 pp. 23-37*, 2012.

98. Paradigm Biosciences Int., Personal Communication (Crocker, M., recipient), January 2012.

99. http://www.accelergy.com/technology_terrasync.html (accessed August 2017).

100. https://en.wikipedia.org/wiki/Lutein (accessed July 2017).

101. Richer, S.; Stiles, W.; Statkute, L.; Pulido, J.; Frankowski, J.; Rudy, D.; Pei, K.; Tsipursky, M.; Nyland, J., Double-masked, placebo-controlled, randomized trial of lutein and antioxidant supplementation in the intervention of atrophic age-related macular degeneration: the Veterans LAST study (Lutein Antioxidant Supplementation Trial). *Optometry - Journal of the American Optometric Association Vol. 75 (4), pp. 216-229*, 2004. http://www.sciencedirect.com/science/article/pii/S1529183904700494.

102. März, U., FOD025C–The Global Market for Carotenoids. *BCC Research Vol. pp.* 2008.

103. Cerón, M. C.; Campos, I.; Sanchez, J. F.; Acién, F. G.; Molina, E.; Fernandez-Sevilla, J. M., Recovery of lutein from microalgae biomass: development of a process for Scenedesmus almeriensis biomass. *Journal of Agricultural and Food Chemistry Vol. 56 (24), pp. 11761-11766*, 2008.

104. Richardson, J. W.; Johnson, M. D.; Zhang, X.; Zemke, P.; Chen, W.; Hu, Q., A financial assessment of two alternative cultivation systems and their contributions to algae biofuel economic viability. *Algal Research Vol. 4 pp. 96-104*, 2014. http://www.sciencedirect.com/science/article/pii/S2211926413001215.

105. Wang, B.; Li, Y.; Wu, N.; Lan, C. Q., CO2 bio-mitigation using microalgae. *Applied microbiology and biotechnology Vol. 79 (5), pp. 707-718*, 2008.

106. http://www.seambiotic.com/News/Scientific-white-papers. (accessed August).

107. Sepúlveda, C.; Acién, F. G.; Gómez, C.; Jiménez-Ruíz, N.; Riquelme, C.; Molina-Grima, E., Utilization of centrate for the production of the marine microalgae Nannochloropsis gaditana. *Algal Research Vol. 9 pp. 107-116*, 2015. http://www.sciencedirect.com/science/article/pii/S2211926415000673.

108. https://www.alibaba.com/product-detail/Organic-100-Natural-Alpha-Linolenic-Acid_60428596173.html?spm=a2700.7724857.main07.10.6f7de77ceXsPod&s=p (accessed July 2017).

109. https://www.alibaba.com/trade/search?fsb=y&IndexArea=product_en&CatId=&SearchText=docosahexaenoic+acid+100%25+pure (accessed July 2017).

110. Cuellar-Bermudez, S. P.; Aguilar-Hernandez, I.; Cardenas-Chavez, D. L.; Ornelas-Soto, N.; Romero-Ogawa, M. A.; Parra-Saldivar, R., Extraction and purification of high-value metabolites from microalgae: essential lipids, astaxanthin and phycobiliproteins. *Microbial Biotechnology Vol. 8 (2), pp. 190-209*, 2015. http://dx.doi.org/10.1111/1751-7915.12167.

111. Gastineau, R.; Turcotte, F.; Pouvreau, J.-B.; Morançais, M.; Fleurence, J.; Windarto, E.; Semba Prasetiya, F.; Arsad, S.; Jaouen, P.; Babin, M.; Coiffard, L.; Couteau, C.; Bardeau, J.-F.; Jacquette, B.; Leignel, V.; Hardivillier, Y.; Marcotte, I.; Bourgougnon, N.; Tremblay, R.; Deschênes, J.-S.; Badawy, H.; Pasetto, P.; Davidovich, N.; Hansen, G.; Dittmer, J.; Mouget, J.-L., Marennine, Promising Blue Pigments from a Widespread Haslea Diatom Species Complex. *Marine Drugs Vol. 12 (6), pp. 3161-3189*, 2014. http://www.ncbi.nlm.nih.gov/pmc/articles/PMC4071570/.

112. http://algosource.com/en/produit/spirulysat/ (accessed August 2017).

113. http://algosource.com/en/ (accessed August 2017).

114. https://en.wikipedia.org/wiki/Chloroplast#Phycobilins (accessed July 2017).

115. National Research Council, Sustainable Development of Algal Biofuels in the United States, The National Academies Press: Washington, DC, 2012; p 246.

116. http://cellana.com/technology/core-technology/ (accessed July 2017).

117. https://www.sciencedaily.com/releases/2007/03/070319175853.htm (accessed July 2017).

118. http://www.greencarcongress.com/2007/03/researchers_dev.html (accessed July 2017).

119. http://www.greencarcongress.com/2008/01/centia-biofuels.html (accessed July 2017).

120. http://pondtechnologiesinc.com/ (accessed July 2017).

121. http://pondtechnologiesinc.com/technology/ (accessed July 2017).

122. http://pondtechnologiesinc.com/technology/carbon-capture/ (accessed July 2017).

123. http://www.genesis-biofuel.com/ (accessed August 2017).

124. http://www.genesis-biofuel.com/Vision.html (accessed August 2017).

125. http://www.genesis-biofuel.com/Technology-The-Process.html (accessed August 2016).

126. http://www.genesis-biofuel.com/Technology-Our-Value-Add.html (accessed August 2017).

127. Olivares, J. National Alliance for Advanced Biofuels and Bioproducts (NAABB) Final Report Section 3. US DOE-EERE Biotechnologies Office 2014. https://energy.gov/eere/bioenergy/downloads/national-alliance-advanced-biofuels-and-bioproducts-synopsis-naabb-final

128. http://www.globalgae.com/technology/ (accessed August 2017).

129. http://www.febico.com/en/index.html (accessed August 2017).

130. http://www.accelergy.com/technology_cbtl.html (accessed August 2017).

131. http://www.globalgae.com/equipment/ (accessed August 2017).